Characterisation of sensory neurons innervating murine skeletal muscle, focusing on one class of Group III afferents

by

Rochelle Peterson

Thesis
Submitted to Flinders University
for the degree of

Doctor of Philosophy

College of Medicine & Public Health

1st August 2019

Characterisation of sensory neurons innervating murine skeletal muscle, focusing on one class of Group III afferents

A thesis submitted in total fulfilment of the requirements of the degree of Doctor of Philosophy

Rochelle Ann Peterson

Bachelor of Medical Science

Bachelor of Science (Honours)

Discipline of Human Physiology and Centre of Neuroscience

College of Medicine and Public Health

Flinders University

Summary

This study aimed to identify and characterise group III and IV sensory nerve endings within skeletal muscle. This population of neurons have terminals in the skeletal muscle and cell bodies in dorsal root ganglia (DRG). They are part of neural pathways that convey muscle work, pain, and fatigue. These sensory endings comprise a mixture of fine myelinated and unmyelinated axons with variable branching patterns. Until now it has been difficult to relate their morphology to their functional characteristics, with the exception of large group I and II afferent endings of muscle spindles and Golgi tendon organs.

An isolated preparation of mouse abdominal muscles was developed. A combination of techniques applied previously in preparations of visceral organs was used, allowing correlation of form and function of small diameter endings for the first time. We validated this preparation by using it to correlate the morphological and functional characteristic of the well-described muscle afferent endings in muscles spindles. This confirmed that these techniques could relate the morphological and functional properties a single class of well-characterised skeletal muscle afferents in detail.

Electrophysiological recordings from nerve trunks, innervating the muscles of the abdominal wall, enabled detailed studies of a distinctive class of group III muscle afferents. These afferents had discrete fields of innervation, were mechanically-sensitive, with distinctive saturating response to both punctate pressure and stretch. They were metabo-sensitive, activated by a known muscle metabolites mix but were insensitive to the TRPV1 agonist, capsaicin. Electrophysiological studies combined with anterograde labelling revealed, for the first time, that these group III muscle afferents have terminals located within the connective tissue between the muscle

layers. Additional immunohistochemical labelling for calcitonin gene related peptide (CGRP), demonstrated these were not CGRP immunoreactive.

Targeted extracellular recordings from these identified afferents, tentatively named CT3 afferents (group III afferents with endings in connective tissue), investigated responses to lactate. We showed lactate can directly excite CT3 afferents, but not all muscle sensory neurons. Real-time PCR demonstrated that mRNA for the G-protein coupled lactate receptor (hydroxyl carboxylic acid receptor 1 or HCAR1) was localised in DRGs containing afferents that innervated abdominal muscles. HCAR1 immunoreactivity was visualised in DRG sensory neurons retrogradely labelled from abdominal muscles. HCAR1 immunoreactivity was present in axons and nerve endings in abdominal muscles, often in CGRP-negative axons; consistent with belonging to CT3 afferents. This suggests that HCAR1 is expressed in a subset of primary afferents that innervate some skeletal muscles. These data are consistent with the novel proposal that lactate activates sensory afferent endings in skeletal muscle via its G-protein receptor, HCAR1.

This work has advanced knowledge of one class of group III muscle afferents (CT3s), revealing a distinctive class of mechanically and metabo-sensitve afferents with terminals in muscle connective tissue. We developed and validated an ex *vivo* preparation and a combination of techniques, in which different classes of group III and IV muscle afferents can be systematically characterised in detail, physiologically and morphologically. We propose that some muscle afferents, including CT3 afferents, can be directly activated by lactate via HCAR1.

Declaration

I certify that this thesis does not incorporate without acknowledgment any material previously submitted for a degree or diploma in any university; and that to the best of my knowledge and belief it does not contain any material previously published or written by another person except where due reference is made in the text.

Signed:

Rochelle Ann Peterson

Acknowledgements

First and foremost, I would like to express my sincerest appreciation and thanks to my primary supervisor, Professor Simon Brookes, for your guidance, expert training, assistance, and constructive criticism over the years. Your encouragement and belief in me has given me the motivation to go further than I thought possible. Thank you for always making me go the extra mile, to do that extra experiment, so that my research was the best it could be.

I would like to thank my co-supervisor, Dr Christine Barry, for all of your helpful feedback, advice, encouragement and support throughout my PhD. You always made sure that you were available to read over a draft, answer any questions. Our little chats in the corridor were always helpful and motivating.

I gratefully acknowledge the funding received towards my PhD, from an Australian Government Research Training Program Scholarship which allowed me to carry out my research.

This PhD would not have been possible without all the help and encouragement that I that received along the way. I would like to especially thank Nan Chen for her contributions to the development of my practical skills, as well as her experimental and laboratory knowledge. Mel Kyloh for sharing your expertise on how to carry out the surgeries for my retrograde labelling studies, and dissections. Luke Wiklendt who created our in-house discriminating program, for taking the time to explain computational and mathematical concepts (Gaussians and Principle components), discussing results and making continual edits to your code and program, so I could carry out different types of analysis. Richard Leibbrandt for helping me whenever my

data decided to crash our in-house discriminating program.

I would also like to thank Pat Vilimas and Yvette Hannig (nee DeGraff) for teaching me about confocal microscopy, our great chats and letting me into the microscopy suite after, yet again, forgetting my code. Dr Alyce Martin and Jastrow Canlas for taking the time out of their own PhD schedules to show me how to carry out PCR, along with the required analysis. Lauren Jones for helping with electrophoresis runs of my PCR products and Tim Hibberd for reviewing and your advice on the fourth chapter of this thesis.

I would like to give a very special thank you to Adam Humenick for your experimental expertise, reviewing this thesis, bouncing ideas around with, troubleshooting set ups, endless coffee runs (I think I owe you more than just a few), and your friendship. To Lauren Keightley for reviewing this thesis, being an absolute amazing friend, a listening ear, and for all the support you have given me throughout this time, I am truly thankful.

I would like to give a heartfelt thank you to my Mother Janine, my Father Michael, and brother Matthew for the always believing in me, supporting and encouraging me to follow dreams. To my loving husband Stephen, you have been with me every step of this crazy journey with me, thank you for your endless love and support throughout my PhD.

Figures and Tables

Abbreviation List

$[K^+]$	Potassium ions
3,5-DHBA	3,5-Dihydroxybenzenioc acid
Ach	acetylcholine
ASICS	Acid sensing ion channels
ASICS3	Acid sensing ion channel 3
ATP	Adenosine triphosphate
Ca^{2+}	Calcium ion
CGRP	Calcitonin gene related peptide
Cl^-	Chloride ion
CP	Creatine phosphate
CT3 afferents	Group III afferents with endings in connective tissue
DI	Dynamic index
DOMs	Delayed onset muscle soreness
DP	Dynamic peak
DRG	Dorsal root ganglia
EC Coupling	Excitation-contraction
GAPDH	Glyceraldehyde 3-phosphate dehydrogenase
GPCR	G-protein coupled receptor
GPR81	G-protein receptor 81 (also known as HCAR1)
H^+	Proton
HCAR1	Hydroxyl carboxylic acid receptor 1
IGLEs	Intraganglionic laminar endings
IUPHAR	International Union of Basic and Clinical Pharmacology
MCT	Monocarboxylate transporters
Mg^{2+}	Magnesium ion
MNE	Mean Normalised Expression
MRGPRs	Mas-related related G-protein coupled receptors
mRNA	Messenger RNA
Na^+	Sodium ion
NF2000	Neurofilament 2000
P2X	Purinergic ligand gated ion channel
P2X2	P2X purinocepter 2
P2X3	P2X purinocepter 3
PAD	Peripheral artery disease
PCR	Polymerase chain reaction
PGP 9.5	protein gene product 9.5
RD	Resting Discharge
SMA	Smooth Muscle actin
SP	Substance P
SR	Static response
TAP block	Transversus abdominis plane Block
TH	tyrosine hydroxylase
TRPA1	Transient receptor potential cation channel, subfamily A, member 1

TRPC3	Transient receptor potential cation channel subfamily C, member 3
TRPC6	Transient receptor potential cation channel subfamily C, member 6
TRPM1	Transient Receptor Potential Cation Channel Subfamily M, Member 1
TRPV1	Transient receptor potential cation channel subfamily V, member 1
TRPV4	Transient receptor potential cation channel subfamily V, member 4
TS	Time Silent

CHAPTER ONE

REVIEW OF THE LITERATURE

Principles of sensory neuron function

For an animal to detect changes in its external or internal environment and generate appropriate responses, it needs to be able to monitor what is happening around it, in an ongoing fashion. Sensory neurons are nerve cells in the body that are dedicated to this purpose. Sensory neurons respond to a variety of mechanical, thermal, light and chemical stimuli. Some sensory neurons give rise to conscious sensations, such as touch, smell, taste, or pain. However, sensory neurons may also activate motor responses that vary from simple reflexes without accompanying conscious sensations, through to complex adaptive motor behaviours. Sensory neurons have receptive endings within peripheral tissues or close to the body's surfaces which detect and encode stimuli. Apart from the special senses, most sensory neurons have cell bodies in segmental spinal ganglia and axons that project via these ganglia to the spinal cord (Basbaum et al., 2008).

Disregarding the more complex arrangements of cranial sensory neurons and the special senses, the cell bodies of a most other sensory neurons are located in the neural crest-derived dorsal root ganglia (DRG). Their single process (neurite) bifurcates into two axons, one of which projects into the periphery in nerve trunks and innervates peripheral tissues such as, the skin, muscle, joints, blood vessels, and the viscera. The other axon branch projects from the dorsal root ganglia into the dorsal horn usually via the dorsal roots, into the spinal cord where it synapses onto central interneurons or occasionally forms monosynaptic reflexes with motor neurons (Perl, 1992). In the head, sensory neurons have their cell bodies within ganglia associated with the cranial nerves; these include the trigeminal ganglia, superior and inferior ganglia of the vagus, superior and inferior glossopharyngeal ganglia, vestibular and spinal ganglia of the inner ear and geniculate ganglion of the facial nerve (Basbaum et al., 2008). There are

also sensory nerve cell bodies within the gut and heart that detect local stimuli and interact with local peripheral circuits, without direct connections with the central nervous system. There are also characteristic arrangements of the sensory neurons involved in the non-tactile "special senses" of vision, audition, olfaction and gustation. Vision is characterised by specialised photoreceptor cells; the rods and cones which synapse onto a complex retinal circuitry from which ganglion neurons project via the optic nerve II to central targets. One class of intrinsically-photosensitive ganglion cells fall outside this arrangement (Do and Yau, 2010). For audition, the situation is more akin to that of somatic mechanoreceptors. Sensory nerve cell bodies in the modiolus of the spiral ganglion each give rise to a neurite that bifurcates, with the peripheral ending receiving input from specialised mechanoreceptor cells; the hair cells. The central axon conducts action potentials via axons in the vestibulo-cochlear nerve (VIII) to terminals in the cochlear ganglia, which then activate higher auditory processing pathways (Hudspeth, 2014). Olfactory receptor cells are activated by occupation of odorant receptors on their cilia located within the mucus layer of the olfactory epithelium. Small clusters of olfactory axons penetrate the cribriform plate, and project into the olfactory bulb. Within the olfactory bulb axons converge and terminate onto the dendrites of second order olfactory neurons in spherical glomeruli. The output from the bulb projects through the olfactory tract to central targets, mainly the olfactory cortex. The olfactory axons collectively constitute the olfactory nerve (cranial nerve I) (Hatt, 2004). The last special sense; taste is mediated by receptors on microvilli that are exposed to the contents of the mouth. Taste cells form synapses onto primary gustatory afferent axons. Taste transduction is different from those described above, it involves several different processes dependent on the tastant (taste stimuli – sweet, sour, salt, bitter, umami and "oleogustus"(Running et al., 2015). The tastant may act directly on ion channels (salt and sour), it may bind and block an ion channels (sour)

or it may bind to a G-protein coupled receptor within the taste cell membrane, initiating a secondary messenger cascade, which opens a select ion channels (bitter, sweet, oleogustus and umami). Each of these results in the activation of the primary gustatory afferent axons, projecting to the gustatory nucleus, via one of the three cranial nerves dependent on the area of the tongue. The anterior two-thirds of the tongue and palate have axons via the facial nerve (VII), while the posterior third via axons in the glossopharyngeal nerve (IX). Information regarding taste from the throat runs via the vagus nerve (X).

Sensory neurons detect the changes in the external and internal environments by their specialised endings within the organ or tissue that they innervate; a process known as sensory transduction. Once an ending has been activated by a stimulus, action potentials are generated and conducted from the sense organ to the spinal cord or brain. The area in which the specialised endings can be activated (detect a stimulus) is its 'receptive field'. The size of the receptive field varies depending on the type of nerve ending and its terminal branching pattern in the organ that it innervates. The stimulus, or combinations of stimuli, that activates a sensory neuron is called its 'adequate stimulus'. The activation of a sensory neuron is determined by the combination of ion channels and receptors on its peripheral ending. These determine the process of transduction (Basbaum et al., 2009).

Sensory transduction

Transduction is the process in which environmental stimuli are converted into electrical signals usually via conformational changes in the structure of specific proteins located on the sensory cells. Transduction may be direct, where the sensory nerve terminal contains all of the cellular machinery required to convert the stimulus

into trains of action potentials. There is also indirect transduction, where the stimulus is detected by a specialised type of cell, which then activates the afferent terminal via a synaptic mechanism. Examples of the latter include hair cells in the inner ear, Merkel cells in the skin and entero-endocrine cells in the lining of the gut mucosa. In the sensory cell, conformational changes of these proteins directly or indirectly (via signalling cascades) trigger the opening or closing of ion channels (Julius and Nathans). Sensory neuron terminals express a large variety of cell surface proteins. The different combinations of expressed surface proteins enable sensory neurons, to not only be differentiated into neuronal sub-classes, but to act as initiators and modulators of stimulus evoked responses (Julius and Nathans).These proteins allow sensory neurons to collect a variety of environmental details. The two cell surface receptor proteins, ion channels, and g-protein coupled receptors have been investigated in extensive detail.

Ion channels are usually multimeric proteins located in the plasma membrane. The proteins are arranged in such a manner as to create a 'pore' or 'channel' which can open or close in response to stimuli. This allows a specific type of ion or combination of ions (Na^+, K^+, Cl^-, Ca^{2+}) to flow passively down their electrochemical gradient, through the plasma membrane, creating a current which alters the plasma membrane potential. This change in membrane potential is referred to as the generator potential. If the generator potential reaches the threshold, one or more action potential is produced at a nearby site (Catterall et al., 2017, Hille, 2001).

Ion channel classification is highly complex and the relationship between genetic classifications and functional classifications is often not clear, especially for heteromeric channels. According to the IUPHAR database

(http://www.guidetopharmacology.org/targets.jsp)(Harding et al., 2017), voltage-gated ion channels have at least 8 major families. As their name suggests, their opening probability varies in response to changes in membrane potential but may be modulated by calcium ions, or other intracellular messengers. Ligand-gated ion channels (10 families) open in response to a specific ligand binding to the extracellular domain of the receptor protein. Other major families (apart from voltage and ligand gated channels) listed by IUPHAR include chloride channels, connexins and pannexins, store-operated ion channels, piezo channels, non-selective sodium leak channels and aquaporins. Ion channels responses are often rapid, enabling the sensory ending to convert the stimuli into neural depolarisation that over a millisecond timescale. They have the capacity for signal integration and control. G-protein coupled receptors generally operate over a much slower timescale between tens to hundreds of milliseconds (Julius and Nathans).

G-protein coupled receptors

G-protein coupled receptors, like ion channels, are membrane proteins that have seven-membrane spanning domains. G-protein coupled receptors transduce information through a multiple component second-messenger based signalling pathways. G-protein coupled receptors respond to a diverse array of signalling molecules, peptides, hormones, neurotransmitters, odorants, tastants and other mediators. Transduction is dependent on a receptor-mediated activation of heterotrimeric G-proteins. These proteins are composed of 3 different subunits Gα, Gβ and Gγ. The binding of extracellular ligands regulates the interaction between the receptor and the g-proteins (Hilger et al., 2018). The binding of a ligand results in a conformational change of the receptor and the g-protein subunits. A g-protein coupled receptor is inactive when all three subunits Gα, Gβ and Gγ are associated and guanosine diphosphate is bound to

Gα. Upon the activation of the receptor guanosine diphosphate at the Gα subunit is exchanged with guanosine triphosphate. The dissociation of guanosine diphosphate causes a conformational change that results in the dissociation of Gα from Gβ and Gγ subunits. Gα subunits come in a variety of isoforms ($G\alpha_s$, $G\alpha_i$, $G\alpha_q$, $G\alpha_0$, $G\alpha_{12}$, and $G\alpha_t$ (in transducin); these determine the secondary messenger targets which include up or down regulation of adenylyl cyclases, cGMP phosphodiesterase, phospholipase C and RhoGEFs. The Gβ and Gγ subunits can affect the recruitment and regulation of g-protein-regulated inwardly rectifying K^+ channels (GRK), voltage-dependent Ca^{2+} channels, adenylyl cyclases, phospholipase C, phosphoinosite 3 kinase and mitogen-activated protein kinases. Once guanosine triphosphate has been hydrolysed to guanosine diphosphate, Gα subunits it again binds with Gβ and Gγ subunits and become inactive (Hilger et al., 2018).

Ion channels along with g-protein coupled receptors together, through active and passive properties, result in the conversion of an external stimulus into an electrical signal essential for the conversion of a generator potential into an action potential that propagates back to the spinal cord. To demonstrate how these mechanisms, operate the following are a few select examples of sensory transduction in a range of different nerve cells to illustrate the variety of mechanisms that operate. In recent years there has been a great amount of progress made, this has largely been due to the combinations of sophisticated techniques including genetic models, electrophysiology and behavioural studies.

Hair cells in the cochlea

Sensory hair cells found within the inner ear transduce mechanical stimuli and thereby active afferent neurons via a basolateral synaptic mechanism. Atop of a hair cell are roughly 60-100 sterocilia, these are arranged in a staircase manner of increasing height. The tip of each of the sterocilia are joined by protein structures called 'tip links'. It is thought that the deflections of the sterocilia cause the tip link to generate enough force that results in the opening of mechanosensitive ion channels. These mechanosensitive ion channels are also located near the tip of each stereocilium. Over the last two decades the identity of this particular mechanosensitve ion channel has been extensively researched and there have been many proposed candidates, including TPV4, TRPA1, HCN1, TRPML3, PKD1, PKD2, TRPC3/TRPC6 and TRPM1 (see review - (Corey and Holt, 2016)). Recent investigations, using targeted mutation of the pore-forming region and protein structural analysis suggest that Transmembrane-channel-like-protein 1 is a pore forming component at the stereocilia tip (Pan et al., 2018). Mutations in TMC1 in human patients, are seen as congenital blindness, this is consistent with the major role of TMC1 in transduction (Kurima et al., 2002).

Merkel cell transduction

Merkel cells are found within touch domes in the epidermis layer of the skin. They are known to respond to light pressure and act as type I slowly adapting mechanoreceptors (Iggo and Muir, 1969). Since their initial description, how Merkel cells transduce sensory information has been debated. Merkel cells have recently been shown to be activated by mechanical stimuli. In a recent study touch domes containing Merkel cells were optogenetically activated via targeted laser illumination, resulting in the activation of slowly adapting type I mechanoreceptors. This method of activation resulted in a sustained response, while touch stimuli results in rapid bursts of firing

before the maintained firing. Mechanoreceptors that innervate touch domes in the Atoh 1 knockout model (lacking Merkel cells), have reductions in both dynamic and sustained components (Maksimovic et al., 2014). Recent studies have demonstrated the expression of Piezo 2, a mechanosensitive channel, in Merkel cells and that it is required for mechanotransduction (Ikeda et al., 2014, Woo et al., 2014). In a Piezo 2 knockout model Woo et al 2014, demonstrated that loss of Piezo 2 in skin cells resulted in a partial deficit in light touch detection, as some mechanosensitivity remained (Woo et al., 2014). Due to this partial deficit in touch detection, it has been suggested that the type I afferent terminals capable of transduction and that they are mechanosensitive, and that this mechanosensitivity is tuned by Merkel Cell input (Maksimovic et al., 2014, Woo et al., 2014). Several studies have suggested that the communication between Merkel cells and their afferent ending is either serotonergic or glutamatergic, although a recent study has described that noradrenaline, acting via Beta 2 receptors, as the required transmitter (Hoffman et al., 2018).

Direct mechanotransduction in intraganglionic laminar endings (IGLEs)

Intraganglionic laminar endings are low threshold mechanosensitive endings of vagal afferents. Intraganglionic laminar endings are located within the myenteric ganglia of the stomach and the oesophagus (Zagorodnyuk et al., 2001, Zagorodnyuk et al., 2003). Four lines of evidence suggests that intraganglionic laminar endings are directly activated via mechanosensitive ion channels of their endings, unlike the slowly adapting type I cutaneous receptors. Firstly, the substitution of extracellular calcium ions or the addition a vesicle-mediated transmitter blocker Cd^{+} ions had no effect on IGLE transduction. Secondly, intraganglionic laminar endings were found to have a transduction delay value that was less then 6 ms, indicating a faster mechanism and not indirect transmission. Transduction delay was calculated by subtracting the spike

delay following electrical stimulation from the following rapid mechanical activation at the same site using a piezo-electric-driven probe. Thirdly, the application of two known rapid mediator antagonists for glutamate and adenosine 5'-triphostate (ATP) did not affect transmission. Lastly, stretch-induced firing of IGLEs was found to be reduced after the application of a known mechanosensitive ion channel blocker benzamil. Altogether, this evidence suggests that intraganglionic laminar endings were likely to be directly mechanosensitive to mechanical stimuli via expression of mechanosensitive ion channels, which remain to be identified at the molecular level.

Modulation of sensory transduction by G-Protein Coupled Receptors (GPCRs) and other receptors

Above are a few examples of the range of mechanisms in which mechanotransduction by ion channels occurs in sensory neurons in mammals. Some ion channels expressed on sensory neurons can be modulated via exogenous ligands, blurring the boundary between transduction and modulation (Hogg et al., 2005). For example, the ion channel transient receptor potential cation channel, subfamily A, member 1 (TRPA1) is expressed on many polymodal nociceptors. TRPA1 is a thermosensitive channel, implicated in noxious cold. Allosteric gating of TRPA1 receptor can occur via a range of exogenous substances including electrophiles; allyl isothiocyanate, allicin and oleocanthal from edible plants, alkenals (e.g. acrolein, crotonaldehyde), some aldehydes (e.g. formaldehyde, acetaldehyde), hypochlorites. Some non-electrophiles also have the ability activate the channel, these occur without co-valent modifications; menthol, icilin, (2-APB), nicotine, delta-9-tetrahydrocannabinol, thymol, low pH, high intracellular pH and polyunsaturated fatty acids.

Not only is TRPA1 able to be allosterically modulated this ion channel can also be modulated via the activation of different receptors. These include g-protein coupled receptors (bradykinin B2 receptor, protease activated receptor2) and several Mas-related related G-protein coupled receptors (MRGPRs) (see review -(Viana, 2016)). This remarkable list refers to just a single ion channel expressed in some nociceptors. Other substances acting modulators, have the potential to modify the sensitivity of sensory endings. An example of these are the substances released during inflammation, and how they potently modify the sensitivity of nociceptors. These substances include: amines (histamine, 5-hydroxytryptamine) eicosanoids and related lipids (leukotrienes, prostaglandins, thromboxanes, endocannabinoids), neurotrophins, cytokines, chemokines, extracellular proteases and protons (see for review (Basbaum et al., 2009)).

Here we have provided a brief account to demonstrate the complexity of the transduction process at sensory neuron terminals. Using mechanotransduction as an example, it has been demonstrated how the process of sensory transduction can be influenced by an enormous range of modulatory signals mediated via a number of cellular targets. In recent years there has been an extensive research in identifying the key species involved in mechanotransduction, although much more is needed to be done to fully understand primary afferent neurons are activated under the full range of physiological and pathophysiological conditions.

Classifications of sensory neurons

Sensory neurons can be classified in many different ways, including their morphological and functional characteristics encompassing, but are not limited to: soma size, microscopic structure of peripheral ending, location, combinations of

expressed ion channels, or the amount of myelination and axonal diameter. Functional characteristics may include: conduction velocity (which relates to myelination and axonal diameter), basal firing rate, peak firing rate, rate of adaptation, low-threshold versus high-threshold, adequate stimulus (i.e. heat, chemical, mechanical load, pressure), sensitivity to one or more modalities, stimulus response functions and sensitivity to hormones, transmitters, modulators, based on their response to substances including capsaicin, bradykinin, purines, adenosine triphosphate (Basbaum et al., 2009, Brookes et al., 2013). In some instances, the morphological characteristics correlate with the functional characteristics of a neuron, for example, the conduction velocity of a sensory neuron depends of the myelination of the axon and axonal diameter. Thus, Group IV afferents with fine axons that have no myelin conduct very slowly, while Group I afferents that are thickly myelinated and of large diameter conduct very quickly (Erlanger and Gasser, 1930).

In addition, another useful method for classifying sensory neurons is by their neurochemical code; i.e.: the combinations of chemical markers they contain (Furness et al., 1989). Using either functional and morphological characteristics to classify different classes of neurons (listed above, for example) can be a limitation. Ideally, as many properties as possible should be established before classifying a sensory. neurons. A neurochemical marker can be any substance that is contained within a cell body, or an ion channel or a receptor in/on the cell membrane of a cell body or nerve ending. Neurochemical coding is a method used to visualise, distinguish and classify neurons by the appearance of chemical markers in combination, allowing each class to be studied in detail, one at a time, without conflating their properties (Furness et al., 1987, Furness et al., 1989, Gibbins et al., 1987). It is usually based on the use of multiple labelling immunohistochemistry although other histochemical markers can

be used. It should be noted that neurochemical markers are not entirely stable; they can change under different conditions. It is possible for the expression of a neurochemical marker to be either reduced or upregulated in different disease states, such as inflammation (Ro et al., 2009). For example, transient receptor potential cation channel subfamily V, member 1 (TRPv1) expression in dorsal root ganglia (L4-L6) has been shown to increase compared to that of controls, in an inflammatory hyperalgesia model. This model used injections of complete Freund's adjuvant to the plantar surface of the hind paw to induce inflammation (Yu et al., 2008).

Understanding sensory innervation

In disorders of the sensory nervous system, afferent neurons may not detect stimuli appropriately. This includes conditions such as chronic pain and congenital analgesia (inability to feel pain). Many of these sensory disorders have unknown aetiology, therefore, there is a great need to understand the mechanisms involved in transduction. It can be argued that in order to understand how the nervous system is affected in disease, the mechanisms that occur in the healthy state also needs to be understood (Basbaum et al., 2008). It is important to be able to study changes in a single homogenous class of neurons, one at a time, in order to avoid conflating or blurring properties between classes. Having the ability to discriminate a particular class or sub-class of sensory neurons, by their morphology, neurochemical code, and functional characteristics in a healthy state, gives a greater understanding of their role and the part they play in the nervous system. This may give an indication as to what might go wrong in disease and provide a means to identify which classes of afferents may be specifically affected.

An example of where the morphology and function of different classes of sensory neurons having been correlated is that of the skin. Because of this, cutaneous sensory innervation in mammals has been characterised in extensive detail (McMahon and Koltzenburg, 2006). The pattern of innervation varies between hairy and non-hairy skin. Within the skin, there are six sensory endings with distinctive morphology and functions. Pacinian corpuscles are tuned to detect high frequency vibrations; Meissner's corpuscles, detect flutter at lower frequencies (Mountcastle et al., 1967). Merkels disks detect steady indentation, as do Ruffini's endings, however, the latter are more directionally sensitive and tend to be aligned with the skin folds. Hair receptors detect the distortion of the hair follicle and unspecialised 'free nerve endings' branch widely under the dermis and respond to a variety of stimuli including heavy pressure, pinching, chemical damage, cutting, burning as well as a number of substance released by damaged cells (Iggo and Andres, 1982, Andres and During, 1990). A detailed account for the sensory innervation of other structures within the body, such as viscera or skeletal muscle lag behind the skin.

Over the last decade, a combination of techniques has been developed that has allowed the extrinsic sensory innervation of viscera to be characterized functionally and morphologically. Five morphological classes of axon terminals have been identified in the gastrointestinal tract, which arise from three different anatomical pathways. Each has specific morphological endings within the gut wall, and their transduction sites can be in a single layer or in multiple layers of the gut wall. Such examples include vagal intraganglionic laminar endings (IGLEs) as the transduction sites of low threshold mechanoreceptors in the stomach and oesophagus (Zagorodnyuk and Brookes, 2000), rectal IGLEs as a distinct class of low threshold sacral mechanoreceptors in the distal bowel (Lynn and Brookes, 2011a) and varicose axons

on blood vessels as transduction sites of mechano-nociceptors in the small and large intestine (Song. X., 2009). Mucosal afferents innervate the mucosa and the intramuscular afferents that have endings within the longitudinal and circumferential muscle layers (Tassicker et al., 1999, Brookes et al., 2013, Chen et al., 2015). These techniques are based on a combination of recording nerve activity in nerve trunks close to the organ of interest. Mechanosensitive sites belonging to a single afferent are then identified by focal probing and are marked on the living specimen, thus delineating the receptive field of one afferent unit. At the end of the recording period, biotinamide is applied in an intracellular solution (Tassicker et al., 1999) to the nerve trunk for a period of several hours in organ culture. The tracer is taken up by most afferent and efferent axons in the recorded trunk and transported down to their terminals in the organ. After fixation and visualisation with fluorophores conjugated to streptavidin, the goal is to identify a single axon that fills the receptive field with its branching. In some cases, this is impossible as several different axons may intermingle in the field, or on some occasions, no filled axon reaches the marked area. Despite these shortcomings, this approach has led to the identification of the morphology of the major classes of extrinsic afferents in the gut wall (Brookes et al., 2013). Potentially, these techniques might help unravel the relationship between structure and function of group III and group IV afferents in skeletal muscle, but this has not yet been attempted.

Basic functional anatomy of skeletal muscle, fascia and tendon

This project focussed on the sensory innervation of skeletal muscle. Before dealing with the details regarding the sensory innervation and endings within the muscle, a morphological context is needed. The skeletal muscles within the human body make up approximately 40% of our body weight and contain a significant proportion (50-75%) of all body protein. These muscles contribute significantly to many bodily

functions. Mechanically, skeletal muscles convert chemical energy into mechanical energy that generates force, power for movements, as well as maintain the body's posture. Skeletal muscles not only creates movements; it also plays a major role in basal energy metabolism. Skeletal muscles also serve as storage for amino acids and carbohydrates, produces heat to maintain body core temperature during shivering, and consumes oxygen and fuel during physical activity and exercise (Frontera and Ochala, 2015).

Basic skeletal muscle macroscopic and microscopic anatomy

At the macroscopic level, a layer of connective tissue surrounds a skeletal muscle, which supports, separates and protects the muscle, while maintaining its shape and integrity during deformation; this is the epimysium. Each muscle is composed of multiple fascicles, which are groups of muscle fibres/cells bundled together. Fascicles are enclosed by perimysium, another connective tissue structure. The muscle fibres/cells within the fascicles are separated from each other by endomysium. The epimysium, perimysium and endomysium, are all connective tissue structures. The epimysium and perimysium contain large amounts of collagen type I, whereas the endomysium contains more collagen type II (Light and Champion, 1984).

A single muscle fibre/cell is made up of many fused cells and is 10-100μm in diameter, varies in length (depending on the size of the muscle) and is delimited by a cell membrane called a sarcolemma. The inside of the muscle fibre/cell is the sarcoplasm. The detailed structure of skeletal muscle has been extensively studied. Below is a simplified account of the main structures. For a more detailed description see (Frontera and Ochala, 2015). Each muscle fibre/cell contains many myofibrils; sarcomeres are repeating units along the length of a myofibril. A sarcomere is the smallest functional

unit within a skeletal muscle and typically measures 2.5μm in length at rest. Sarcomeres contain many different specialised proteins, some of which contribute to the structure of the cytoskeleton, while others are associated with filamentous structures and are involved in the contraction of the muscle.

The two most abundant myofilaments are thin actin and thick myosin filaments. These filaments interdigitate and slide past each other during contraction and relaxation according to the 'sliding filament theory' (for detail see below ((Huxley and Niedergerke, 1954, Huxley and Hanson, 1954)). It is the orientation and alignment of the myofilaments, sarcomeres and myofibrils, that give the skeletal muscle its very orderly and characteristic striations. Within the sarcomere there are light and dark bands. The I band is where there is actin without myosin, for example where it attaches to the Z band that forms the border of the sarcomere in the long axis. The A band is where the actin and myosin interdigitate past each other. The myofibrils are arranged in a way that the myosin thick filaments and actin thin filaments of adjacent fibrils align (Frontera and Ochala, 2015).

Due to the technological advances, in the last few decades, and the use of proteomic analysis, the study of muscle proteins has allowed for greater insight into different proteins and their roles within the muscle. A portion of these proteins contribute to the mechanical and physiological properties of the muscle. Titin, for example, is a large elastic protein that attaches to the Z-line of the sarcomere and the myosin thick filament. The role of titin is described to help stabilise and align the thick filament (Greising et al., 2012). Nebulin, also a large protein, that is thought to have a regulatory role involving the length of the thin filaments (Ottenheijm and Granzier, 2010). Both of these proteins contribute to the integrity of the sarcomere. Other proteins that are

now known to play important role in the structure composition of the sarcomere are α-actinin and desmin. α-actinin serves as an attachment point for actinin at the Z-disk and desmin connects the Z-disk to the sarcomere and extracellular matrix. Dysfunction in these different proteins are involved in some myopathies (Frontera and Ochala, 2015).

Other cellular elements that are present in the sarcoplasm, within the muscle fibre/cell, that play important part in the production of force and contraction are the sarcoplasmic reticulum, the transverse tubular system (T-tubule), and the mitochondrial network. The sarcoplasmic reticulum main functions include the storage, release and the re-uptake of calcium (Ca^{2+}) after activation. The ends of the sarcoplasmic reticulum are called the cisternae. The calcium is stored within the terminal cisternae and is in close contact with the transverse tubule system. There are two cisternae located either side of the T-tubule, together (2 cisternae, 1 T-tubule) these make a structure called the triad (Lamboley et al., 2014). There are two proteins that contribute to the binding and re-uptake of calcium to the sarcoplasmic reticulum. Sarcoplasmic reticulum Ca^{2+} - ATPase, is involved in the re-uptake of Ca^{2+} into the cisternae and calsequestrin, the protein that binds Ca^{2+} to the cisternae. Lastly, the mitochondrial network, which is a three-dimensional network, that it throughout the muscle cell, and generates most of the ATP required for muscle action when oxygen is present (Dahl et al., 2015).

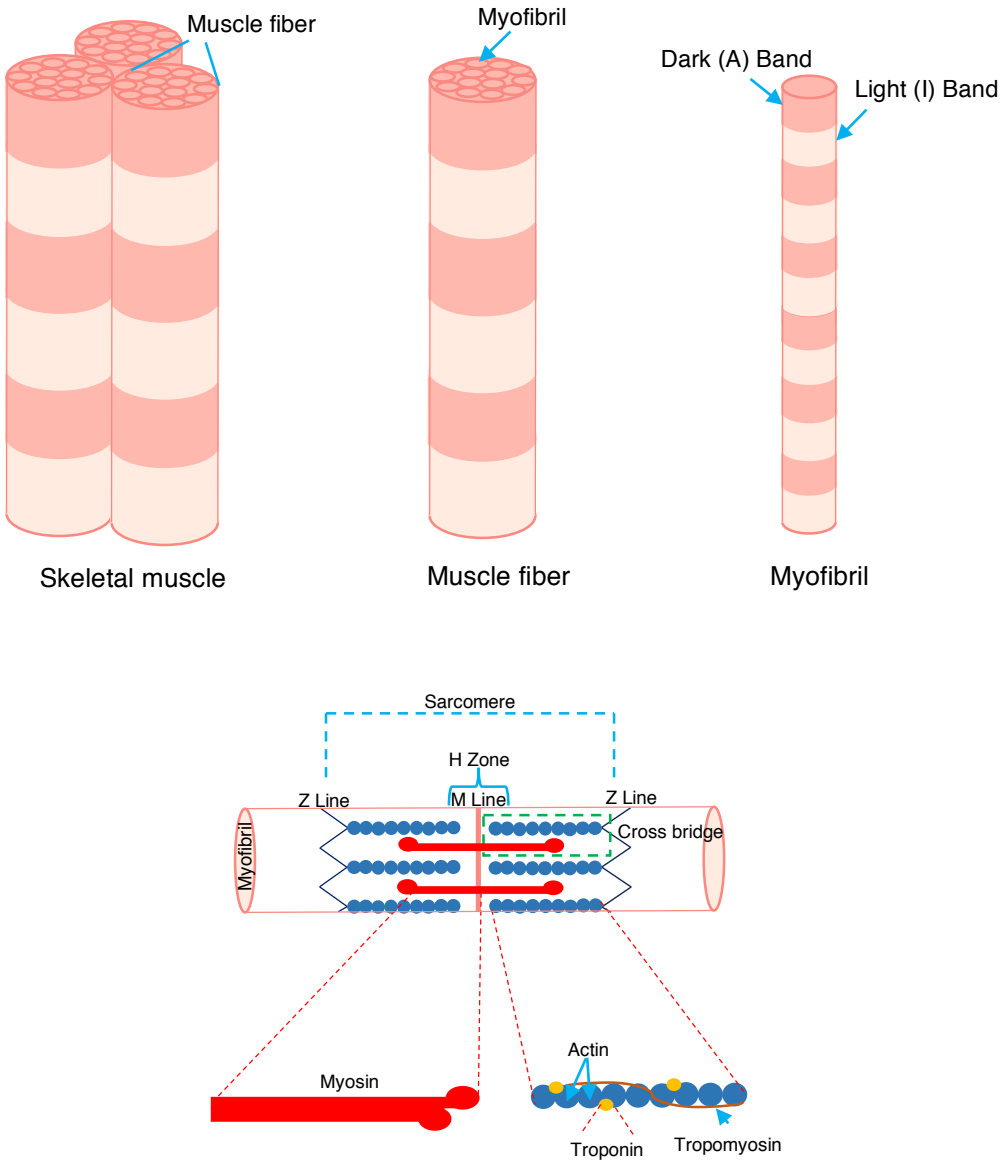

Figure 1.1. The macroscopic and microscopic anatomy of skeletal muscle
The body of a muscle is made up of many muscle cells. These muscle cells can be further broken down into the smallest functional and moving components. The smallest components are the myosin and actin filaments, which move over each other during muscle contraction. The distinctive striations of skeletal muscle are well established to arise from the precise alignment of myofilaments in the hugely elongated muscle cells.

A brief overview of contraction in skeletal muscle

There are two processes required for the generation of muscle force, these are excitation-contraction (EC) coupling and cross bridge cycling. Briefly, EC-coupling includes the arrival of the muscle action potential generated at the motor endplate and its transmission down the t-tubule to the triad, followed by the release of Ca^{2+} into the sarcoplasm. The interactions of actin and myosin form the cross bridges which are at the centre of the contractile mechanism (Frontera and Ochala, 2015). While the 'sliding filament theory' explains the basic mechanism by which the muscle fibre/cell generates force by individual actin-myosin cross-bridges. Each of these are described briefly below; for in-depth explanations see (Huxley and Niedergerke, 1954, Huxley and Hanson, 1954).

An action potential travels along an alpha-motor neuron axon, and upon arrival at the neuromuscular junction on a muscle fibre; it causes the release of acetylcholine (ACh). The ACh diffuses across the synaptic cleft to the muscle cell membrane, acting on Type IV nicotinic receptors, causing the muscle cell to depolarise. This generates a sodium-dependent muscle action potential which spreads over the surface of the muscle and is conducted to the interior of the muscle cell via the T-tubule system (Frontera and Ochala, 2015). The action potential arrives at the triad, where the voltage gated subunit on the dihydropyridine receptor on the T-tubule opens. This, in turn acts on nearby ryanodine receptors in the terminal cisternae of the sarcoplasmic reticulum, releasing a large quantity of Ca^{2+} into the sarcoplasm (Rebbeck et al., 2014). The release of Ca^{2+} increases the concentration of Ca^{2+} within the cell and binds to a regulatory protein troponin C on the actin myofilament. This binding modifies the troponin complex and initiates the displacement of another protein tropomyosin, which normally masks the myosin-binding site of the actin filament. The exposure of

the actin-binding site allows the head of myosin to bind with the actin. Adenosine triphosphate (ATP) then binds to the myosin head facilitating the detachment of the myosin from one actin-binding site. The action of the myosin ATPase then triggers the formation of a new cross-bridge further along the thin filament, resulting in the sliding of actin along the myosin filaments, shortening the sarcomere and contracting the muscle (Huxley and Niedergerke, 1954, Huxley and Hanson, 1954). Physiologically, skeletal muscle can perform four types of contractions: *concentric (shortening),* a reduction in length of the muscle and/or the generation of force. This can be broken down into *isotonic contraction,* a change in the muscle length without a change in the force exerted, *isometric contraction,* increasing the force produced without a change in muscle length. In fact, auxotonic contraction which involves changes in both length and tension accounts for most concentric contraction. E*ccentric (lengthening) contractions,* occur when the muscle lengthens due to an external force, with the muscle's force generating mechanism resisting the lengthening. This can decelerate or control a movement (Frontera and Ochala, 2015).

Types of muscle fibres

Over the decades muscle fibres have been classified using a range of different criteria. It has long been known that they could be distinguished on the basis of their colouring (red vs white) correlating to the content of myoglobin, contractile properties in response to the electrical stimulation of a motor unit, and the speed of shorting during a single twitch (fast vs slow) (Needham, 1926, Schiaffino and Reggiani, 2011).This lead to the theory that there were two distinct muscle fibres types. Type I muscle fibres that were, slow, rich in myoglobin (red), high levels of mitochondria, and slow contractile properties. While Type II muscle fibres were fast, had low levels of myoglobin (white) and mitochondria, and fast contraction and relaxation.

In the late 1960's Edstrom and Kugelberg (1968) using a glycogen depletion technique demonstrated the heterogeneity of fast motor units correlating their physiological and histochemical properties. By stimulating the motor unit, they were able to establish the twitch properties of muscle fibres. Glycogen depletion was then induced, and corresponding muscle fibres were identified by periodic acid-Schiff (PAS) staining and enzyme histochemistry for succinate dehydrogenase activity, to reflect oxidative metabolism, in serial sections. In this rat model, they showed that muscle fibre types could be distinguished based in their succinate dehydrogenase staining. They showed that muscle fibres were homogenous in composition based succinate dehydrogenase staining, that small succinate dehydrogenase positive (oxidative) or large succinate dehydrogenase negative (glycolytic) muscle fibres are both fast-twitch fibres. It was also shown that muscle fibre with low to no succinate dehydrogenase staining had a rapid decline in tension following stimulation and therefore fatigable, whereas, those abundant with succinate dehydrogenase staining had a greater resistance to fatigue (Edström and Kugelberg, 1968).

It was also known that myosins within the muscle fibres differed between fast and slow fibre types, including the ATPase activity of myosin, which correlates to the speed of muscle shortening (Bárány, 1967). The idea of heterogeneity and that there are two distinct types of fast muscle fibres was supported by the visualization of 'myosin' ATPase activity in tissue sections. ATPase activity studies revealed that there is in fact two different types of fast (Type II) muscle fibres. The two types were referred to as IIA and IIB, they were abundant in fast muscles (type II) and distinct from slow type I fibres (Brooke and K, 1970). A further contribution towards this characterisation was carried out in biochemical studies investigating the levels of oxidative and glycolytic enzymes. This led to the classification of Type I slow

oxidative, Type IIA fast-twitch oxidative glycolytic, and Type IIB fast-twitch glycolytic fibers (Peter et al., 1972). The metabolic properties between the different muscle fibres types was carried out more precisely by the introduction of microdissection of individual muscle fibres which demonstrated a variety of enzyme activities (Schiaffino and Reggiani, 2011).

The discovery of a third muscle fibre type took place during the late 80's to early 90's by the expression of myosin heavy chain protein isoforms. Monoclonal antibodies raised against myosin heavy chains resulted in the identification of muscle fibre type IIx (LaFramboise et al., 1990, Schiaffino et al., 1998, Schiaffino et al., 1989). Type IIx were found to have similar twitch properties to that of types IIA and IIB, while their level of fatigability and contractile properties were between that of type IIA and type IIB (Bottinelli et al., 1991, Larsson et al., 1991). Currently, the myosin heavy chain protein isoforms have been found to be the most fibre type specific marker to distinguish skeletal muscle fibre types across different species (mice, rats, and human) (Schiaffino, 2018). From the above studies have it been determined that there are four major fiber types in the mouse (Type I, Type IIA, Type IIB, and Type IIx). While there are only three fiber types in human muscle, with type IIB being present only in trace amount in human leg muscle samples (Schiaffino, 2018). The most frequently used classification of adult human limb muscles to date is type I – slow, oxidative, fatigue resistant, type IIa – fast, oxidative, intermediate metabolic properties, and type IIx – fastest, glycolytic, fatigable (Frontera and Ochala, 2015, Schiaffino, 2018).

Skeletal muscle energy production

All contractions by muscle require energy in the form of adenosine triphosphate (ATP). The metabolic energy pathway used to produce and maintain muscle actions depends on the duration and intensity of the activity. There are three energy pathways that a muscle can use:

1) ATP and CP (Creatine phosphate), that supports high intensity, short duration (few seconds) activities because the amount of ATP and CP reserves in muscle fibres is small.
2) Anaerobic glycolysis – produces ATP quickly from glycogen/glucose to sustain muscle actions for a couple of minutes but the end-products (H^+, lactate) impair muscle function and maybe associated with muscle fatigue. Critically, it does not require oxygen consumption.
3) Glycolysis and oxidative phosphorylation – energy for exercise performed at intensities that can be sustained for longer durations from minute to hours, is supplied by oxidative phosphorylation within the mitochondrial network. Carbohydrates (plasma glucose and muscle glycogen) and fats (free fatty-acids) are the two main fuels utilised by the muscle cell to produce ATP via these mechanisms. A network of capillaries transports oxygenated blood to the active muscle fibres. This network supports and assists with the metabolic demand on the muscle fibre (Frontera and Ochala, 2015). Oxygen is absolutely essential to this pathway and all of it is delivered via the bloodstream apart from the component stored as myoglobin in muscle fibres. Myoglobin is a cytoplasmic, oxygen (O_2) binding haemoprotein, expressed in cardiac myocytes and skeletal muscle. Myoglobin is a well-accepted O_2-storage protein in muscle, that has the ability to release O_2 during periods of hypoxia and anoxia (Ordway and Garry, 2004).

Basic Tendon anatomy and function

Tendons predominantly connect muscle to bone, although there are some instances where tendons connect to other structures, including other muscles and fascia. Fundamentally, tendons transmit tensile forces generated by muscle to the bone; they may also be subject to compression and shear. Tendons come in various shapes and sizes; a general rule is that extensor tendons tend to be flattened, while flexor tendons are more rounded, or oval in cross section (Benjamin et al., 2008). However, round tendons in particular become more flattened as they approach their attachment site. Tendons are largely composed of structural collagens and proteoglycans. Of these components, type I collagen predominates, but other collagens (II, III, V, VI, IX, XI) are also present. The primary role of collagen fibres is to resist tension, although still allowing compliance. Compared to the collagens, proteoglycans are responsible for the viscoelastic behaviour of the tendon, but do not make major contribution to the tensile strength (Benjamin et al., 2008).

Collagen fibres are overall a significant component of the dense connective tissue that make up tendons. The cell responsible for collagen assembly and turnover is the tenocyte; these are specialised fibroblasts that are arranged in rows in close proximity to the collagen fibrils. Collagen molecules consist of polypeptides chains, three of which combine to form a densely packed helical tropocollagen molecule. Five tropocollagen molecules constitute a microfibril. Microfibrils aggregate together and form fibrils; these fibrils are grouped into fibres. Fibres are bound together into bundles and these bundles into fascicles (Benjamin et al., 2008).

Basic tendon function

An important feature within a tendon is the ability for the tendon fascicles to slide independently of one another, allowing the transmission of tension despite the changing angles when a joint moves (Fallon et al., 2002). This also allows the tendon to change shape as the muscle contracts. To facilitate sliding of fascicles, a thin layer of loose connective tissue is present between fascicles, called the endotenon, it also occurs in the proteoglycan-rich matrix surrounding the fascicles. Its presence between the fascicles and fibre bundles promotes the movement between structures. This sliding within the tendon is not only limited to the fascicles. This movement is also seen between fibrils, this is thought to account for the longitudinal deformation or strain on the tendon (Screen et al., 2004). Because of their in-series location at the ends of muscles, tendons are ideally situated to detect tension in the body. Unsurprisingly, they receive a distinctive innervation by large diameter sensory neurons that make specialised endings in the tendon body; the Golgi tendon organs (see below).

As well as tendons, fascia transmits force from some muscles to other structures in the body. For example, the plantar fascia, helps to maintain the arch at the bottom of the foot, transmitting force from the back of the foot to the front. Fascia can also have a protective role. The palmer aponeurosis protects the nerves and vessels that lie underneath it between the wrist and fingers (Benjamin, 2009).

Basic definition, structure and classification of fascia

The original meaning of fascia was a vague Latin term for a band or bandage, used by gross anatomists to encompass a spectrum of undifferentiated mesenchymal tissue wrapped around specialised organs and the tissues of the body (Benjamin, 2009). Today fascia is defined as a connective tissue composed of irregularly arranged

collagen fibres, distinguished from the regular arrangement in tendons, ligaments and aponeurotic sheets (Willard et al., 2012). Collagen is the key structural component that gives connective tissue its ability to resist tension. Type 1 collagen is the most abundant type of collagen in fascia. Fascia also contains an array of collagen type combinations, which include, but are not limited to I, III, IV, V, VI, XI, XII, XIV, XXI (Kumka and Bonar, 2012). The collagen fibrils are important to the integrity and function of the fascia, as it is the irregular arrangement of the collagen which enables the fascia to withstand stresses in multiple directions (Willard et al., 2012). Within the structure of fascia there are various types of cells that help regulate and maintain the connective tissue, including fibrocyctes (fibroblasts and myofibrolasts), adipocyctes and migrating white blood cells.

Within the body there are four fundamental types of fascia. The first, is pannicular or superficial fascia, described as a loose connective tissue that encases much of the body. The second is the deep fascia, which surrounds the musculoskeletal system, and which forms a dense layer of connective tissue. Thirdly, the meningeal fascia or meninges, including the dura, pia and arachnoid mater, invests the central nervous system. Last is the visceral or splanchnic fascia, this invests the body cavities and their organs (Schleip et al., 2006, Schleip et al., 2012).

Innervation of skeletal muscle, fascia and tendon

Innervation of Skeletal Muscle

Sensory neurons innervating skeletal muscle have been classified into four groups; using two methods. Erlanger and Gasser (1930) classified the sensory neurons using conduction velocity, naming the classes with capital Roman letters and Greek lower case letters, similar to the nomenclature used to distinguish classes in the skin(Erlanger

and Gasser, 1930). The second method developed by Lloyd in 1943 distinguished the sensory fibres by their axonal diameter (which would be expected to be closely related to that of conduction velocity) denoted by the Roman numerals (I-IV). Lloyd's nomenclature is still commonly used for sensory fibres in skeletal muscle (see **Table 1.1.** (Lloyd, 1943b)).

Table 1.1. Classification of sensory fibres in skeletal muscle

Myelination	Classification (Lloyd, 1943)	Classification (Erlanger & Gasser, 1930)	Functional endings examples	Diameter (μm)	Mean Conductance velocity (ms)
Thick myelinated	Group I	Aα	Muscle Spindles (Ia)	15	100
		Aα	Golgi tendon organs (Ib)	15	100
	Group II	Aβ	Muscle Spindles secondary Nociceptors (?)	8	50
Thin myelinated	Group III	Aδ	Ergoreceptors Nociceptors	<3	15
			Mechanoreceptors Pacinian Corpuscle	<3	15
Unmyelinated	Group IV	C	Ergoreceptors Nociceptors	1	1
			Mechanoreceptors	1	1

Table Modified from (Mense and Gerwin, 2010)

Group I and II

As can be seen above in **Table 1.1**, some large diameter sensory axons in skeletal muscle have specialised endings, as seen in the skin and viscera. The three specialised endings within skeletal muscles that have been extensively investigated are the (i) primary muscle spindle, (ii) the 'flower spray ending' or the secondary afferent ending and (iii) the Golgi tendon organs. These are the functional endings of group Ia, group II and group Ib muscle afferents respectively.

Muscle spindles are complex receptive structures that measure the length and the rate of change in length of the muscle (Tiegs, 1953, Bewick and Banks, 2015). In 1898, Angelo Ruffini provided the first detailed description and drawings of the fine structure of muscle spindles. He described them as having a large "annulospinal" or primary nerve ending that wrapped around the equatorial region of elongated intrafusal muscle fibres (Ruffini, 1898). Sherrington, only four years earlier (1894), had showed the muscle spindles were sense-organs (Sherrington, 1894). In a class study, Adrian and Zottermann (1926) recorded the firing of frog muscle spindle primary endings and identified the principle of frequency coding of afferent firing (Adrian and Zotterman, 1926). B.H.C Matthews in 1933 carried out some of the early recordings from muscle spindles. These recordings were made from the central end of the muscle spindle, transecting it distally until a discharge was evoked by stretching the muscle was resultant from one unit. It was identified as a muscle spindle afferent by the decrease seen in the resting discharge when the muscle was made to twitch via motor nerve stimulation (Matthews, 1933).

It is now accepted that the primary receptive ending of the spindle forms loops around the central portion of the intrafusal fibres (as described by Ruffini). Lengthening of the muscle, especially its central portion, causes the loops to deform and in doing so, evokes a train of action potentials to the central nervous system. Matthews also noted that, when stretching a muscle to a new length, the spindle afferent fired more rapidly as the stretch was being applied (during the dynamic stage). Then after reaching and/or adapting to the new final length, the firing rate was dependent on both the rate and the on-going degree of stretch (Matthews, 1933). The fibres that project from the spindle ending to the central nervous system are classified as group Ia; they are thick myelinated fibres and are amongst the fastest conducting axons in the body (Lloyd,

1943a). The generator potential that gives rise to these patterns of firing have been recorded from primary endings in the presence of tetrodotoxin, which blocks action potential production (Hunt et al., 1978). The non-linearities in the responses were shown to be present in the generator potential and in the tension developed in the tissue, suggesting that the complex dynamic-biased response is at least partly a result of mechanical coupling to the sensory ending (Hunt and Wilkinson, 1980).

In his description of the primary spindle ending, Ruffini (1898) described a second type of afferent ending in muscle spindles. He described these as 'flower spray' endings and noted that they flanked the larger primary endings. Their axons were smaller than those projecting from the primary endings. The secondary afferent fibres described by Ruffini are Group II muscle afferents (Lloyd, 1943a) and have a slower conduction velocity than group I muscle afferents; 50 m/s compared with 100 m/s. Copper (1961) described some of the functional characteristics of secondary afferent endings. Group II muscle afferents lacked the large dynamic response, seen in group Ia muscle afferents, but responded to the amount of strain applied. The secondary afferent receptors were described as length receptors, as the firing was largely independent of the ongoing fusimotor activity. Small movement of a resting muscle often lead to spontaneous firing by primary endings, while the secondary endings respond more sedately, needing significant maintained mechanical changes to alter their firing patterns (Cooper, 1961). Between them, primary spindle and secondary endings provide the central nervous system with separate, but linked channels of information about the mechanical state of each major muscle group.

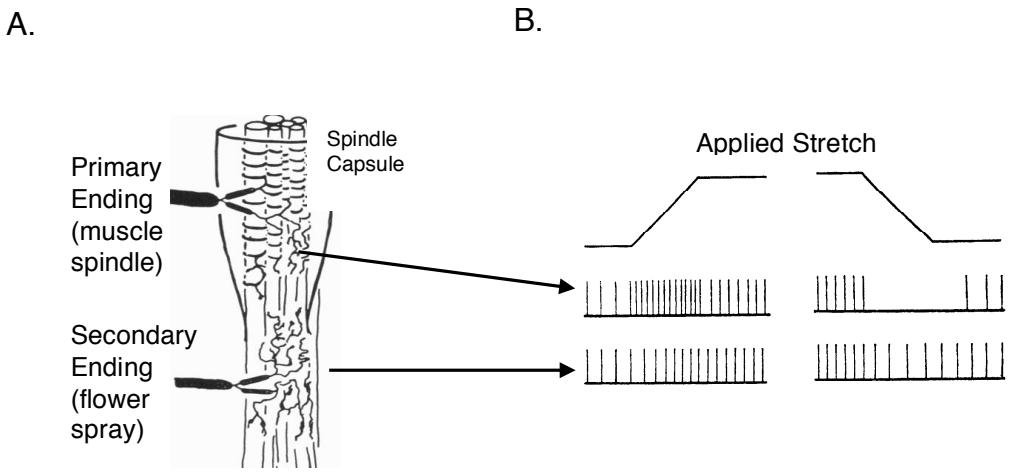

Figure 1.2. Neuroanatomical illustration and physiological responses of Group Ia and II afferent endings.
A. An illustration based on observations of primary endings and secondary endings impregnated by the modified de Castro method. This demonstrates the spiral ending of the muscle spindle, looping around the intrafusal muscle fibres, along with 'flower spray' ending of group II endings (Modified Figure From: (Stacey, 1969)). **B**. The physiological response of a primary ending and a secondary ending to a linear stretch. Primary endings increase their firing during the dynamic phase and cease firing once the stimulus is removed before returning to spontaneous firing. Secondary endings increase their firing during the static phase of the stretch and return to spontaneous firing once the stretch has been removed (Modified Figure From: (Matthews, 1964)).

Golgi tendon organs were reported and characterised by Golgi in 1878 and 1880 (Golgi 1878 and 1880 -see (Schoultz and Swett, 1972)). He described them as being musculo-tendinous organ endings. Now known commonly as Golgi tendon organs, they form another type of encapsulated sensory nerve endings. Golgi tendon organs are commonly distributed along the musculo-tendinous boundaries of skeletal muscle, in-series with the contractile elements (Brown, 1975). These sensory nerve endings are sensitive to mechanical force exerted in the muscle and tendon during passive stretch (Schoultz and Swett, 1972). Cattaneo (1888) established the sensory nature of the Golgi tendon organs by cutting the ventral roots and thereby the motor supply to the dog's hind limb. The Golgi tendon organ and its nerve remained intact indicating that

the axon had not been severed from its cell body and thus, by inference, must have a cell body in the dorsal root ganglion (Brown, 1975, Schoultz and Swett, 1972).

Golgi tendon organs contain bundles of collagen fibres that connect small fascicles of muscle to the whole muscle tendon or aponeurosis (Schoultz and Swett, 1972). Golgi tendon organs thus form an 'in series' alignment within the musculo-tendinous border. The innervation of a Golgi tendon organ is by an individual large diameter group Ib muscle afferent, that enters the capsule near the equator of the receptive ending (Jami, 1992). The Ib afferent then bifurcates, one branch projects proximally (towards the muscle) and the other distally. These main branches further divide into smaller collaterals that intertwine between the collagen fibres (Nitatori, 1988, Schoultz and Swett, 1974). The collagen within the Golgi tendon organs capsule is distributed unsymmetrically with two types of collagen packaging. Firstly, there is the collagen fibres that border the capsule, these are packed closely together and run in parallel. while the collagen bundles occupying the capsule lumen, are densely pack at either end, but become looser as they approach the centre. These 'loose' collagen fibre therefore does not run in parallel, but form a complex network. It is this collagen network that is directly innervated by the Golgi tendon organ ending that entwines its branches around the individual collagen fibres (Schoultz and Swett, 1974).

Golgi tendon organs are biological force transducers, converting tensile forces between muscle fibres and tendons, into a train of action potentials in Ib afferent fibres (Houk and Henneman, 1967b). Upon the activation of a motor unit, the muscle fibre within the Golgi tendon organs capsule straightens some of the complex network of loose collagen fibres. This straightening of the collagen fibres compresses and depolarises the pressure-sensitive afferent ending (Fukami and Wilkinson, 1977).

Throughout the literature, many idiosyncrasies in Golgi tendon organ afferent behaviour have been reported (Mileusnic and Loeb, 2006). For example, after a sudden step activation of muscle units, Golgi tendon organs generate a burst of action potentials (dynamic) in response, which then gradually decays to constant firing rate (static/tonic) as a result of damping and dependency on force generation. Golgi tendon organs' dynamic response during motor unit activation decreases after prior activation of the same motor unit (self-adaptation) or from other motor units (cross-adaptation) (Gregory et al., 1985, Gregory and Proske, 1979). And lastly, Golgi tendon organs demonstrate non-linear summation, when multiple muscles are activated (Gregory and Proske, 1979). Exactly how these different behaviours occur is unknown, but two mathematical models of Golgi tendon organ activity have been created which emulate these physiological behaviours (Houk and Henneman, 1967b, Mileusnic and Loeb, 2006). These models have been used to predict the relationships between Golgi tendon organ recruitment, forces and overall Golgi tendon organ activity under various normal, pathological and therapeutic conditions (Houk and Henneman, 1967a, Loeb and Mileusnic, 2016, Mileusnic and Loeb, 2006).

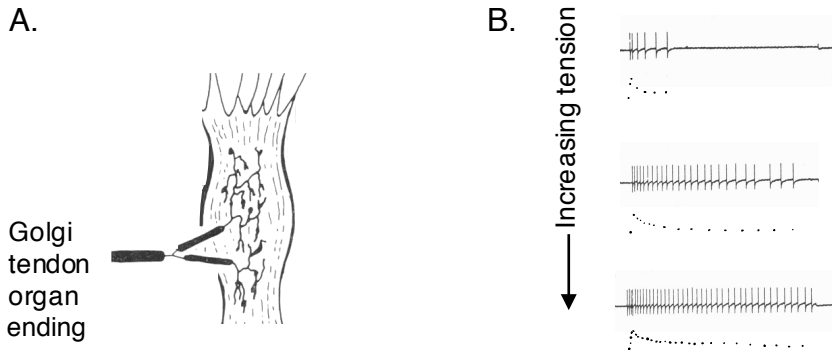

Figure 1.3. Neuroanatomical illustration and physiological response of Group Ib muscle afferents.
A. An illustration based on observations of group Ib Golgi tendon organ ending impregnated by the modified de Castro method, demonstrating their encapsulated endings in series alignment with the musculo-tendinous boarder (Modified Figure From: (Stacey, 1969)).**B.** The firing pattern of a single activated Golgi tendon organ; increasing tension (ramp portion) results in increased firing (Modified Figure From: (Fukami and Wilkinson, 1977)).

Group III and IV

The morphology of group III and IV afferent endings have not been as extensively investigated as those of group I and II afferents. Group III and IV afferents have low conduction velocities of 2.5-30 m/s and 0.5-2.5 m/s respectively (Erlanger and Gasser, 1930, Lloyd, 1943b), **see Table 1.1**. Group III fibres are described as thinly myelinated, whereas group IV fibres are unmyelinated. Group III fibres mostly correspond to the cutaneous Aδ fibres, and group IV to C-fibres (Lloyd, 1943b).

The first comprehensive report on the morphology of sensory endings within skeletal muscle was published by Stacey (1969); his study focused on group III and IV fibres, which were reported to comprise ‘free nerve endings’. Free nerve ending, have no corpuscular structures in light microscopy (Stacey, 1969, Mense and Gerwin, 2010). Free nerve endings of group III and IV afferents were visualised in skeletal muscle

connective tissue, between muscle fibres and in the adventitia of arteries and veins (Stacey, 1969). Group III afferents have been described to also supply Pacinian corpuscles in connective tissue near muscles. Using electron microscopy, Düring and Andres (1990) reported group III and IV endings, located in the epineurium of larger or smaller nerve bundles, in the adventitia of veins and arteries and within the connective tissue; perimysium proper (von Düring and Andres, 1990). Immunohistochemical studies for calcitonin gene-related peptide (CGRP) and Substance – P (SP) have reported small diameter fibres within the skeletal muscle surrounding the same structures (Tamura et al., 1996, Tsukagoshi et al., 2002, Tsukagoshi et al., 2006).Early experiments reported that activation of some small afferent fibres was associated with muscle pain (Weddell and Harpman, 1940). Since then, the role of small diameter group III and IV afferents to detect a range of stimuli and to mediate pain has been investigated. Further support has been provided that small diameter fibres are responsible for pain sensations (Abrahams, 1986) through an array of functional studies.

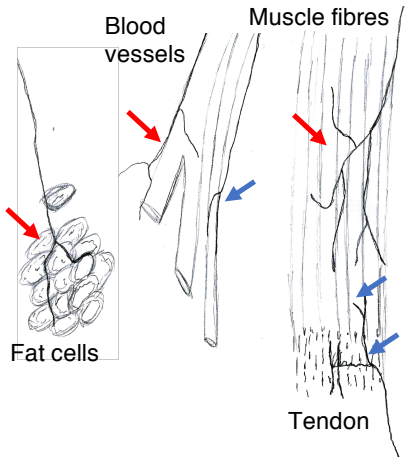

Figure 1.4. Neuroanatomical illustration of the location of Group III and Group IV muscle afferents.
An illustration based on observations of group III and IV muscle afferent endings impregnated by the modified de Castro method. Group III (blue arrows) and IV (red arrows) were found to terminate in and around arteries, fat cells, muscle fibres, and along the musculo-tendinous boarder (Modified Figure From:(Stacey, 1969).

Many functional studies have been carried out on both group III and IV fibres to define their functional properties during inflammation and pain behaviours (Jankowski et al., 2013). Paintal (1960) was one of the first to investigate the discharge properties of group III afferents and demonstrated that some could be activated by pressure applied via a smooth glass rod to the hind limb muscle in cats (Paintal, 1960). Other studies focussed on more physiological properties. Around 40% of group III and group IV fibres do not exhibit spontaneous firing at rest, and have low-threshold mechanosensitivity (LTM), in the innocuous range, and can be activated by non-painful deformation of muscle tissue. They are assumed to be non-nociceptive, and may detect work of the muscle and are likely to be group III afferents (often referred to as "ergoreceptors"). The other 60% of group III fibres and group IV were described as having nociceptive properties resembling mechano-nociceptors in the skin. (Djouhri and Lawson, 2004, Lawson, 2002, Lawson, 1992) These were characterised by: high-threshold mechanosensitivity, and discharges elicited by noxious mechanical stimuli. Their discharge often outlasted the duration of the stimulus, with a pronounced after-discharge, lasting from a few seconds to several minutes. The mechanisms underlying the after-discharge are currently unknown. Afferents that have these properties were more likely to be group IV (Ellrich and Makowska, 2007, Hoheisel et al., 2004, Hoheisel et al., 2005, Kaufman et al., 2002, Reinöhl et al., 2003). Discharge properties of group III and IV fibres from a number of studies are summarised in **Table 1.2.**

It also needs to be noted that afferents having conduction velocities within the range of group II range have also been described as having nociceptive properties (Djouhri and Lawson, 2004)

Table 1.2. Discharge properties of group III and group IV muscle afferents

	Discharge Property	References
Group III	Mostly consists of Low-Threshold Mechanosensitive (LTM) receptors	(Hoheisel et al., 2005, Mense, 1993, Mense and Gerwin, 2010)1}
	Small proportion of High-Threshold Mechanosensitive (HTM) receptors	(Hoheisel et al., 2005, Mense, 1993, Mense and Gerwin, 2010)1}
	That about half respond to either intermittent tetanic or maintained static contraction	(Kaufman et al., 2002, Kaufman and Rybicki, 1987, Kaufman et al., 1983, Mense and Stahnke, 1983, Paintal, 1960)
	About half respond to intra-arterial injection of bradykinin	(Kaufman et al., 1982, Mense, 1981, Mense, 1997, Mense, 2009, Mense and Schmidt, 1974)7
	Respond to non-noxious punctate pressure	(Jankowski et al., 2013, Kaufman et al., 2002, Kestell et al., 2015, Martin et al., 2009, Mense, 1996)
	Believed to be polymodal i.e. respond to both mechanical and chemical stimuli	(Kumazawa and Mizumura, 1977, Mense, 1996)
	Respond vigorously at the onset of tetanic contraction, first impulse within 200 milliseconds of the contraction	(Kaufman et al., 1983)
	Increase their response to tetanic contractions as peak tension in muscle increases	(Kaufman et al., 1983, Mense and Stahnke, 1983)
	Decrease discharge rate during a static contraction, as muscle fatigues	(Hayes et al., 2005) (Kaufman et al., 1983, Mense and Stahnke, 1983)
	Capable of synchronising their discharge with a constantly oscillating stimulus e.g. 5 Hz twitch stimulus	(Kaufman et al., 1984, Ross et al., 2014)
	Gadolinium attenuates mechanical sensitivity	(Hayes and Kaufman, 2001, Hayes et al., 2009)}
	Stimulated by metabolic substances such as: Adenosine tri-phosphate, lactate, changes in pH	(Diehl et al., 1993, Ellrich and Makowska, 2007, Fock and Mense, 1976, Hoheisel et al., 2004, Hoheisel et al., 2005, Mense, 1981)
Group IV	Display a latency to contraction of 5-30s	(Kaufman et al., 1983, Kaufman et al., 1984, Mense and Stahnke, 1983)
	Response to dynamic exercise not attenuated by gadolinium	(Hayes and Kaufman, 2001, Hayes et al., 2009)}
	Response to contraction in ischemic conductions increase by half	(Kaufman et al., 1983)
	60% of Group IV mechanosentive are HTM	(Kniffki et al., 1978, Mense, 1993, Mense, 2009, Mense and Gerwin, 2010, Rotto and Kaufman, 1988)
	Less sensitive to mechanical stimuli, requiring noxious stimulus	(Diehl et al., 1993, Ellrich and Makowska, 2007, Fock and Mense, 1976, Hoheisel et al., 2004, Hoheisel et al., 2005, Mense, 1981)
	Stimulated by metabolic substances such as: Adenosine tri-phosphate, Lactate and changes in pH	(Diehl et al., 1993, Ellrich and Makowska, 2007, Fock and Mense, 1976, Hoheisel et al., 2004, Hoheisel et al., 2005, Mense, 1981)

Many group III and group IV muscle afferents are polymodal (Kaufman et al., 1982). Polymodal Group III and group IV afferents respond to various combinations of: mechanical distortion with mechanical probes, changes in length (strain), changes in tension, and compression of the muscle (Abrahams, 1986, Diehl et al., 1993, Hoheisel et al., 2004, Mense and Meyer, 1985), chemical stimuli (i.e. accumulation of CO_2, lactate, adenosine triphosphate (ATP))(Jankowski et al., 2013), inflammatory mediators (i.e. prostaglandins, interleukins (IL-6), nerve growth factor) (Ellrich and Makowska, 2007, Hoheisel et al., 2005), thermal stimulation (28°C, 35°C & 42°C) (Mense and Meyer, 1985) and circulatory responses (Haouzi et al., 2004, Haouzi et al., 1999). These afferents express receptors for substances known to be involved in pain transduction (Mense and Gerwin, 2010), including receptors for bradykinin, serotonin, pH-sensitive ion channels (ASICs), adenosine triphosphate (ATP), nerve growth factor, and glutamate - all of which are algogenic and for capsaicin, the agonist of TRPv1 channels (Fock and Mense, 1976 , Franz and Mense, 1975, Mense, 1981, Kaufman et al., 1982, Hoheisel et al., 2004, Mense, 2009).

Group III and IV Spinal Cord Projections

Centrally, Group III and group IV muscles afferents project to both spinal and supraspinal levels (Laurin et al., 2015). Group III and IV afferents synapse in the dorsal horn of the spinal cord, specifically in laminae I, II IV and V (Murphy et al., 2011, Laurin et al., 2015, Mense and Craig Jr). Jankowski et al (2013) functionally characterised group III and group IV muscle afferents then intracellularly filled them with neurobiotin to determine their central projections. They demonstrated that out of the 12 cells they labelled, 2 were group III, and 10 were group IV afferents. The two group III muscle afferents had central projections located in laminae I and II, and had additional pronounced projections to laminae IV-V. One was activated by cold and the other responded to a mixture of metabolites. Group IV afferents' central projections were almost exclusively limited to laminae I and II. Their

projections only extended over one segment of the spinal cord immediately rostro-caudal to the point of entry into the spinal cord. There were no obvious differences in projection patterns between the functional classes of group IV afferents; 1 responded to no stimuli, 6 were activated by a high concentration metabolite mix and 3 were activated by a low concentration metabolite mix) (Jankowski et al., 2013).

In addition to synapses onto spinal interneurons, central terminals of group III and group IV muscle afferents were associated with large diameter afferents endings (Group Ia afferents) (#Torne Della et al 1996) and may directly synapse onto alpha-motorneurons (Gandevia, 2001, Kniffki et al., 1981, Weavil et al., 2015).

Group III and IV morphology and function

Previous studies have characterised some of the functional features of group III and group IV afferents, but many of their anatomical and physiological properties are still poorly defined (Jankowski et al., 2013). Hinsey (1927) was unable to establish the connectivity between parent nerve trunks and their endings, due to the exclusive use of sectioned material. Sections do not allow the visualisation of the whole nerve fibre at the same time as its terminal branching patterns (Hinsey, 1927).

Dye fills of cell bodies of functionally identified group III/IV muscle afferents after intracellular recordings have been correlated with the neurochemical coding e.g. TRPV1 immunoreactivity (Hoheisel et al., 2004, Jankowski et al., 2013). These studies provide a wealth of information regarding the size and chemical coding of cell bodies, but much less information regarding the endings within target tissues; the morphology and location of their endings largely remains unknown. Surprisingly; unlike viscera and skin, whole-mount dye filled and immunohistochemical preparations have not been extensively used to study

muscle afferent ending. This is likely to be due to the thickness of most muscles and the relative opacity which makes it difficult to trace axons reliably. This maybe one of the reasons why it is not possible to correlate the morphological and functional characteristics of group III and IV nerve endings within skeletal muscle (Hinsey, 1927).

Innervation of tendon

Much of the literature devoted to the innervation of tendons by group III and IV fibres has concentrated on the Achilles tendon. This tendon is poorly innervated; the majority of the nerve fibres are located at the muscle-tendon border, within the connective tissue surrounding the tendon itself, or in connective tissue between the fascicles (Benjamin et al., 2008). Immunolabelling has shown that there is actually a mix of autonomic and sensory fibres in these locations. To determine the presence of autonomic fibres within the tendon, neurochemical markers neuropeptide Y, noradrenaline, tyrosine hydroxylase was used to visualise sympathetic nerve fibres. Similarly, vasoactive intestinal peptide was used to visualise parasympathetic nerve fibres. Overall, autonomic nerve fibres were associated with blood vessels and the majority were sympathetic, although there was a significant population that was parasympathetic (Ackermann et al., 2001).

Four major classes of sensory endings have been described in tendons. These include Ruffini's endings, Pacinian corpuscles, Golgi tendon organs, and free nerve endings. Ruffini endings and Pacinian corpuscles have been located at the proximal end of the tendon close to where the muscle and tendon meet. They occurred singly or in groups of 2-3 (Zaffagnini et al., 2003) and their axons entered the tendon from the muscle end. Ruffini endings had a "flower spray" receptor ending of varying complexities. Golgi tendon organs, as previously described, measure the tension of the muscle, and are arranged in series with the extrafusal muscle fibres, usually located at the transition between the skeletal muscle and the tendon.

The receptive endings are interwoven between the collagen fibre bundles of the tendon (Benjamin et al., 2004). Free nerve endings arose from both myelinated and non- myelinated small diameter fibres, and are found throughout the connective tissue that surrounds the tendon, and around the tendon bundles (#Stilwell 1957 and Andres 1985). Many free nerve endings in tendons branch in the connective tissue layers, or are associated with arteries, veins and lymphatics (Andres et al., 1985, Stilwell, 1957).

It interesting to note that the innervation of the tendon, (in particular that of the sensory innervation) is concentrated near the transition zone between muscle and tendon. Benjamin (2008) speculates that the absence of nerve fibres in the body of the tendon is associated with the heavy loading to which the tendon is subjected which might damage delicate unprotected nerve endings(Benjamin et al., 2008).

Innervation of fascia

The fascia has largely been considered as an amorphous layer of collagen rich tissue whose function is inert structural support and organ containment (Stecco et al., 2007). Combined electron microscopy and staining procedures have demonstrated sensory nerve fibres in many regions of fascia. It has been suggested that the fascia contributes to functions such as proprioception, nociception and may be responsive to pressure, temperature or vibration (Stecco et al., 2007, Tesarz et al., 2013). Fascia of the upper and lower limbs, and the thoracolumbar region, have similar types of sensory nerve endings. Combinations of 3,3-diaminobezidine (DAB) (Stecco et al., 2007, Willard et al., 2012), haemotoxylin and eosin (H&E) and Azan-Mallory (Stecco et al., 2018) staining of human fascia have been used to describe the innervation of sensory nerve endings. Described endings include small diameter nerve fibres that terminate as free nerve endings (likely involved in pain). These are numerous, and often associated with blood vessels. The other major types of endings are

encapsulated. These include Ruffini-like endings, Golgi-Mazzoni-like endings and Pacinian corpuscles.

Pacinian corpuscles have an ovoid structure with a central core surrounded by multiple layers of laminar structures. The lamellae are what gives the sectioned corpuscle an appearance of an opened onion. Golgi-Mazzoni's endings are similar elongated corpuscles, of an irregular shape, that are smaller in diameter and have fewer internal laminae, compared to Pacinian corpuscles. Ruffini's endings resemble balls of fine twisted nerve fibres, or flower spray endings. They have extensive arborisation surrounded by a delicate capsule. Understanding the innervation, structure, and function of fascia is important in its own right. In addition, fascia may hold some of the keys for understanding other mechanisms such as muscle action and musculoskeletal pain (Stecco et al., 2007, Stecco et al., 2018, Willard et al., 2012).

Reflexes involving skeletal muscle sensory fibres

As described in detail above muscle spindles detect changes in muscle length and Golgi tendon organs detect changes in muscle tension. Muscle spindles and Golgi tendon organs are examples of proprioceptors. These receptors are a part of the somatic sensory system, in which we are aware of the position and/or movements of our bodies and limbs, also called proprioception. How muscle spindles and Golgi tendon organs play a role in proprioception is described below.

Stretch (Myotatic) Reflex

The stretch reflex (myotatic reflex) was first described by Liddel and Sherrington (1924), when they demonstrated that rapidly stretching a muscle evoked a sudden contraction, which tends to restore the muscle to its former length. This was shown to be a neural reflex as it

required afferent signals from the muscle to the spinal cord (Liddell and Sherrington, 1924). Since then it has been shown that the sensory fibre responsible, make direct connections with motor neurons of the same muscle, forming monosynaptic reflex circuit (Lloyd, 1943b, Merton, 1951). The afferent receptors involved in this case are muscle spindles, group Ia fibres. Muscle spindles are located within the belly of the muscle. When the muscle is stretched, the receptors themselves are also stretched, generating firing at an increased rate. In the spinal cord, the sensory axon forms monosynaptic excitatory connections with the α motor neuron that innervates the same muscle (De Nó, 1935). This results in a rapid contraction of the stretched muscle, which restores the muscle to its former length, thereby acting as a negative feedback loop (Houk and Henneman, 1967a)

Golgi tendon organ reflex (inverse myotatic reflex)

Golgi tendon organs also play an important role in the regulation of motor activity and have been extensively studied, for more detailed reviews see (Houk and Henneman, 1967a, Jami, 1992). When a muscle contracts, the force acts directly via the tendon, leading to an increase in the tension of the collagen fibrils and compression of the intertwined Golgi tendon organ axons as described above. Centrally, the Ib axons from Golgi tendon organs contact inhibitory interneurons which synapse with alpha-motor neurons that innervate the same muscle, thereby creating a negative feedback loop that regulates maximal muscle tension (Houk and Henneman, 1967a). This reflex circuit is also active at sub-maximal levels of force. Under these conditions it tends to counteract the small changes in muscle tension caused fluctuations in firing of the alpha-motor neurons (Houk and Henneman, 1967b). Thus, Golgi tendon organs tend to maintain a steady level of force within the muscle. This reflex is not a closed loop as the Ib inhibitory interneurons receive inputs from a variety of other sources (cutaneous receptors, joint receptors and descending motor neuron pathways) which modulate the responsiveness of Ib activity to muscle tension (Jami, 1992).

Unlike the reflexes described above the axon reflex occurs within the muscle, and describes how the activation of the afferent ending can have multiple influences.

The Axon reflex

Some nociceptors may release neuropeptides from their peripheral endings and these may influence nearby cells (Haouzi et al., 2004, Haouzi et al., 1999, Mense, 1977, Mense, 1993). This is the basis of an axon reflex in which a nociceptive ending in the connective tissue gives rise to an axon collateral on a blood vessel; usually an artery or arteriole. If the afferent ending in the connective tissue is activated by a noxious stimulus, action potentials propagating centrally also invade the perivascular branch, causing the release of neuropeptides CGRP and SP onto the arteriole. These can then cause vasodilation and/or plasma extravasation (Brain et al., 1985). This whole process forms an axon reflex and contributes to neurogenic inflammation. This type of response activated in the skin is also referred to as the 'Triple response' (Bruce, 1913, Lewis, 1926).

Skeletal muscle in exercise

Neural control of cardiovascular responses to exercise

In the early 1900s it was shown that during different kinds of exercise of varying degrees of intensity, there was an increase in cardiovascular and respiratory activity (Bowen, 1904). Strenuous exercise increases arterial pressure, heart rate, and ventilation (Kaufman et al., 2002). The mechanisms, which cause these responses, are still not fully understood, but two theories that have been suggested to underlie these increases in cardiovascular and respiratory activity. The first is the 'central command theory', it suggests that increased cardiovascular and respiratory responses may be due to the action of the motor cortex or subthalamus on the medullary and spinal neuron pools that control ventilation and cardiovascular function. The second proposed mechanism is that a metabo-reflex originates

from sensory neurons (ergoreceptors) innervating the exercising skeletal muscle itself. These two theories are not mutually exclusive (Kaufman et al., 2002). These two mechanisms; central command and the exercise pressor reflex are not the only cardiovascular and respiratory adjustments to exercise. The arterial baroreflex is also involved in the regulation of blood pressure especially during exercise. Mitchell (1990) estimated the contributions of the central command, exercise pressor reflex and the arterial baroreflex components to the adaptation to exercise. They showed that the various contributions depended on the type of exercise (static or dynamic), the intensity of the exercise, the time after onset (immediate, steady state and exhaustive) and the ability of blood flow to meet the metabolic needs of the contracting muscles (Mitchell, 1990). Together, they are responsible for these reflex adjustments, through complex interactions controlling the cardiovascular and hemodynamic changes in an intensity dependent manner (Fadel, 2015).

Central Command Theory

Central command, originally termed 'cortical irradiation' (Krogh and Lindhard, 1913), is a concept that involves descending neural signals from higher brain centres capable of influencing cardiovascular responses during exercise (Krogh and Lindhard, 1913, Williamson, 2010). Central command is typically defined as 'a feedforward mechanism involving the parallel activation of motor and cardiovascular centres' (Goodwin et al., 1972). Central command has been extensively studied and is widely accepted (Williamson et al., 2006). The neural control of circulation during exercise is a complex phenomenon involving many sites within the central nervous system (Williamson, 2010, Williamson et al., 2006). The hypothesis that central signals drive respiratory and autonomic cardiovascular responses to exercise was established and supported by early observations that heart rate increased at the onset of exercise. Krogh and Lindhard (1913) measured the changes in heart rate, blood flow, and respiratory changes that took place in the first few minutes of light and heavy

exercise, of human subjects, while they carried out cycling exercises on a bicycle ergometer at varying difficulties. It was determined that this response was too rapid to be explained by a reflex mechanism driven by changes in the contracting muscles (Krogh and Lindhard, 1913, Gasser and Meek, 1914).

Several of the pivotal studies investigating the role of central command theory, used passive cycling (Williamson et al., 1995) and partial motor paralysis (neuromuscular blockade) to alter the level of central command influence. These studies demonstrated that the initial increases in heart rate in response to voluntary contractions was not affected by the neuromuscular blockade, thereby demonstrating that the resultant response (increase in heart rate) was not related to a feedback mechanism from the contracting muscle alone (Iwamoto et al., 1987, Secher, 1985). It is now widely accepted that this initial increase in heart rate, is due to descending central inputs (Fisher, 2015).

Due to the complexity of the central command system, the identification of specific central pathways responsible for evoking autonomic adjustments remains elusive (Fisher et al., 2015). However, numerous animal studies have identified putative sites using direct electrical or chemical stimulation of neural structures. These include: the sub-thalamic Fields of Forel and motor cortex, insular cortex, mesencephalic and subthalamic regions, capable of generating both motor and cardiovascular responses (Eldridge et al., 1985, Waldrop et al., 1986, Bandler and Carrive, 1988, Fisher et al., 2015).

Advances in neuroimaging have provided opportunity for translating these finds to humans. The insular and anterior cingulate cortices have been suggested as regions that are activated by the central command during exercise. Electrical stimulation of midbrain areas during neurosurgery (deep brain stimulation) has enhanced our understanding (Green et al., 2005,

Basnayake et al., 2010, Abrahams et al., 1960)The thalamus, periadqueductal grey, subthalamic nucleus, periventricular grey, substania nigra, may all be involved in mediating the centrally generated cardiovascular response to exercise (Fisher et al., 2015).

Central Command has been viewed as contributing to the increase in heart rate at the onset of exercise (Fisher, 2014, Krogh and Lindhard, 1913). It has now been shown that an individual's perception of effort contributes to the magnitude of central command during exercise, independent of the actual force produced (Fisher et al., 2015). Ratings of perceived exertion (Borg, 1973) have been widely used to assess the magnitude of central command; how these signals modify perceived exertion and its influence on central command has not been clearly defined (Williamson, 2010, Williamson et al., 2006).

Exercise Pressor Reflex

The exercise pressor reflex gives rise to increases in cardiovascular and respiratory function during exercise. Alam and Smirk (1937) were among the first to provide experimental evidence that a reflex was responsible for these physiological responses to exercise. During the study participants carried out rhythmic forearm and calf contractions. They first carried out the exercises under patent conditions. Secondly, the exercises were done with circulation to the limb occluded, so that it was ischemic during and for some time after exercise. The occlusion trapped exercise-induced metabolites within the previously active muscle. It was reported that exercise increases blood pressure, and that this persists even when the circulation to the active muscle had been interrupted. Furthermore, occlusion prolonged the increase in blood pressure after exercise had stopped. The maintained rise in blood pressure was suggested to be due to the retention of metabolic products within the muscle created by the exercise. Once these products were cleared, blood pressure returned to its normal level. Because of the change in blood pressure after the arrest of circulation, it was proposed by

default to be due to a neural reflex (Alam and Smirk, 1937). Support for this hypothesis was provided by later human and animal studies (Coote et al., 1971, Kaufman et al., 1988, McCloskey and Mitchell, 1972).

Coote et al (1971) described an increase in mean arterial pressure, heart rate and ventilation evoked by electrical stimulation of the ventral roots (L6-S1), which contracted skeletal muscle of the triceps surae. They also demonstrated that severing L6 – S1 dorsal roots abolished the responses to the electrically driven exercise, and that occluding the arterial supply evoked an even greater pressor response (Coote et al., 1971). To identify which sensory nerves were involved, nerve blocks on the dorsal roots were used. Firstly, an anodal block was applied with direct current, which blocked large diameter nerve fibres before small diameter fibres. Second, a local anaesthetic agent was applied which blocks small fibres before larger fibres. Anodal block, had little effect on cardiovascular and respiratory activity evoked by exercise. When a local anaesthetic was applied to the dorsal roots (lignocaine 0.125%), the cardiovascular and respiratory responses to exercise were rapidly abolished (McCloskey and Mitchell, 1972). When the anaesthetic was washed out, responses returned. These results suggest that larger nerve fibres (group I and II) had relatively little contribution to the pressor reflex whereas; the smaller diameter axons (group III and IV) played an important role. From this report and other similar studies (Kaufman et al., 1984, McCloskey and Mitchell, 1972, Tibes, 1977, White, 2014), it has become clear that group III and IV muscle afferents form the afferent arm of the exercise pressor reflex.

The discharge properties of group III and group IV afferent have been investigated in some detail. Hayes et al (2009) used gadolinium, a lanthanide, to block mechano-gated ion channels, showing that it blocked the response of group III afferents to static contraction and tendon stretch, but did not affect group IV afferents to these stimuli (Hayes et al., 2009,

Kaufman, 2012). Circulatory occlusion during muscle contraction, was used to determine the response of group III and IV afferents to metabolic products (Kaufman et al., 1984, Iwamoto et al., 1985). This study suggested that group III afferents were predominantly mechanosensitive, while group IV afferents were predominantly metabosensitive. Overall, in this study 50% of group IV afferents increased firing to metabolic products produced from working muscles, compared to 12% of group III afferents.

The specific central pathways activated by muscle afferents to evoke the exercise pressor reflex, currently remain unknown. However, activation has been detected in areas in the brainstem related to cardiovascular control such as the nucleus tractus solitarius (NTS), rostral ventral medulla and caudal ventral medulla (Dampney, 2016, Drew, 2017, Michelini et al., 2015, Murphy et al., 2011).

Arterial Baroreflex

The arterial baroreflex, is a feedback mechanism that normally regulates blood pressure within narrow limits. It coordinates the appropriate response to different stressors, including exercise, to maintain an adequate blood pressure (Drew, 2017). The receptive endings involved in the arterial baroreflex are un-encapsulated free nerve endings, located at the medial adventitial border of arteries in the carotid-bifurcation and aortic arch (Coote and Dodds, 1976).

Alterations in blood pressure cause conformational changes in the baroreceptive endings, leading to changes in afferent firing; when blood pressure increases, firing increases. This results in an increase in parasympathetic nerve activity (causing temporary bradycardia) and a decrease in sympathetic nerve activity (slowing heart rate and decreasing stroke volume). Autonomic adjustments result in appropriate increased venous capacitance, reduced cardiac

output and lowered total peripheral resistance to promptly correct pressure changes (Fisher et al., 2015, Michelini et al., 2015). It has been shown in animals (Coote and Dodds, 1976, Walgenbach and Donald, 1983) and healthy subjects (Fadel et al., 2001) that during exercise the arterial baroreflex continues to regulate blood pressure, but with an elevated set-point. In human studies, neck cuffs have been extensively used to allow pressure changes to be applied directly to the carotid sinus at rest and during cycling exercises (Papelier et al., 1994). These studies have shown that the carotid sinus pressure and systematic blood pressure have a linear relationship and that during exercise the response curve is increased with increasing exercise intensity.

These three mechanisms of neural control (central command, afferent feedback from muscles and baroreflexes) during exercise are not mutually exclusive. They work in concert with some overlap and redundancy (Drew, 2017, Mitchell, 2017). The extent and nature of the interactions between these mechanisms needs further investigation.

Exercise induced skeletal muscle vasodilation

At the onset of muscular contraction, there is a rapid vasodilation in active skeletal muscle; usually coinciding with an increase in blood pressure. However, on occasions there may be a decrease in blood pressure, or no change, depending on the exercise modality and intensity (Fisher et al., 2015). A local vasodilation allows an increase in blood flow to the muscle and thus may help meet the oxygen and metabolic demands driven by the contractile machinery. The cause of this rapid vasodilation remains unresolved and has been attributed to a number of factors; these include the muscle acting as a pump so that the contractions of the muscle forces venous blood out of the muscle (Saito et al., 1993). It is also believed that metabolic factors released from working muscles have local vasodilatory properties (including potassium ions, adenosine, carbon dioxide/H^+, lactate, and nitric oxide) that diffuse to

arterioles to elicit changes in vasomotor tone. Interestingly, there is little support for any single vasodilator being essential for this process; it appears to require a mixture of factors (Clifford and Hellsten, 2004). Thirdly, local withdrawal of sympathetic vasoconstriction may also contribute. The peripheral vasoconstriction during high intensity whole body exercise is important to redistribute cardiac output away from inactive muscles and splanchnic tissues, and towards the active skeletal muscle. However, in the active muscle, there is a 'blunting' of the vasoconstrictor response in order to ensure adequate oxygen delivery. The concept of a sympathetically mediated vasodilatory mechanism has not been confirmed to date (Hearon Jr and Dinenno, 2016).

This project was largely carried out on abdominal muscles because their thinness made them suitable for detailed morphological studies. Nevertheless, these muscles are involved in a variety of both active behaviours and postural adjustments and may be subject to similar sensory demands as other major muscle groups. For this reason, it is valuable to give an account of abdominal muscles and their roles in posture and movement.

Abdominal muscles

The abdominal wall is composed of four muscles, the rectus abdominis, external and internal obliques, and the transversus abdominis. The abdominal muscles generate force to produce movement of the spinal column (Brown et al., 2010, Masani et al., 2009). They are involved in multiple movements including trunk flexion, lateral bending, creating torque and twisting of the spine (McGill and Norman, 1986, Arjmand et al., 2008). They can increase intra-abdominal pressure for coughing, defecation, vomiting and parturition (Cholewicki et al., 1999). The forces created by the abdominal muscles also play a significant role in stability of the trunk (Reeves et al., 2007), during functional tasks involving the limbs such as

running, jumping and lifting, (Urquhart et al., 2005) and other movements of the trunk (Knežević and Mirkov, 2013).

Anatomy of the abdominal wall

The most superficial layer of muscle is the external oblique. The external oblique attach to the iliac crest, the pubic tuberale, and the linea alba (Gilroy et al., 2012). Its apponeurosis extends medially over the rectus abdominis and the internal oblique where it attaches to the linea alba in the mid line. The body of muscle runs obliquely, following an inferiomedial direction (Urquhart et al., 2005). The main functions of the external oblique are to pull the thorax inferiorly, compress the abdominal cavity, assist in contralateral axial rotation, and ipsilateral side bending of the trunk (Brown et al., 2010, Gilroy et al., 2012). The external oblique is innervated via the anterior rami of the lower 6 thoracic spinal nerves T7-T12.

The internal oblique is the next muscle, deep to the external oblique. The internal oblique insert onto the 10^{th} and 12^{th} rib, iliac crest and the linea alba. It also wraps around the torso and attaches to the thoracolumbar fascia. The muscle fibres of the internal oblique are aligned superiomedially, inferiomedially from the iliac crest across the torso to the linea alba (Gilroy et al., 2012, Urquhart et al., 2005). The internal oblique acts in some ways as an antagonist to the diaphragm, reducing the volume of the thoracic cavity during forced expiration(Brown et al., 2010). It also flexes the trunk, helps with ipsilateral rotation, and side bending of the trunk (Brown et al., 2010, Brown et al., 2012, Brown et al., 2011).The thoracic spinal nerves T7-T12, L1 and the iliohypogastric and ilioinguinal nerves, innervate the internal oblique.

The rectus abdominis muscle (the six-pack muscles) has attachments to the sternum and pubis and is positioned ventrally both sides of the midline, bisected by the linea alba. It

contains several tendinous insertions throughout the belly of the muscle and is located deep to the internal and external tendons. The muscle fibres of the rectus abdominis run superiorly along the abdomen and terminate at the symphysis pubis and the xiphoid process. This muscle is involved in compressing the contents of the thoracic cavity, flexing the vertebral column of the lumbar spine and tensing the abdominal wall. It is innervated by the intercostal T5 – T12 spinal nerves.

The transverses abdominis muscle is deep to the obliques, with fibres running horizontally toward the linea alba. It origins are at the 7^{th} to 12^{th} costal cartilage, thoracolumbar fascia and the iliac spine and it inserts into the linea alba and pubic crest. The transversus abdominis compresses the ribs and the abdominal cavity (Brown et al., 2010). It also provides both thoracic and pelvic stability (Hodge, 2003). The transversus abdominis is innervated by the intercostal T7 to T12 spinal nerves and L1, the iliohypogastric and ilioinguinal nerves (Gilroy et al., 2012).

Table 1.3. Abdominal wall muscles

Muscle name	Origin	Insertion	Innervation
Rectus abdominis	Crest of the pubis	Xiphoid process, costal cartilages 5th and 7th ribs	Intercostal T5-T12
External oblique	5th to 12th ribs	Linea alba, pubic tubercle, iliac crest	Intercostal T7-T12
Internal oblique	Thoracolumbar fascia (deep), iliac crest, iliac spine and iliopsoas fascia	10th and 12th ribs and linea alba	Intercostal T7-T12 iliohypogastri and ilioinguinal
Transversus abdominis	7th to 12th costal cartilage, thoracolumbar fascia iliac spine and iliopsoas fascia	Linea alba, pubic crest	Intercostal T7-T12 iliohypogastri and ilioinguinal

Modified from (Gilroy et al., 2012).

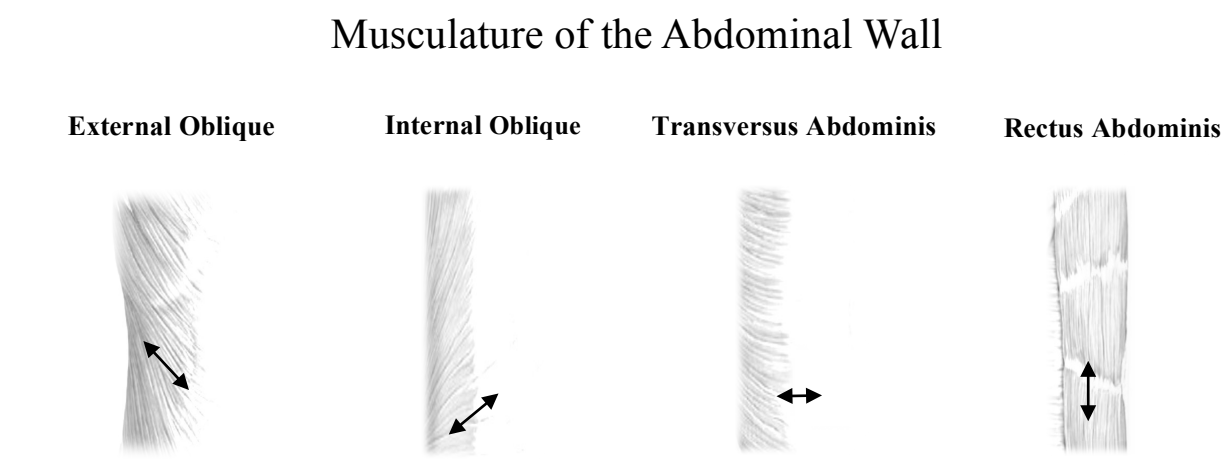

Figure 1.5. Abdominal wall musculature
The layers of the abdominal wall are shown running from superficial (starting left) to the deepest layer or rectus abdominis to the right. Each of muscle layer has its own directionality and insertion points described in **Table 1. 3.** A similar layout is present in the mouse: the subject of this study. Modified from (Gilroy et al., 2012)

The morphology, architecture, and how human utilise their abdominal muscles has been described in detail above. Cats, dogs, rats, and mice have all previously been used as animal models to investigate the innervation of skeletal muscles. One can compare bipedal animals such as humans to quadrupeds (animals listed above). The differences in posture, methods of locomotion, general size, and dimensions of fore and hind limbs are all areas in which may be specialised, depending on the species. Brown et al (2010) investigated the differences between human abdominal muscles and that of Sprague-Dawley rats. Architectural and morphological characteristics including force-generation (physiological cross-sectional area of the muscle) and excursion (fascicle length), sarcomere lengths, relative muscle size and muscle fibre orientation were all compared. Based on these characteristics, rat and human abdominal muscles were all quite similar. These results may not be surprising, humans are bipedal, but are not always upright. We have the ability to bend (pick up a box off the ground), reach (getting something off the top shelf) and get on

all fours. One of the major morphological difference between the species was in the lower region of the abdominal musculature. The external oblique in humans becomes aponeurotic around the level of the superior iliac spine, while in rats the external oblique muscle continues to the pelvic insertion (Brown et al, 2010). How these similarities and differences reflect the functional requirements of humans and rats needs to be discussed. Listed above (page 67) are the ways that the abdominal muscles are utilised in humans. The abdominal muscles in rats are also utilised during the expiration phase of ventilation, during locomotion. In addition, rats use a combination of their external obliques and internal obliques phasically, relating to the contralateral hind limb stance (Brown et al., 2010). The role of the human abdominal muscles in supporting the lumbar spine has also been described. Muscle mass, relative to size, is larger in rats compared to humans, which suggests that the abdominal muscles play a greater stabilising role. This may reflect their greater ability to twist and climb (Brown et al., 2010). Despite some differences in architectural and morphological properties, how the abdominal musculature are functionally used in rodents and humans is strikingly similar.

Clinical applications

At the onset of exercise there are highly co-ordinated cardiovascular, hemodynamic adjustments to meet the metabolic and oxygen needs of activated skeletal muscle (Fadel, 2015, Hearon Jr and Dinenno, 2016). Alterations in the sympathetic and parasympathetic nervous systems are responsible for many key cardiovascular responses to exercise, including: increased cardiac output, heart rate, skeletal muscle blood flow, and initial increase in blood pressure (Fisher et al., 2015).

Hypertension

Hypertension (or high blood pressure) is a common and sometimes preventable cardiovascular disease risk factor. Clinically it is defined by having a systolic blood pressure equal to or greater than 140 mmHg and a diastolic equal of greater to 90 mmHg, which occurs repeatedly over time. It increases the risk of developing coronary heart disease, peripheral artery disease, stroke, renal disease, and heart failure (Pescatello et al., 2015, Smith et al., 2006). In 2017-2018, 10.6 % of all Australians aged 18yrs and over (2.6 million people) had hypertension (Statistics, 2018). In the US, approximately 80 million Americans (33%) have hypertension and another 36% have pre-hypertension. Predictions indicate that by 2030 over 40% of adults in the US will be hypertensive and the total direct costs will triple from US$ 130.7 to US$389.9 billion (Pescatello et al., 2015).

Before exercise begins, individuals with hypertension already have elevated arterial blood pressure. They then typically show excessive increases in arterial blood pressure, heart rate and sympathetic efferent activity in response to exercise (Mitchell, 2017, Smith et al., 2006). These abnormal cardiovascular haemodynamics make the patient more prone to angina, acute myocardial infarction, cardiac arrest, and stroke during physical activity (Mitchell, 2017).

Smith et al (2006) used a spontaneously hypertensive rat model and demonstrated that the abnormal cardiovascular response to physical activity in hypertension is, in part, mediated by an overactive exercise pressor reflex. Using electrically induced static muscle contractions, spontaneously hypertensive rats showed a greater elevation in arterial blood pressure and heart rate than the control rats. The percent increase of blood pressure due the exercise pressor reflex was also increased. As cardiac output and systemic vascular resistance determine arterial pressure, the changes seen in response to muscle contraction seen in hypertensive rats were thought to be the result of increases in sympathetic vascular

resistance. Using ganglionic blockade with hexamethonium, they demonstrated that spontaneously hypertensive rats have elevated basal sympathetic drive. Further, using a sympathetic blockade with hexamethonium and phentolamine showed that the exaggerated pressor response in response to muscle contraction was completely abolished in hypertensive rats. These results are consistent with the exercise pressor reflex being overactive (Smith et al., 2006). The aetiology of the dysfunction of the exercise pressor reflex is currently unclear but may also involve a shift in the sensitivity of muscle metaboreceptors and mechanoreceptors (Murphy et al., 2011).

Heart Failure

Heart failure is typically as the result of a myocardial insult or exaggerated afterload (pumping blood against a heightened arterial pressure), both of which compromise myocardial performance and subsequent systemic haemodynamics (Poole et al., 2012). Patients with heart failure exhibit decreased cardiac output, chronically elevated sympathetic nerve activity and peripheral endothelial dysfunction. Additionally, in patients with heart failure, exercise evokes excessive increase in blood pressure, heart rate, sympathetic activity, and excessive hyperventilatory responses (Ives et al., 2016, Olson et al., 2010).

The exercise pressor reflex is exaggerated in heart failure patients. It is thought that this in due, in part, to muscle reflex abnormalities, including exaggerated afferent feedback (Garry, 2011). Amann et al (2014) has studied patients with heart failure who performed single leg knee extensions. These activated group III/IV muscle afferents. Intrathecal fentanyl was then applied to block ascending spinal pathways. The presence of fentanyl attenuated sympathetic outflow reflected by cardiac output, compared to trials without fentanyl. Thus, group III/IV afferents have strong effects in heart failure patients on the pressor response. The reduction of sympathetic outflow caused by i.t. fentanyl was also manifested as a

reduction in femoral artery vasoconstriction, which led to an increase in leg vascular conductance. The conclusion from this study was that activation of group III/IV afferents had exaggerated effects on sympathetic outflow in patients with heart failure (Amann et al., 2014). The exact driver for increased Group III/IV activation is not clear in heart failure patients, but evidence suggests that release and accumulation of H^+ ions in active muscle may be a major contributor (Scott Adam et al., 2003).

Peripheral artery disease

Peripheral artery disease (PAD) is a progressive narrowing of arteries predominantly supplying the lower limbs. This narrowing is caused by an accumulation of atherosclerotic plaques on arterial walls (Falk, 2006). PAD affects 8-12 million people in the US, and patients with PAD have an increased risk of myocardial infarction and stroke (Stone and Kaufman, 2015). Due to the accumulation of plaques there is a decrease in blood flow to the muscles, thereby reducing the muscles' ability to function during dynamic exercise. Concomitant changes in blood pressure are thought to be caused due, in part, to an exaggerated exercise pressor reflex. Due to their involvement in the exercise pressor reflex, group III/IV muscles afferents have been investigated to determine if they are involved in this exaggerated response (Stone and Kaufman, 2015). A rat femoral artery ligation model, replicating the impaired blood flow (seen in patients with peripheral artery disease), has shown that ASICS3 channels (Tsuchimochi et al., 2011), TRPV1 (Stone and Kaufman, 2015), and μ-opioid receptors (Harms et al., 2018, Tsuchimochi et al., 2010b) expressed on group III/IV muscle afferents, play a role in the exaggerated pressor response seen in patients with peripheral artery disease.

Muscle Fatigue

Muscle fatigue limits physical performance and other strenuous or prolonged activity, progressively reducing the muscles ability to produce force and/power during exercise.

There is accumulating evidence that group III/IV sensory fibres play a role in generating fatigue. Muscle fatigue can affect us during our daily life, for example when carrying a shopping bag or child. This type of muscle fatigue can be rectified by either swapping from one set of muscle to another (changing arms) or by periods of rest (placing the shopping or child on the ground) or reducing overall activity (Taylor et al., 2016). However, in many disorders, muscle fatigue restricts daily life. Such disorders include McArdle's disease (Lucia et al., 2008), myasthenia gravis (Hoffmann et al., 2016, Westerberg et al., 2018), chronic fatigue syndrome (Staud et al., 2015) and heart failure (Amann et al., 2015), but it is also associated with ageing and frailty, and after any period of forced inactivity or deconditioning. Fatigue can alter overt performance, such that the task is performed more slowly or clumsily or may even prevent it being performed successfully. Sensations that accompany muscle fatigue, such as muscle pain or discomfort, and perception of increased effort, also impact on quality of life (Taylor et al., 2016).

Muscle fatigue can be defined as the reduced performance during continuing exercise of a sufficient duration and intensity. Exercise-induced decrease in performance is caused by both peripheral and central components (Allen et al., 2008, Gandevia, 2001). 'Peripheral fatigue' encompasses biochemical changes within the contracting muscle leading to as attenuated force/power response to motor neuron input (i.e.: changes on excitation/contraction coupling). This may involve changes in membrane excitability, intracellular calcium release/ excitation contraction coupling or muscle metabolism (Fitts, 1994).'Central fatigue', refers to the decrease in force/ power secondary to a reduction in descending motor drive. In combination, these factors result in a decrease in the output from spinal motor neurons and thus voluntary muscle activation (Sidhu et al., 2014, Amann et al., 2015).

It is now known that muscle afferents (group III/IV) are involved in slowing the development of peripheral fatigue during exercise through the exercise pressor reflex. However, they also play an important driving role in the development of central fatigue. Group III and group IV afferents can modulate the development of central fatigue. In part, this occurs via their inhibitory effects on the output of spinal moto neurons which causes a reduction in muscle activation and thereby reduce performance during exercise (Amann et al., 2015, Weavil et al., 2015). These mechanisms are dealt with in more detail in Chapter 5

Chronic Fatigue

Chronic fatigue syndrome, also called "myalgic encephalomyelitis", is a complex disorder that is characterised by severe and prolonged mental and physical fatigue, not alleviated by rest, and which is exacerbated by exercise (Staud et al., 2015). Additional symptoms include sleep disturbance, musculoskeletal pain, attention and short-term memory impairments (Holgate et al., 2011). Chronic fatigue syndrome affects 0.2-0.7% of the Australian population. Estimating the prevalence of chronic fatigue syndrome is complicated by the multiple comorbidities that patients often present with (Johnston et al., 2016). Patients with chronic fatigue syndrome suffer reduced productivity and may be forced to give up work, study and interests due to the physical and mental impacts. Many experience loss and reduced self-worth and their relationships also suffer; their careers and supporters are affected, with the fatigue preventing social contact and intimacy (Roberts, 2018).

A hallmark of chronic fatigue syndrome is long-lasting fatigue after only minor physical activity. It is hypothesised that muscle metabolites, that build up during muscle contraction, activate fatigue pathways excessively (Staud et al., 2015). A study using 31P nuclear magnetic resonance showed that CFS patients had normal levels of metabolites and similar changes in exercise, but the changes occurred more rapidly during the course of the exercise

than in healthy subjects (Wong et al., 1992). Patients with chronic fatigue syndrome have increased fatigue ratings, compared to healthy controls after forearm blood supply occlusion (via a pressure cuff), and after hand grip exercises to exhaustion. Blood supply occlusion after exercise resulted in worsening of overall fatigue, providing evidence for sensitisation of metaboreceptor/ergoreceptor pathways. As there was an overall increase in general fatigue, and not just local fatigue, both peripheral and central pathways may be affected (Staud et al., 2015). Given the role of muscle ergoreceptors in both fatigue and pressor responses to exercise, it would be of considerable interest to know if abnormal Group III/IV afferent activation contributes to the abnormal sensations that characterise this disorder.

Delayed onset muscle soreness

Delayed onset muscle soreness is a common occurrence after strenuous exercise, especially if the exercise involved eccentric muscle contractions (Mizumura and Taguchi, 2016). Delayed onset muscle soreness is different from the acute pain felt during or directly after exercise; discomfort increases after a pain free period lasting between 12 and 24 hours after the exercise stopped. It usually peaks at 24 -72 hours and disappears within a 7-day time period after the exercise (Armstrong, 1984, Newham, 1988, Graven-Nielsen and Arendt-Nielsen, 2003). The presence of this pain free period (first 24 hours) that gives delayed onset muscle soreness its name, is intriguing. Establishing the mechanisms involved represents a considerable challenge.

Delayed onset muscle soreness is characterised by muscle tenderness, stiffness, movement-induced pain in the exercised muscle, but usually an absence of pain at rest (Cheung et al., 2003, Mizumura and Taguchi, 2016, Taguchi et al., 2005b). The sensation intensity can vary from a slight muscle stiffness, all the way to severe debilitating pain that restricts movement. This discomfort and pain may interfere with daily life, not only preventing further exercise

but also disrupting on-going daily tasks. Delayed onset muscle soreness affects people who exercise irregularly or not at all and those who have re-started training after an extended period without exercise that allows deconditioning. However, delayed onset muscle soreness can also affect the performance of elite athletes, even though they train daily, especially if they engage in an unfamiliar sport or exercise routine (Mizumura and Taguchi, 2016). Delayed onset muscle soreness has been described as possibly one of the most common and recurrent forms of sports injury (Cheung et al., 2003). Even though delayed onset muscle soreness has such a high incidence, it is usually classified as a sub-clinical injury as sufferers usually tolerate it privately and recover from it without any medical treatment (Cheung et al., 2003, Taguchi et al., 2005b). However, delayed onset muscle soreness can lead to more debilitating and chronic injuries (Hayashi et al., 2017), resulting in chronic pain and/or hyperalgesia, with plastic changes in the central nervous system (Sluka et al., 2012). It also acutely affects range of movement and peak force development in the affected muscles (Cheung et al., 2003). Therefore, effective methods to prevent delayed onset muscle soreness or treat it more effectively would be of considerable value.

Delayed onset muscle soreness is known to be associated with unfamiliar high force muscular work and eccentric muscle actions (Armstrong et al., 1983, Asmussen, 1956). Eccentric contractions cause it more effectively than concentric work (Armstrong, 1984, Newham, 1988, Pyne, 1994). Eccentric muscle contractions are defined as the forced elongation of a muscle during its simultaneous contraction often in an attempt to decelerate limb or body movement (Proske and Morgan, 2001). Examples of eccentric exercises include walking down a hill, resisted cycling, lifting weights, and resistance training (Cheung et al., 2003). Due to the relationship between delayed onset muscle soreness and eccentric muscle contraction, researchers investigating delayed onset muscle soreness have induced muscle soreness using many of these activities in both human and animal studies

(Cheung et al., 2003, Taguchi et al., 2005b). Many of these investigations have found histochemical, ultrastructural, biochemical and physical changes within the muscle. These include micro-lesions within the muscle, the widening of I-bands (detected by toluidine blue), the presence of mononuclear cells, the presence of macrophages within muscle fibres (by methylene blue), the distortion and/or loss of Z-lines, and the increase plasma enzyme glucose-6-phosphate dehydrogenase (Armstrong et al., 1983, Newham et al., 1983).

The mechanisms that underlie delayed onset muscle soreness remain unclear (Cheung et al., 2003, Mizumura and Taguchi, 2016, Taguchi et al., 2005b). Over the decades many mechanisms have been proposed. These include lactic acid build-up which damages the muscle fibres (Schwane et al., 1983), muscle spasms (Cheung et al., 2003), connective tissue damage (Hough, 1902), muscle fibre damage (micro-injuries i.e. distortion of sarcomeres, widening of I-bands) (Proske and Morgan, 2001), release of enzymes from damaged muscle fibres ((Armstrong, 1984, Gulick and Kimura, 1996)- see (Cheung et al., 2003))and inflammation (Hikida et al., 1983). The most widely accepted cause for delayed onset muscle soreness is micro-damage of the subcellular structures of muscle fibre and the subsequent inflammation that this induces. This theory has recently come into question because of reported cases of delayed onset muscle soreness without muscular damage (Mizumura and Taguchi, 2016, Taguchi et al., 2005b). In addition, the timescale of micro-injury occurrence may not match that of delayed onset muscle soreness (Newham, 1988). Furthermore, anti-inflammatory drugs (NSAIDs) are not helpful in many cases in reducing delayed onset muscle soreness (Cheung et al., 2003).

To further investigate the cause of delayed onset muscle soreness, Taguchi et al (2005) established an animal model of mechanical hyperalgesia in exercised rats. Previous findings demonstrated the existence of muscle tenderness using behavioral pain tests, combined with

c-Fos protein expression in the spinal dorsal horn neurons in response to mechanical stimulation of the muscle 2 days after applying forced eccentric contraction in their *in vivo* rat model (Taguchi et al., 2005a, Taguchi et al., 2005b). Taguchi et al (2005) then investigated the role of group III and IV muscle afferents in delayed onset muscle soreness (Taguchi et al., 2005b). Single-fibre afferent recordings were made in the rat extensor digitorum longus muscle /peroneal nerve preparations *in vitro* two days after eccentric contractions (Taguchi et al., 2005b). These recordings provided evidence that the mechanical threshold of the thin-fibre sensory receptors in the muscle was reduced in exercised rats compared to controls. Furthermore, the magnitude of afferent responses to mechanical stimulus were also enhanced (Taguchi et al., 2005b). This strongly supports the idea that peripheral sensitisation of group III and/or group IV muscle afferents is involved in delayed onset muscle soreness.

In later studies Mizumura et al (2016) the same group showed that muscle hyperalgesia can occur without any visible sign of microscopic damage to the muscle in their animal model. They suggest that bradykinin may play a key role in initiation of muscle soreness. They also describe the maintenance of soreness, during delay onset muscle soreness, may involve nerve growth factor (NGF) as it is upregulated in hyperalgesic muscle and antibodies to NGF can reverse the soreness. NGF also sensitises some thin fibre muscle afferents (Murase et al., 2010). The situation is complex however. Based on pharmacological studies with blockers, Cyclo-oxygenase 2 may also be involved in initiation of delayed onset of muscle soreness, but not in its maintenance, which may also involve glial-derived neurotrophic factor (GDNF); another modulator of group III/IV muscle afferents (Murase et al., 2014). Clearly the mechanisms underlying delayed onset muscle soreness are more complex than once thought but closely involve group III and IV afferents from striated muscles.

Aims of this project and summary of findings

This project aimed to investigate the neurobiology of fine sensory nerves that innervate skeletal muscle in a mammal. Currently, there is no established method to correlate the morphological features of group III and IV fibres with their functional properties recorded in electrophysiological studies (Jankowski et al., 2013). Techniques to achieve this goal have been developed in the host laboratory for visceral primary afferents (Brookes et al., 2013, Song. X., 2009, Tassicker et al., 1999, Zagorodnyuk and Brookes, 2000). Pilot studies suggested that the abdominal muscles may be an appropriate preparation for the visualisation and characterisation of sensory nerves within skeletal muscle. Their thin flat structure removes the need for sectioning or 3-D reconstruction, as the innervation could be clearly seen, and they were easy to isolate from the animal. The preferred species for this study were mouse and guinea pig, as tissue from both species was readily available and thin enough for whole-mount immunohistochemistry. We tested whether these techniques could be used to identify, discriminate and visualise muscle afferent endings within an abdominal skeletal muscle preparation.

In the present studies, we aimed to use a combination of electrophysiology, anterograde labelling and immunohistochemistry previously used in visceral organs, to successfully and informatively correlate the morphological and functional characteristics of sensory neurons that innervate abdominal skeletal muscles. In **chapter 2**, we showed that we could successfully identify the action potentials of muscle spindle afferents, demonstrate their well described functional characteristics and correlate this to their known distinctive morphology. This study validated the novel preparation and methods and showed that they can be used to relate the morphological and functional characteristics of muscle afferents. This methodology will allow individual classes to be studied systematically and in detail, one at a time without conflating their properties (**Chapter 2**). This simple approach, in which

essentially a single functional class is studied in detail, has the potential to contribute significantly to a better understanding of the basis of sensation from muscle groups.

In **chapter 3** we used the newly-validated preparation and methods described above to make recordings from a distinctive population of axons innervating preparations of abdominal skeletal muscles. Due to their characteristic features, we were able to describe for the first time a class of group III muscle afferents that are mechanosensitive metaboreceptors, present within the connective tissue in skeletal muscles in mice, group III connective tissue afferents (hereafter referred to as CT3s) (**Chapter 3**). These studies revealed that CT3 afferents were readily distinguishable and had discrete fields of innervation sensitive to von Frey hairs, showed saturating responses to graded muscle stretch, and were highly responsive to a mixture of metabolites. The morphology of CT3 afferents formed fine branching endings that were not immunoreactive for CGRP, and which were located in the deep connective tissue layers between the layers of muscle. These studies revealed that group III muscle afferents were easily identifiable in such preparations by their saturating mechanical responses to both von Frey hairs and step-stretch. These data were exploited in **chapter 4** to identify CT3 afferents, so that they could be characterised further.

Observations made in **chapter 3** showed that CT3 muscle afferents are activated by a metabolic mix. In **chapter 4** we aimed to characterise this population of group III neurons further, specifically their response to the metabolite lactate alone. We show for the first time, the G-protein coupled lactate receptor, hydroxyl carboxylic acid receptor 1 (HCAR1), is expressed in a subset of primary afferents that innervate the abdominal muscles. We show that superfusion of lactate can excite identified CT3 afferents, but not all sensory neurons. We show, for the first time, that the G-protein coupled lactate receptor, hydroxyl carboxylic acid receptor 1 (HCAR1), is expressed in a subset of primary afferents that innervate the

abdominal muscles in mice. We show that HCAR1 mRNA was localised in dorsal root ganglia and that HCAR1 immunoreactivity was visualised in the somata of dorsal root ganglion sensory neurons retrogradely labelled from abdominal muscles. We describe a population of these cell bodies were HCAR1+/CGRP-, along with HCAR1 immunoreactivity in nerve fibres and nerve endings in wholemounts of mouse abdominal muscle in many cases in CGRP- negative axons, which is consistent with belonging to CT3 afferents. Therefore, we propose that lactate activates sensory afferent endings in striated muscle, at least in part, via its G-protein receptor, hydroxyl carboxylic acid receptor 1, HCAR1.

The major themes arising from the results of all the present studies are presented and discussed in **chapter 5**.

Note to reviewers

Chapters 2 and 3 include some data that was acquired before enrolment in PhD studies. This includes the first isolation of the abdominal muscle as a preparation (chapter 2), some initial immunohistochemical studies (results not shown), and feasibility studies on biotinamide labelling experiments (chapter 3). Results sections in which these data are included have headings marked by asterisks (also noted in the table of contents). However, substantial additional analysis has been carried out that replaces most of this data during the course of the PhD.

CHAPTER TWO

IDENTIFICATION AND EXTRACELLULAR RECORDINGS FROM SPONTANEOUSLY FIRING AFFERENTS IN MOUSE ABDOMINAL MUSCLES

INTRODUCTION

Sensory neurons encode mechanical, thermal, chemical and light stimuli, and often give rise to conscious sensations, including, but not limited to, touch, smell, taste, and pain. Sensory neurons detect changes in the external and internal environment by the process of transduction at their specialised endings within the organ or tissue they innervate (Basbaum et al., 2009). Accounting for sensory neuron function it is an important part of understanding the neural basis of behaviour. A comprehensive description of sensory neuron structure and function provides a sound start for such understanding. (Li et al., 2015, Zeng and Sanes, 2017). A sound understanding of the different classes of sensory neurons, and their roles in evoking sensations, is important to be able to target these neurons therapeutically.

The sensory neurons that innervate skeletal muscle are usually classified into four groups, denoted by the Roman numerals (I-V) (Lloyd, 1943a), based on their conduction velocity (Erlanger and Gasser, 1930)and axonal diameter (Lloyd, 1943a). Group I and group II muscle afferents have been extensively investigated and are known to terminate in specialised endings. These specialised endings are Golgi tendon organs (group Ib) and muscle spindles, which includes both the primary (group Ia) and secondary (group II) endings.

Golgi tendon organs were described by Golgi in 1878 and 1880 (Jami, 1992). These receptors are concentrated along the muscle-tendinous boundaries of skeletal muscles. Golgi tendon organs convert tensile force into action potentials and are therefore known as tension receptors, whereas, muscle spindles are known to sense changes in muscle length.

Muscle spindles contain receptive endings that detect the length and dynamic changes in length of the muscle (Bewick and Banks, 2015, Tiegs, 1953). Ruffini in 1898 provided the first detailed description of muscle spindles, drawing their detailed structure. Primary endings were described as having a large 'annulospiral' endings that wrapped around the elongated intrafusal muscle fibre (Ruffini, 1898). It is now accepted that the primary receptive ending of the spindle forms loops around the central portion of the intrafusal muscle fibre. Lengthening of the muscle, especially in the central portion, causes these loops to deform, and in doing so evoking a train of action potentials, probably by opening a mechano-gated ion channel. Recent evidence suggests that the same mechanogated ion channel, Piezo2, may be responsible for the mechanosensitivity of annulospiral endings and Golgi tendon organs (Woo et al., 2015). The primary endings give rise to group Ia muscle axons, that are thickly myelinated and have fast conduction velocities.

Ruffini in 1898, described a secondary ending of a muscle spindle; the 'flower spray' ending. These were described as being located either side of the primary afferent ending. Their axons are smaller than those that terminate in primary endings Ruffini, 1898 #432}. These are group II fibres with smaller axonal diameter and their slower conduction velocities. Secondary endings lack the large response during the dynamic phase of a stretch, that is seen when primary endings are activated. Instead they respond in a more proportional manner to the amount of stretch applied to the muscle (Cooper, 1961). Thus, secondary endings are described as length receptors rather than change-in-length receptors (ie: primary endings). Secondary endings respond more sedately, needing considerable elongation to alter their firing pattern (Cooper, 1961).
Compared to the extensive knowledge of groups I and group II, the morphology of group III and group IV muscle afferents has not been as extensively investigated.

Group III and group IV have much slower conduction velocities than groups I and II (Jankowski et al., 2013, Lloyd, 1943a). Group III fibres are thinly myelinated, whereas group IV fibres are unmyelinated. Group III and group IV fibres have been suggested to terminate as 'free nerve endings'. These nerve endings are bare, having no specialised capsular or corpuscular structure. Free nerve endings of group III and group IV fibres have been identified in connective tissue, surrounding blood vessels, running alongside muscle fibres and within larger nerve trunks (von Düring and Andres, 1990). A number of laboratories have investigated the functional characteristics of these two groups of muscle afferents, yet many of the basic anatomical and physiological properties of group III and group IV muscle afferents are still unknown. Standard methods to identify the morphology of functionally identified group III and group IV afferents have not been readily available (Jankowski et al., 2013). It is unknown if different functional subtypes of group III and group IV endings have different structural properties. It is also unknown if functional subtypes of group III and group IV afferents differ in their endings' locations or if any of these factors have any influence on their predicted function. For example, different classes of group III and group IV muscle afferents are known to be activated by a metabolite mix (ATP 1 μM, lactate 15 mM, and pH 7.0). These metabolites are released from the working muscle and activate muscle afferents that signal muscle work, although, the location of the responsive free nerve endings within the muscle is yet to be established (Jankowski et al., 2013, Light et al., 2008).

Studies that investigated group III and group IV afferents have been largely carried out *in vivo*; many of these studies have concentrated on functional characteristics. These have included recordings from cell bodies from the dorsal root ganglia, using intracellular micro-electrodes, while activating the nerve ending within the tissue. This

enabled them to linked the immunohistochemistry of cell bodies and electrophysiological properties of sensory neurons corresponding to these functional tests (Jankowski et al., 2013). This type of methodology relates cell bodies to endings but gives no information about the morphology of the functionally characterised ending in the periphery. Another productive approach has been to use anterograde labelling from the dorsal root ganglia to label sensory endings in the periphery, allowing their visualisation within the tissue or organ. However, it is difficult to identify the functional characteristics of each morphological type of ending (Spencer et al., 2018a). Thus, these methods do not allow the morphology of afferent endings to be correlated with their functional characteristics.

Methods that can relate the structure of sensory endings to their functional characteristics have been used extensively in visceral preparations (Lynn and Brookes, 2011a, Song. X., 2009, Zagorodnyuk and Brookes, 2000, Zagorodnyuk et al., 2003). These preparations have the ability to obtain and study in detail the peripheral branching patterns of sensory nerves and relate this to their functional properties, allowing a deeper understanding of gastrointestinal afferents (Tassicker et al., 1999, Brookes et al., 2013).

This study aimed to:

a) Established an ex vivo preparation of skeletal muscle from a laboratory animal that allows optimal visualisation of sensory endings while allowing electrophysiological characterisation
b) Determine if the combination of techniques previously used in visceral preparations can be transferred successfully to correlate the morphological and functional characteristics of sensory nerves that innervate skeletal muscle,

without the need for sectioning or 3D-reconstruction of endings. This validation was carried out on a distinctive class of sensory neuron that showed high, constant rates of spontaneous electrical firing that had previously been shown to belong to muscle spindle afferents (Matthews, 1933, Bewick and Banks, 2015).

METHODS AND MATERIALS

Ethical approval

C57Bl/6 mice (n=10, 1 female and 9 male), between the ages of 4-8 weeks (bred in-house), given *ad libitum* access to food and water, were euthanized by a lethal dose of isoflurane by inhalation, followed by removal of the heart or decapitation. All procedures were performed in accordance with *Australian Code for the Care and Use of Animals for Scientific Purposes* (8th ed, 2013, National Health and Medical Research Council of Australia) and were approved by the Animal Welfare Committee (permit #890/15) of Flinders University.

Isolation of the abdominal muscles

The abdominal wall muscles were then excised, as an intact structure, including wall musculature (external oblique, internal oblique, transversus abdominis and rectus abdominis muscles) along with the lower ribs on the right side, for orientation. The external oblique and rectus abdominis were then removed, leaving a preparation of internal oblique and transversus muscle which was pinned in a petri dish lined with

Sylgard (Dow Corning, Midland MI), superfused with Krebs solution (in mM: NaCl, 118; KCl, 4.75; NaH_2PO_4, 1.0; $NaHCO_3$, 25; $MgCl_2$, 1.2; $CaCl_2$, 2.5; glucose, 11; bubbled with 95% O_2/5% CO_2) and warmed to 37°C.

Close extracellular single unit recordings

Several fine nerve trunks (2-4 trunks) entering the preparation were dissected free of muscle and connective tissue over a length of 5-8mm. Preparations were then transferred to a 15ml, Sylgard-lined recording chamber and the dissected nerve trunks were pinned under slight tension to the Sylgard base using 50µm tungsten pins. The chamber was continuously superfused, via a peristaltic pump (Watson Marlow, Digital, Wilmington, MA) with warmed, oxygenated Krebs solution. A paraffin oil bubble was attached to the base of the chamber, and the end of the dissected nerve trunk was then pinned inside the oil bubble. Single unit recordings were made from the exposed nerve trunk inside the paraffin bubble with a 100µm Pt/Ir wire electrode insulated to within 200µm of its tip. Signals were amplified (ISO-80, WPI, Sarasota, FL), recorded at 20-40kHz (PowerLab16s/p, LabChart 7 Pro software, AD Instruments, Sydney, Australia) and visualised on an oscilloscope (National, VP-5220A). Single units were discriminated by amplitude and duration using Spike Histogram software (Spike Histogram software, ADInstruments). Further discrimination of units was carried out using a custom made in-house program that used principle component analysis for feature extraction and Gaussian mixture modelling for clustering written in Python. Usually, several nerve trunks were tested until a single unit could be clearly discriminated, based on minimal interspike intervals longer than 5 milliseconds, (Zagorodnyuk and Brookes, 2000). In some preparations, two recording electrodes, attached to separate amplifiers, were placed on the same nerve trunk in two separate paraffin bubbles, several millimetres apart. The conduction

velocity of an individual unit was calculated by dividing the distance between the two recording electrodes by the time delay between discriminated action potentials (n=6, 9 units).

Focal compression

With the muscle under 5 mN resting tension, mechano-transduction sites were identified by probing the muscle with a 1.0 mN von Frey hair. Transduction sites were identified by bursts of action potentials and were marked on the tissue, using fine carbon particles **(Figure 2.5 B)** applied via the tip of the von Frey hair. The tip of the hair was dipped into a droplet of concentrated sucrose solution which was then allowed to evaporate. The sticky sucrose then allowed carbon particles to attach and then be placed accurately on the preparation. Within a second or so, the sucrose dissolved in the Krebs solution, leaving the carbon particles adhering to the preparation. In this way, the receptive fields of mechanosensitive afferents could be accurately mapped on the preparation. The live preparation with carbon marks was then photographed. A range of von Frey hairs were then tested (20mg, 50mg and 100mg) to produce a stimulus response curve.

Stretch

In all preparations, a purpose-built 8-mm array of hooks (Biomedical Engineering, Flinders Medical Centre, South Australia) was used to connect the preparation via a cotton thread to the lever of an isotonic transducer (52-9511, Harvard Bioscience, South Natick, MA, USA). By adding counterweights to the isotonic lever, constant force could be applied, thus stretching the muscle evenly across its width, while measuring changes in the dimensions of the preparation. Counterweights of 1 – 4 g

were applied to the isotonic lever for 20 s. A minimum rest period of 3 min was allowed between stretches.

Additional stretch data analysis

Firing rate were calculated at four different stages of the step stretch, modified from that described in Wilkinson et al (2012) and depicted in **Figure 2.7.B**. Resting discharge was calculated as the mean firing rate during the 10 s before the start of the stretch and the "dynamic peak discharge" was the difference between the highest discharge frequency at the end of the ramp phase and the resting discharge. The "dynamic index" was the frequency difference between the highest frequency of the ramp phase and the frequency 1 s after. The "static response" was defined as the firing rate difference between the firing rate 1 s from end of the stretch and resting discharge and "static sensitivity" was the static response divided by the magnitude of stretch. The time that the unit was silent following the release of the stretch was also determined (Wilkinson et al, 2012).

Application of metabolic products

To determine if these afferents are activated by metabolic products released from the muscle, preparations were exposed to an oxygenated "low" metabolite mixture (15mM lactate, 1μM ATP, pH 7.0) dissolved in Krebs solution. The adenosine triphosphate (ATP) was added to the mixture immediately prior to the delivery into the bath. The concentrations of metabolites were chosen based on the previous studies by Light et al (2008), and Jankowski et al (2013). While the metabolic mix was present in the bath, three stretches (1, 2 and 4g) were applied to the preparation to determine if the presence of the metabolites had an effect on the afferents sensitivity to stretch.

Bolus application of capsaicin

A stock solution of 10^{-2} M capsaicin was made in ethanol (Sigma; V913). It was kept refrigerated and diluted to the working concentration in Krebs solution shortly before use. The effect of capsaicin (1μM final concentration) was then recorded.

Application of increased potassium concentrations [K^+] of Krebs solution

The preparations were exposed to two increased potassium concentrations [K^+], to determine the effects on firing rate in these afferents. In the first solution, K^+ concentration was increased from 4.75mM KCl (normal concentration in Krebs solution) to 6.75 mM KCl. In the second, K^+ concentration was increased to 9.75 mM KCl. The preparations were superfused with the different solutions for 10 minutes, before a 15-minute wash period. While each of the potassium solutions were present, three stretches (1, 2, 4g) were applied to the preparation to determine if the presence of the increased potassium concentrations (6.75 and 9.75 mM, respectively) had an effect on the afferents' responses to stretch. At the end of the recording period, the preparation was removed from the recording chamber and transferred to a new chamber for anterograde labelling.

Anterograde labelling

At the end of the recording the preparation was pinned in a new purpose-built chamber for anterograde labelling of axons in the nerve trunk (Zagorodnyuk and Brookes, 2000). The end of the nerve trunk was led into a side-chamber filled with paraffin oil (sealed with a partition made from a cover slip, with a silicon grease seal (Ajax Chemicals, Castle Hill, NSW, Australia). A drop of biotinamide solution (Molecular Probes, Eugene, OR, USA) in "artificial intracellular medium" (150 mM monopotassium L-glutamic acid, 7 mM $MgCl_2$, 5 mM glucose, 1 mM EGTA, 20 mM

HEPES, 5 mM disodium adenosine-triphosphate, 0.02% saponin, 1% dimethyl sulphoxide) was placed onto the de-sheathed nerve trunk under the paraffin and the main chamber was filled with sterile culture medium (Tassicker et al., 1999). Preparations were incubated for 4 hours on a rocking tray in a humidified incubator at 37°C, 5% CO_2 in air, then fixed overnight in modified Zamboni's fixative (as above) at 4°C. Preparations were permeabilised and cleared using the immunohistochemical protocol described below. Biotinamide was visualised by CY3-conjugated streptavidin (1:500, Molecular Probes, 4 hours). Preparations (n=5) were, rinsed three times in PBS and mounted in 100% carbonate buffered glycerol (pH 8.6). Preparations were mounted between two coverslips, with the lower coverslip fixed to a 1mm thick aluminium surround so that they could be viewed from either side.

Tissue fixation and processing

Preparations were fixed in modified Zamboni's fixative (0.2% saturated picric acid in 2% paraformaldehyde in 0.1 mol L^{-1} phosphate buffer, pH 7.2) for 24 hours. The tissue was then washed in phosphate buffered saline (PBS) (3x 10 minutes), permeabilised and cleared with dimethyl sulphoxide (DMSO) (2x 10 minutes, 1x 30 minutes) and rinsed in PBS (3 x 10 minutes). The samples were then treated with Triton X-100 (0.5%) in PBS on a mixing tray at room temperature overnight. After 24 hours, the samples were rinsed in PBS, then further permeabilised in 100% glycerol with 0.1% sodium azide, on a rocking orbital mixer (OM5, Ratek, Victoria, Australia) in a humidified incubator at 37°C for 24 hours. Samples were then washed with PBS solution (3 x 30mins) to remove the glycerol.

Microscopy and processing

Immunohistochemically stained preparations were viewed and analysed on an Olympus IX71 inverted fluorescence microscope, fitted with appropriate dichroic mirrors and filters. Images of labelled neural structures were captured via a CoolSNAP ES digital camera (Roper Scientific, (Photometerics), Tucson, AZ, USA) using analySIS 5.0 software (Soft Imaging System, Gulfview Heights, South Australia, Australia). Image processing was restricted to brightness and contrast adjustments, cropping and formation of photomontages using Adobe Photoshop (CS6, Adobe Systems Inc., San Jose, CA).

Statistical Analysis

Statistical analysis was performed by Student's paired or unpaired two-tailed *t* tests or by repeated measures analysis of variance (ANOVA, one-way or two-way) using Prism 7 software (GraphPad Software, Inc., San Diego, CA, USA). Differences were considered significant if $P < 0.05$. Results are expressed as means ± 95% confidence intervals except when stated otherwise. The number of animals used in each set of experiments is indicated by '*n'*. NS denotes a non-significant finding ($P > 0.05$).

RESULTS

Identifying a suitable preparation*

For this study, we needed to establish a small animal, *ex vivo* preparation that allows optimal visualisation of sensory nerves and their terminals within muscle. This preparation would allow the optimal conversion of techniques previously used in visceral preparations to be applied to skeletal muscle. The criteria the preparation needed to meet were (i) to be thin, to remove the need for sectioning or 3D-reconstruction, (ii) easy to remove from the animal without damaging the muscle or the innervation and (iii) to have a visible nerve supply. A range of skeletal muscles preparation were investigated to determine which best met all the required criteria, these included: hindlimb muscles (gastrocnemius, rectus femoris muscles), forelimb (biceps, triceps) and back muscles (trapezius), all of which were discarded. The forelimb and hindlimb muscles were too thick to visualise the innervation. Some of these muscles were difficult to isolate in a timely manner without damaging either the preparation or the innervation.

The abdominal wall muscles met all of the criteria. The abdominal muscles (external oblique, internal oblique, transversus abdominis and rectus abdominis) are thin, translucent, their innervation is clearly visible, and they are easily isolated from the animal (Figure 2.1.). From this point forward, the internal oblique and the transversus abdominis were used as the preparation.

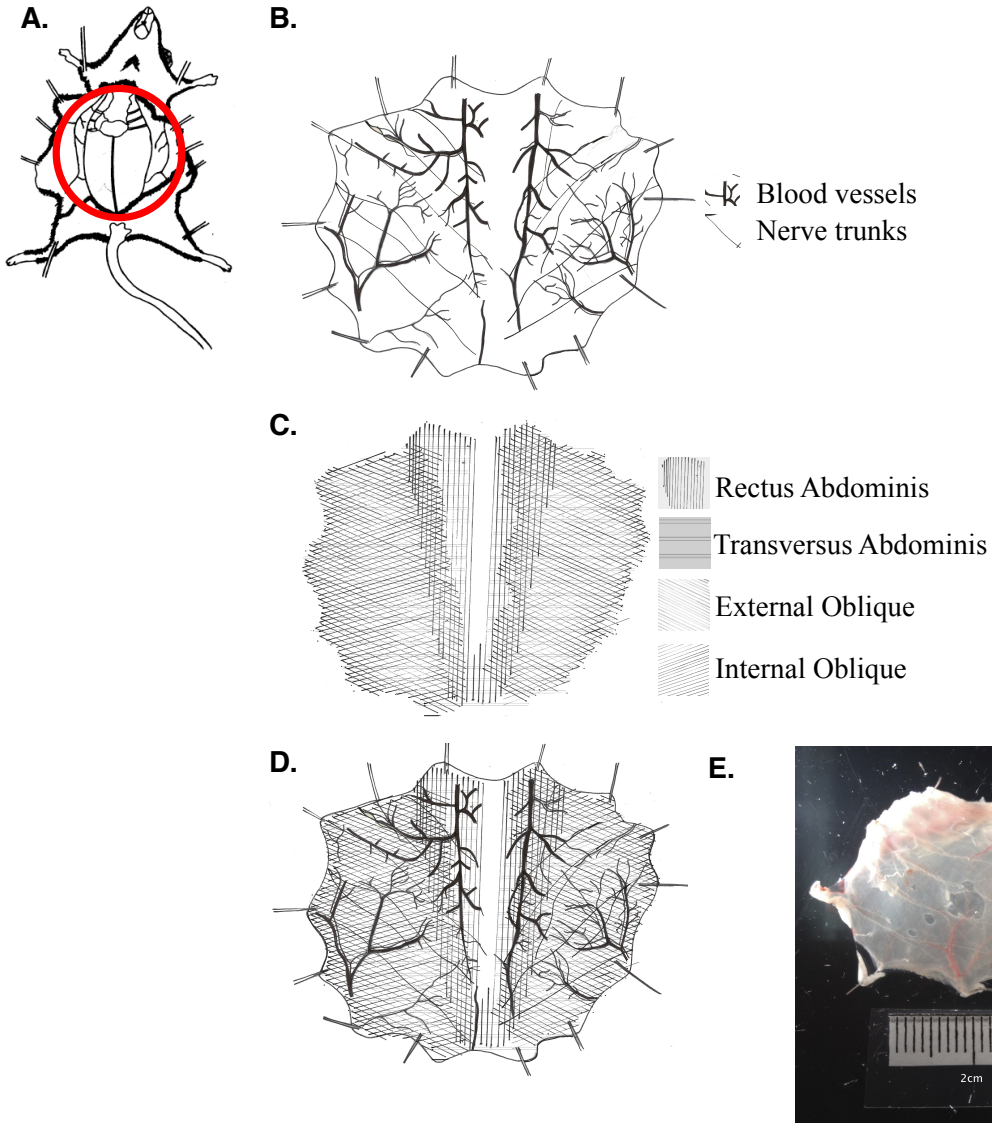

Figure 2.1. Schematic of mouse dissection and the microscopic and gross anatomy of the mouse abdominal muscles.
A. The gross anatomy and location of the abdominal muscles, the red circle indicates the location of the abdominals in relation to the gross anatomy of a mouse. **B.** The blood vessels and nerves that were visualised to supply the abdominal muscles. Note that the major nerve trunks and vessels did not run in parallel although fine peri- and parasvascular nerve trunks were often revealed by immunohistochemical staining. **C**. The anterior view of the abdominal muscles, and the various muscle fiber directions of each muscle layer. Note that each muscle's fibres have a distinctive orientation which determined the directionality of intramuscular nerve endings, but not endings in the connective tissue layers that separated the muscles **D.** Combined images of **B** and **C**, to demonstrate how the abdominal muscles looked after dissection. **E**. A micrograph of the abdominal muscles of a mouse to give a representation of the scale of the preparations used in the study.

Landmarks and components of the preparation*

The abdominal musculature was removed from the animal as an intact whole. As seen in **Figure 2.1 E**, our preparation included the bottom of the rib cage for orientation. In the middle of the preparation is the linea alba, a fine layer of connective tissue joining the left and right sides of the abdominal musculature (**Figure 2.1. C-E**). The preparation is supplied by five different arteries. The two prominent blood vessels can be seen in **Figure 2.1. B & E** entering from the top and the bottom of the preparation; these are the superior and inferior epigastric arteries, respectively. There are also smaller blood vessels that travel alongside the nerves that innervate the preparation from between and beneath the ribcage that branch towards the midline. These are the intercostal and subcostal arteries respectively, these can also be seen in **Figure 2.1. B&E.** The last to artery that innervates the preparation are the branches of the deep circumferential iliac artery, these are deeper within the tissue and cannot be seen while the preparation is intact. The major nerve trunks that innervate the preparation can clearly be seen but these usually divided into finer branches that became increasingly difficult to trace under the dissection microscope. In **Figure 2.1. E**, a micrograph of the preparation the innervation of these muscles is clearly seen as large white nerve trunks that enter the preparation either between the intercostal spaces or subcostal. The branching pattern of these larger nerve fibres could be seen by the naked eye as they head medially. The different muscle layers were also clearly visible, which assisted during the dissection. The rectus abdominis or 'six-pack' muscles were easily identifiable as they run cranially along the abdomen close to the linea alba (**Figure 2.1. C&E**). The rectus abdominis was not chosen as a preparation to investigate the sensory innervation due to its thickness; this can clearly be seen when comparing it to the other muscles in **Figure 2.1. E** The external oblique muscle fibres run inferiomedially. The internal oblique (aligned superiomedially and inferiomedially)

and the transversus abdominis (running horizontal to the linea alba) were easily visible when the external oblique was removed, see the small window removed in **Figure 2.1. E.** The anatomical landmarks used to establish this preparation ensured that each preparation was anatomically consistent.

Spontaneously firing afferents

Early in the project, when the nerve trunk was placed on the recording electrode, most preparations contained easily identified distinctive single units that fired spontaneously at high rates with little variation in frequency. These action potentials tended to be the largest recorded from the nerve. In 6 preparations 9 units were investigated. Six of these units (n=6) fired spontaneously and the other 3 units were only activated when mechanical stimuli were applied (discussed in detail below). The spontaneously active discriminated units had an average firing frequency of 12.6 ± 0.5 Hz (n=6) measured before any stimuli were applied (**Figure 2.2.**).

It was hypothesised that these afferents were muscle spindle afferents. To determine whether this was the case, we investigated their conduction velocity, responses to punctate force, responses to applied load, and sensitivity to a metabolic mix, capsaicin, and increased concentrations of extracellular K^+. These functional properties were then followed by anterograde labelling to visualise the endings of these spontaneous afferents, to relate their morphology with their functional characteristics.

Conduction velocity

The conduction velocity was calculated for all 9 units (n=6) from two recording sites on the same nerve trunk. In every preparation action potentials that occurred at the first electrode were also seen at the at the second recording site, in a one to one fashion (**Figure 2.3A**). The average distance between the two recording sites was ~3.45 mm. The average conduction velocity of these spontaneous afferents was 22.9 ± 4.8 m/s (range 13.64 m/s – 35.28 m/s, **Figure 2.3.B**).

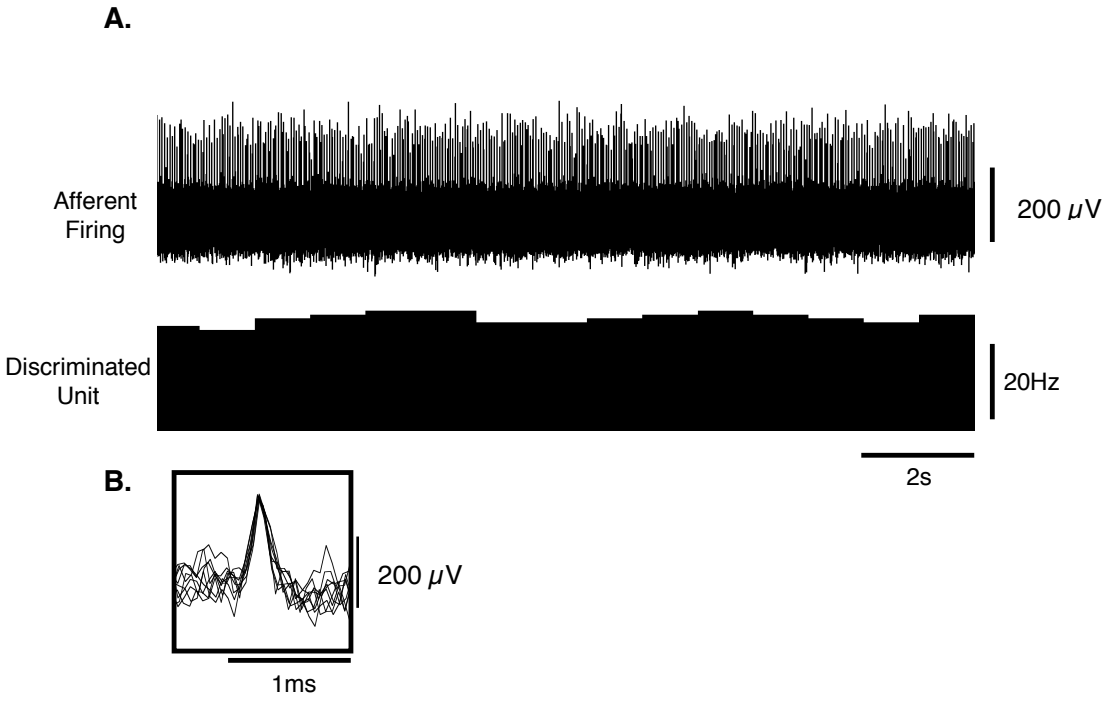

Figure 2.2 Spontaneous afferent firing

A. A typical trace of spontaneous firing of identified units. A large unit fires at a constant rate close to 30 Hz; a smaller unit fires intermittently. **B**. The spike shape of the large unit discriminated in software, has a clearly distinguishable waveform (9 superimposed action potentials).

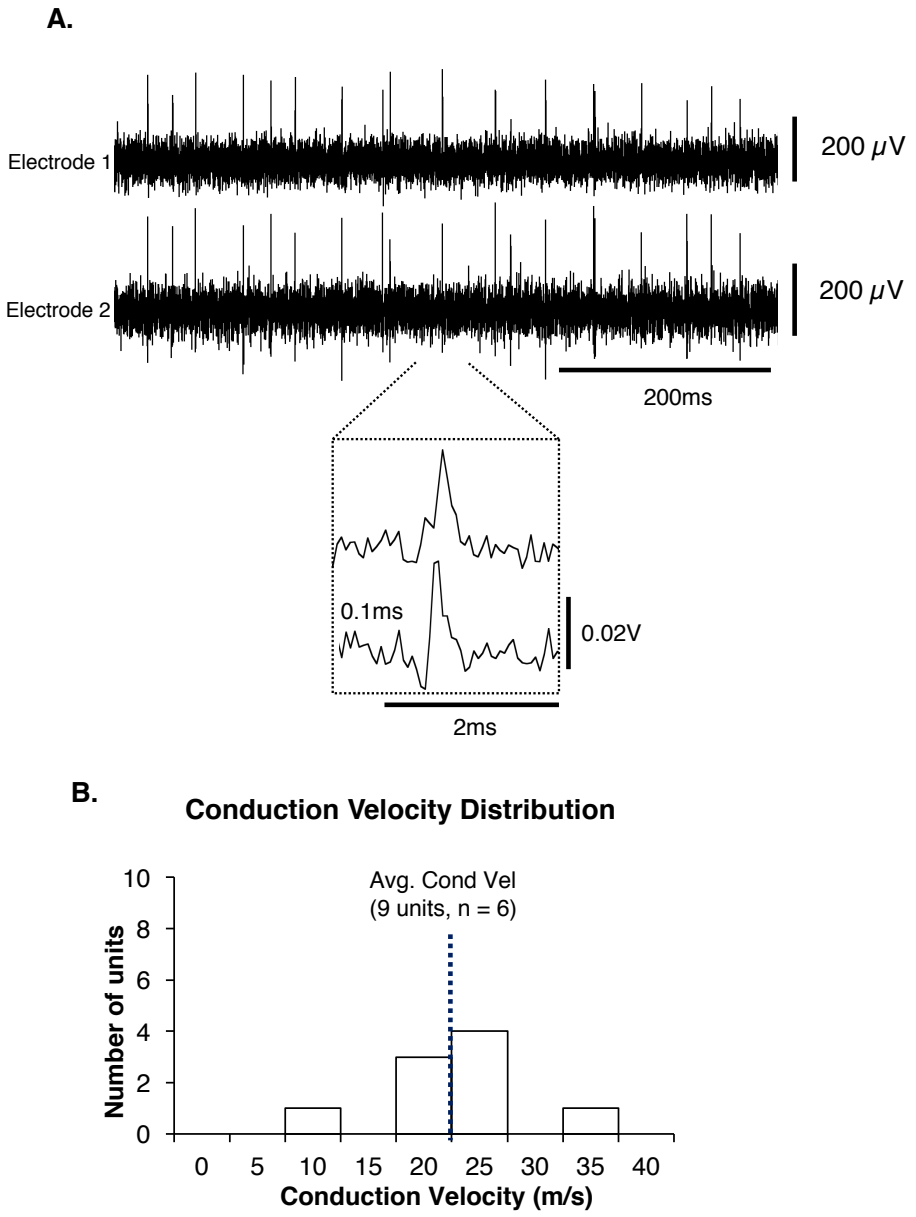

innervating the abdominal muscles.

A. A set of paired recordings showing nearly 1:1 of action potentials in both traces, although the amplitude can differ between the two. Electrode 1 is the electrode that is closest to the preparation, while electrode 2 is the electrode that is closest to the severed end of the recorded nerve. An expanded time base (in the insert) demonstrates the conduction delay between the same unit's action potential at the two recording sites. **B**. The distribution of conduction velocities of spontaneous afferents (9 units, n=6). Note the dotted line indicates the average conduction velocity of 23 m/s of all 9 units, $n = 6$.

Von Frey hair Responses

A standard calibrated 1 mN von Frey hair (which exerted a force equivalent to ~100mg) was applied to numerous locations on the muscle surface, to identify and map mechanosensitive sites (hot spots) of the discriminated units (9 units, n=6). The mean action potential amplitude of these identified afferents was 0.041 ± 0.015 V and the mean half peak duration was 0.184 ± 0.027 ms (**Figure 2.4.**). When a von Frey hair was applied to a hot spot, the afferent would increase its firing from basal, and once removed the afferent would return to basal firing (**Figure 2.5.A**). We tested a small range of von Frey hairs (20, 50 100mg), which evoked increasing responses to the increasing force (**Figure 2.5. C**). The maximum instantaneous firing rate of activated units to the stiffest von Frey hair was found to be 52 ± 12 Hz.

Receptive field

The receptive fields of discriminated units were then mapped in detail on a micrograph of the live preparation, with carbon particles applied at multiple points to act as visual landmarks (n=5). Sites at which a 100 mg von Frey hair evoked firing ("hot spots") were then plotted on a micrograph of the live preparation, relative to the carbon particle landmarks. From this we were able to confirm that the identified units had a single, elongated receptive field aligned in the direction of the muscle fibres. Receptive fields had an average area of 0.54 ± 0.16 mm^2, and were surrounded by non-responsive sites (**Figure 2.5.B)**. Their long axis averaged 1.52 ± 0.29 mm and their short axis averaged 0.3 ± 0.05 mm.

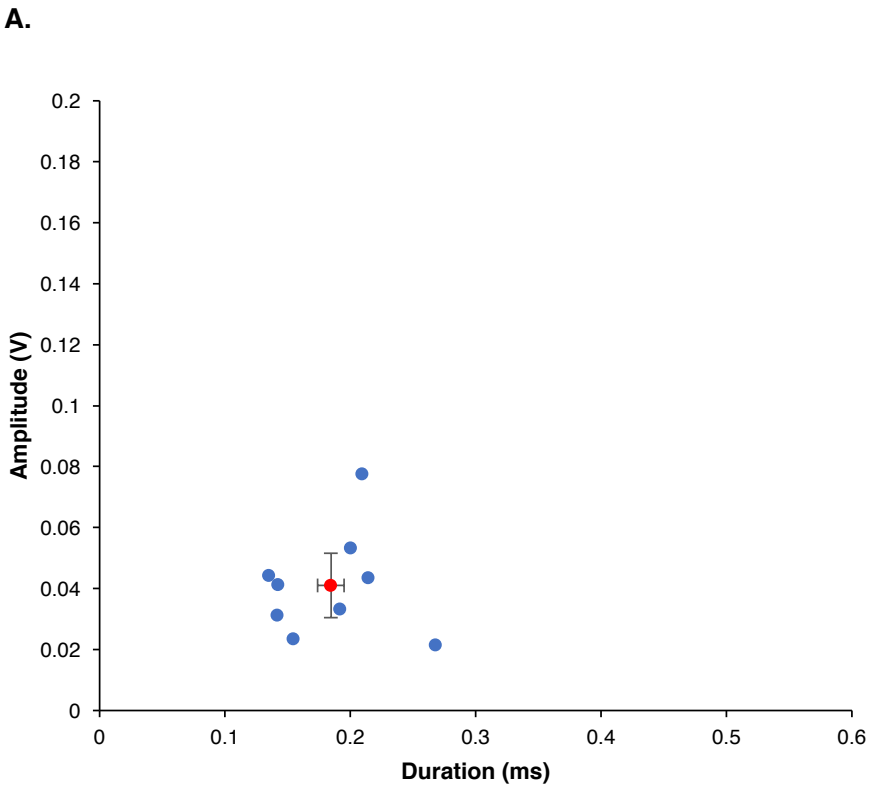

Figure 2.4. Characteristics of spontaneous units by amplitude and duration

A. A scatterplot of recorded unit's amplitudes and duration, to demonstrate that spontaneous afferent action potentials are quite closely clustered, indicating that they have a restricted range of similar amplitudes and durations. Individual units are in blue and the average amplitude and duration is in red with 95% confidence intervals as error bars.

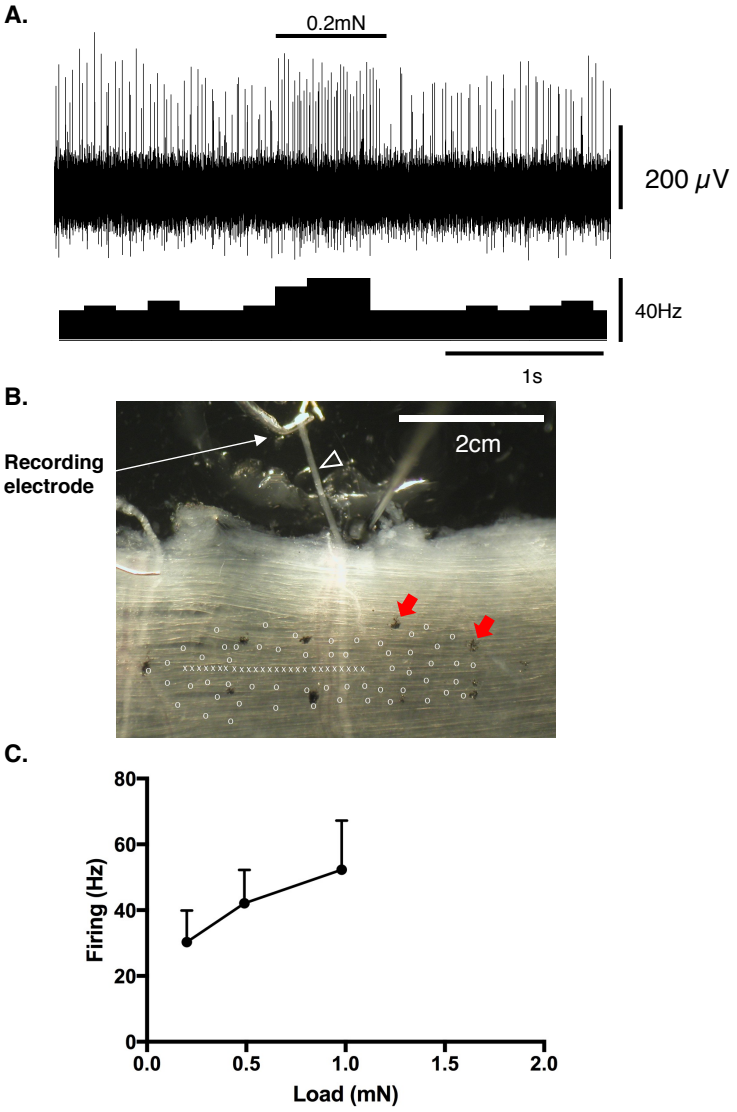

Figure 2.5. Firing evoked by von Frey hairs.

A. An example of mechanically evoked increase in firing evoked by probing with a 1mN von Frey hair on the surface of a preparation. **B.** A micrograph taken of the preparation of abdominal muscle during extracellular recording. Multiple black carbon markers can be seen on the surface of the internal oblique (examples are indicated by red arrows). The white open circles are sites where the preparation had no response to the von Frey hair, while the white crosses mark the responding sites i.e.; receptive field of this unit. Also visible is the recording electrode (white arrow) and the nerve trunk that is being recorded (arrow head). It should be noted that the receptive field is long and elongated in shape. The receptive fields were also aligned with the direction of the muscle fibres. **C.** Combined mean data from 14 units showing peak firing frequency to a range of von Frey hairs with higher firing with stiffer von Frey hairs. Von Frey hairs above 1mN were not used as previous data had suggested that the application of von Frey hairs above this load would potentially damage the receptive endings within the preparations.

Responses to stretch

Loads of 1,2 and 4g were applied to the arm of the isotonic transducer and the changes in muscle length and firing were recorded. Step stretches evoked an abrupt increase in firing in all units (**Figure 2.6.A-D**). From the mean data, the maximum firing rate in response to stretch was 35 ± 3 Hz. Overall, firing of all units increased in response to increasing graded load (**Figure 2.7. A**).

Dynamic responding units

Out of the 9 units, 6 units had spontaneous firing before the stretch was applied and increased their firing in response to the applied stretch (**Figure 2.7. B**). Five out of these 6 spontaneous units displayed an abrupt increase in firing which partially adapted within ~4 seconds, but the firing rate remained elevated compared to basal firing. Once the stretch was removed the spontaneous firing of these units was typically diminished or abolished, returning to the control basal rate after a silent period of 1- 11 seconds.

Static responding units

Out of the 9 units (n=6), 3 units were only activated after stretch was initiated. These unit fired tonically throughout the duration of the stretch and, when the load was removed, they ceased firing. One of the 6 spontaneously firing units showed a similar firing pattern to the 3 non-spontaneous units. This unit did not have a silent period when the stretch was removed but simply returned to its basal firing rate (**Figure 2.7. C**).

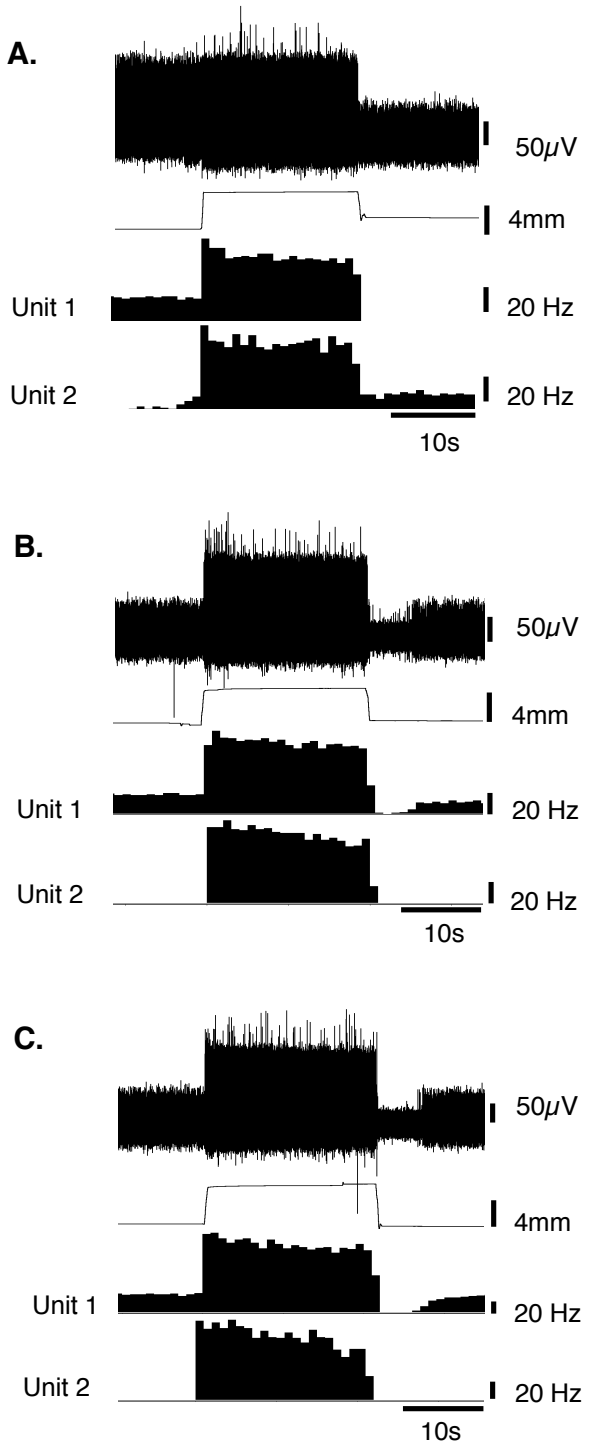

Figure 2.6. Typical responses of identified spontaneous muscle afferents to muscle stretch by applied loads of 1, 2, and 4 g.

The upper trace of each example shows a multi-unit recording. Firing rates (1s bins) are shown for two different discriminated stretch-responsive units both of which show maintained firing during the 20 s stretch. Unit 1 demonstrates a unit with spontaneous firing which increases during applied stretch, and upon release of the load becomes silent before spontaneously firing again. Unit two is only activated once the load is applied to the preparation. (9 units, n=6) **A.** 1g **B**. 2g **C**. 4g

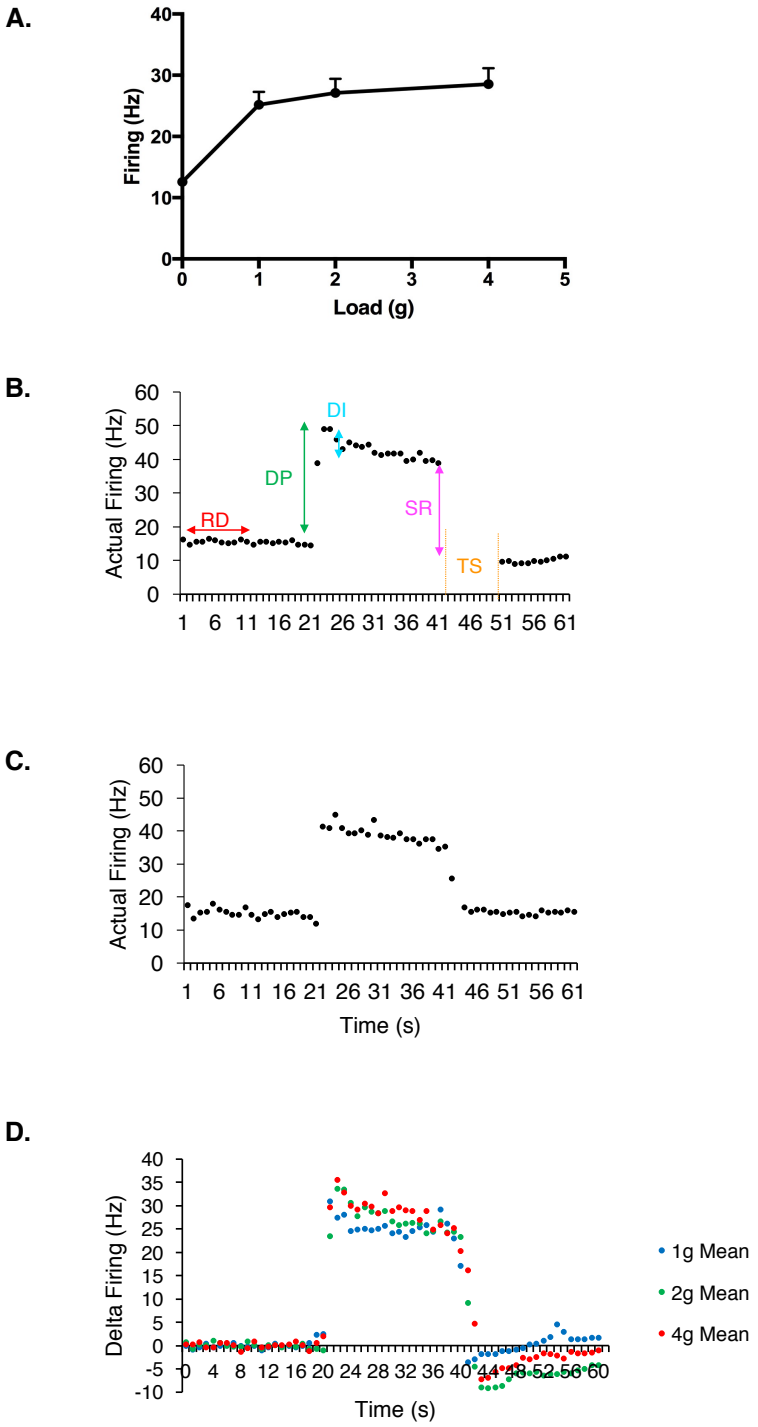

Figure 2.7. Mean data of identified stretch responsive units
A. Mean change in firing rate to increasing loads (20 s duration, 1, 2, 4 g; 9 units, *n* = 6). Responses increase with increasing load but the curve appears to flatten towards the right, suggesting saturating responses. **B.** The mean response of 6 units (6 units, n=6) that displayed an increased dynamic peak and time silenced after the removal of stimulus, arrows indicate time points of Resting Discharge (RD), Dynamic Peak (DP), Dynamic Index (DI), Static Response (SR) and Time Silenced (TS). **C**. The response of a unit that had spontaneous firing that increased in parallel to the static component of the stretch, then returned to spontaneous firing when the stimulus was removed **D**. Change in firing rate of all 9 units (n=6) at 1, 2 and 4g over a 60 s time period shows the modest increase in response with increasing load.

We utilised the data analysis described by Wilkinson et al (2012) for the murine extensor digitorum longus muscle, to relate the discharge patterns of muscle spindle afferents presented in this study with previously established functional properties of muscle spindles in *ex vivo* preparations.

Resting discharge, Dynamic peak, Dynamic index, Static response and Time silent data analysis

All stretches (1g, 2g, and 4g) were applied in the presence of three experimental solutions (a metabolite mix, 6.75 mM [K^+] and 9.75 mM [K^+]), as well as the control Krebs solution. In the section below, we will describe the results of each of these solutions.

Resting Discharge

The resting discharge was measured as the mean spontaneous firing of the identified unit for 10 s before the application of the stretch. The resting discharge was measured and used to compare changes in firing during the stretch. Six units exhibited a resting discharge before stretch (9 units, n=6) and this remained constant between stretches separated by intervals of 60 seconds. In Krebs solution, the mean resting discharge averaged before 1, 2, and 4 g stretches was 13.24 ± 2.5 Hz.

Increasing the [K^+] concentration to 6.75 mM [K^+] had non-significant effects on resting discharge when compared to normal Krebs solution. The average resting discharge in the presence of 6.75 mM [K^+] was 9.7 ± 1 Hz (9 units, n =6, NS, $P > 0.05$, $P = 0.098$, df = 8, One-way ANOVA). Increasing [K^+] concentration to 9.75 mM [K^+] also had a non-significant effect on the resting discharge, the average resting discharge increased to 17.20 ± 2.3 Hz (9 units, n = 6, NS, $P > 0.05$, $P = 0.064$, df = 8, One-way

ANOVA). The resting discharge was consistent over all stretches applied in both [K^+] solutions.

Stretches were also applied in the presence of a metabolite mix (ATP 1 μM, lactate 15 mM and pH 7.0). This particular metabolite mix has been shown to activate muscle afferents activated by muscle work (Light et al., 2008). These metabolites have also been used to activate group III and IV muscle afferents (Jankowski et al., 2013) (see **Chapter 3**). We tested if this metabolite mix had an effect on the spontaneous afferent firing in the present study. In the presence of the metabolite mix the resting discharge significantly decreased from an average of 13.24 ± 2.5 Hz in Krebs solution to 8.03 ± 0.1 Hz (9 units, $n = 6$, $P < 0.05$, $P = 0.018$, $df = 8$, One-way ANOVA) (**Figure 2.8. A**). This was a significant decrease in resting discharge when compared to the Krebs solution. The resting discharge remained consistent throughout the applied stretches.

Dynamic Peak

The dynamic peak is the peak frequency near the onset of the stretch. Throughout the preparations (9 units, n=6), the dynamic peak firing increased with increasing load in each solution (**Figure 2.8. B**). However, dynamic peaks at each of the applied loads showed some variability between repeats under each condition. The dynamic peaks were significantly less in the 6.75 mM [K^+] (9 units, $n = 6$, $P < 0.05$, $P = 0.004$, $df = 8$, One-way ANOVA) and the metabolite solution (9 units, $n = 6$, $P < 0.05$, $P = 0.0003$, $df = 8$, One-way ANOVA), than in normal Krebs solution. There was no significant difference between the dynamic peaks in the 9.75 mM [K^+] solution compared to the normal Krebs solution (9 units, $n = 6$, $P > 0.05$, $P = 0.257$, $df = 8$, One-way ANOVA).

Dynamic Index

The dynamic index is the difference between the peak frequency of the dynamic phase (dynamic peak) and the static response, measured 1s after the dynamic peak, thereby measuring the slowing of discharge. The dynamic index provides a method to measure the dynamic sensitivity of the recorded ending. The dynamic index increased at each of the applied loads in 9.75 mM [K^+] and in the metabolite mix, but not in the 6.75 mM [K^+] solution. In this latter solution, there was an increase between the dynamic index at 1 and 2g, but it dropped away again at 4g (**Figure 2.8.C**). The largest dynamic index was seen in normal Krebs solution; in all other solutions, the dynamic index was reduced. This reduction was significant in both the 6.75 mM solution [K^+] (9 units, n = 6, P <0.05, P = 0.017, df = 8, One-way ANOVA) and the metabolite mix (9 units, n = 6, P <0.05, P = 0.025, df = 8, One-way ANOVA), but not the 9.75 mM [K^+] solution (9 units, n = 6, P >0.05, P = 0.484, df = 8, One-way ANOVA).

Static response

The static response is the difference in firing frequency 1 s before the end of the applied stretch and the resting discharge. This reflects how much firing was stably raised above basal during maintained stretch. In each solution, the static response to load did not significantly increase with the loads applied. The largest static response was seen in the normal Krebs solution, followed by the 9.75 mM [K^+] solution, which was not significantly different (9 units, n = 6, P >0.05, P = 0.004, df = 8, One-way ANOVA). Then the 6.75 mM [K^+] (9 units, n = 6, P <0.05, P = 0.037, df = 8, One-way ANOVA). and metabolite mix had significantly lower responses (9 units, n = 6, P <0.05, P = 0.028, df = 8, One-way ANOVA) (**Figure 2.8. D**).

T*ime Silent*

Time silent was the time at which the afferents remained silent after the load was removed. In the presence of 6.75 mM [K^+] and the metabolite mix the time silent increased very slightly with greater applied load. In the presence of 9.5 mM [K^+] solution, no such increase was seen (**Figure 2.8. E**).

Before comparing the discharge patterns between the data in the current study and that of Wilkinson et al (2012), it should be noted that there are a few differences between the two studies that only qualitative patterns of firing to be compared rather than permitting quantitative comparisons. The present study uses an applied step-load method to stretch the preparation, compared to Wilkinson et al who used a ramp-and-hold stretch stimulus. Due to the difference in stretch application, Wilkinson et al were able to calculate instantaneous firing frequencies throughout the range of stretches, while the present study utilised firing frequency over discrete intervals. Therefore, this comparison is restricted to a comparison of discharge patterns of the muscle afferents.

The firing patterns observed in the present study were very similar to those described in Wilkinson et al (2012). Both studies reported a majority of their units having spontaneous firing. The resting discharge in both studies was consistent between stretches, therefore it can be assumed that the muscle was returning to its initial length between stretches.

In both the present study and Wilkinson et al (2012), the dynamic responses to stretch were similar even though the time-course of stretches were different. Both studies described the dynamic peak, dynamic index and static responses all increasing with the greater lengths of the muscle. Our results for dynamic index were lower than those

described by Wilkinson et al. This could be attributed to the step stretch we applied, as the stretch was applied much more quickly (as an applied load). A rapid ramp-stretch might allow a greater build-up of firing. Both studies reported an increase in static response as the muscle lengthened, thus in both cases afferents encoded the magnitude of the stretch. The time silent after the stretch removed tended to increase with muscle length in both studies. Like Wilkinson et al. (2012), it was not possible to discriminate with confidence group I and group II muscle afferents based on their dynamic properties. Despite the different methodologies between these studies, this brief analysis suggests that the ex vivo preparation of abdominal muscles provided comparable results to those of Wilkinson et al.

Discriminating primary (group Ia) and secondary (group II) afferents

Muscle spindles are innervated by two types of endings: a primary 'annulospiral' (Ia) sensory ending and a secondary 'flowerspray' (Ib) ending. These types of endings have been reported to respond differently to stretch stimuli. Primary sensory endings are more intensely activated by the dynamic phase of a stretch; their response at the onset phase is much greater than during the static phase of maintained stretch. Primary endings are typically silent for a few seconds after a stretch has been removed, before returning to basal firing rate. Secondary endings are activated much less during the dynamic phase; they increase their firing from basal more linearly once the stretch has been applied and fire tonically throughout the duration of the stretch. When the stretch is removed, they return to basal firing without a silent period. Along with their distinctive responses to stretch, these sensory neurons can also be discriminated by conduction velocity. Primary endings, have a larger diameter and are thickly myelinated and have a fast conduction velocity (*in vivo* range Group I $<42.9 \pm 4.3$ m/s in the hindlimb of mice (Steffens et al., 2012), *ex vivo* range group I/II 29 to 7 m/s in

a mouse plantar muscle-tibial nerve preparation (Wenk and McCleskey, 2007) in mice). In contrast, group II muscle fibres terminate as secondary endings, these fibres are smaller in diameter and have a slightly lower conduction velocity (*in vivo* range group II 38 – 22 m/s (Steffens et al., 2012), *ex vivo* range group I/II 29 to 7 m/s (Wenk and McCleskey, 2007), < 14 m/s (Jankowski et al., 2013) in mice).

We used the criteria above to try to identify the afferents we recorded as either primary or secondary. Out of the 9 units ($n = 6$), 6 units displayed the firing pattern of a primary ending. These units had abrupt increases in firing during the first 4 seconds of the stretch, before adapting and firing tonically at an elevated rate throughout the rest of the stretch. Once the load was removed, these units ceased to fire for 1 – 11 s (**Figure 2.7. B**). These afferents had similar conduction velocities ranging from 19.16 – 35.5 m/s; mean conduction velocity was 27.9 ± 3.9 m/s. The other 3 units displayed firing patterns more comparable to secondary endings. These afferent units increased firing rate more gradually at the onset of the stretch, fired tonically throughout the stretch and returned to basal firing with less of an undershoot in firing rate once the stimulus was removed. The conduction velocities of these 3 afferents ranged from 10.64 – 18.07 m/s, with a mean conduction velocity of 15.59 ± 3.96 m/s (**Figure 2.7. C**). Based on these two characteristics our data is consistent with the existence of the two classes of muscle spindle endings that have been previously distinguished.

A.

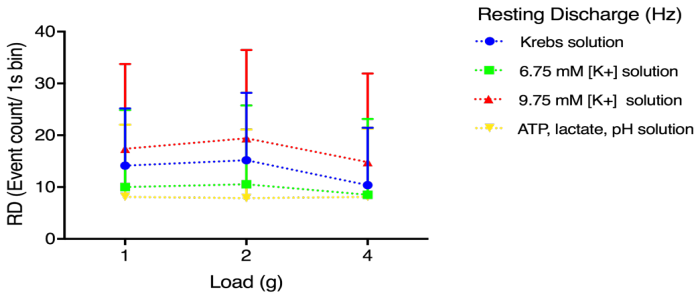
RD (Event count/ 1s bin)
40
30
20
10
0
1
2
4
Load (g)
Resting Discharge (Hz)
Krebs solution
6.75 mM [K+] solution
9.75 mM [K+] solution
ATP, lactate, pH solution

B.

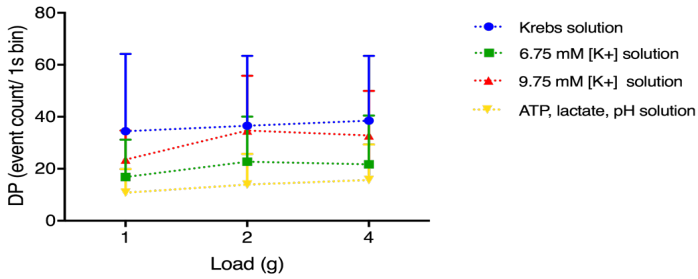
DP (event count/ 1s bin)
80
60
40
20
0
1
2
4
Load (g)
Dynamic Peak (Hz)
Krebs solution
6.75 mM [K+] solution
9.75 mM [K+] solution
ATP, lactate, pH solution

C.

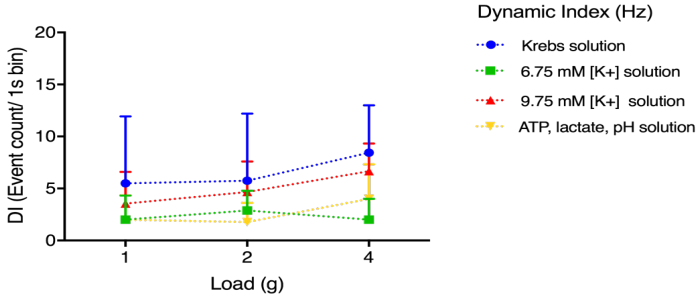
DI (Event count/ 1s bin)
20
15
10
5
0
1
2
4
Load (g)
Dynamic Index (Hz)
Krebs solution
6.75 mM [K+] solution
9.75 mM [K+] solution
ATP, lactate, pH solution

D.

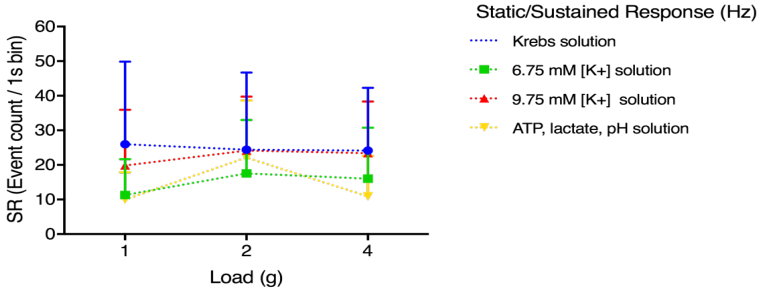
SR (Event count / 1s bin)
60
50
40
30
20
10
0
1
2
4
Load (g)
Static/Sustained Response (Hz)
Krebs solution
6.75 mM [K+] solution
9.75 mM [K+] solution
ATP, lactate, pH solution

E.

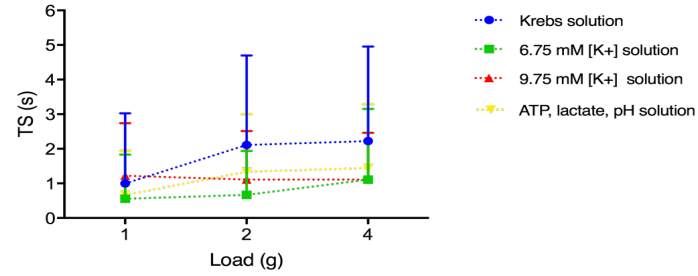
TS (s)
6
5
4
3
2
1
0
1
2
4
Load (g)
Time Silent (s)
Krebs solution
6.75 mM [K+] solution
9.75 mM [K+] solution
ATP, lactate, pH solution

Figure 2.8. Effects of applied load

The responses of 5 measured variables to 1, 2, and 4 g applied loads (x-axis) in 4 superfusing solutions: Krebs solution (4.75 mM [K^+], and three experimental solutions containing 6.75 mM [K^+] Krebs solution, 9.75 mM [K^+] Krebs solution, and a 'low metabolic mix' containing 15 mM lactate, 1 μM ATP and pH 7.0. **A**. Resting discharge (i.e. spontaneous firing rate) was slightly raised in 9.75 mM [K^+], but reduced in 6.75 mM [K^+] and in the metabolite mix (compared to Krebs solution). **B**. Dynamic Peak is calculated as the difference between the highest discharge frequency at the onset of the stretch and the resting discharge (see **Figure 2.7.B**). There was a tendency for a small increase in dynamic peak with load. Notably, dynamic peaks were suppressed in raised [K^+] and in the metabolite mix. **C**. Dynamic Index is the fall-off in firing rate between the dynamic peak response and the sustained response, reflecting adaptation to the maintained stimulus. Unsurprisingly, dynamic index parallels Dynamic Peak response (**B**) with raised [K^+] and metabolite mix having smaller responses. All responses except for 6.75 mM [K+] show an increase in their dynamic index, while the response to 6.75 mM [K+] decreased. This is to be expected, as during the application of 6.75 mM [K+] firing was reduced (for further details see (**Figure 2.12.**) **D**. Static Response is the level of maintained firing above resting discharge. This was not proportional to load, reflecting the saturating response at 2-4 g. **E**. Time silent after the removal of the load showed a slight tendency to increase with load. Again, responses in control Krebs solution were higher than that of all experimental solutions. Error bars indicate 95% confidence intervals in all graphs.

Response to 'Metabolic Mix'

The metabolite mix (ATP1 μM, Lactate 15 mM, pH 7.0) was applied by superfusion to 6 preparations with identified spontaneous firing afferents. Averaged across the 6 preparations (8 units), the addition of the metabolite mix evoked a small increase in basal firing rate in 4 units, no change in another 2 units and a small decrease in 2 unit (**Figure 2.9. A**). The average basal firing before the addition of the metabolite mix was 14.9 ± 9.4 Hz. The average firing rate after 5 minutes of superfusion of the metabolite mix was 15.9 ± 9.7 Hz (8 units, n = 6, P = 0.484, NS, t = 0.739, df =7, paired t-test). From the time of the application of the metabolite mix, the maximum firing rate of 19.5 ± 8.9 Hz occurred with a considerable delay, which averaged 9 minutes after initial exposure to the mix (**Figure 2.9 B**).

We have described above the responses of the 9 units to 1,2 and 4g stretches in the presence of Krebs solution and solutions with increased [K^+]. These responses changed in the presence of the metabolite mix. Out of the 9 units, 1 did not respond to any of the 3 stretches in the presence of the metabolite mix. Four units fired throughout the stretch, whilst 4 units had either a small burst of firing when the stretch was applied or when the stretch was removed. In the presence of the metabolite mix, the responses to 1, 2, and 4 g stretches were significantly decreased compared to Krebs solution; 1g (8 units, n = 6, P < 0.05, P = < 0.0001, t = 19.24, df = 19, paired t-test), 2g (8 units, n=6, p< 0.05, p = 0.0087, t = 2.926, df = 19, paired t-test) and 4g (8 units, n = 6, P < 0.05, P = < 0.0001, t = 18.93, df = 19, paired t-test). Mean data for the 1g and 4g stretch show the firing pattern of these afferents were similar to that observed in the Krebs solution. The 2g firing pattern was slightly different, which could be due to 2outliers in the data set (**Figure 2.10.**).

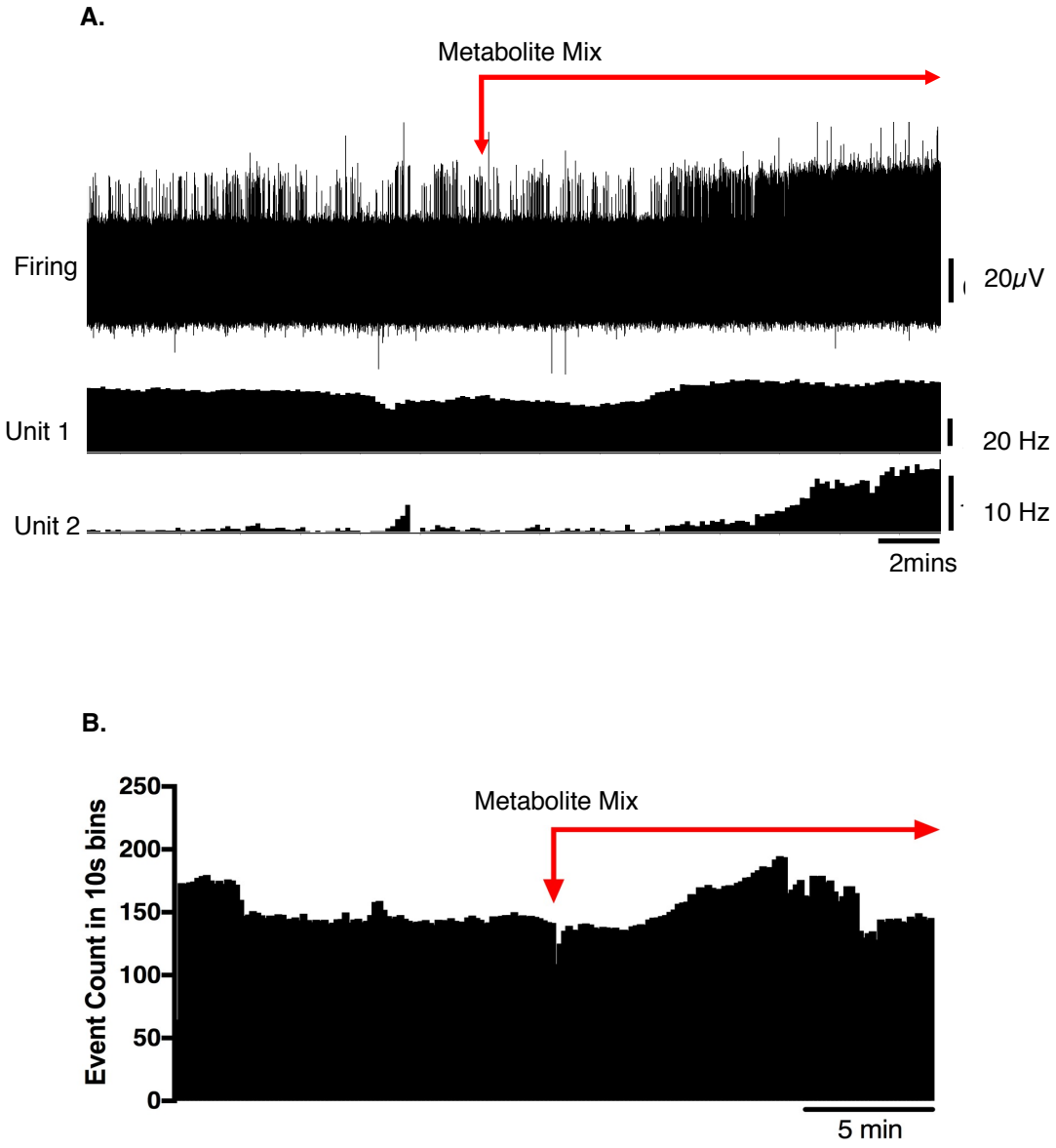

Figure 2.9. Direct activation of discriminated afferents by the metabolite mix (ATP 1μM, Lactate 15 mM and pH 7.0).

A. Typical example of the effects of application of the metabolite mix on spontaneous firing; unit 1 fired spontaneously and showed a modest response to the metabolite mix. Unit 2 was an unidentified afferent within the preparation that had slow spontaneous firing but increased its firing significantly after the application of the metabolite mix. **B**. The mean spontaneous firing rate of eight discriminated units (n = 6) during the application of the metabolite mix, averaged over 15mins (10 sec bins). Arrows demonstrate the time the metabolite mix was present. The change in firing was not significant when averaged over the 8 units P = 0.484.

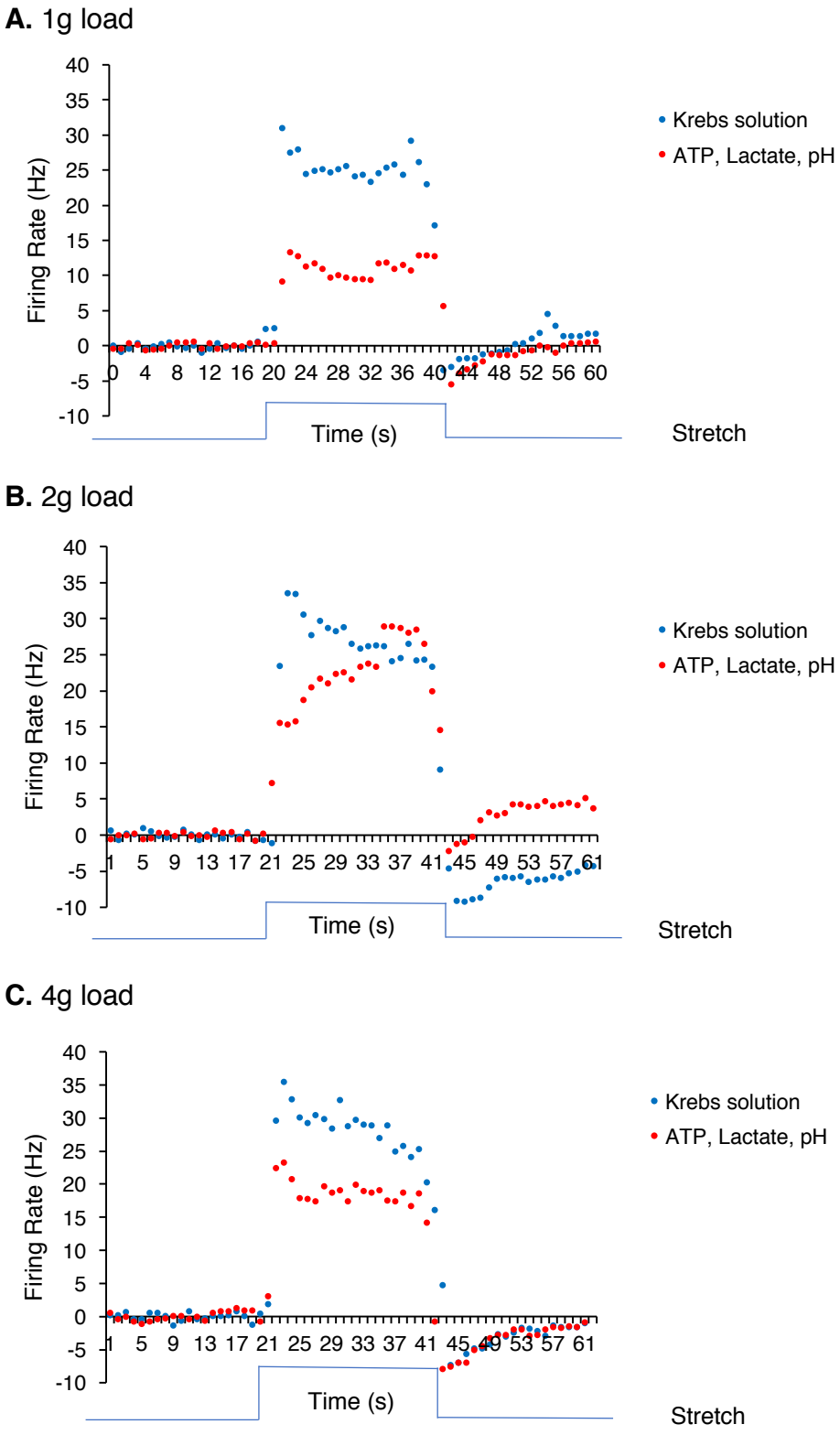

Figure 2.10. Mean responses to applied load in the presence of the metabolite mix Averaged responses to stretch responses in Krebs solution to the stretch response in the presence of the metabolite mix (red; 8 units, n = 6) were typically smaller than those in Krebs solution (blue). **A**. 1g **B**. 2g **C**. 4 g even when changes in spontaneous firing were subtracted.

Capsaicin Responses

Capsaicin (10^{-6} M) was directly applied as a single bolus dose to preparations (8 units, n = 6). None of the identified spindle afferents showed an increase in spontaneous firing rate (**Figure 2.11. A**). The average firing rate of spontaneously active afferents before the application was 10.6 ± 6.8 Hz, which is not significantly different from the average firing rate after capsaicin 11.7 ± 8.7 Hz (8 units, n = 6, P < 0.05, P = 0.2199, NS, t =1.37, df = 6, paired t-test, **Figure 2.11.B**).

Increase in potassium concentrations [K^+]

Increased potassium concentrations were used to depolarise afferents. Increasing the bathing solution concentration of [K^+] from 4.75 mM to 6.75 mM caused no increase in spontaneous firing of the afferents (**Figure 2.12. A**). The average basal firing was 12.3 ± 13.2 Hz in normal Krebs solution, while the average firing rate after the application of 6.75 mM [K^+] was 10.5 ± 11.3 Hz (8 units, n = 6, P < 0.05, P = 0.415, NS, t = 0.864, df =7, paired t-test). During the basal period, some units had occasional bursts of higher frequency firing. After application of [K^+], firing tended to become more regular, thereby evening out the spontaneous afferent firing rate (**Figure 2.12 B**).

While a small increase in potassium concentration had no effect on the spontaneously firing afferents, a larger concentration of 9.75 mM did increase basal firing (**Figure 2.13. A**). The average basal firing before the application was 13.24 ± 9.6 Hz and increased to 17.79 ± 10.3 Hz (8 units, n = 6, P < 0.05, P = 0.0272, t = 2.784, df = 7) after application, with the maximum firing occurring within the last ~5mins (**Figure 2.13. B**). Changes in firing rate were not accompanied by a detectable change in length of the preparation measured with the isotonic transducer.

Stretches of 1,2 and 4g were applied while raised of [K^+] was present in the bath. Stretches in 6.75 mM [K^+] all showed a decreased response when compared to normal Krebs solution. This was clearest with one- and two-gram loads (**Figure 2.14. A&B**) (1g (8 units, *n* = 6, P < 0.05, P = <0.0001, t = 10.22, df = 19), 2g (8 units, *n* = 6, p < 0.05, P = <0.0001, t = 12.95, df = 19)). The 4g load mean response in 6.75 mM [K^+] showed an only slightly decreased response (8 units, *n* = 6, P < 0.05, P = 0.0233, t = 2.467, df = 19, **Figure 2.14. C**).

Stretches applied in the presence of 9.75 mM [K^+] had similar results to that of the 6.75 mM [K^+] solution, although less marked. Mean responses to the 1g and 4g load showed a slight decrease in firing throughout the stretch, compared to that seen in the normal Krebs solution (1g (8 units, *n* = 6, P < 0.05, P = <0.0001, t = 6.906, df = 19, **Figure 2.15 A&C**), 4g (8 units, *n* = 6, P < 0.05, P = <0.0001, t = 17.42, df = 19)). The effect with 2g loads were slightly smaller (8 units, *n* = 6, NS, P < 0.05, P = 0.2947, t = 1.078, df = 19, **Figure 2.15. B**).

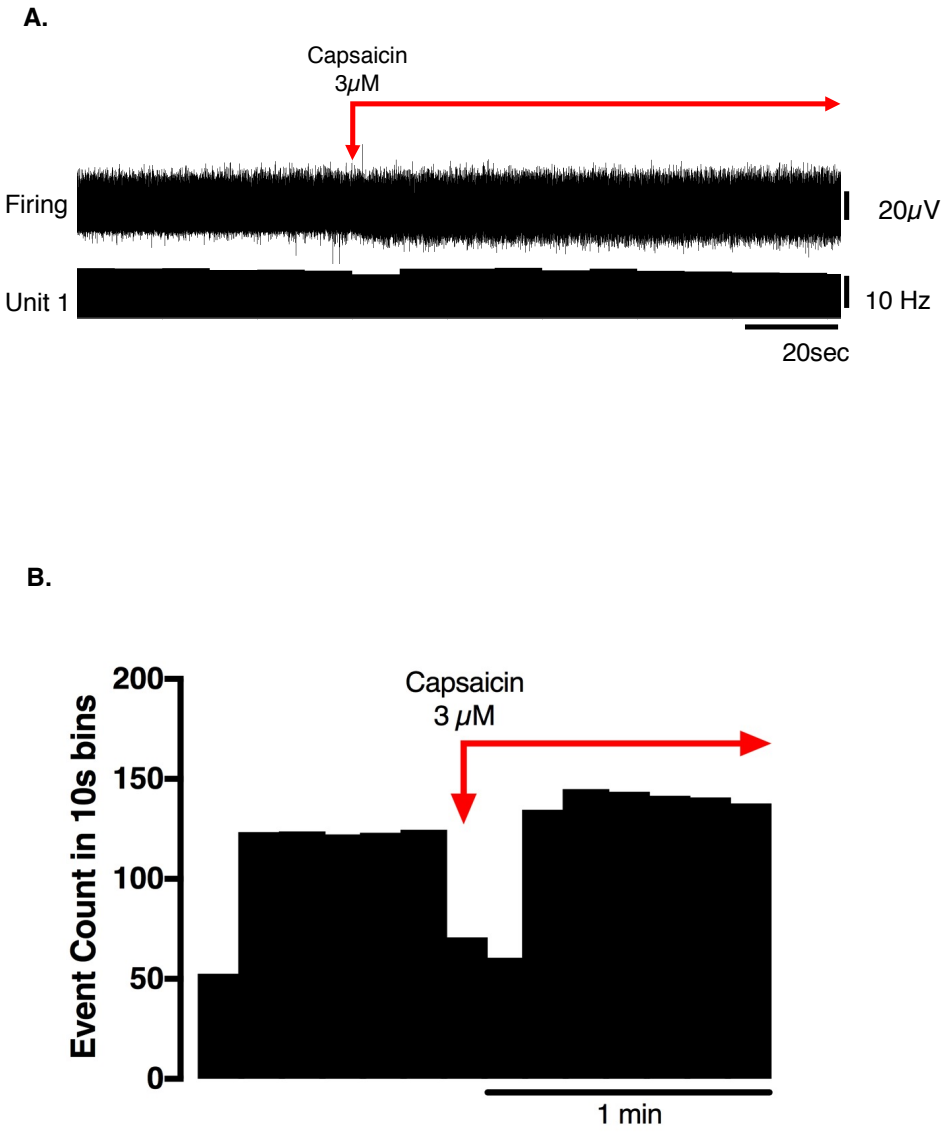

Figure 2.11. Spontaneous afferents do not respond to the application of capsaicin. **A**. Typical example of the effects of 10^{-6} M capsaicin; there was no change in basal firing rates in discriminated afferents after the application of capsaicin indicating that there were not excited by this TRPV1 agonist. **B.** The mean firing rate of spontaneously active units during the application of capsaicin 2 minutes in 10 sec bins (8 units, $n = 6$). Note that there is an artefactual drop in the firing at the same time that the capsaicin was added. This was due to mixing capsaicin into the bath with the pipette which caused noise which interfered with single unit discrimination. In other preparations in the laboratory (visceral afferents) where capsaicin has an effect on afferent firing, it causes an increase in firing that lasts several minutes (data not shown) making it unlikely that an effect was masked by the artefact.

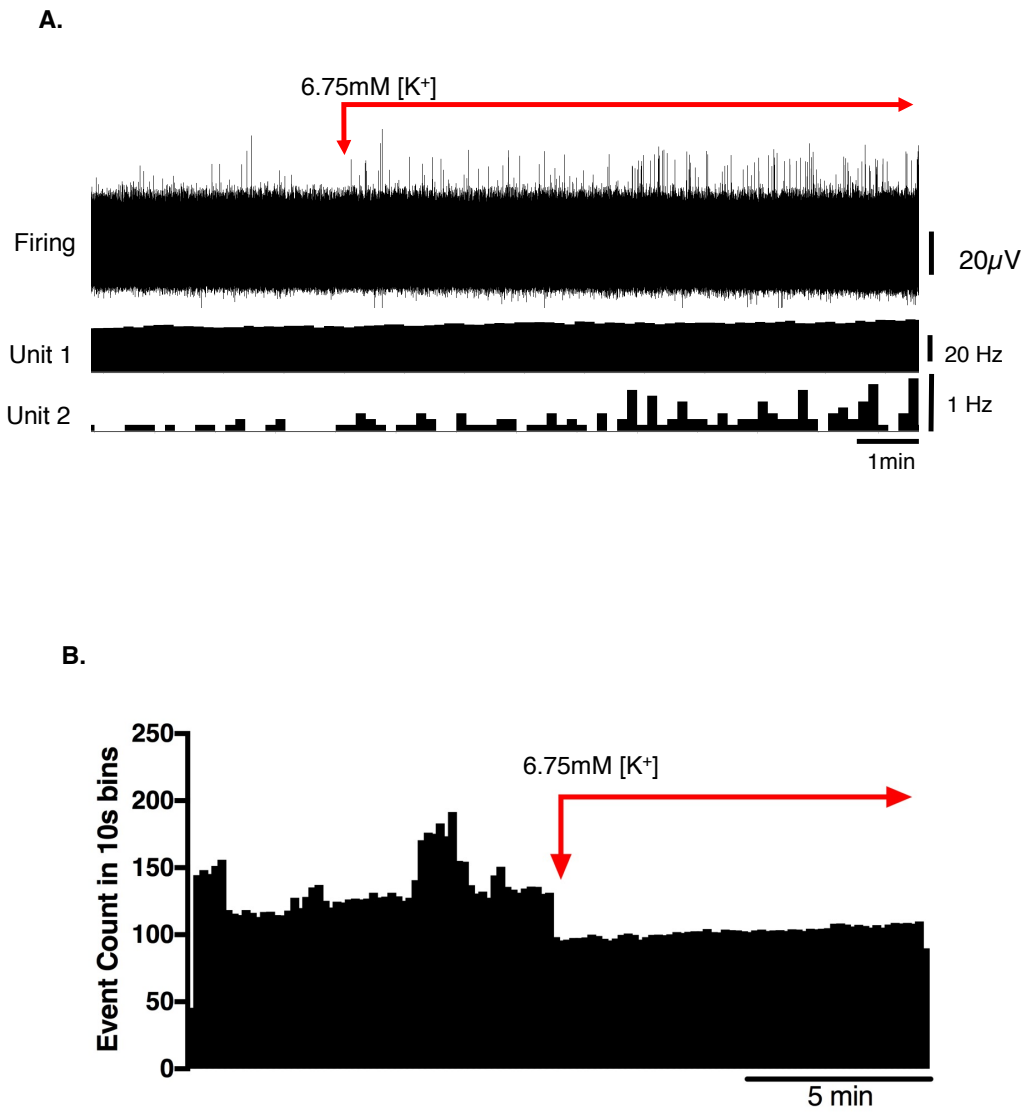

Figure 2.12. Activation of spontaneous units with increased [K^+] from 4.75 mM to 6.75 mM [K^+].

A. Typical example of the effects of application of 6.75 mM [K+] Krebs solution; unit 1 is a spontaneously firing, stretch sensitive unit that did not respond to this rise in $[K^+]_{out}$. Unit 2 showed a moderate increase in firing, demonstrating a bursty firing pattern. **B.** This figure shows the mean firing rate of 9 discriminated units (n = 6) averaged over a 10 minute period. Note that there are variations of spontaneous activity in the basal period due to occasional prolonged bursts of firing in a few units, but once the [K+] was increased (red arrows), the averaged firing became more regular, but was not increased overall.

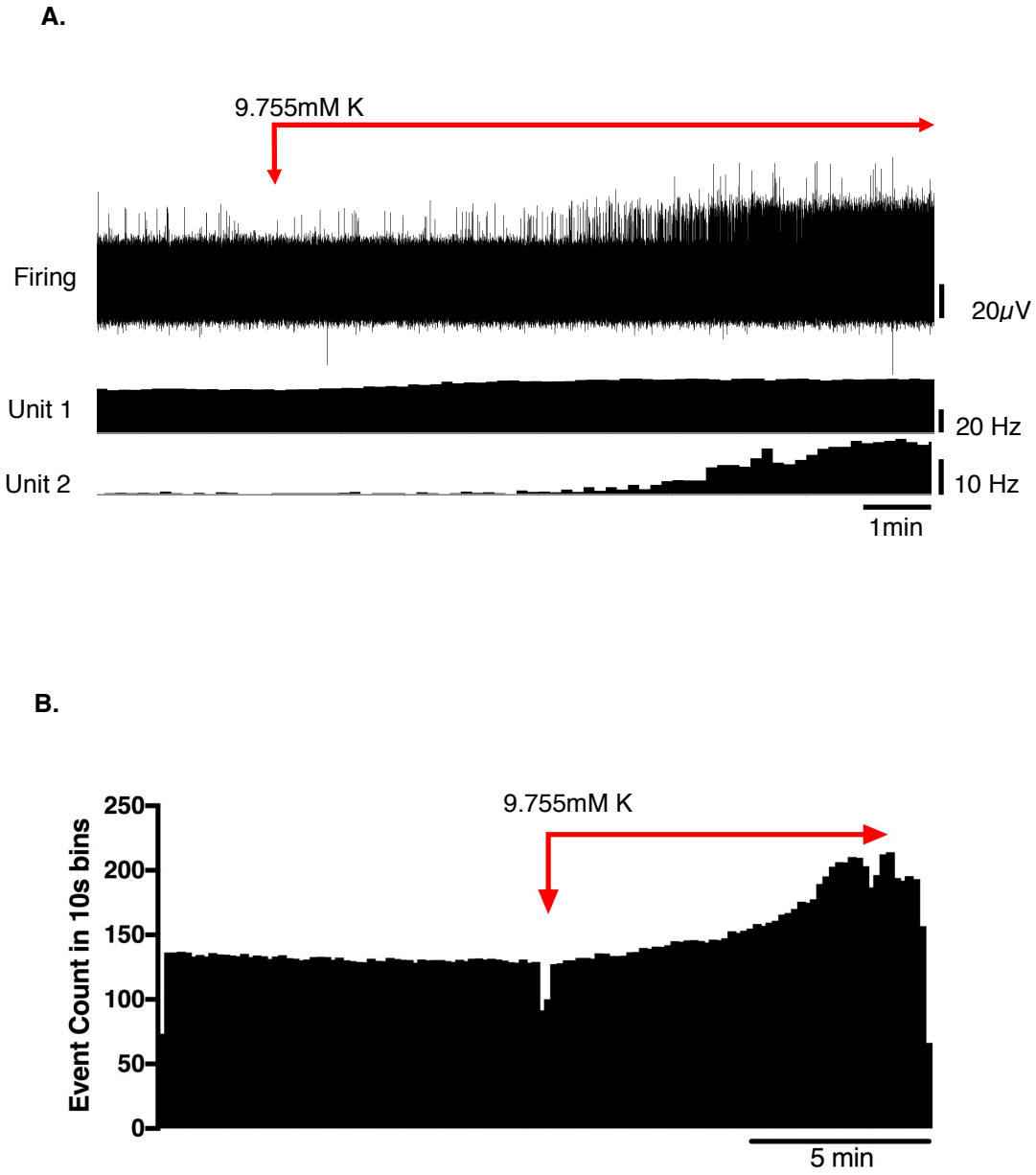

Figure 2.13. Activation of spontaneous units with increased [K+] from 4.75 mM to 9.75 mM [K+].

A. Typical example of the effects of application of 9.75 mM [K+] Krebs solution; both units are spontaneously firing. Unit 1 increases firing moderately in response to the application of 9.75 mM [K+] Krebs solution. While unit 2 increases its firing rate quite dramatically in response to the 9.75 mM [K+] Krebs solution. Note the delay before the increasing response. **B.** The mean firing rate of 8 discriminated units (n = 6) averaged over 10 minutes in 10 s bins.

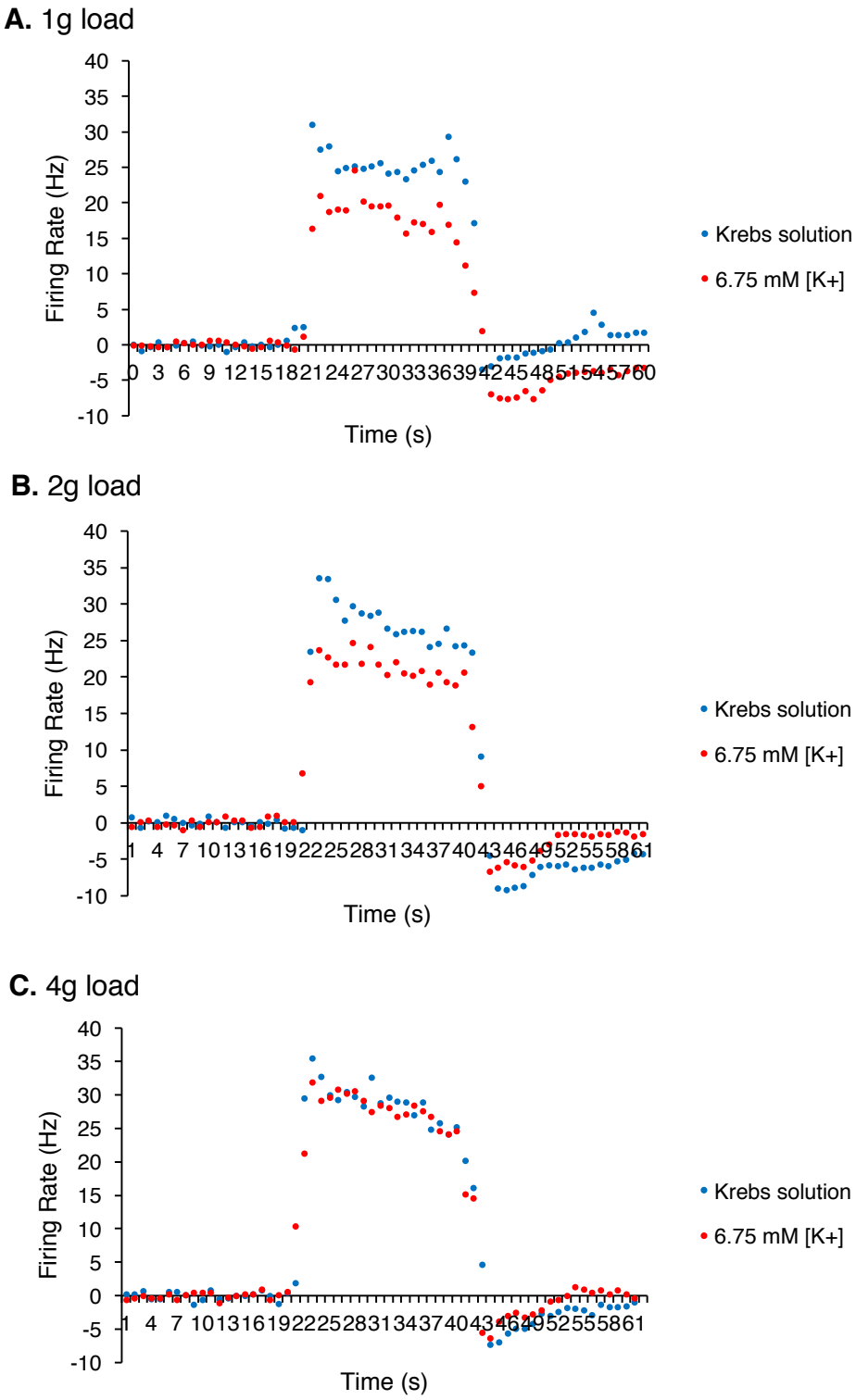

Figure 2.14. Mean responses to applied load in the presence of 6.75 mM [K+] solution.

Comparing responses in normal Krebs solution to the stretch response in the presence of the 6.75 mM [K^+] Krebs solution (9 units, n = 6, Blue dots = Krebs solution, Red dots = 6.75 mM [K^+] Krebs solution). Responses at **A**. 1g and **B**. 2g were significantly decreased compared to the responses in normal Krebs solution, while this was less pronounced with 4g loads (**C**).

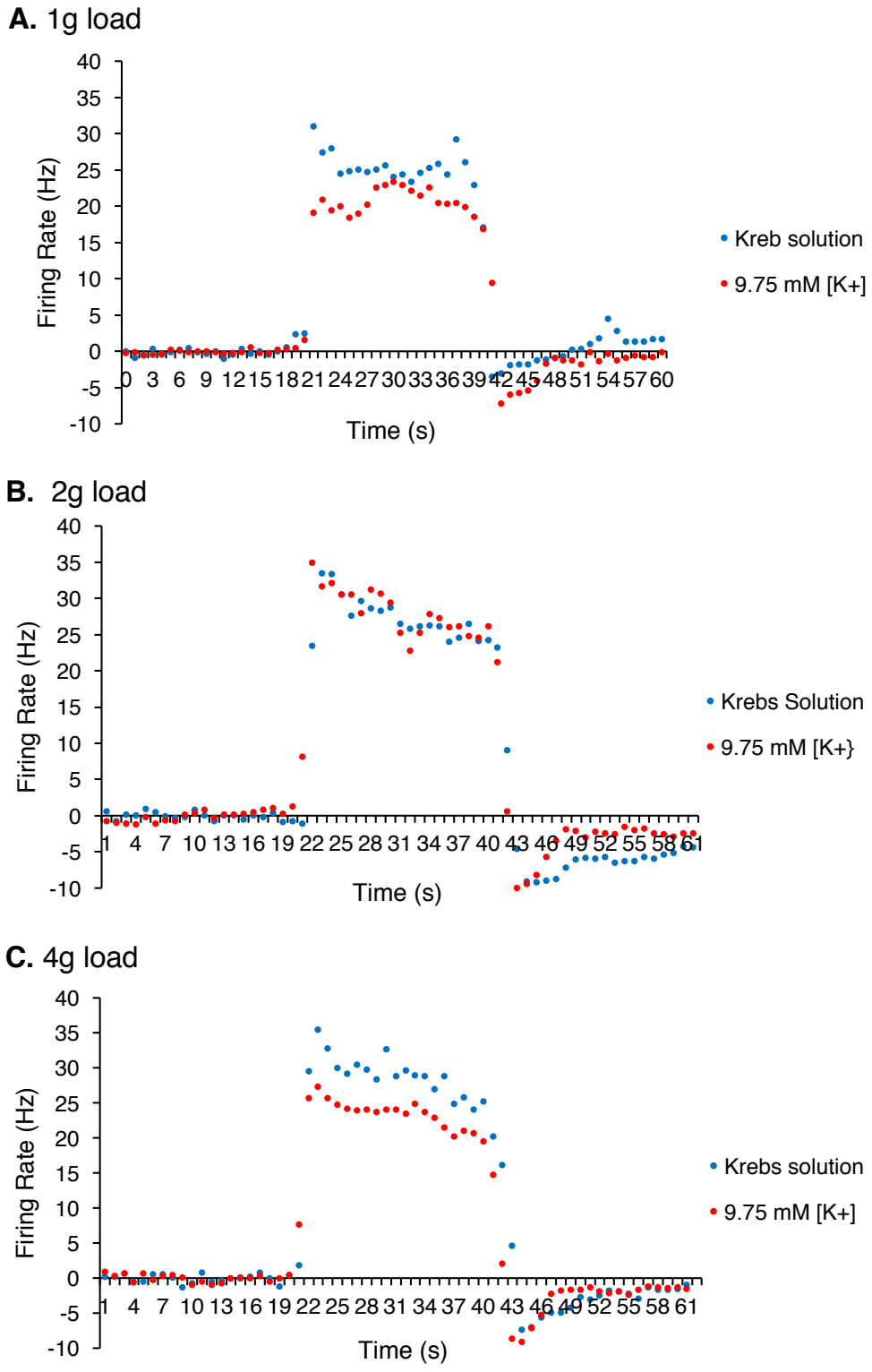

Figure 2.15. Mean response to applied load in the presence of 9.75 mM [K^+] solution.

Comparing responses in normal Krebs solution to the stretch responses in the presence of the 9.75 mM [K^+] Krebs solution (9 units, n = 6). Overall the firing rate of stretch-responsive units was decreased in the presence of the 9.75 mM [K^+] Krebs solution. This was evident at 1 g and 4 g (**A**, **C**) but, was less apparent in 2 g (**B**). (Blue dots = Krebs solution, Red dots = 9.75 mM [K^+]).

Correlation of electrophysiology and morphology

After mapping the receptive fields of the spontaneous afferents on a micrograph of the preparation, rapid anterograde tracing was applied to the recorded nerve trunk for a period of 4 hours in organ culture conditions. The carbon particle landmarks applied to the surface of the preparation mostly remained visible after fixation and were used to identify precisely the extent of the receptive field in the fixed, labelled preparation. Preparations were mounted between two coverslips so that they could be viewed from either side (see methods). Out of the 7 preparations with identified, mapped spontaneously active units, we were able to identify the discriminated axon and ending in 5 preparations unequivocally. In these five preparations, a single axon was present in the receptive field. It terminated with an elongated spiral ending, with axonal rings wrapped around the muscle fibre (**Figure 2.16.A & Figure 2.17. A**). A capsule was seen surrounding the ending, and these endings were aligned with the muscle fibres. Based on the literature, the muscular ending we describe here were muscle spindle afferents. In each case, our dye fills revealed the primary ending of the muscle spindle (**Figure 2.16. B**). Secondary or 'flower spray' endings may also have been labelled (**Figure 2.17 B.)** in 2 out of 5 preparations but fine axonal branching could not be adequately resolved due to high background labelling, autofluorescence and blurring in the thick tissue of the muscle spindles.

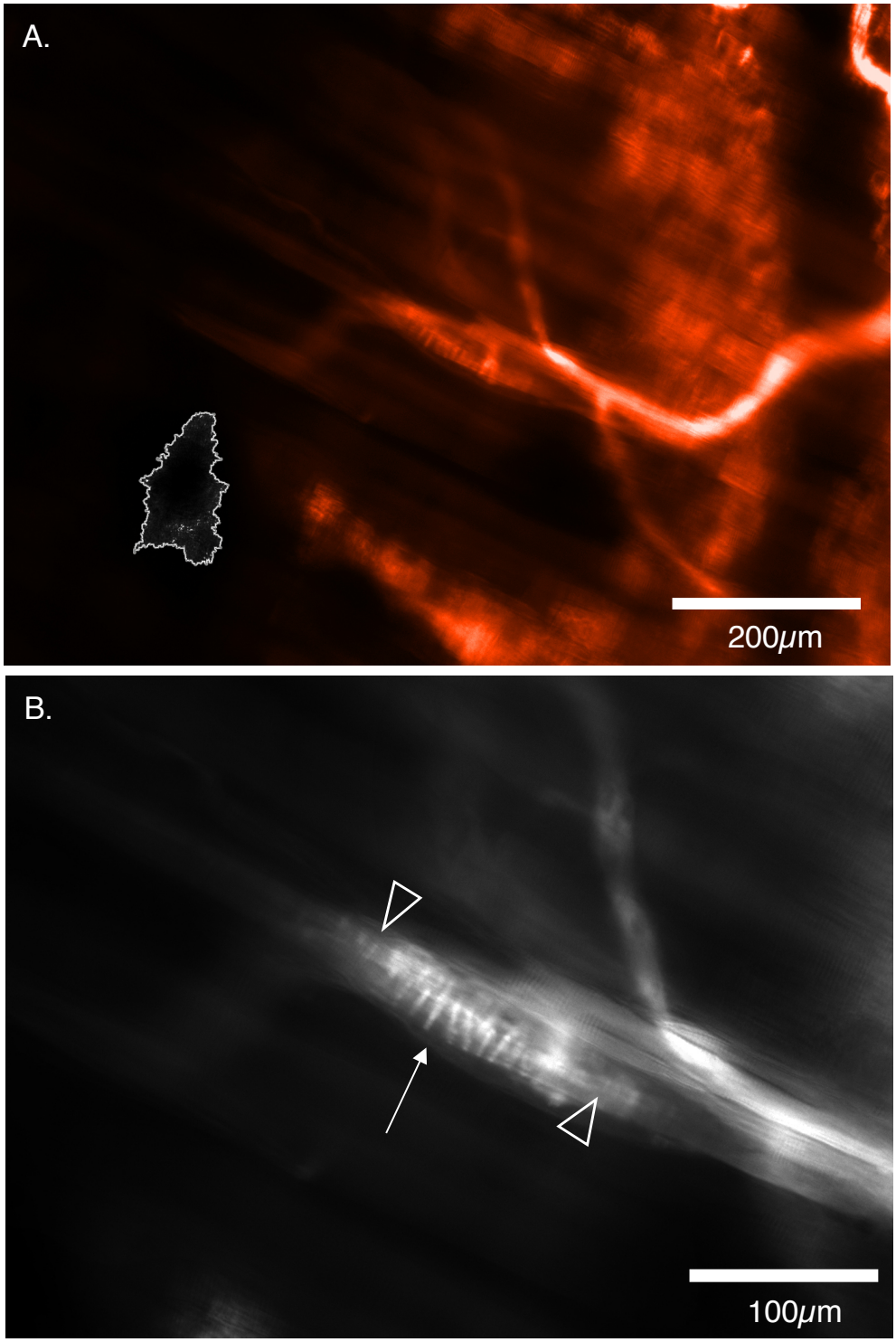

Figure 2.16. Specialised endings of identified spontaneous afferents.
A. Medium power micrograph of a biotinamide filled spontaneous afferent identified as the only axon and ending within the mapped field of innervation. Superimposed and outlined in white is a carbon marker used to locate the receptive field. **B**. A higher power micrograph of the same ending. Note the continuous smooth axon that terminates with a spiral ending, that appears to wrap rings around a muscle fibre and the capsule that surrounds it (white arrow). There may also be secondary endings behind and alongside the first larger spiral ending, indicated by the arrow head.

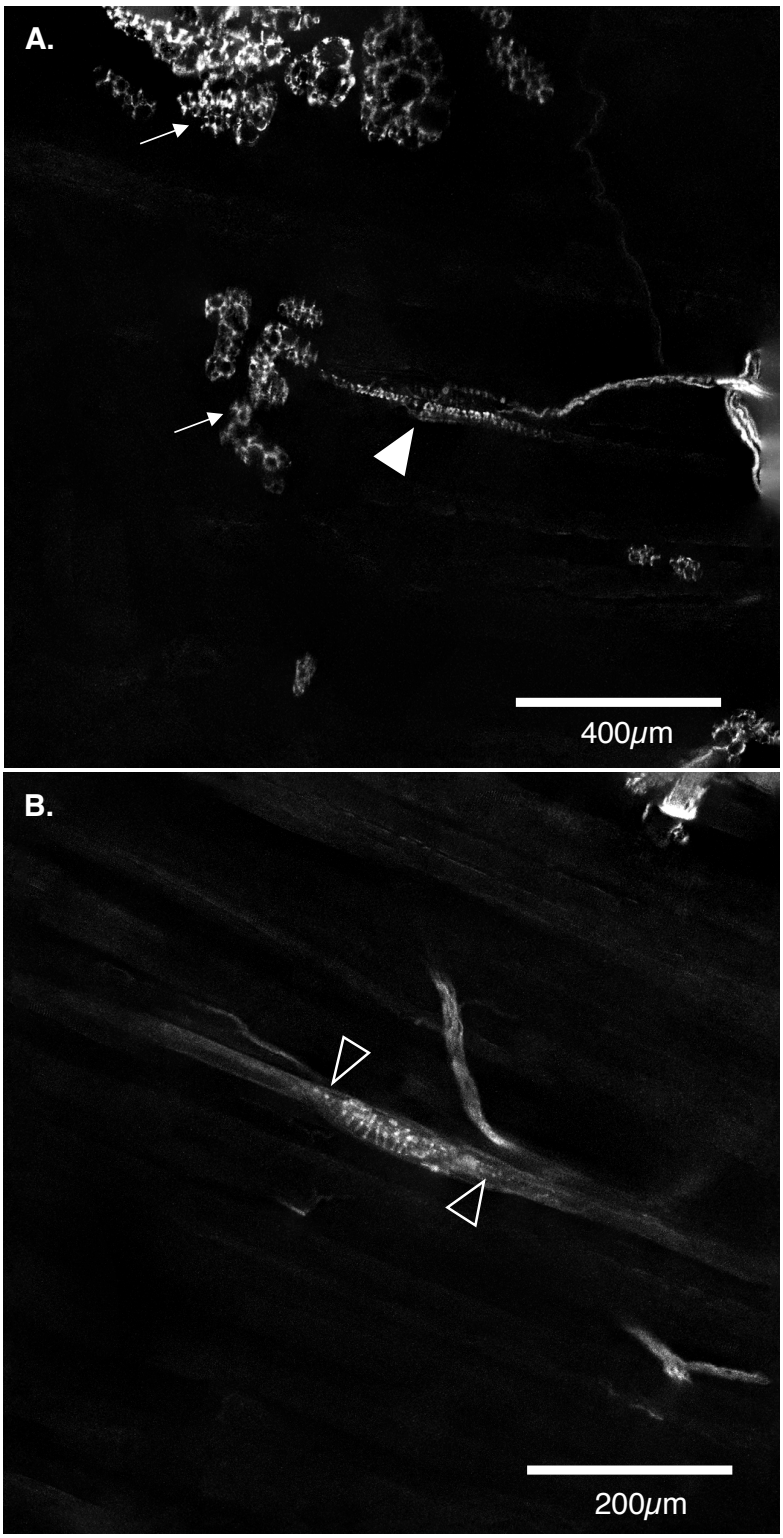

Figure 2.17. Confocal images of axonal branching and spiral endings of identified spontaneous afferents.

A. A biotinamide labelled axon that terminates as a long thin spiral ending (white arrow head). Note that streptavidin also labels endogenous biotin present within fat cells (white arrows). **B**. Higher power micrograph of another identified afferent, demonstrating the spiral structure of the primary ending in the centre of the fibre. Note the arrow heads, indicating possible secondary endings that are visible either side of the spiral ending.

DISCUSSION

In the present study, we adapted a combination of techniques previously used in preparations of visceral organs, to successfully investigate the sensory innervation of skeletal muscle. We established a whole-mount abdominal muscle preparation that allowed the correlation of morphological characteristics of functionally identified sensory neurons in a systematically controlled environment. In this chapter, we recorded the functional characteristics of extensively studied muscle spindle afferents and correlated this to their known distinctive morphology. This demonstrating the utility of the preparation and the suitability of the techniques to characterise somatic afferent endings both physiologically and morphologically.

A preparation that has the ability to relate morphology to functional characteristics has been reported for several classes of visceral afferent neurons in the gut, using a rapid anterograde tracing technique (Tassicker et al., 1999), which can be combined with *ex vivo* afferent recordings. These techniques have identified vagal intraganglionic laminar endings (IGLEs) as the transduction sites of low threshold mechanoreceptors in the stomach and oesophagus (Zagorodnyuk and Brookes, 2000), rectal IGLEs as a distinct class of low threshold sacral mechanoreceptors in the distal bowel (Lynn and Brookes, 2011b, Lynn and Brookes, 2011a) and varicose axons on blood vessels as transduction sites of mechano-nociceptors in the small and large intestine (Song. X., 2009). In skeletal muscle, methods to unequivocally relate the morphology of group III and IV afferent endings to their functional characteristics have not previously been reported (Diehl et al., 1993, Mense, 2009).

In the present study, we used well-known sensory endings (muscle spindle afferents) to validate our preparation and techniques. We adapted methods to an *ex vivo*

preparation of murine abdominal muscles, which allowed the visualisation and characterisation of muscle spindle afferents in a flat sheet preparation. The preparation could be viewed microscopically as a wholemount, thus removing the need for sectioning or 3D reconstruction. Mounting the preparations between pairs of coverslips allowed viewing from both sides, often improving visualisation of fine nerve endings that would otherwise be blurred by looking through the thickness of the preparation. In such preparations, the fields of innervation of single afferent axons could be mapped on the surface of the preparation from their mechanonsensitive responses to von Frey hairs. Subsequent immunohistochemical labelling and anterograde tracing could then be related to the axons of single, characterised afferents. With all the precautions taken when selecting the preparation, and the techniques used to visualise afferent endings, the thickness of muscle itself was still a limitation. Even with using the double-sided slides, when viewing the muscle using higher magnification, blurring and distortion occurred. When labelled structures were within the middle of a thick part of the preparation, some details were obscured even with the use of confocal microscopy.

We have shown using our preparation that we are able to record the well described functional characteristics of muscle spindles, both primary and secondary afferent responses. These responses have been described as early as the 1960's, in cats, frogs, rabbits and other species (Matthews, 1964). Muscle spindle primary afferents and secondary afferents can both have spontaneous firing, as described in the present study. Recent human studies using microneurography, a technique in which a fine tungsten electrode can be inserted into nerves of an awake human, have shown that muscle spindle afferents also show spontaneous firing (Macefield and Knellwolf, 2018). However, spindles in muscles involved in body weight loading, for example in

the foot, are often not spontaneously active (Knellwolf et al., 2019).We have demonstrated that the firing patterns in response to von Frey hairs and stretch seen in the present study are similar to those previously described in the literature (Franco et al., 2014, Macefield and Knellwolf, 2018, Matthews, 1964, Matthews, 2015, Wilkinson et al., 2012). Primary muscle spindle afferents have a characteristic large initial response to the dynamic phase of the stretch, which exceeds the maintained firing rate ("static component") during prolonged stretch. Once the stimulus is released these afferents cease firing temporarily, taking up to seconds before the spontaneous firing of these afferents reoccurred (Franco et al., 2014, Matthews, 1964, Merton, 1951, Wilkinson et al., 2012). Secondary muscle afferents do not give rise to this large dynamic response but increase firing within the static portion of the stretch. Typically, they return to spontaneous firing rates once the stretch in removed (Bewick and Banks, 2015, Jansen and Matthews, 1962). Both types of responses were seen in the present study of mouse abdominal muscles ex vivo.

A difference between the current study and previous studies in the literature is the method in which the stretch was applied. The type of stretch applied in the present study was a step-stretch. Many previous studies that investigated muscle spindle afferents specifically used a ramp and hold stretch or sinusoidal stimuli. This could explain the why dynamic peak and dynamic index values in the present study vary from those cited in the literature (Franco et al., 2014, Wilkinson et al., 2012). The dynamic phase in these preparations, due to the type of the stretch, is shorter and the preparation is pulled quickly in response to the applied load. Even though this was the case, some units still had a significant increase in firing during the dynamic phase of this type of stretch, while others fired tonically throughout the stretch. The conduction velocities recorded in this study align within what is stated within the literature for

mice. Our mean conduction velocity was 22.2 ± 4.8 m/s and ranged from 13.6 – 35.8 m/s. Like previous studies that have investigated these afferents *ex vivo*(Franco et al., 2014, Wilkinson et al., 2012). It should be noted that with the small sample size used in this validation study, we were not able to discriminate between group Ia and group II based only on their conduction velocity.

In the current study, we investigated the response of muscle spindle afferents to increased $[K^+]_{out}$. Increasing $[K^+]_{out}$ concentration should depolarise endings, via changes in the K^+ equilibrium potential and thus excite afferents (Adrian, 1956). In the studies at hand, increasing $[K^+]$ had an opposite effect, thereby, suggesting that there were additional effects, probably mediated by complex interactions of ion channels. It has previously been reported that increasing external $[K^+]$ reduces the generator potential in frog muscle spindle afferents and it is possible that this mechanism contributes to the reduced firing to stretch (Husmark and Ottoson, 1971). One potential explanation is that increasing $[K^+]_{out}$ activates an inwardly rectifying K^+ channel such as $K_{IR}2.1$, which can evoke hyperpolarisation in some cells (Longden et al., 2017). To confirm the mechanism behind these responses would require more detailed studies.

We also describe the responses of muscle spindle afferents to a metabolite mix. Superfusion of the metabolite mix had no effect on muscle spindle afferent firing but significantly reduced their response to stretch. The metabolite mix was applied as a mixture that had been reported to activate metaboreceptor/ ergoreceptor sensory neurons responsive to muscle activity (Jankowski et al., 2013, Light et al., 2008)(for further details see **Chapter 3**).

Primary endings of muscle spindles are described as having a large ‘annulospiral’ ending that forms loops around the central portion of the intrafusal muscle fibre (Adal, 1984, Barker, 1948, Bewick and Banks, 2015, Ruffini, 1898). In the current study, we have anterogradely labelled functionally identified units with endings that match the description above. The endings are surrounded by a capsule, with the ending itself forming loops around an individual muscle fibre. We could not visualise the fine details of secondary endings within our preparations probably due to the poor optics caused by the thickness of the preparation. Although, a wholemount preparation allows the ability to follow nerves through the preparation, distortion caused by the bulk of tissue made it difficult to focus into the middle of the preparation. The tissue clearing process and mounting solution called "ScaleS" (Hama et al., 2015) was tested, but did not improve the optical qualities of the preparations (data not shown). After discriminating the recorded units, based on their firing pattern in response to stretch, three out of the nine units were tentatively classified as possible secondary endings. The preparation and techniques used within this study have been validated, although it may be hard to resolve adequately fine details of structures deep within the thickest parts of the muscle preparation, despite using double-sided slides.

Overall, the lack of knowledge about distinct types of sensory neurons that innervate skeletal muscle has hindered the development of a comprehensive understanding of the basic sensations from the skeletal muscle, such a pain and muscle fatigue. The present study provides a new preparation and method in which these problems can be addressed. This allows a wide range of studies to identify the morphology of functionally characterised group III and group IV muscle afferents for the first time.

CHAPTER THREE

CHARACTERISATION OF ONE CLASS OF GROUP III SENSORY NEURONS INNERVATING ABDOMINAL MUSCLES OF THE MOUSE

INTRODUCTION

Muscle afferents have cell bodies in dorsal root ganglia, with axon terminals that transduce stimuli in muscles and associated tissue. Muscle afferents are commonly classified as Groups I - IV, based on conduction velocity. Group I and II fibres are fast conducting with specialised endings in muscle spindles or tendon organs, whereas group III and IV afferents are slower conducting, with roles in nociception and encoding muscle metabolic and mechanical states (Rotto and Kaufman, 1988, Mense, 1993). Group III and IV fibres play important roles in the exercise pressor reflex as described in the review of literature (**chapter 1**)(Amann et al., 2015, Amann and Light, 2015).

Early studies reported that some small-diameter afferent fibres were associated with muscle pain (Messlinger, 1996, Weddell and Harpman, 1940). Since these initial experiments, the functional roles of group III and IV muscle afferents have been widely investigated. It has been established that some group III and group IV muscle afferents are nociceptive, responding to noxious levels of mechanical, chemical, and thermal stimuli (Jankowski et al., 2013, Mense, 1977, Diehl et al., 1993, Mense, 2009). Other group III and group IV afferents are probably non-nociceptive, being activated by chemical, mechanical, and metabolic stimuli within the physiological range. A subset of group III and group IV muscle afferents function as ergoreceptors, which are activated by contraction, stretch, and by metabolites released by working muscles (Amann et al., 2015). Group III and group IV ergoreceptors regulate circulation and ventilation via the exercise pressor reflex in both animal and humans (Alam and Smirk, 1937, Amann et al., 2015, Weavil et al., 2015). Group III and group IV afferents have been extensively investigated in terms of function, although many of their basic

anatomical and morphological properties remain largely unknown (Jankowski et al., 2013, Diehl et al., 1993, Mense, 2009).

Stacey (1969) examined the morphology of afferent terminals in striated muscle and described 'free nerve endings' that terminated throughout the muscle without corpuscular or specialised receptive endings (Stacey, 1969). These were attributed to Group III and group IV afferents. Immunohistochemical localisation of calcitonin gene-related peptide (CGRP) and substance P revealed numerous small diameter fibres within the skeletal muscle, some with structures similar to the Group III and IV endings described by Stacey (Barry et al., 2015, Tamura et al., 1996, Tsukagoshi et al., 2002, Tsukagoshi et al., 2006).Free nerve endings do not comprise a homogenous group, but probably consist of several functionally and morphologically different types (Diehl et al., 1993). However, to date, it has not been possible to relate the morphological features and physiological characteristics of any group III or group IV muscular afferents. However, methods to achieve this have been used extensively in visceral preparations (Lynn and Brookes, 2011a, Song. X., 2009, Zagorodnyuk and Brookes, 2000) and **Chapter 2** validated the use in skeletal muscle and somatic sensory neurons. In the present study, mechanoreceptors were electrophysiologically recorded in nerve trunks to the abdominal wall musculature *ex vivo*. Their fields of innervation were marked on the tissue, then their morphology was determined by anterograde labelling of axons in the recorded nerve trunk.

METHODS AND MATERIALS

Ethical approval

C57Bl/6 mice (n= 55, 40 female and 15 male), between the ages of 4-8 weeks (bred in-house), given *ad libitum* access to food and water, were euthanized by a lethal dose of isoflurane by inhalation, followed by removal of the heart. All procedures were performed in accordance with *Australian Code for the Care and Use of Animals for Scientific Purposes* (8^{th} ed, 2013, National Health and Medical Research Council of Australia) and were approved by the Animal Welfare Committee (permit #890/15) of Flinders University. The abdominal wall musculature (external oblique, internal oblique, transversus abdominis and rectus abdominis) was removed from the animal, along with the lower ribs on the right side, for orientation. The external oblique and rectus abdominis were then removed, leaving a preparation of internal oblique and transversus muscle which was pinned in a petri dish lined with Sylgard (Dow Corning, Midland MI), containing Krebs solution (in mM: NaCl, 118; KCl, 4.75; NaH_2PO_4, 1.0; $NaHCO_3$, 25; $MgCl_2$, 1.2; $CaCl_2$, 2.5; glucose, 11; bubbled with 95% O_2/5% CO_2) and warmed to 37°C.

Tissue fixation and processing

Samples used for immunohistochemistry were fixed in modified Zamboni's fixative (0.2% saturated picric acid in 2% paraformaldehyde in 0.1 mol L^{-1} phosphate buffer, pH 7.2) for 24 hours. The tissue was then washed in phosphate buffered saline (PBS) (3x 10 minutes), permeabilised and cleared with dimethyl sulphoxide (DMSO) (2x 10 minutes, 1x 30 minutes) and rinsed in PBS (3 x 10 minutes). The samples were then treated with Triton X-100 (0.5%) in PBS on a mixing tray at room temperature overnight. After 24 hours, the samples were rinsed in PBS, then further permeabilised in 100% Glycerol with 0.1% sodium azide, on a rocker tray in a humidified incubator

at 37°C for 24 hours. Samples were then washed with PBS solution (3 x 30mins) to remove the glycerol.

Immunohistochemistry

Preparations of abdominal muscle (*n*=4*)* were incubated with primary antisera at room temperature for 2 days (anti-protein gene product 9.5 (PGP9.5- RA95101; Ultraclone, Wellow, UK; raised in rabbit, 1:400), anti-calcitonin gene-related peptide (CGRP-IHC6006; Peninsula, CA, USA; raised in rabbit, 1:1000) or (CGRP Arnell, NY, USA; raised in goat, 1:1000), anti-smooth muscle actin (SMA) (A2547; Sigma-Aldrich, MO, USA; raised in mouse, 1:1000) or anti-tyrosine hydroxylase (TH) (Ab113; Abcam, Cambridge, MA, USA; raised in sheep, 1:500). Preparations were rinsed three times in PBS and incubated with the appropriate secondary antisera for 4 hours (all raised in donkeys and obtained from Jackson ImmunoResearch: anti-rabbit IgG CY3, 1:100 and 1:400, anti-sheep IgG CY5, 1:100, anti-mouse IgG AMCA 1:100, anti-mouse IgG CY3, 1:200) at room temperature. Details of antibody combinations are summarised in Table 3.1. After final rinse with PBS, preparations were equilibrated with 50%, 70% and 100% carbonated-buffered glycerol and mounted in 100% carbonate buffered glycerol (pH 8.6).

Table 3.1. Primary and Secondary antibodies combinations

Primary Antibody	Source	Species	Dilution	Secondary Antisera	Dilution	Source
Calcitonin Gene Related Peptide	Arnell	Goat	1:1000	Donkey anti-sheep CY5	1:100	Jackson
Protein Gene Product 9.5	Ultraclone	Rabbit	1:400	Donkey anti-rabbit CY3	1:100	Jackson
Smooth Muscle Actin	Sigma	Mouse	1:1000	Donkey anti- mouse CY3	1:100	Jackson
Tyrosine Hydroxylase	Abcam	Sheep	1:500	Donkey anti-sheep CY3	1:100	Jackson
Biotinamide	(See	below)		CY3-conjugated Streptavidin	1:500	Molecular Probes

Anterograde labelling

The preparation was pinned in a purpose-built chamber for anterograde labelling of axons in the nerve trunk (Zagorodnyuk and Brookes, 2000). The end of the nerve trunk was led into a side-chamber filled with paraffin oil (sealed with a partition made from a cover slip, with a silicon grease seal (Ajax Chemicals, Castle Hill, NSW, Australia). A drop of biotinamide solution (Molecular Probes, Eugene, OR, USA) in "artificial intracellular medium" (150 mM monopotassium L-glutamic acid, 7 mM

$MgCl_2$, 5 mM glucose, 1 mM EGTA, 20 mM HEPES, 5 mM disodium adenosine-triphosphate, 0.02% saponin, 1% dimethyl sulphoxide) was placed onto the de-sheathed nerve trunk under the paraffin and the main chamber was filled with sterile culture medium (Tassicker et al., 1999). Preparations were incubated for 4 hours on a rocking tray in a humidified incubator at 37°C, 5% CO_2 in air, then fixed overnight in modified Zamboni's fixative (as above) at 4°C. Preparations were permeabilised and cleared using the immunohistochemical protocol described above. Biotinamide was visualised by CY3-conjugated streptavidin (1:500, Molecular Probes, 4 hours). Preparations were then immunohistochemically labelled (n=10), rinsed three times in PBS and mounted in 100% carbonate-buffered glycerol (pH 8.6) as described above. Preparations were mounted between two coverslips, with the lower coverslip fixed to a 1mm thick aluminium surround so that they could be viewed from either side on the microscope.

Close extracellular single unit recordings

A total of 41 preparations were studied electrophysiologically during the course of this study. Single unit recordings were made from the exposed nerve trunk inside the paraffin bubble with a 100µm Pt/Ir wire electrode. Signals were amplified (ISO-80, WPI, Sarasota, FL), recorded at 20-40kHz (PowerLab16s/p, LabChart 7 Pro software, AD Instruments, Sydney, Australia) and visualised on an oscilloscope (National, VP-5220A). Single units were discriminated by amplitude and duration using Spike Histogram software (Spike Histogram software, ADInstruments). In some preparations, two recording electrodes, attached to separate amplifiers, were placed on the same nerve trunk in two separate paraffin bubbles, several millimetres apart. Conduction velocity of individual units was calculated by dividing the distance

between the two recording electrodes by the time delay of discriminated action potentials between them (n= 10).

Transduction delay

Transduction delays were measured for identified CT3 afferents comparing latencies of responses to mechanical and electrical stimuli. Firstly, the receptive field of a CT3 afferent was mapped on the preparation and mechanosensitive "hotsposts" were marked with carbon-particles applied via the tip of the von Frey hair. Then, the distance between the identified receptive field and the recording electrode was measured. A purpose-designed piezoelectric probe was positioned over a marked transduction site (hotspot) in a way in which it just contacted the preparation without activating it mechanically. When the probe was activated by a large electrical pulse, it generated sufficient movement to locally distort the preparation and reliably activate the afferent ending. This led to an action potential being recorded at a fixed latency after the stimulus was applied. This same afferent was then activated electrically via a stimulating electrode placed at exactly the same marked site. A single electrical pulse that was just supra-threshold was administered to the preparation (variable voltage, 0.5 ms duration) to just evoke an action potential at the recording electrode.

By comparing the delays of the responses to mechanical and electrical stimuli, the transduction delay could be calculated. It was assumed that the response to the focal electrical stimulus was instantaneous. The mechanical stimulus always evoked an action potential with a longer delay. Part of this was due to the time taken to distort the tissue. This was measured by using the probe as a switch in a small battery-operated circuit. When the probe advanced it closed the switch and the battery voltage was recorded; the delay to move the probe was measured as 0.7 ms.

Static and Dynamic Stretch

In preparations, a purpose-built 8-mm array of hooks (Biomedical Engineering, Flinders Medical Centre, South Australia) was used to connect the preparation via a cotton thread to the lever of an isotonic transducer (52-9511, Harvard Biosicence, South Natick, MA, USA). In all cases there was a resting counterweight of 0.5 g, due to the weight of the metal hook, and the weight of the isotonic transducer lever. The preparation was placed on the metal hook (and thereby 5 mN tension) before recording started, therefore, ensuring that the recording and firing of afferents were not affected by the addition of the hook afterwards. Static or step stretches were applied by applying additional counterweights to the isotonic lever. Constant forces could thus be applied, stretching the muscle evenly across its width, while measuring changes in the length of the preparation. Counterweights of 1 - 20g were applied to the isotonic lever for 30 s. A minimum rest period of 3 min was allowed between all stretches. Graded loads were applied by infusing fluid into a reservoir (0.5g resting weight corresponding to ~5mN load) that formed the counterweight at 0.02, 0.043, 0.08, 0.16 g/s) to a peak level of 2.0g (~ (see (Lynn et al., 2005, Lynn et al., 2003)).

Focal compression and capsaicin application

With the muscle under 5 mN resting tension, mechano- transduction sites were localised by probing the muscle with a 1.0 mN von Frey hair. Transduction sites were identified by bursts of action potentials and were marked on the tissue, using fine carbon particles applied via the tip of the von Frey hair. At the end of the mapping period, preparations with carbon marks were photographed (Olympus C-4040 digital camera) in the dissecting microscope (Olympus, SZ-STU1). The field of innervation was then mapped in detail using the von Frey hair and plotted on a printout of the

micrograph. In some studies, a range of von Frey hairs was tested (20mg, 50mg, 100mg, 200mg, 300mg, and 400mg). The effect of capsaicin (1μM final concentration) was also recorded (capsaicin stock; 10^{-2} M solution in ethanol).

Application of metabolite mix

Some preparations were exposed to an oxygenated "low" metabolite mix (15mM lactate, 1μM ATP, pH 7.0) dissolved in Krebs solution. After a 45-minute washout period, the preparation was then exposed to a "high"-metabolite mix (50mM lactate, 5μM lactate, pH6.6). The adenosine triphosphate (ATP) was added to the mixture immediately prior to the delivery into the bath. The two concentrations of metabolites were chosen based on the previous studies by Light et al (2008), and Jankowski et al (2013). At the end of the recording period, the preparation was removed from the recording chamber and transferred to a new chamber for anterograde labelling (see above).

Dynamic stretch and presence of metabolite mix

In four preparations, graded loads were applied by infusing fluid into a reservoir (0.5g resting weight) thereby increasing the counterweight to a peak level of 2.0g (0.02, 0.043, 0.08, 0.16 g/s) in Krebs solution. The preparations were then superfused with the "low" oxygenated metabolite mixture and the same mechanical stimulus was applied to characterise interactions between metabolic and mechanical stimuli.

Microscopy and processing

Immunohistochemically stained or biotinamide-labeled preparations were viewed and analysed on an Olympus IX71 inverted fluorescence microscope, fitted with appropriate dichroic mirrors and filters. Images of labelled neural structures were

captured via a CoolSNAP ES digital camera (Roper Scientific, (Photometerics), Tucson, AZ, USA) using analySIS 5.0 software (Soft Imaging System, Gulfview Heights, South Australia, Australia). Image processing was restricted to brightness and contrast adjustments, cropping and formation of photomontages using Adobe Photoshop (CS6, Adobe Systems Inc., San Jose, CA).

Axonal Mapping

Two Mitutoyo linear scales (1 μm resolution), fixed to the microscope stage, were connected to a Mitutoyo 2dimensional ALC Decoder (ALC-3701, Mitutoyo Corporation, Japan). This was connected via an RS232/USB connector to a personal computer and coordinates, corresponding to the stage position, were downloaded to the computer running Microsoft Office Excel via Bill Redirect Software (http://www.billproduction.com/) together with an identifying keypress. Data was then plotted as smoothed line segments or symbols in the spreadsheet software.

Statistical Analysis

Results are expressed as means ± 95% confidence intervals, with *N* referring to the number of discriminated afferent units and *n* referring to the number of animals. Two means were compared using Student's paired or unpaired two-tailed *t* tests. Differences were considered significant if $P < 0.05$.

RESULTS

Immunohistochemistry*

Antiserum raised against PGP9.5, a ubiquitin hydrolase enzyme, is widely used as a general marker for nerve cells and their processes (Day and Thompson, 2010). Fibres immunoreactive for PGP 9.5 were found in all layers of wholemounts of abdominal muscle preparations. The most prominent PGP-labelled structures were bundles of large- diameter axons, which gave rise to clusters of motor endplates concentrated in one or more regions. In most preparations, one or two muscle spindles were identified by characteristic beaded, branching axons that filled the centre of the spindle-shaped structures. Both the internal oblique and transversus abdominis muscles were also innervated by an extensive network of finer axons, some clearly varicose, either running parallel to muscle fibres within the sheets of muscle, or branching in the connective tissue between the muscle layers, without specific alignment to the muscle. In places, there were also modest perivascular and paravascular plexuses around larger blood vessels. Apart from muscle spindles, no other corpuscular endings were observed.

Immunoreactivity for the neuropeptide, CGRP, was not present in either motor endplates or muscle spindles. However, numerous thin axons-of-passage were visible within major nerve bundles and fine single fibres, often varicose, were visible, branching extensively. Some of these were located in the connective tissue at the edges of sheets of muscle, and some ran within the muscle, predominantly parallel to the myocytes. CGRP-immunoreactive axons were especially prominent in the perivascular and paravascular plexuses. CGRP-IR fibres entered the preparations via two pathways: (i) accompanying blood vessels that penetrated the surface of the

muscle, (ii) in the larger segmental nerve trunks that carried the main motor supply to the muscles.

Tyrosine hydroxylase (TH) is a marker of sympathetic nerve fibres and was localised in a few axons within the muscle layers of the preparation, but was most abundant in the perivascular and paravascular plexuses. Occasional single axons with TH immunoreactivity branched away from blood vessels and penetrated the muscle layers. TH-IR fibres had no apparent association with motor endplates or muscle spindles.

Axonal tracing combined with immunohistochemistry*

To identify the morphology of single nerve endings, rapid anterograde labelling of axons in intercostal and subcostal nerve trunks was carried out with the tracer, biotinamide. This appeared to fill most axons in the large nerve trunks, including both thick and thin axons. Biotinamide-labelled motor neuron axons were smooth, had a large diameter and usually branched extensively, giving rise to multiple motor endplates. A few biotinamide- filled axons terminated in muscle spindles (usually 1 or 2 per preparation). Fine varicose axons were often labelled by biotinamide in the perivascular and paravascular plexuses; their location was confirmed by labelling vessels with antisera to smooth muscle actin. Some of the filled perivascular axons were CGRP-immunoreactive; others were TH-immunoreactive. There were also smaller numbers of fine beaded/varicose axons travelling either in small bundles of 2-4 axons, or as single axons either running parallel to muscle fibres, or meandering within the connective tissue, usually with extensive branching. Some, but not all of these biotinamide-filled single axons were CGRP immunoreactive. Thus, biotinamide filling appeared to label all the types of axons labelled with PGP or CGRP antisera.

From this analysis (n = 10), six major types of biotinamide -labelled neuronal structures could be distinguished after filling from segmental nerves; (i) thick motor neuron axons that gave rise to motor endplates; (ii) muscle spindle afferents; (iii) varicose axons in the perivascular and paravascular plexuses with CGRP immunoreactivity and (iv) varicose peri/paravascular axons with TH immunoreactivity; (v) axons in the connective tissue which were usually fine, smooth or varicose, and branched extensively, but usually not closely aligned with muscle fibres (vi) fine axons running within the muscle sheets were identified, usually aligned for much of their length with muscle fibres (see **Figure 3.1. A-H**). It is possible that the same parent axon may have given rise to two or more of these specialised types of endings; the density of labelling precluded unequivocal identification of the entire branching patterns of single axons, in most cases. The range of group III and group IV afferents recorded electrophysiologically from muscles are likely to form subsets of the axons described above. In the present study, by using additional techniques, it was possible to identify the morphology of just one specific type of group III afferent (see below).

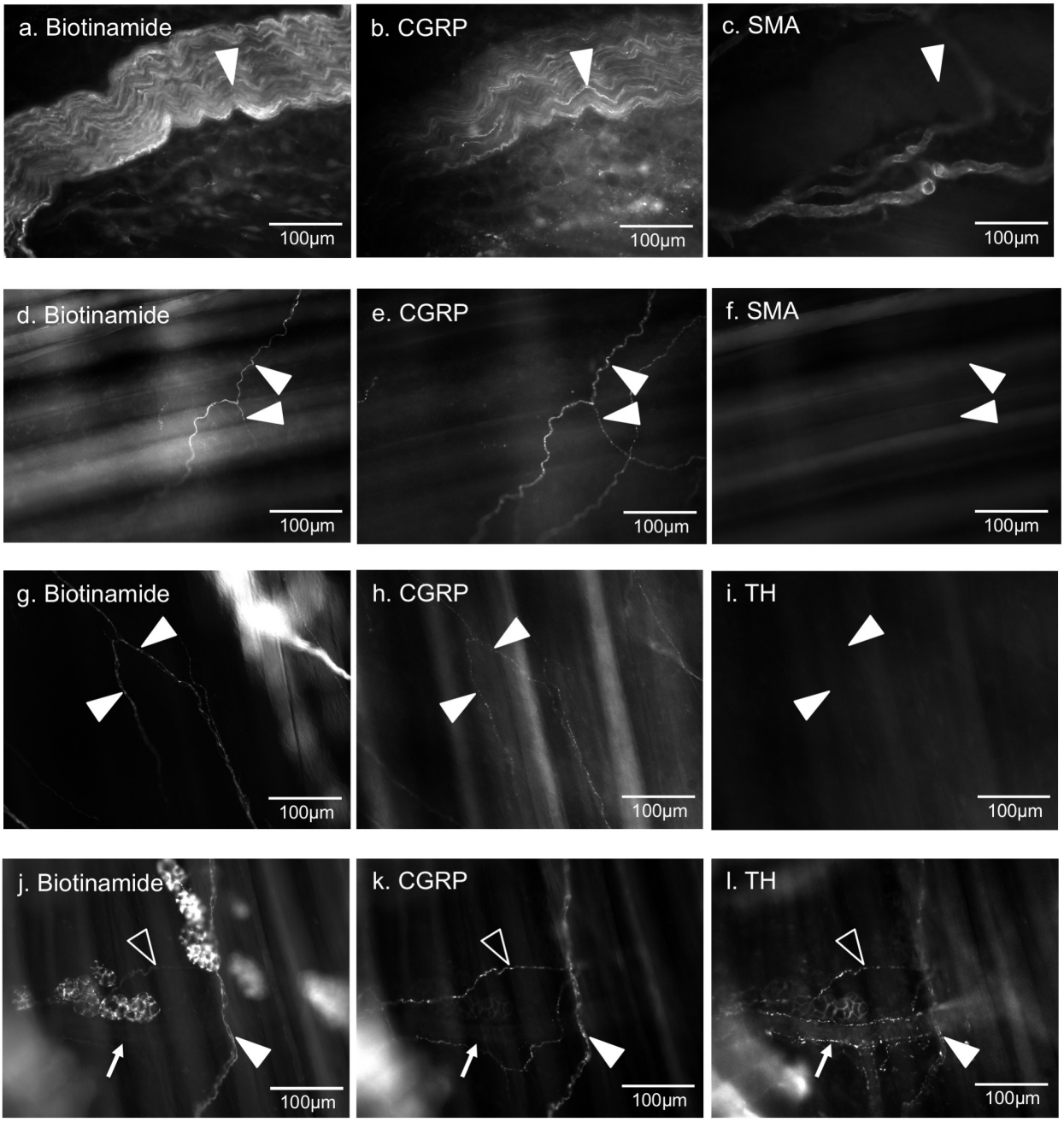

Figure 3.1. Biotinamide filling of neurons innervating mouse abdominal muscle, combined with CGRP, TH and SMA immunoreactivity shows multiple types of endings.

(**a, b & c**) an axon of passage in a large nerve trunk, some of which were CGRP-immunoreactive (solid arrow). This image suggests that some sensory fibres accompanied large diameter motor fibres in the major nerve trunks that supplied the abdominal muscles. A nearby network of blood vessels can be seen in (c). (**d, e & f**) biotinamide filled branching axon in connective tissue which lacked CGRP immunoreactivity but ran alongside a CGRP-immunoreactive axon, with no surrounding blood vessels (f). (**g, h & i**) axons running close to- and parallel with muscle fibres also lacked TH and CGRP immunoreactivity(**j, k & l**) axons running close to a blood vessel, one of which was CGRP and TH immunoreactive (open arrow head); the other lacks CGRP or TH (solid arrow head). TH immunoreactivity could also be seen running tightly alongside blood vessels (full white arrow).

Electrophysiological recordings

Extracellular recordings were made from desheathed segmental nerve trunks close to the edge of the preparations (n = 41 preparations). In some studies, recordings were made from two sites on a single nerve trunk, separated by 5-7 mm. Analysis was confined to single units (n = 41, N = 41) that could be discriminated by amplitude, duration or shape (see methods). Spontaneous action potentials were recorded from all intact nerve trunks, although some discriminated single units did not fire under resting conditions. One type of unit, which we called "CT3" (Group III connective tissue units: see below) was especially recognisable in many recordings. CT3 units usually had little spontaneous activity, responded modestly to stretch but were readily activated by light von Frey hairs applied to the upper surface of preparations. Recordings were concentrated on these units, which were relatively abundant; other units were ignored. Of 41 CT3 units (n = 41 animals), 3 had spontaneous firing (averaging 26.2 ± 2.2 Hz, mean ± 95% confidence interval). The other discriminated units had no spontaneous firing but were excited by a range of mechanical and/or chemical stimuli.

Mechanosensitive responses to von Frey hairs

A standard calibrated 1 mN von Frey hair (which exerted a force of equivalent to ~100 mg) was applied to numerous sites, to map mechanosensitive site (hotspots) of single, discriminated CT3 units (N=9, n=41). We also tested a range of von Frey hairs (20, 50, 100, 200 and 500 mg) which evoked increasing responses which tended to saturate (see **Figure 3.2.**). Maximum instantaneous firing rate of CT3 units during probing with a von Frey hair was 57.4 Hz ± 15.8 (N = 30, n = 30). In most cases, CT3 units activated by von Frey hairs returned to being silent after removal of the probe.

Receptive fields

The receptive fields of discriminated CT3 units were mapped on a micrograph of the live preparations with carbon marks at multiple points to act as visual landmarks (*n = 6)*. Sites at which a 100mg von Frey hair evoked firing (i.e.: "hotspots") were marked on a printout of the micrograph, relative to the carbon particle landmarks. From this, we were able to confirm that CT3 units had a single, irregular receptive field that averaged 0.38 ± 0.18 mm^2, surrounded by non-responsive sites (**Figure 3.2. B**). Identified receptive fields were not aligned with either the internal oblique or transversus abdominis. The shape of the receptive fields measured were elliptical or slightly oval in shape.

Twin recordings from the same nerve

Conduction velocity was calculated for 19 discriminated single units in 10 preparations which had 2 recording sites on the same nerve ($n = 10$). In every case, action potentials occurred first at the recording site near the preparation and occurred a moment later at the more distant recording site. Conduction velocities were initially calculated using the measured distance between recording electrodes. However, it became clear that the slight tension on the nerve caused by the electrodes introduced an artefactual overestimation of the distance. This amounted to an average strain of 1.23 ± 0.06 compared to the nerve with minimal tension (14 nerve trunks from n=6). Correcting for this, unidentified units had conduction velocities ranging from 5-14 m/s (average: 9±3 m/s; N=12, $n = 10$). CT3 units, characterised by von Frey hair responses (see above), had conduction velocities that ranged from 8-20 m/s (7 units, $n = 10$) (average 14 ± 4 m/s, 7 units, $n = 7$) slightly faster than the non-CT3 population ($P < 0.01$, $t = 2.93$, $df = 17$) **(Figure 3.3.)**. These paired recordings from single nerve trunks provided additional information. First, the recordings were very similar at the two sites. All

spikes at the site far from the muscle were also recorded at the site near the tissue. However, some spikes at the near site did not have equivalents at the far site. This suggests that spikes arose from sensory endings in the muscle and were propagating away from the preparation (i.e.: centrally), but some spikes failed at or after the first recording site. No spikes occurred at the far site that had not passed via the near recording site (n=10). Action potentials at the far site (i.e.: recorded near the cut end of the nerve) were typically rather monophasic, whereas those at the site near to the muscle were usually more biphasic, although this was not the case in all recordings.

Transduction delay

To determine the transduction delay for a mechanical stimulus by CT3 afferents, the time taken from the initiation of the electrical stimulus to the first depolarisation of the action potential was calculated. This averaged 10 ± 3.3 ms (range: 3 – 14 ms, n = 7). The delay from the mechanical stimulus (piezoelectric probe) was similarly measured and it average 11 ± 2.7 ms (range: 6 – 15 ms, n = 7). The difference between the two, minus the probe delay of 0.7ms was then calculated. This provided an estimate of the transduction delay for CT3 afferents of 1.5 ± 0.8 ms (7 units, n = 7). A typical example is shown in **Figure 3.4**. The ability of the sensory ending to respond to a mechanical stimulus in less than 2ms strongly suggests that the ending is not indirectly activated via release of a neurotransmitter from a nearby cell. Thus, it is likely that CT3 afferents express mechanosensitive ion channels on their terminals that can be activated by muscle stretch.

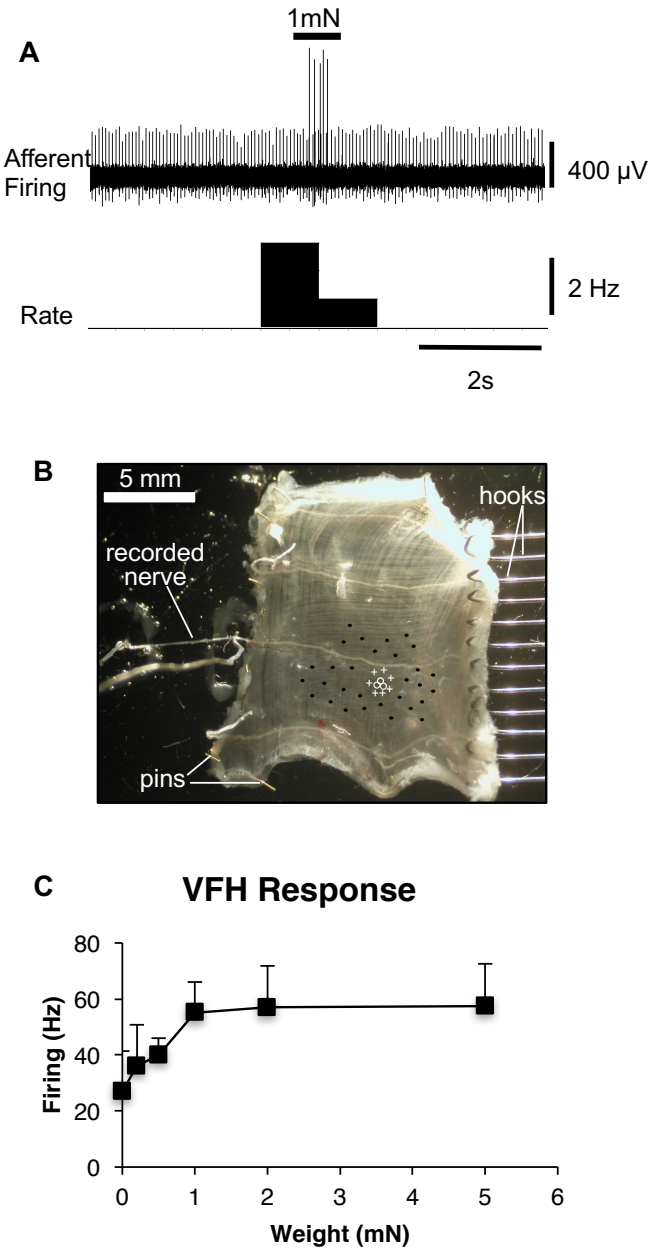

Figure 3.2. Firing evoked by von Frey hairs

A. Burst of firing evoked by probing the surface of a preparation with a 1mN von Frey hair in an afferent subsequently identified as a CT3 afferent. **B.** Image of a typical preparation in the recording chamber. Carbon particle landmarks are shown as white crosses. Sites where von Frey hair probing evoked firing ("hot spots") are shown as open white circles; black dots represent sites without a response. Notice the cluster of hotspots, corresponding to the receptive field, located within the ring of carbon landmarks. **C.** Combined data from 23 identified CT3 units showing maximal instantaneous firing rate to a range of von Frey hairs; note the saturating responses with the stiffest hairs (N = 23, *n* = 23).

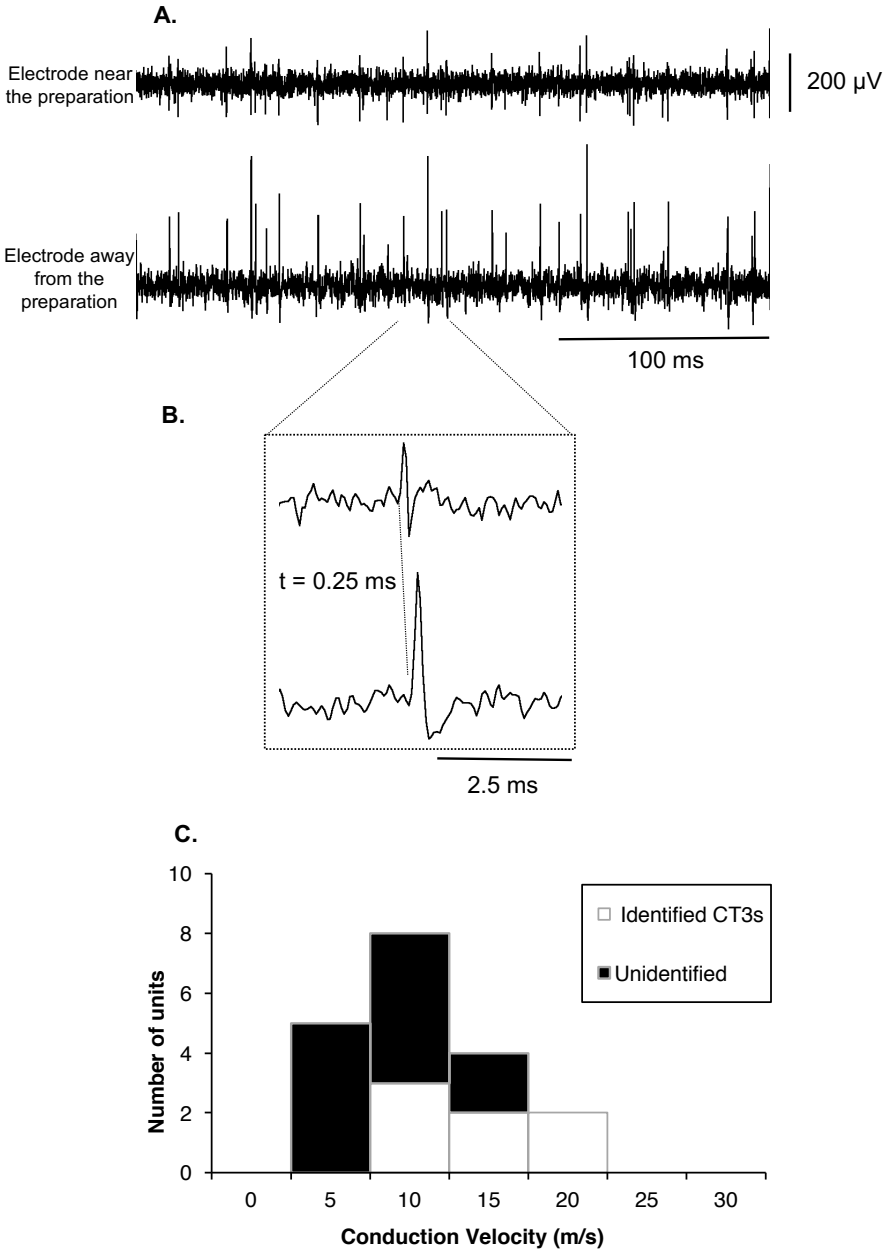

Figure 3.3. Simultaneous recordings from 2 sites on a single nerve trunk innervating mouse abdominal muscle

A. Paired recordings from a single nerve trunk ex vivo show 1:1 correspondence of action potentials at the two recording sites although amplitudes differ between the traces. **B**. An expanded time-base shows measurements of transmission delay, used to calculate conduction velocity (dotted line). Note that the action potential at the site closest to the preparation (upper trace) and was more bipolar than the recording close to the cut end of the nerve (lower trace). **C.** The distribution of conduction velocities of muscular afferents, for identified CT3 units (white) and unidentified units (black), the average conduction velocity of identified CT3 was 14 m/s (7 units, n = 7). CT3 units tended to have faster conducting action potentials than other units recorded from the same nerve trunks.

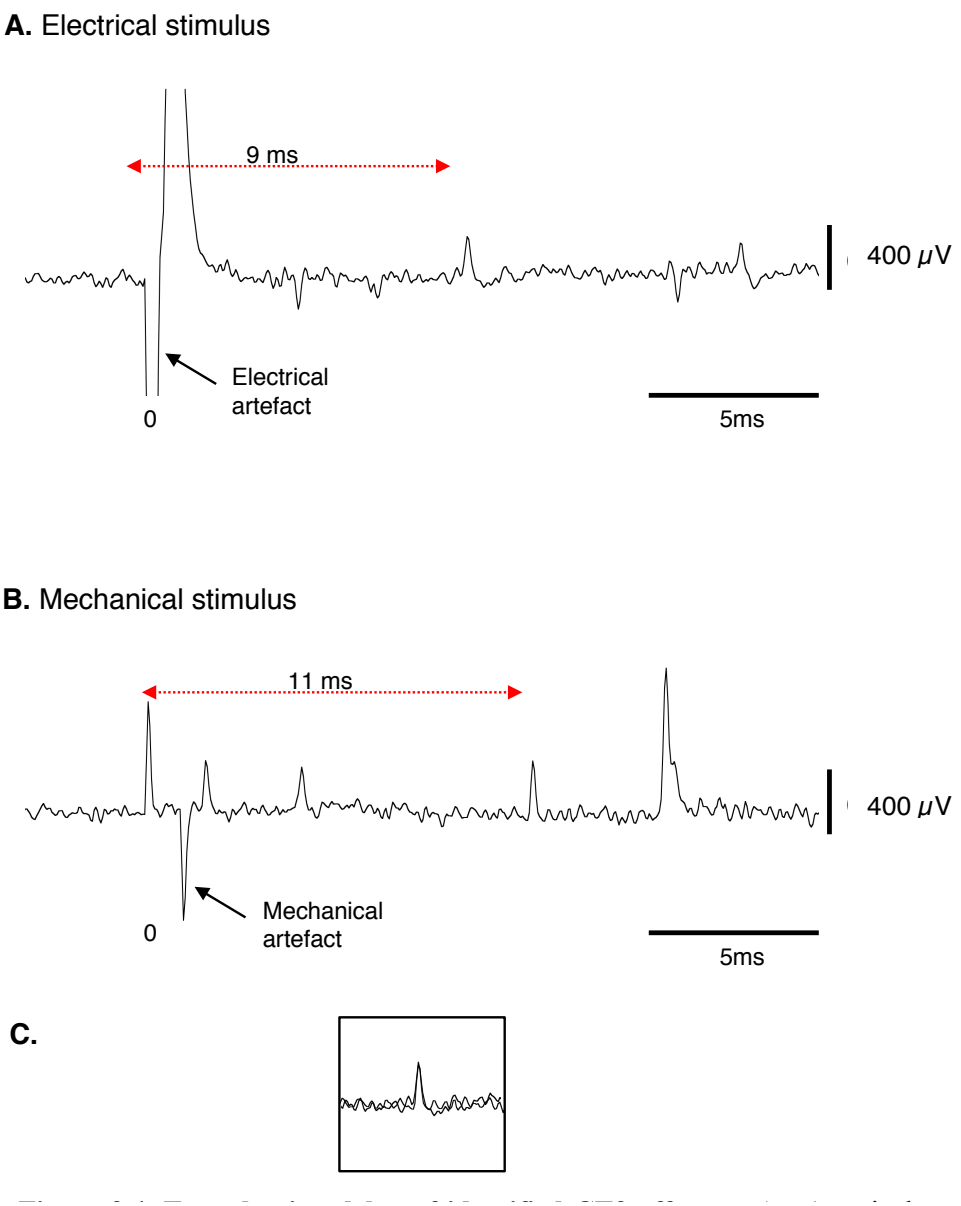

Figure 3.4. Transduction delay of identified CT3 afferents
A A typical trace demonstrating the time taken from the start of an electrical stimulus artefact to the first deflection of a CT3 afferent action potential at the recording electrode. **B**. A typical trace demonstrating the time taken from the start of a mechanical stimulus artefact (from a piezoelectric probe at the same site as the electrical stimulating electrode) to the arrival of a CT3 afferent action potential. Note that the delay to the mechanical stimulus is 2 ms longer than that of the electrically-evoked response. This represents the transduction delay required for the afferent terminal to generate an action potential from a mechanical deformation. Care was taken to measure delays to the time-locked spikes to avoid confounding them with spontaneous action potentials from other units. **C.** The overlay of the two-action potential from the traces from **A** and **B** demonstrating that they are from the same unit. Note that both the electrical and mechanical stimulus created an artefact, the transduction delay was calculated from the start of this artefact to the first deflection of the CT3 afferent action potential.

Maintained Stretch

Preparations were pinned securely down one edge and the opposite edge was attached by a "rake" to an isotonic transducer, via a pulley. Loads (1 - 20g) were applied to the arm of the isotonic transducer and changes in length of the preparation were recorded. Of 41 CT3 units (distinguished by von-Frey hair responsive sites), 3 were not affected by any load, up to 20g. The remaining 38 units increased firing when the muscle was put under load (**Figure 3.5**). Of these, 20 units (n = 41) fired tonically throughout the duration of the stretch with little adaptation, especially with higher loads. The other 7 units fired phasically at the onset (and sometimes offset) of the load. Overall, the stimulus/response curve showed an initial load-responsiveness, but responses typically saturated above 5g (**Figure 3.6 A&B**). The average peak rate of firing to stretch was ~12Hz +/- which was slower than the maximum firing rate evoked by von Frey hairs (57.4 Hz ± 15.8 (N = 30, n = 30)).

Dynamic Stretch

Dynamic ramp stretch was applied to six preparations with identified CT3 afferents at four speeds; 0.2 mN/s, 0.43 mN/sec, 0.8 mN/s, and 1.6 mN/s. All six CT3 afferents were activated by dynamic ramp stretch (n = 6), with faster firing as load was increased, up to a rate at which responses saturated (**Figure 3.7.**). There was a modest effect of rate of distension, so that at any given load, or length, firing was slightly faster with 0.8 mN/s compared to 0.2 mN/s (see **Figure 3.7.B, 3.7.C)**. CT3 afferent firing rate during dynamic stretch had a high correlation with both force (R 0.94, 0.91, 0.94, 0.96 for the four rates tested, n = 6) and change in length (R 0.97, 0.93, 0.97, 0.97).

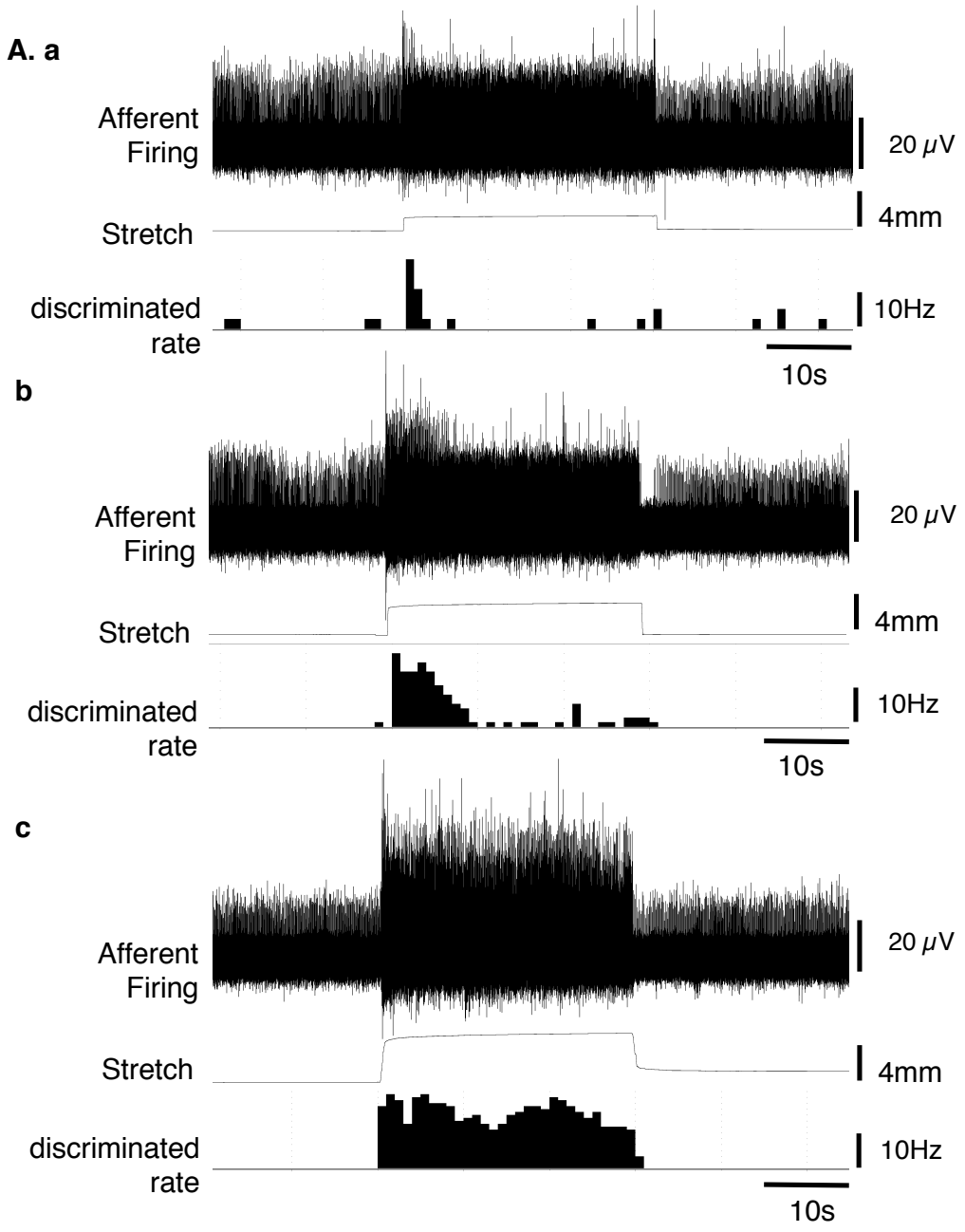

Figure 3.5. Response of identified CT3 afferents to muscle stretch by increasing loads

A. Typical responses to applied load **a**: 2 g; **b**: 6 g and **c**: 20 g are shown for the same identified CT3 afferent unit in one preparation. Upper traces show raw multi-unit recordings made using the extracellular recording electrode; the lowest trace shows the discriminated rate of firing of the identified CT3 unit (1s bins). The middle trace shows the change in length of the preparation recorded with an isotonic transducer, in response to the applied load. Note the increase in firing during stretch, with a dynamic response at the onset followed by some adaptation in firing rate (not as clear with the highest load (**C**).

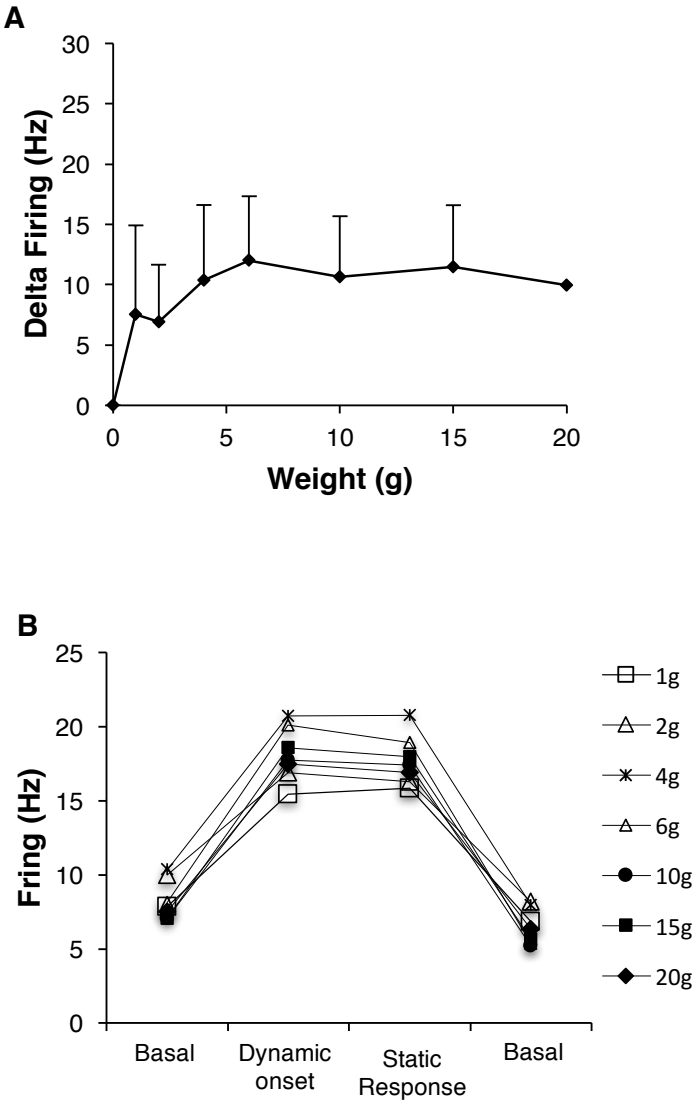

Figure 3.6. Response of identified CT3 afferents to muscle stretch by increasing loads (1 – 20 g)

A. Mean responses load (27 units from 27 animals) are shown for stretches applied for 30 s at 3 minute intervals. Note that responses to the increasing loads saturate above 5g. **B.** Combined data from 27 units shows absolute firing rates during application of loads for 30s, averaged over a 25 s period before the load, at the onset of load, during maintained load and after load was removed. Note that the largest responses occurred with 4-6g loads and that there was little adaptation (between 2nd and 3rd points) while the load was applied indicating that CT3 afferents have, on average, small dynamic responses at the onset of the stretch stimulus.

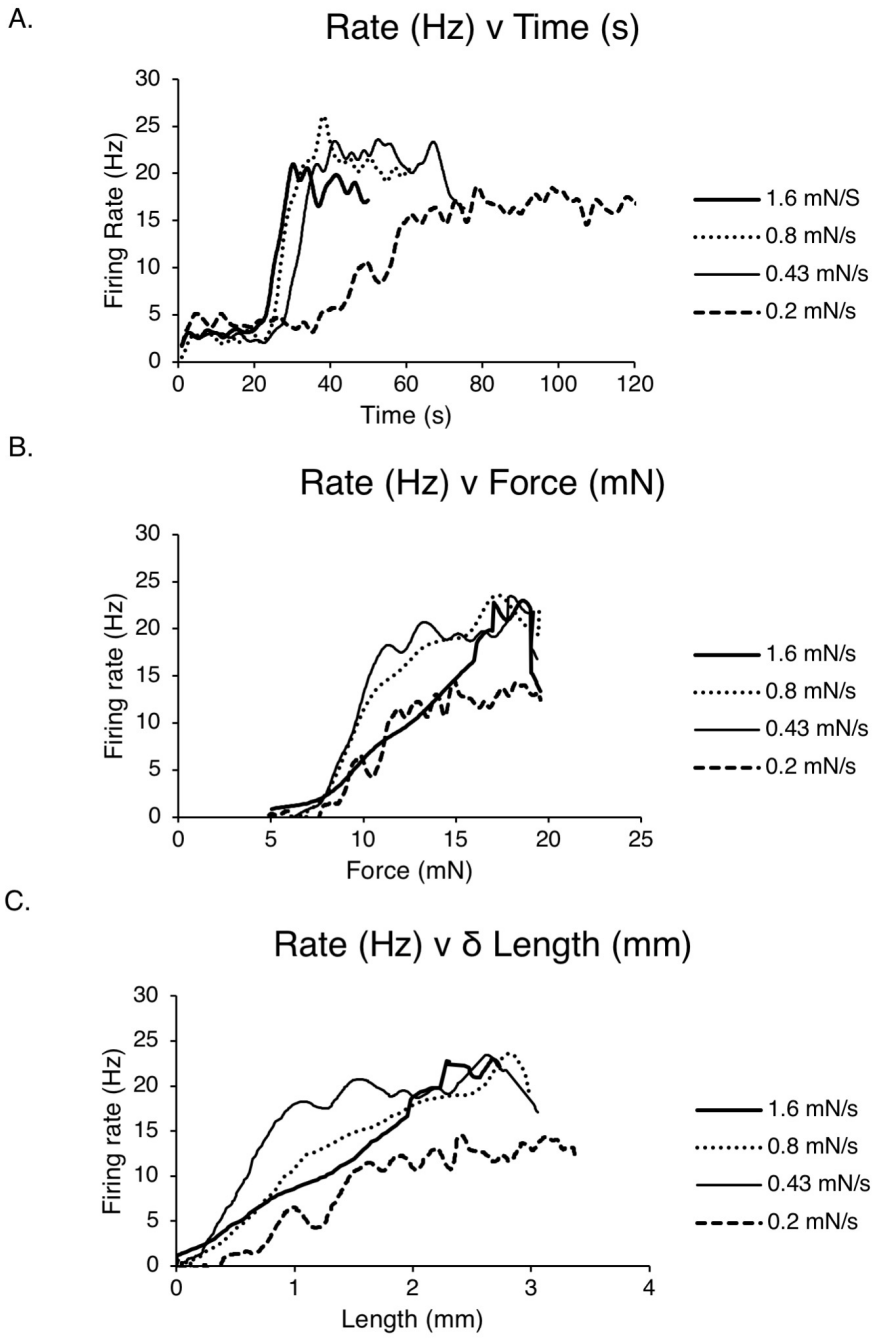

Figure 3.7. Activation of CT3 afferents by different rates of dynamic stretch. Load on the muscle started at an initial value of 5 mN and was increased to 20 mN at four different rates (0.2 – 1.6 mN/s) **A.** Mean firing response of CT3 identified afferents to increasing dynamic stretches plotted against time. **B**. The same data with firing rate replotted against load, shows that for any given load, firing was generally higher at the highest rates of distension. **C**. Using the same data, firing was re-plotted against the change in length of the preparation. Again, for any given change in length, firing was generally higher with the faster rates of distension (6 units, $n = 6$).

Capsaicin

Capsaicin (10^{-6}M) was directly applied as a single bolus to the identified receptive field of 14 discriminated CT3 units; none was activated (data not shown). The mean spontaneous firing rate of non-discriminated units before the application (5.5 ± 0.1 Hz) was not significantly different from mean firing rate immediately after capsaicin application (5.8 ± 0.8 Hz).

Metabolite Mix

'Low' metabolite mix (15 mM lactate, 1µM ATP, pH 7) and a 'high' metabolite mix (50 mM lactate, 15µM ATP, pH 6.6) were applied to 5 preparations with identified CT3 units (n = 5) (Light, 2008, Jankowski, 2013). Both low and high mixtures caused firing of many afferent units, which had a wide variety of amplitudes, durations and shapes (**Figure 3.8.)**. For identified CT3 units, all (n=5) were potently activated by the low metabolite mixture. Average latency to the first response was 60s, but individual latencies were highly variable, ranging from 2 s to 240 s. For these identified units, firing frequency peaked at 29.7 ± 10.1 Hz compared to basal firing of 0.2 ± 0.3 Hz ($P < 0.05$). After a 45-minute washout period, the 'high' metabolite mixture was then applied. All identified units were also excited by the high metabolite mixture (**Figure 3.8. B**). The time taken to the first increase in firing was shorter (20-50s). Firing rates could not be accurately discriminated because of the number of units excited and their high discharge frequencies, but firing appeared to be higher than with the low metabolite mix.

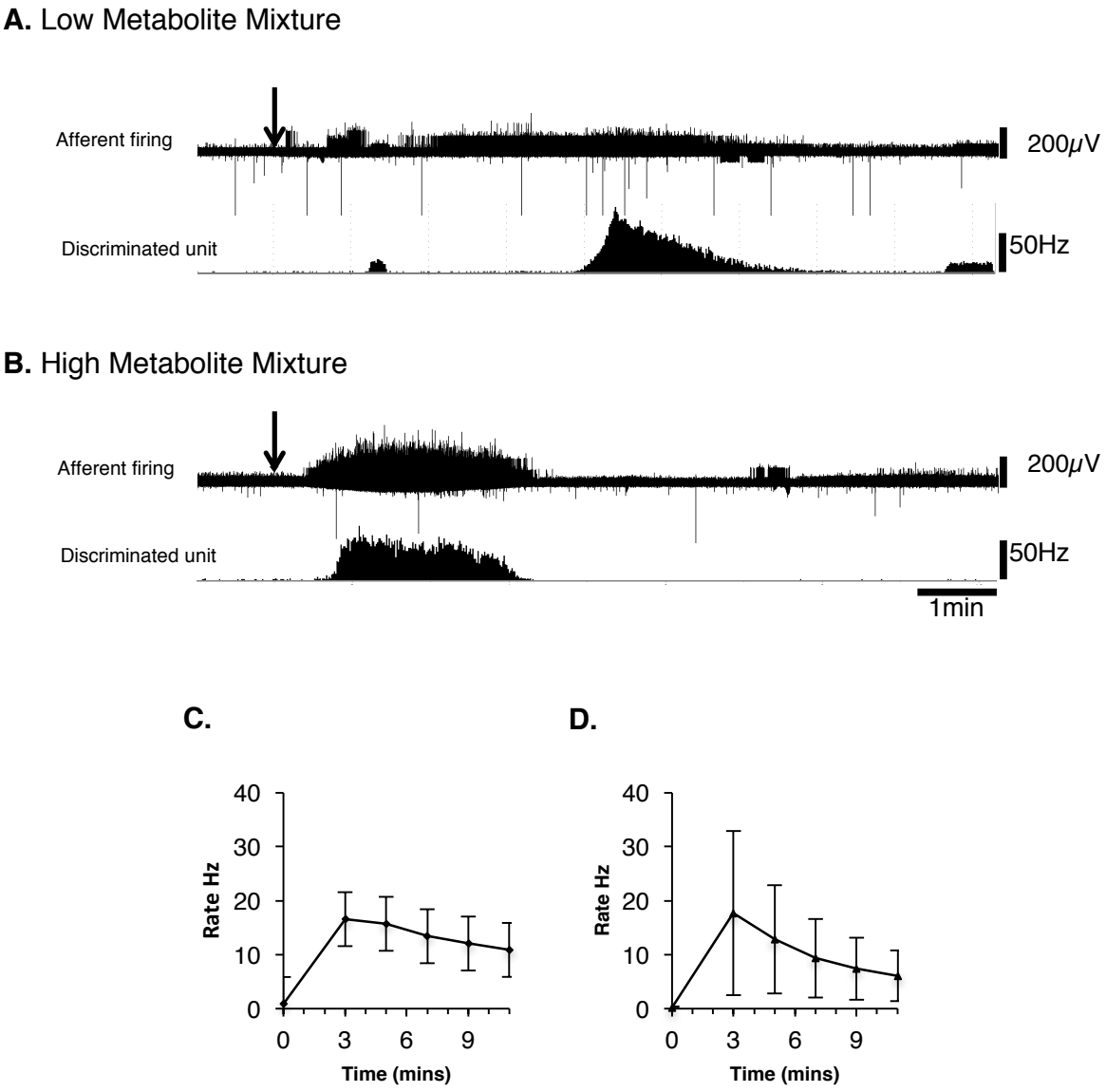

Figure 3.8. Activation of CT3 afferents by low and high concentration 'metabolite mixes'

A. Typical example of response to application of low metabolite mixture (black arrow) to a preparation; discriminated CT3 unit firing (identified single unit) shown on the lower trace. Note the long delay before the main response. Several other units (not CT3 afferents) were also activated by the mix. **B.** Trace (from the same unit) showing response to the high metabolite mixture. Note the shorter latency period and slightly higher mean firing. **C & D.** The mean firing of 6 discriminated units during the application of the low metabolite mixture which was applied at time t = 0. (**C**) low metabolite mix and (**D**) high metabolite mix are averaged over 3-minute bins (6 units, $n = 6$). Note the similarity of the responses; mean responses for the more concentrated mixture were not significantly greater than the low metabolite mix.

Interactions between metabolites and mechanosensitivity

The response of CT3 afferents to stretch was compared in control Krebs solution and after addition of the low metabolite mix, investigate interactions between mechanical and chemical stimuli. As described above, the low metabolite mix caused an increase in basal firing, from 2.7 ± 0.3 Hz in Krebs solution to 13.3 ± 1.2 Hz in the metabolite mix. Firing further increased during dynamic ramp stretch in the presence of the metabolite mix; an additive effect. Average firing in response to dynamic stretch was not significantly higher in the metabolite mix than in Krebs solution, despite the higher basal firing rate (peak: 17.6 ± 0.65 Hz in Krebs solution; 28.9 ± 1.5 Hz in metabolite mix) (**Figure 3.9.**). Similar patterns were seen when firing rate was plotted against either force or length (**Figure 3.9.B & 3.9.C**). CT3 afferent firing rate during dynamic stretch in the presence of metabolites when compared to Krebs solution, had a high correlation with both force (R values in Krebs; 0.92, Metabolite mix 0.98, n = 4) and change in length (R values Krebs 0.94, Metabolite mix 0.99).

Correlation of electrophysiology, morphology and immunohistochemistry

After mapping the receptive field of CT3 afferents on a micrograph of the preparation, rapid anterograde tracing was applied to the recorded nerve trunk, followed by immunohistochemical processing for CGRP. The carbon particle landmarks applied to the preparation's surface usually remained visible after fixation and were used to identify precisely the extent of the receptive field in the fixed, labelled preparation. Out of 41 preparations with an identified mapped CT3 unit, we were unable to identify the discriminated axon unequivocally in 34 preparations. This was either because multiple axons branched within the area of the receptive field, or occasionally because no filled axons were visible in it ("failure to fil"). However, in 7 preparations, a single axon filled the receptive field with its axonal branching (**Figure 3.10.A)**. In all 7 cases, the axon had similar morphology. The thin, parent axon branched repeatedly (**Figure**

3.10.F), with some branches tending to run in parallel to one another, but not usually aligned with muscle fibres. The axons typically had a beaded or varicose appearance near their terminations. None of these 7 axons showed any obvious association with blood vessels, muscle fibres, muscle spindles or motor endplates. Rather, they were confined to the most superficial layer of connective tissue in the preparation (i.e.: connective tissue between the internal and external oblique muscle layers). Of these 7 units, none was immunoreactive for CGRP (n = 7), despite the fact that there were other CGRP axons visible in every preparation **(Figure 3.10.C and 3.10.D)**. In several cases, CGRP-immunoreactive axons were present in the same fine nerve trunk as the biotinamide-filled axon.

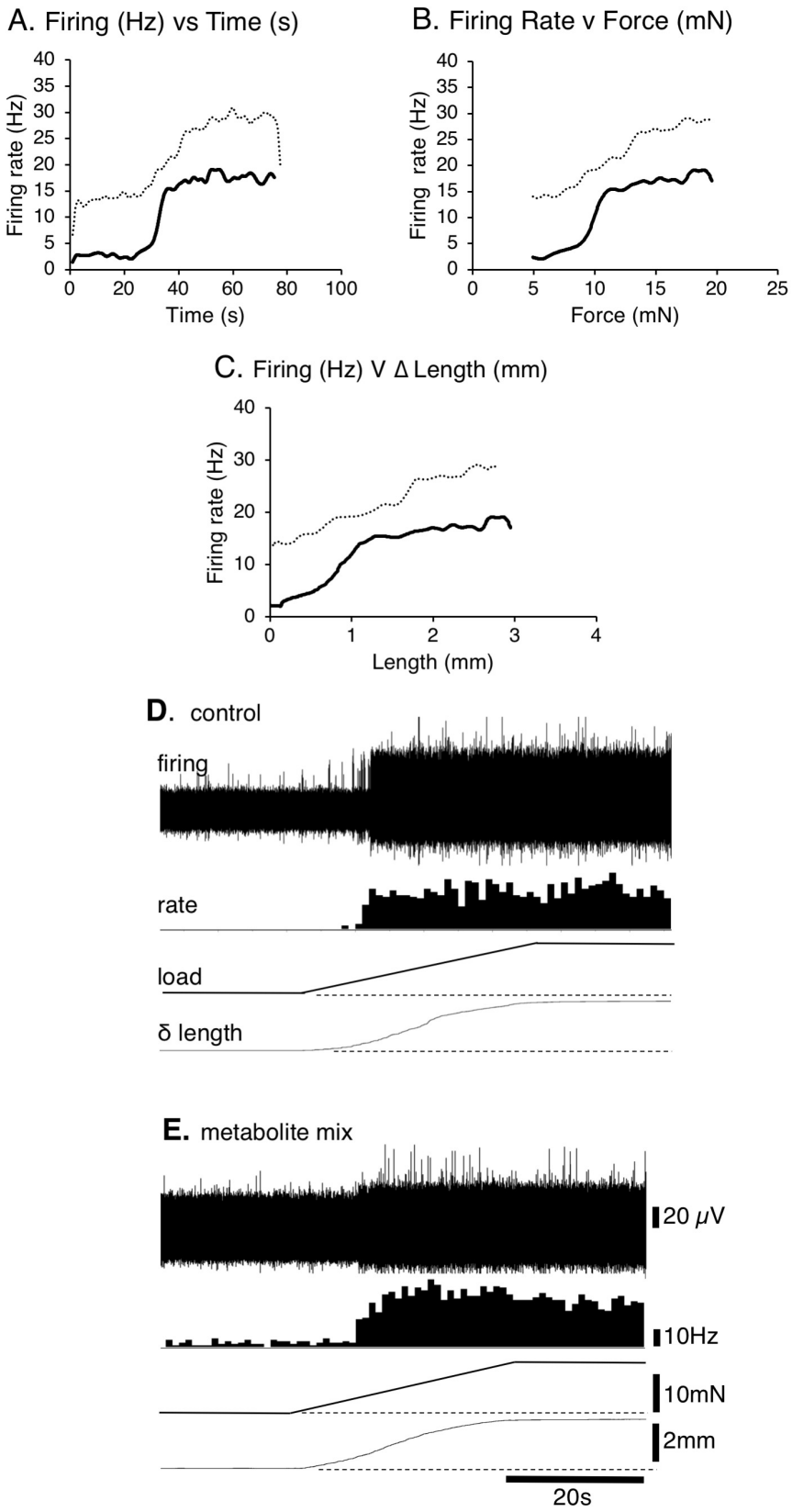
A. Firing (Hz) vs Time (s)
Firing rate (Hz)
Time (s)
B. Firing Rate v Force (mN)
Firing rate (Hz)
Force (mN)
C. Firing (Hz) V Δ Length (mm)
Firing rate (Hz)
Length (mm)
D. control
firing
rate
load
δ length
E. metabolite mix
20 μV
10Hz
10mN
2mm
20s

Figure 3.9. Responses of identified CT3 afferents to dynamic stretch at a fixed rate (at 0.043 g/s) in the presence and absence of the low metabolite mix.
A. Mean change in firing in Krebs solution and in the low metabolite mix plotted against time. **B.** Mean changes in firing plotted against load, again comparing Krebs solution and low metabolite mix. **C.** The same data was replotted as firing against change in length. Note that in all graphs that the basal firing and maximum firing rate are similarly increased in the presence of the low metabolite mixture, compared to the Krebs solution suggesting an additive effect. **D and E.** Typical responses of identified CT3 afferents to dynamic stretch in Krebs solution (**D**) and in low metabolite mix (**E**). Note that this unit has no spontaneous firing in Krebs solution but does have a small basal firing rate in the presence of the metabolite mix.

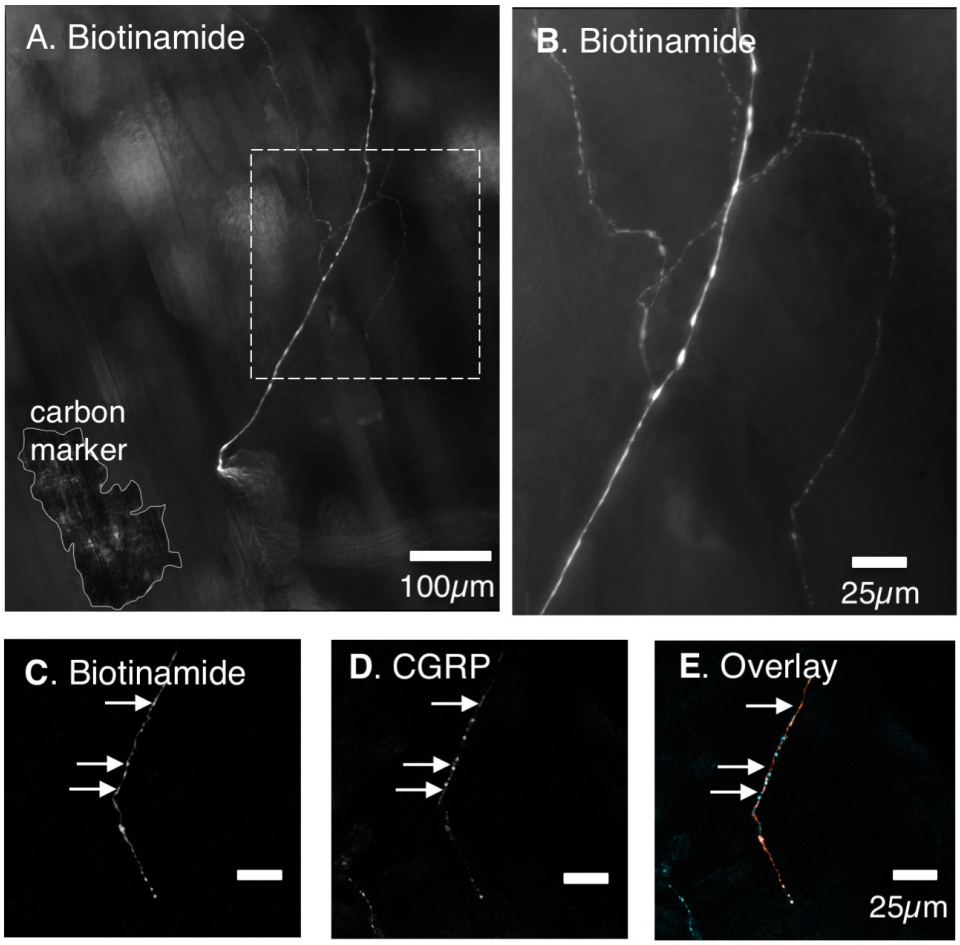
A. Biotinamide
carbon
marker
100μm
B. Biotinamide
25μm
C. Biotinamide
D. CGRP
E. Overlay
25μm
F. Biotinamide
1 mm
G. Map of axon branching
1 mm

Figure 3.10. Axonal branching of identified CT3 afferent in muscle.
A. Medium power micrograph of biotinamide filled CT3 axon identified as the only filled axon within the mapped field of innervation. Note the beaded appearance of the parent axon and the more pronounced varicosities on finer branches. **B**. shows detail from **A** (white dashed outline) revealing varicose axons and branching at higher magnification. **C**. Detail of single axon revealed by biotinamide (confocal image) which ran parallel to a CGRP immunoreactive axon (**D**) but was not itself immunoreactive for CGRP. This can be discerned by the different appearance and spacing of the labelled varicosities. **E**. A coloured overlay of **C** & **D**. **F.** The CT3 axon branching shown at low power. The open arrowhead indicates the parent nerve trunk from which recordings were made and to which biotinamide was applied. The solid arrow shows the point at which the single CT3 axon could be distinguished. **G.** Map of full branching pattern of the CT3 axon from **F**, recreated from the stage coordinates of the microscope (see methods) measured with linear scales with 1 μm resolution. Note that axons branched multiple lines but were not aligned with muscle fibres (orientation identical to **E**).

DISCUSSION

Summary of Results

This study used a novel *ex vivo* protocol to correlate the morphological and physiological properties of muscular afferents within the abdominal muscles of mice. Six populations of sensory endings could be distinguished on the basis of rapid anterograde filling combined with immunohistochemical labelling. These were: (i) muscle spindle endings (ii) axons of passage, (iii) perivascular or paravascular sensory axons, (iv) sympathetic perivascular or paravascular axons (v) axons ramifying in the connective tissue and (vi) axons ramifying close to and parallel with muscle fibres. In extracellular recordings of muscle afferents, one type of mechanosensitive metaboreceptor afferent was readily distinguished (CT3 afferents). These sensory nerves had conduction velocities in the range of 15-30 m/s, had discrete fields of innervation sensitive to von Frey hairs, showed saturating responses to graded muscle stretch, and were highly responsive to a mixture of metabolites. Morphologically, the axons of these mechanosensitive metaboreceptors formed fine branching endings, that were not immunoreactive for CGRP and which were located in the deep connective tissue layers between the layers of muscle.

Morphological identification of afferent neurons

In studies of the sensory innervation of the skin, the morphology of many physiologically-identified cutaneous afferents have been established (Iggo, 1960). This has provided a firm foundation for understanding cutaneous sensation (Iggo and Andres, 1982). In skeletal muscle, methods that have the ability to indisputably relate functional characteristics to the precise morphology of group III and group IV afferent endings have not been previously reported (Mense, 1993, Mense, 2009). In the

previous chapter (**Chapter 2**) we described and validated an abdominal muscle preparation, and a combination of techniques, previously only used to identify sensory endings within visceral organs (Tassicker et al., 1999), (Lynn and Brookes, 2011a) (Song. X., 2009), to relate the morphology and functional characteristics of the well described muscle spindle afferents. Thereby, demonstrating that this preparation and techniques can be successfully utilised to identify and distinguish peripheral somatic sensory neurons.

In the present study, we utilised this *ex vivo* preparation of abdominal muscles and combination of techniques to definitively identify and distinguish a single class of group III mechanosensitive metaboreceptor muscle afferents. We have also listed potential axonal candidates, for further functional investigation to determine their role based on the location of their endings within the muscle. Skeletal muscle afferents are classified into four groups based on conduction velocity. Group I and II have conduction velocities averaging 100m/s and 50m/s respectively, while groups III and IV average 15m/s and 1m/s respectively. These figures refer to large animals and humans: velocities are typically slower in rats and mice. Group I and II afferents have been extensively investigated and shown to originate from muscle spindles (group Ia and group II) (Bewick and Banks, 2015, Matthews, 2015) and see **Chapter 2** and Golgi tendon organs (group Ib) (Jami, 1992). Muscle spindles are considered to lie in-parallel with muscle fibres and primarily detect changes in muscle length, while Golgi tendon organs lie in-series and detect changes in muscle tension.

Stacey (1969) showed that group III and IV fibres comprise small diameter free nerve endings either in muscle connective tissue, running between individual muscle fibres, or surrounding blood vessels (Stacey, 1969). Electron microscopic analysis by von

During and Andres (1990) described afferents in large and small nerve bundles, with endings similar to those described by Stacey (von Düring and Andres, 1990). Biotinamide tracing in the present study also confirmed the same populations of axons; axons of passage, peri- and para-vascular bundles running near blood vessels, axons ramifying in the connective tissue between the muscle layers and axons that run in parallel and close to muscle fibres.

Physiological identification of afferent neurons

Many studies have described the functional properties of group III and IV muscles afferents *in vivo*. Early studies reported that a sub-population of small diameter afferents was responsible for pain (Weddell and Harpman, 1940). These nociceptors include high threshold mechanoreceptors, which respond to pinching or squeezing of the muscle, firing at up to 20-40Hz. Firing by high threshold mechanoreceptors often outlasted the stimulus; they made up approximately 60% of group IV muscle afferents, but fewer group III.

In the present study, CT3 afferents had conduction velocities between 11-23 m/s; within the range of group III afferents (Steffens et al., 2012). Conduction velocity, as a classification method to discriminate classes of muscle afferents has been used since the pivotal classification by Erlanger and Gasser in 1930 (Erlanger and Gasser, 1930). Technically, conduction velocity can be measured in several ways. These include from electrically-evoked compound action potentials, electrical stimulation on the muscle of single axons or by using two recording points on the same nerve trunk as seen in the present study. Estimates of conduction velocity have limits to their accuracy, depending on the method used. For example, compound action potentials can be measured to discriminate group I, II, III and IV muscle afferents, however it is often

difficult to identify exactly where the compound action potential starts. This is due to the time scales overlapping and the action potential waves being too close together (Wenk and McCleskey, 2007). Inaccuracies can arise in measuring the length of the nerve being stimulated and recorded, thereby. The methods used in the present study to determine conduction velocity of CT3 afferents, allows conduction velocities to be calculated reasonably accurately. There is a known, measurable distance between the recording electrodes and the delay between action potentials could be readily measured. However, the method is affected by the degree of tension under which the nerve trunk was pinned. This was taken into account in the present study in order to make the conduction velocities comparable to those recorded *in vivo*. One surprise of the present study is that, we did not record afferents with conduction velocity in the group IV range (< 2.5m/s). Consistent with this, we also failed to record any axons that were excited by capsaicin, which include group IV/ C-fibres (Szolcsányi, 1987). Why this was the case, when small diameter CGRP immunoreactive axons were present in the perivascular plexus, is not clear. It is possible that vascular afferents entered the preparation alongside blood vessels rather than via the segmental nerves that were the targets of recordings.

Approximately two thirds of group III muscle afferents are low threshold mechanical afferents that are typically silent at rest but are activated by low to moderate pressure. They are considered non-nociceptive, as they respond to stimuli within the physiological ranges of muscle work. Often referred to as ergoreceptors, they appear to be involved in reflex adjustments of respiration and circulation during exercise (Kaufman and Rybicki, 1987, Rotto and Kaufman, 1988, Kaufman, 2012). From their responses to low intensity compression with von Frey hairs, saturating responses to modest load and their dynamic responses to changes in muscle length and tension, they

are likely to function as chemosensitive low threshold mechanoreceptors, and to correspond to a subset of ergoreceptors.

A subset of group III afferents has previously been reported to respond to both chemical and mechanical stimuli (Kaufman and Rybicki, 1987, Kumazawa and Mizumura, 1977, Kaufman et al., 1984)}. These afferents are variously activated by CO_2, lactate (Rotto and Kaufman, 1988), H^+ ions, adenosine triphosphate (ATP))(Jankowski et al., 2013), inflammatory mediators (i.e. prostaglandins, interleukins (IL-6), nerve growth factor) (Ellrich and Makowska, 2007, Hoheisel et al., 2005), bradykinin, serotonin, nerve growth factor, and glutamate (Fock and Mense, 1976, Franz and Mense, 1975, Mense, 1981, Kaufman et al., 1982, Hoheisel et al., 2004, Mense, 2009) and raised $[K^+]$ (Kumazawa and Mizumura, 1977, Mense, 1977, Mense and Meyer, 1985). The mechanosensitive CT3 afferents in this study were also consistently chemosensitive: they responded to the low and high metabolite mixtures described by Light et al (2008), which were based on physiological levels of mediators (lactate, H+ and ATP) detected in active muscle. Whether they respond to all of the inflammatory mediators listed above will require further study. Previous studies have distinguished two subtypes of metabo-receptive muscle afferents. One responds to low metabolite mixtures generated during normal exercise and the other requires higher concentrations present in muscular ischemia (Jankowski et al., 2013, Light et al., 2008);Naves, 2005 #40}. CT3 afferents, in the current study were activated by both low and the high concentration of metabolite mixtures, suggesting that they may be active during normal muscle activity and fatigue.

Afferents that respond to metabolites released during muscle activity stimulate sympathetic reflexes (Alam and Smirk, 1937) including the exercise pressor reflex.

This reflex increases mean arterial pressure, heart rate, stroke volume, cardiac output and ventilation during exercise in animals and humans (Alam and Smirk, 1937, Coote et al., 1971, McCloskey and Mitchell, 1972). Group III and group IV muscle afferents include the afferents that make up the sensory arm of the exercise pressor reflex (Kaufman et al., 1984, McCloskey and Mitchell, 1972). With the onset of exercise, group III and group IV afferents increase their firing (Light et al., 2008);M, 1983 #42} and this is associated with a graded, intensity-dependent increase in efferent sympathetic discharge, with simultaneous parasympathetic withdrawal (Murphy et al., 2011). It is feasible that the CT3 afferents characterised in the present study contribute to these mechanisms. Consistent with this, passive stretch of the type that activated CT3 afferents has been shown to excite transiently muscle sympathetic nerve discharge (Cui et al., 2006).

Mechanically activated group III afferents may be sensitised by metabolites, particularly when perfusion of the muscle is limited, causing accumulation of released substances (Cui et al., 2008, Murphy et al., 2011); this can enhance the pressor reflex(Kaufman and Rybicki, 1987). However, a recent study has suggested that interactions between mechanical stimuli (passive stretch) and metabolite stimulation (using cuff occlusion) may be limited (Rossman et al., 2012). In the present study, CT3 afferents were activated by metabolites, and this activity appeared to sum geometrically with mechanosensitive responses to stretch. It should be noted however, that the level of metabolites used in the present study was similar to that seen in exercising muscle rather than the higher concentrations seen in ischemic or fatigued muscle. Group III and IV afferents may play complex roles in the adaptations required for motor activity. On one hand, they activate the pressor reflex and increase ventilation; on the other, they also limit central motor output to cause central fatigue

and thus protect against excessive peripheral fatigue and muscle failure (Amann et al., 2011b, Amann et al., 2008, Amann et al., 2009). Understanding the physiological responses of morphologically characterised group III and group IV muscle afferents may help identify their contributions to the pressor reflex and fatigue mechanisms during exercise.

Limitations

In the present study, one class of mechanosensitive and metabosensitive afferent fibres - CT3 afferents were characterised morphologically and physiologically in abdominal muscles of the mouse. The abdominal muscles were ideal for the techniques used in the study, as they were thin, could be dissected without excessive damage, survived well *ex vivo* and were suitable for recording sensory nerve activity. It should be noted that they may not be considered as primarily locomotor muscles. Most studies on exercise pressor reflex have elicited it using limb muscles which are certainly important in locomotion. This means that the actual contributions of CT3 afferents to the exercise pressor reflex may be questioned. However, group III and group IV afferents have been detected in many skeletal muscles and it has been suggested that small diameter afferents from trunk muscles and respiratory muscles may contribute to these reflexes (Michelini et al., 2015). Furthermore, abdominal muscles may be considered to have both ventilatory and locomotor functions (Deban and Carrier, 2002). Further studies would be required to determine whether CT3 afferents actually contribute to the pressor reflex and whether group III/IV afferents in other muscle groups have similar properties to CT3 afferents.

CHAPTER FOUR

TARGETED CHARACTERISATION OF CT3 AFFERENTS AND THEIR RELATIONSHIP WITH LACTATE

INTRODUCTION

Lactate is a metabolite formed and released in large quantities in active muscle and in lesser amounts in a wide range of other cells throughout the body (Brooks, 2018, Ferguson et al., 2018, Hall et al., 2016). Muscle lactate is mostly formed through glycolytic conversion of glucose to pyruvate. The enzyme, lactate dehydrogenase, then converts pyruvate into lactate. This sequence occurs in both the absence and presence of oxygen and during exercise (Brooks, 2018). After its discovery in 1780, lactate was often labelled as a metabolic waste product, associated with multiple deleterious effects such as, muscle fatigue and oxygen debt (Ferguson et al., 2018).

In the 1980's the introduction of the cell-cell shuttle theory (Brooks, 1985, Brooks, 2007), shifted the lactate paradigm (Brooks, 2009, Brooks, 2018). Lactate was shown to have more functional roles than previously thought, and is a major player in the coordination of whole-body metabolism. These functions include, but are not limited to: glial cell-neuron lactate shuttles and brain energy metabolism (Bergersen, 2007, Hertz, 2004, Pellerin and Magistretti, 1994), volume transmission for signalling brain metabolic state (Lauritzen et al., 2014), cell signalling (Lauritzen et al., 2014, Liu et al., 2009), and volume regulation (Halestrap, 2013). Lactate may mediate effects on emotional behaviour (Carrard et al., 2016), while augmented lactate production and the dysregulation of lactate metabolism are key elements in carcinogenesis (San-Millán and Brooks, 2017) .

In the previous chapter, we characterised a class of group III mechanosensitive and metabosensitive muscle afferents, CT3's. They were activated by a metabolite mix comprising of ATP, lactate and low pH. The sensory signalling mechanisms of ATP

and low pH are better characterised than for lactate. ATP responses are largely mediated via P2X receptors; P2X2 and P2X3 receptor in particular are located on many sensory endings (Bernier et al., 2018, Burnstock et al., 2013, Burnstock and Williams, 2000, Reinöhl et al., 2003). pH changes are often detected via ASIC channels, particularly by sensory neurons and skeletal muscle ASIC3 (Gregory et al., 2015, Molliver et al., 2005, Naves and McCleskey, 2005).

However, fewer studies have specifically investigated sensory responses to lactate. Where this has been done, lactate or lactic acid was injected into the arterial blood supply (Rotto and Kaufman, 1988), or directly into muscles (Gregory et al., 2015, Pollak et al., 2014). Other studies have recorded lactate production and efflux pre-and post-exercise (Amann et al., 2011a, Amann et al., 2010, Amann et al., 2011b). In addition, responses to a 'mix' of metabolic products (ATP, lactate and pH) at varying concentrations (Light et al., 2008, Light and Perl, 2003), occlusion of muscle blood supply (Iwamoto et al., 1985, Kaufman et al., 1984, Kaufman et al., 2002, Kaufman and Rybicki, 1987) or application of a metabolite mix in an *ex vivo* setting (Jankowski et al., 2013)have been described.

Few studies have investigated the effects of lactate alone and whether it can activate sensory endings directly within the muscle (Xu et al., 2010). Additionally, effects of high concentrations of lactate are complicated by the phenomenon that lactate chelates calcium and magnesium ions in extracellular solution, thereby modifying the availability of divalent cations. Decreases in divalent cations enhance ASICs', responses to protons (particularly ASIC3) (Immke and Mc Cleskey, 2001, Molliver et al., 2005, Naves and McCleskey, 2005). Thus, it has been suggested that the effects of

lactate are on sensory afferents may be indirect, mediated by modulation of ASIC3 channels through this mechanism.

Another mechanism, by which lactate could act directly on sensory neurons, is through the G-protein-coupled-receptor 81 (GPR81) or hydroxy carboxylic acid receptor 1 (HCAR1). This receptor was classified as an orphan receptor until 2008, when lactate was identified as an endogenous ligand (Cai et al., 2008, Liu et al., 2009). HCAR1 is primarily expressed in white and brown adipose tissues (Offermanns et al., 2011). However, it has also been detected in lower amounts in other tissues, including heart, stomach, intestine, hippocampus, cerebellum and skeletal muscle (Liu et al., 2009). It is currently unknown if lactate directly activates primary afferents via HCAR1.

Here, we demonstrate that lactate anions, but not reduced [Ca^{2+}] and [Mg^{2+}], can activate CT3 identified afferents in our *ex vivo* preparation. We show that HCAR1, the receptor for lactate, is expressed in dorsal root ganglia (DRG) that provide sensory innervation of abdominal muscles. In addition, we showed that cell bodies retrogradely labelled from mouse abdominal muscles, are immunoreactive for HCAR1, and that HCAR1 immunoreactive axons are present in wholemount abdominal muscles preparations. This suggests that CT3 afferents can be directly activated by lactate via its GPCR HCAR1.

METHODS AND MATERIALS

Dissection

C57Bl/6 mice (*n*=26, 6 female and 20 male), between the ages of 4-8 weeks (bred in-house), given *ad libitum* access to food and water, were euthanized by a lethal dose of isoflurane by inhalation, followed by removal of the heart or decapitation. All procedures were performed in accordance with *Australian Code for the Care and Use of Animals for Scientific Purposes* (8th ed, 2013, National Health and Medical Research Council of Australia) and were approved by the Animal Welfare Committee (permit #890/15) of Flinders University. Unless stated otherwise in the following methods, the abdominal wall musculature (external oblique, internal oblique, transversus abdominis and rectus abdominis) was removed from the animal, along with the lower ribs on the right side, for orientation. The external oblique and rectus abdominis were then removed, leaving a preparation of internal oblique and transversus muscle which was pinned in a petri dish lined with Sylgard (Dow Corning, Midland MI), containing Krebs solution (in mM: NaCl, 118; KCl, 4.75; NaH_2PO_4, 1.0; $NaHCO_3$, 25; $MgCl_2$, 1.2; $CaCl_2$, 2.5; glucose, 11; bubbled with 95% O_2/5% CO_2) and warmed to 37°C.

Anterograde labelling

The preparation was pinned in a purpose-built chamber for anterograde labelling of axons in the nerve trunk (Zagorodnyuk and Brookes, 2000). The end of the nerve trunk was led into a side-chamber filled with paraffin oil (sealed with a partition made from a cover slip, with a silicon grease seal (Ajax Chemicals, Castle Hill, NSW, Australia). A drop of biotinamide solution (Molecular Probes, Eugene, OR, USA) in "artificial intracellular medium" (150 mM monopotassium L-glutamic acid, 7 mM $MgCl_2$, 5 mM glucose, 1 mM EGTA, 20 mM HEPES, 5 mM disodium

adenosine-triphosphate, 0.02% saponin, 1% dimethyl sulphoxide) was placed onto the de-sheathed nerve trunk under the paraffin and the main chamber was filled with sterile culture medium (Tassicker et al., 1999). Preparations were incubated for 4 hours on a rocking tray in a humidified incubator at 37°C, 5% CO_2 in air, then fixed overnight in modified Zamboni's fixative (as above) at 4°C. Preparations were permeabilised and cleared using the immunohistochemical protocol described above. Biotinamide was visualised by CY3-conjugated streptavidin (1:500, Molecular Probes, 4 hours). Preparations were then immunohistochemically labelled (*n*=10), rinsed three times in PBS and mounted in 100% carbonate buffered glycerol (pH 8.6) as described above. Preparations were mounted between two coverslips, with the lower coverslip fixed to a 1 mm thick aluminium surround so that they could be viewed from either side.

Immunohistochemistry

Tissue fixation and processing

Samples used for immunohistochemistry were dissected and fixed in modified Zamboni's fixative (0.2% saturated picric acid in 2% paraformaldehyde in 0.1 mol L^{-1} phosphate buffer, pH 7.2) for 24 hours.

Wholemounts

The samples were then treated with Triton X-100 (0.5%) in PBS on a mixing tray at room temperature overnight. After 24 hours, the samples were rinsed in PBS, then further permeabilised in 100% glycerol with 0.1% sodium azide, on a rocking orbital mixer (OM5, Ratek, Victoria, Australia) in a humidified incubator at 37°C for 24 hours. Samples were then washed with PBS solution (3 x 30mins) to remove the glycerol. Preparations of abdominal muscle (n=5) were incubated with primary antisera at room temperature for 2 days; primary antibodies are described in **Table 4.1**.

The HCAR1 antibody, GPR81 s296 (Cat# SAB1300090; Sigma-Aldrich), was raised in rabbit against the N terminal extracellular domain of HCAR1(1:200). The antibody specificity and the use of this HCAR1 antibody for immunohistochemical studies has previously been described. Immunohistochemical staining of mouse cortical neurons and western blot analysis demonstrated the labelling of HCAR1 protein. HCAR1 protein expression corresponded to the expected 39 kD molecular mass, as a predominant dark band with only a faint lighter band below 37 kD demonstrating antibody specificity (Bozzo et al., 2013). Preparations were rinsed three times in PBS and incubated with the appropriate secondary antisera for 4 hours at room temperature, all raised in donkey and obtained from Jackson ImmunoResearch (MI, USA). Details of antibody combinations are summarised in **Table 4.1**. After final rinse with PBS, preparations were equilibrated with 50%, 70% and 100% carbonate-buffered glycerol and mounted in 100% carbonate buffered glycerol (pH 8.6).

Sections of dorsal root ganglion

Immersion fixed dorsal root ganglia (*n*=5, T11 to L1) were placed in PBS containing 3% sucrose as a cryoprotectant overnight before being embedded in O.C.T (Optimal Cutting Temperature) compound (Tissue-Tek, Torrance, CA, USA). The ganglia were cut into 12µm thick sections on a cryostat (Lecia- Riechert Cryocut 1800 Cryostat, Germany) at -19C and thaw-mounted onto polyethyleneimine-coated slides. Every third section was collected on the same slide to avoid double counting and approximately 24 sections were counted for each ganglion. Slides were allowed to dry overnight at room temperature and subsequently stored at 4°C, protected from light. Normal donkey serum (10%) for 30 minutes was used as a blocking agent. Antisera against HCAR1, CGRP and NF200 were then applied to sections (Table 4.1.). Sections were incubated in primary antisera at room temperature overnight. The preparations

were then washed with PBS (three 10-min washes) and incubated with appropriate secondary antibodies (Table 4.1.) for 2 hours. After washing with PBS preparations were mounted as described.

Table 4.1. List of primary and secondary antibodies.

Primary Antibody	Source	Species	Dilution	Secondary Antisera		Source	Dilution
GPR81/HCAR1	Sigma	Rabbit	1:200	Donkey CY3	Anti-Rabbit	Jackson	1:400
CGRP	Abcam	Sheep	1:500	Donkey CY5	Anti-Sheep	Jackson	1:200
NF200	Sigma	Mouse	1:1000	Donkey AMCA	Anti-Mouse	Jackson	1:100

Close extracellular single unit recordings

Results are presented from 13 recordings in which CT3 afferents were positively identified. Extracellular recordings, focal compression and stretch stimuli were carried out as described in **Chapter 3**.

Application of lactate

In early experiments a bolus dose of lactate was added to the bath to reach the desired bath concentration (1, 2, 5, 10, 15, 20, 50 mM) with an identical volume bolus of Krebs solution used as a control.

After determining that perfusion was the ideal lactate application method, initial recordings suggested that buffering was needed to maintain a constant pH during the

addition of lactate. To achieve this the recorded afferents were first identified in standard Krebs solution, then the solution was switched to a control HEPES buffered Krebs solution (139 mM NaCl; 4.7 mM KCl; 1.2 mM $MgCl_2$; 11 mM Glucose; 5 mM HEPES; and 2.5 mM $CaCl_2$, pH 7.4) and allowed to equilibrate for 15 minutes during superfusion at 4ml/min. After preparations had equilibrated, they (n = 13) were exposed to 15 mM lactate dissolved in the HEPES buffer solution (15 mM Sodium Lactate; 124 mM NaCl; 4.7 mM KCl; 1.2 mM $MgCl_2$; 11 mM Glucose; 5 mM HEPES; and 2.5 mM $CaCl_2$) at pH 7.4. The NaCl concentration within this solution was reduced to compensate for the addition of sodium lactate. The solution was then titrated back to a pH of 7.4 using 300 mM HCl. The solution was perfused for 15 minutes, then replaced with the HEPES solution for a further 15 minutes. This ensured that addition of lactate occurred independent of changes in pH, osmolarity or temperature.

Application of HCAR1 agonist 3,5-Dihyroxybenzoic acid

In some preparations (n = 5), the effect of the HCAR1 agonist 3,5-Dihydroxybenzoic acid (300μM) (Liu et al., 2012) was measured by superfusing the solution into the bath for 10 minutes at a rate of 4mls/min.

Application of low calcium and magnesium ion solution

To test whether chelation of calcium and magnesium ions could explain the effect of this lactate, we used a previously described solution that 'mimics' the effects of lactate on divalent cation availability (Immke and Mc Cleskey, 2001, Naves and McCleskey, 2005). The solution were calculated based on the free ion concentrations in various lactate solutions from published equilibrium constants (Immke and Mc Cleskey, 2001, Martell, 1977). The 'mimic' solution has a lower concentration of both calcium and

magnesium ions (130 mM NaCl, 5 mM KCl, ***0.88 mM $MgCl_2$***, 10 mM Glucose, 5 mM HEPES, ***1.77 mM $CaCl_2$***, pH 7.0). Lowering the concentration of the calcium and magnesium ions, emulated the effects caused by chelation by 15 mM lactate of these divalent cations. Therefore, if this mimic solution affected CT3 afferent firing in a similar manner to lactate solution, chelation of divalent cations could explain its action.

In these studies, preparations (n = 6) were equilibrated in a HEPES solution containing (130 mM NaCl, 5 mM KCl, ***1 mM $MgCl_2$***, 10 mM Glucose, 5 mM HEPES, ***2 mM $CaCl_2$***) for 15 minutes. The preparations were then exposed via superfusion to the 'mimic' solution. After a 30-minute washout period the preparations were then exposed for 15 minutes to a modified 15 mM lactate solution. This solution with increased concentration of calcium and magnesium ions (115 mM NaCl, 5 mM KCl, ***1.12 mM $MgCl_2$***, 5 mM HEPES, ***2.35 mM $CaCl_2$***, 15 mM lactate) to compensate for chelation of divalent cations (Immke and Mc Cleskey, 2001).

RNA isolation and Quantitative real-time PCR

Quantitative real-time PCR was used to detect mRNA for the lactate G-protein coupled receptor HCAR1.This was compared in freshly dissected hippocampus, gastrocnemius muscle, dorsal root ganglia, and abdominal adipose tissue (white fat) of C57/BJ6 mice (n=4). Tissues were harvested and placed into Trizol (Sigma), then homogenized using a tissue lyser (Qiagen, Melbourne, Victoria, Australia). RNA was extracted using the Direct-zol RNA mini prep- with on-column DNase treatment (Zymo-Spin ICC Columns, Zymogen, Irvine, CA, USA) according to the manufacturer's instructions. RNA purity and concentration were determined using a Nanodrop 2000 (ThermoFischer Scientific, Scoresby, Victoria, Australia). cDNA was produced from the isolated RNA using IScript Reverse Transription Supermix according to the

manufacturer protocols (Superscript II, Biorad, Australia). Real-time PCR was performed using the StepOnePlus cycler (Life Technologies, Scoresby, VIC, Australia). Target-genes were identified and amplified using predesigned primers and probes from Taqman (Cat#4331182, ThermoFischer Scientific, Scoresby, Victoria, Australia) HCAR1, the samples were normalised to β-actin and GAPDH (see Table 4.2) based on comparable expression of this protein in different tissue types. A sample with no cDNA template served as the negative control, with all samples run in triplicate. Primer efficiencies were determined for each target. Resultant PCR products were separated on a 2% SB agarose gel with 100 bp DNA ladder (Invitrogen Scoresby, Victoria, Australia, Cat# 15628-019) and imaged using the Gel Doc EZ Imager (Bio-rad, Gladesville, NSW, Australia) and Image Lab software (Bio-rad). Target gene expression was determined relative to the endogenous controls using Q- Gene analysis software (Simon, 2003).

Table 4.2. TaqMan Primer assays.

Primer	Accession no.	Amplicon length (bp)	Reference
GPR81/ HCAR1	Mm00558586_s1	82	Lauritzen, 2014
β-actin	Mm02619580_g1	143	Liu, 2009
GAPDH	Mm99999915_g1	109	Lauritzen, 2014

Retrograde labelling

To identify the spinal sensory neurons that innervate the abdominal muscles (external and internal obliques, transversus abdominis) retrograde labelling was performed. Male and female C57BL/6 mice (n = 4) were anaethetised by isoflurane inhalation

(induced at 4%, maintained at 1.5% in O_2). While under anaesthesia, a 10 mm long incision was made to the ventral abdomen, approximately 15 mm lateral from the midline, to expose the abdominal wall musculature on the right-hand side. Five microliters of Cholera toxin subunit B (CTxB) conjugated with Alexa Fluor 488 (1mg/mL; Molecular Probes, Vic, Australia was used to fill a glass micropipette (outer diameter: 1.5 mm, inner diameter: 1.12 mm; Cat# TW 150-4; World Precision Instruments, WPI) pulled on a Flaming Brown micropipette puller (Model P- 87; Sutter Instrument Co.) with tip diameters of approximately 5µm. Micropipettes were advanced into the abdominal wall, and solution was injected into the muscle using a custom-made pressure ejection system (Biomedical Engineering, Flinders University). This delivered controlled puffs of nitrogen pulses (1 s duration @ 0.3 Hz; 70 kPa) to the microelectrode. The fine microelectrode tips caused little visible damage to the injected abdominal muscles. Following tracer injection, the skin was closed using 5.0 suture (Dynek, Australia) and a layer of OpSite spray (Cat# 66004978; Smith & Nephew, Hull, UK) was applied. Mice were given at least 7 days to recover after the abdominal muscle injection, before being euthanized by isoflurane inhalation overdose, followed by removal of the heart. The abdominal muscles (internal and external obliques and transversus abdominis), dorsal root ganglia (T9-L1), spinal cord and skin surrounding the incision site were removed from the animal, then the tissue was fixed and permeabilised as previously described. DRG's (T9-T11) were sectioned, as described above. To avoid double counting of CTxB-488 cells, every fourth section of DRGs was collected on the same slide. Out of these four slides every second slide was processed with antisera for HCAR1, CGRP and NF200.

Microscopy and processing

Immunohistochemically stained preparations were viewed and analysed on an Olympus IX71 inverted fluorescence microscope, fitted with appropriate dichroic mirrors and filters. Images of labelled neural structures were captured with a CoolSNAP ES digital camera (Roper Scientific, (Photometerics), Tucson, AZ, USA) using analySIS 5.0 software (Soft Imaging System, Gulfview Heights, South Australia, Australia). Image processing was restricted to brightness and contrast adjustments, cropping and formation of photomontages using Adobe Photoshop (CS6, Adobe Systems Inc., San Jose, CA).

Statistical Analysis

Statistical analysis was performed by Student's paired or unpaired two-tailed *t* tests or by repeated measures analysis of variance (ANOVA, one-way or two-way) using Prism 7 software (GraphPad Software, Inc., San Diego, CA, USA). Differences were considered significant if $P < 0.05$. Results are expressed as means ± 95% confidence intervals except when stated otherwise. The number of animal used in each set of experiments is indicated with '*n'*. NS denotes a non-significant finding ($P > 0.05$).

RESULTS

Identifying CT3 afferents

CT3 afferents were identified in recordings by their distinctive responses to graded von Frey hair probing and to stretch, as described in **Chapter 2**. Single units were discriminated by action potential waveform after probing with von Frey hairs. In each case, they had increasing action potential firing rates to von Frey hair probing of increasing force. Firing responses tended to saturated above probing forces of 1.0 mN. This characteristic, along with tonic firing throughout the duration of graded stretch with little adaptation, was used to identify CT3 afferents which were the focus of this study (see **chapter 3**). Units that did not have these characteristics were disregarded.

A 1 mN von Frey hair was applied to numerous sites on the preparation (units 14, n=13), to identify the mechanosensitive sites (hotspots) of a single unit. Once a hotspot was localised, a range of von Frey hairs (0.2, 0.49, 0.98, 1.96 and 4.9mN) was applied. The maximum instantaneous firing rate of activated units was found to be 53.8 ± 13.7 Hz comparable to rates reported in Chapter 3 (14 units, n=13, **Figure 4.1.**). All preparations (units 14, n=13) were stretched by imposed loads of 1-6g. Distension evoked a dynamic response at the onset in all 14 units, with firing maintained at an elevated rate throughout the duration of the stretch, with little adaptation (**Figure 4.2.**). As the identified units have similar properties to that of the CT3 afferents described in chapter 2, we are confident that all results in this study were obtained from CT3 afferents.

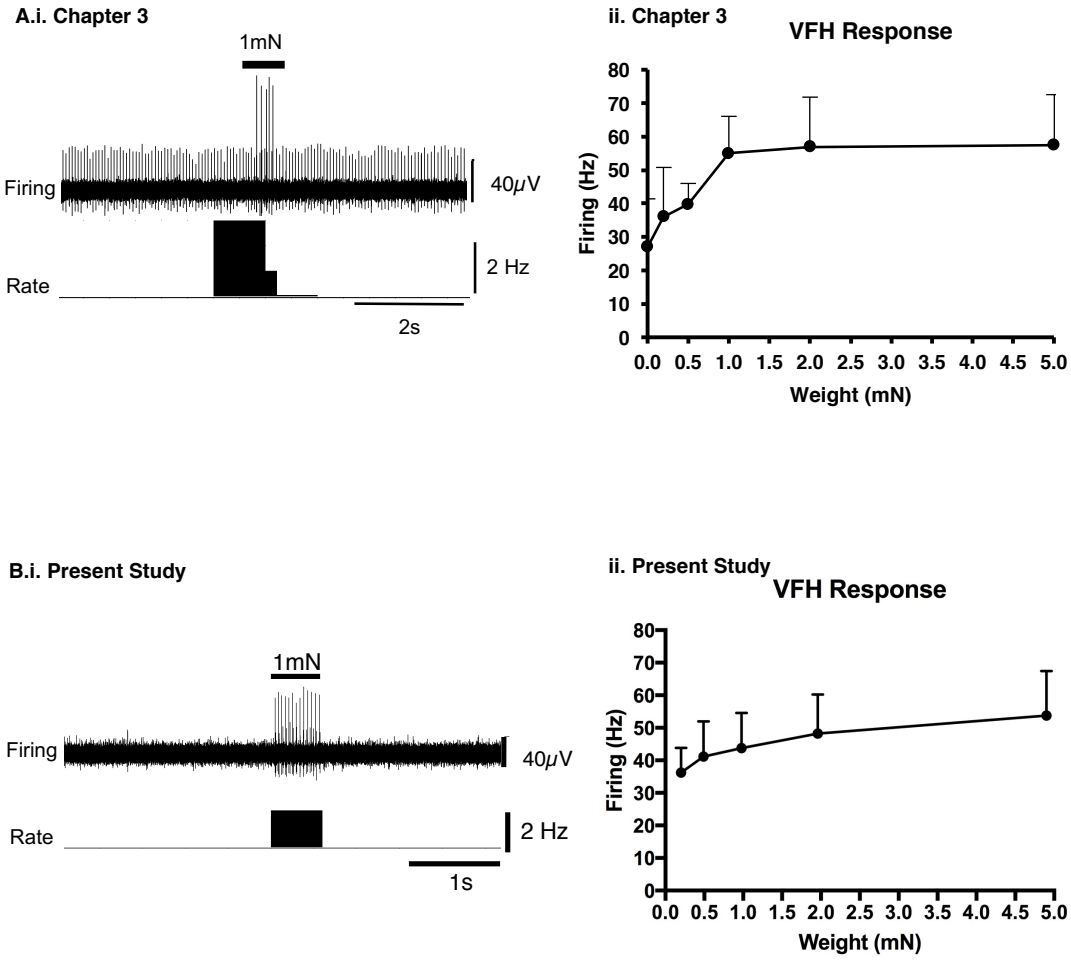

Figure 4.1. Identification of CT3 afferents by responses to von Frey hairs.
Typical responses to 100mg von Frey hair from a unit in the present study and from the first study characterising CT3 afferents (**Ai** and **Bi**). The responses are similar in frequency and dynamics. Mean results of von Frey hair stimulus response curve for 9 units presented in **Chapter 3** (**Aii**) and for 14 units in the present study. This suggests that the same populations of nerve cells (CT3 afferents) were investigated in both studies.

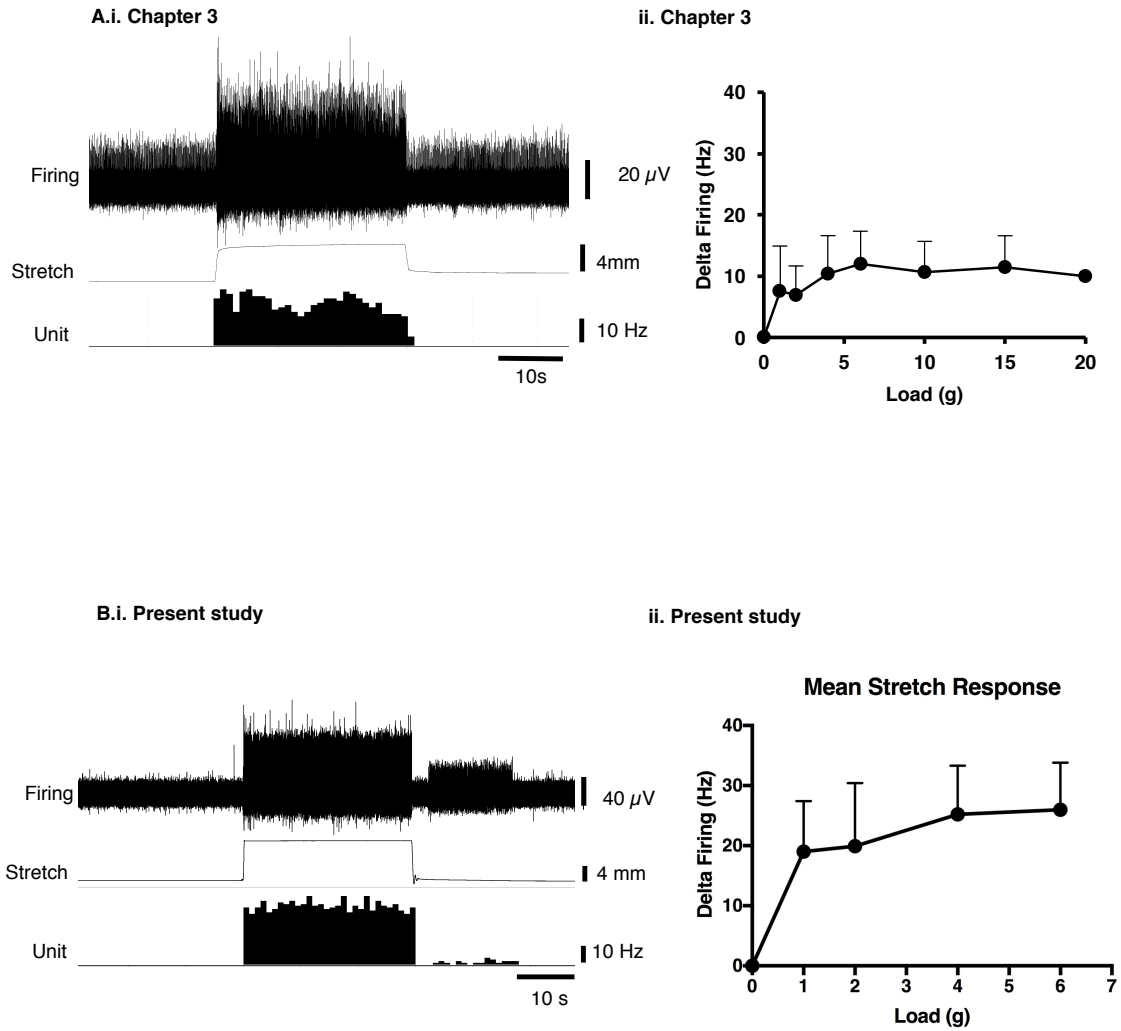

Figure 4.2. Responses of identified CT3 receptors to muscle stretch
Typical response to a 2g load in the study in **Chapter 3** (Ai) and identified CT3 afferents in the present study (**Bi**) are similar in amplitude and dynamics. Mean responses to load/firing curves in **Chapter 3** (9 units) and in the present study (14 units, n = 13, in **Bii**) show the same, characteristics flattening at higher loads, indicating a saturating response. This again supports the suggestion that the criteria used to identify CT3 afferents define populations with similar characteristics.

CT3 afferent response to 15 mM lactate in Krebs

Lactate was initially applied as a bolus dose into the bath to obtain final concentrations of 1, 2, 5, 10, 15, 20, 50 mM. The delivery of a bolus caused a variety of effects on the afferent recordings. The firing of many afferent units was abolished after lactate application (**Figure 4.3.**). Bolus application also caused muscle contractions which sometimes caused tugging on the recorded nerve trunk which affected recording patency. Additionally, muscle contractions made difficult the interpretation of effects on mechanosensitive neurons.

In many studies, direct application of a small drugs bolus into the recording chamber is a simple, rapid and reliable way to test the drug's effects, especially when it acts in the micromolar range. Here however, the final concentrations of lactate were required to be in the millimolar range and this necessitated addition of boluses of large volume (up to 150µl in a 10ml bath). From the preliminary results, we recognised that this method of application could perturb bath temperature, pH, and osmolarity. Each of these factors was addressed individually.

1) **Movement artefact**: Upon the application of a bolus dose of lactate, the muscle was sometimes seen to contract, pulling the recorded nerve and changing action potential amplitudes. To fix preparations in position and eliminate mechanical interference with nerve recordings, twenty or more 50 µm pins were inserted along the top of the preparation, down the side of the preparation and along the nerve within the preparation: this eliminated muscle movements being transmitted to the recorded nerve.
2) **Bath temperature**: The bath temperature was recorded when the bolus was added to the bath. No change in overall bath temperature (32 - 34°C) was

detected but localised temperature change could not be ruled out. Pre-warming the bolus to 32 - 34°C, had no effect on the responses.

3) **Changes in pH**: The pH of the lactate solution and the bath were measured: lactate solutions were more basic than Krebs solution, (pH 8.0 vs pH 7.4 respectively). Lactate solutions were therefore adjusted to a pH of 7.4 using small volumes of 1M HCl, in the HEPES buffered Krebs solution, to maintain constant pH.

After correcting for movement, temperate and pH, there was still visible movement of the preparation (but not the nerve) after bolus application, raising the possibility that the osmolarity of the solutions we were applying was affecting the preparation.

4) **Osmolarity**: Adding 15 mM of sodium lactate, would increase the osmolarity of bath solutions by approximately 30 mOsM. To avoid this, the solutions were balanced so that the sodium lactate replaced part of the sodium chloride in the HEPES-buffered Krebs solution.

Due to the issues regarding bolus application, the administration of lactate was changed from a bolus dose to superfusion. Accordingly, the bath volume was decreased from 10 ml to 4 ml, and flow rate was increased to 4 ml/min in order to speed change-over. pH of the lactate solution was corrected and buffered and the osmolarity was controlled. To ensure that pH, osmolarity, and temperature were maintained throughout the experiment, we substituted Krebs solution for a HEPES buffered solution. From this point on, the recorded afferents were first identified in Krebs solution, then the solution was switched to a HEPES buffered Krebs solution (139 mM NaCl; 4.7 mM KCl; 1.2 mM $MgCl_2$; 11 mM Glucose; 5 mM HEPES; and 2.5 mM $CaCl_2$, pH 7.4) and allowed to equilibrate for at least 15 minutes.

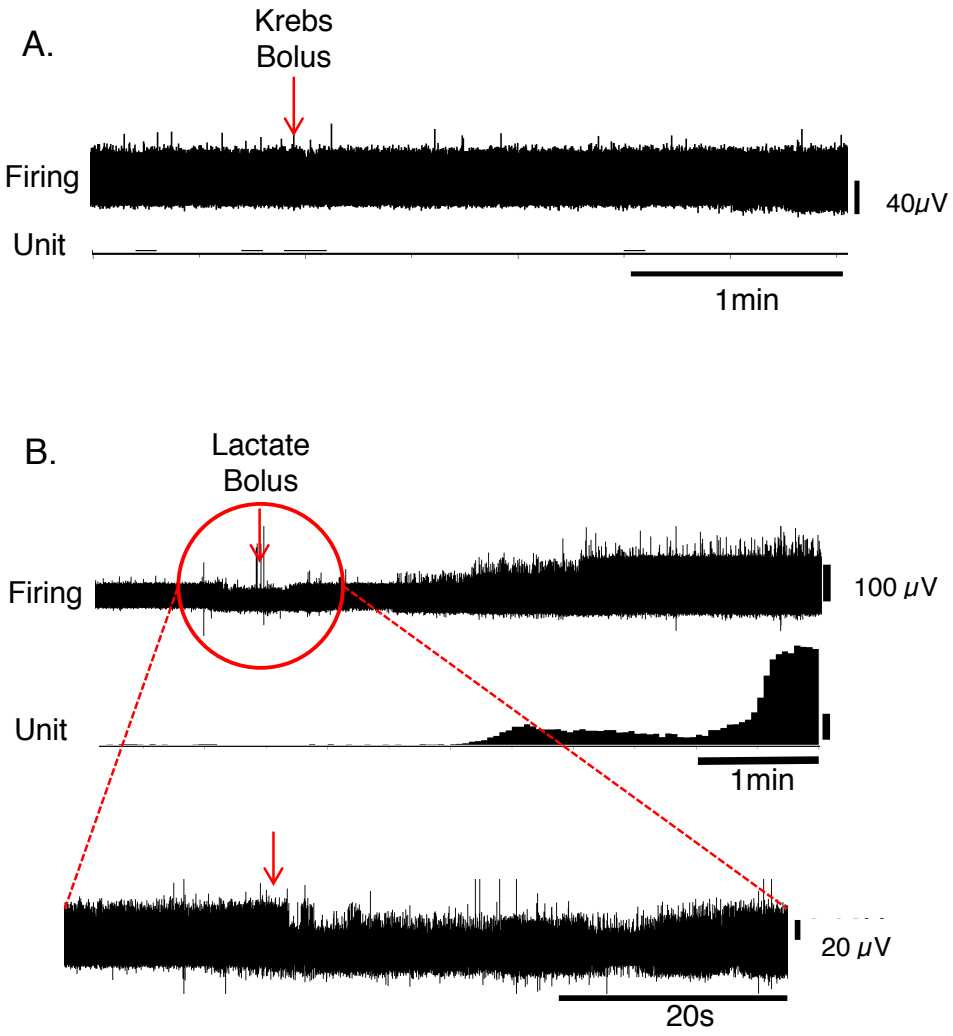

Figure 4.3. Typical effects of bolus application on identified CT3 afferent units. **A.** An identified CT3 unit with minimal spontaneous firing was not detectably affected by application of a bolus of Krebs solution directly into the bath. **B.** In this case, the effects of a bolus of sodium lactate (800µl of 150mM sodium lactate) directly into the bath is shown. With a bath volume of 8mls, this bolus of isosmotic lactate would deliver a final concentration of 15mM. There appears to be an increase in firing of the CT3 unit (B, middle trace) after a delay of 2 minutes. However, there were also changes in the extracellular recording trace (B, bottom trace) with at least one unit dropping out and a notable change in amplitude of the spike envelope, suggesting that the nerve had moved on the recording electrode. Because of artefacts like these, administration of lactate solution was changed over to superfusion, in which temperature, mechanical artefacts, osmolarity and pH could all be better controlled, albeit at the cost of slower wash-in to the bath.

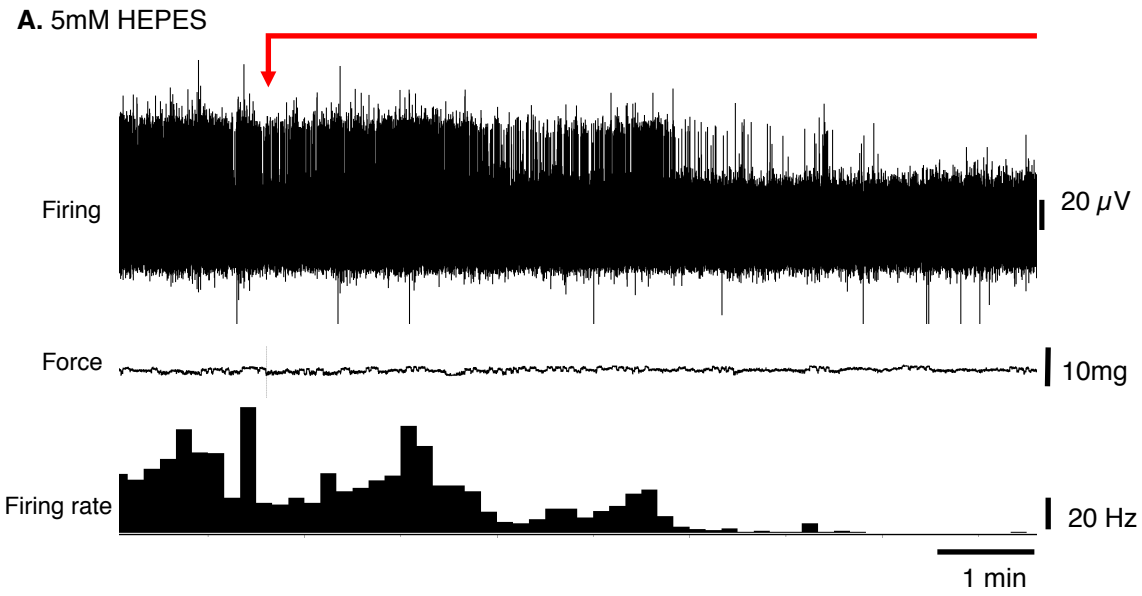

Figure 4.4. Change in firing patterns between Krebs and HEPES.
A. Typical baseline firing of a spontaneously active CT3 unit is shown in the upper trace. At the red arrow, superfusion was switched from Krebs solution to 5 mM HEPES. This caused a rapid loss of spontaneous firing in this unit and in all CT3 units tested. For this reason, the effects of lactate were measured after at least 15 minutes of equilibrium in HEPES containing solution before switching to HEPES solution containing 15 mM lactate.

It was apparent that changing over from Krebs solution to HEPES-buffered Krebs solution reduced the spontaneous firing rate of all afferent units (Fig 4.4). HEPES-buffered Krebs solution does not contain sodium bicarbonate; a difference between the two solutions, which may reflect the overall decrease in spontaneous firing once it is perfused. For this reason, we allowed a period of at least 15 minutes for preparations to equilibrate before recordings were made.

Effects of ATP and low pH on CT3 afferents

As shown in the last chapter, CT3 afferents showed robust responses to the low and high metabolite mix which contained H+, ATP and lactate. We examined the effects of these components applied individually. Typical examples for H+ and for ATP are shown in Figure 4.5. In both cases, the agents at the concentration present in the high metabolite mix (pH 6.6 and 5μM) had negligible effects on CT3 afferents.

CT3 afferent response to 15 mM lactate in HEPES

Fourteen identified CT3 afferents were exposed to 15 mM lactate by superfusion (13 preparations). On average, 15mM lactate by superfusion evoked a small but significant increase in firing. Average basal firing was 6 ± 0.7 Hz and in the presence of 15 mM lactate this increased to an average of 11.7 ± 6.7 Hz (14 units, n=13, $P < 0.05$, $P = 0.0484$, $t = 2.178$, $df = 13$, paired t-test, **Figure 4.6**). From the time of application there was a gradual increase in firing, with the maximum firing rate of 16 ± 9 Hz (averaged across all 14 units) occurring 14 minutes after first arrival in the bath. Of all 14 units exposed to 15 mM lactate, 3 units responded within 10s of lactate arriving in the bath, while the other responding units showed latencies of up to 5 minutes after the start of the superfusion. Of the 14 units, 8 units showed a clear increase in firing after the application of lactate; 4 units showed no detectable changes in firing. The remaining

two units had large bursts of spontaneous firing within the 15-minute basal recording period (average basal firing 9.7 ± 3.7 Hz) and actually showed an overall decrease in firing after lactate arrived in the bath (by 2.8 ± 2.8 Hz). Where present, the large bursts of firing in the baseline period may have overwhelmed either excitatory or inhibitory response to lactate, but this could not be ascertained with confidence.

Response of CT3s to HCAR1 (GPR81) agonist 3,5-Dihyroxybenzoic acid (3,5-DBHA

3,5-Dihydroxybenzenioc acid (300μM, 3,5-DHBA) has been reported to be an HCAR1 agonist (Lui, 2012). The application of 3,5-DHBA evoked no change in the firing rate of CT3 afferents. The average firing rate in 3,5-DHBA was 16 ± 13 Hz was compared to the average basal firing 14 ± 10 Hz, it was not significant (7 units, *n*=5, P > 0.05, P = 0.05057, t = 0.7077, df = 6 paired t-test, **Figure 4.7**).

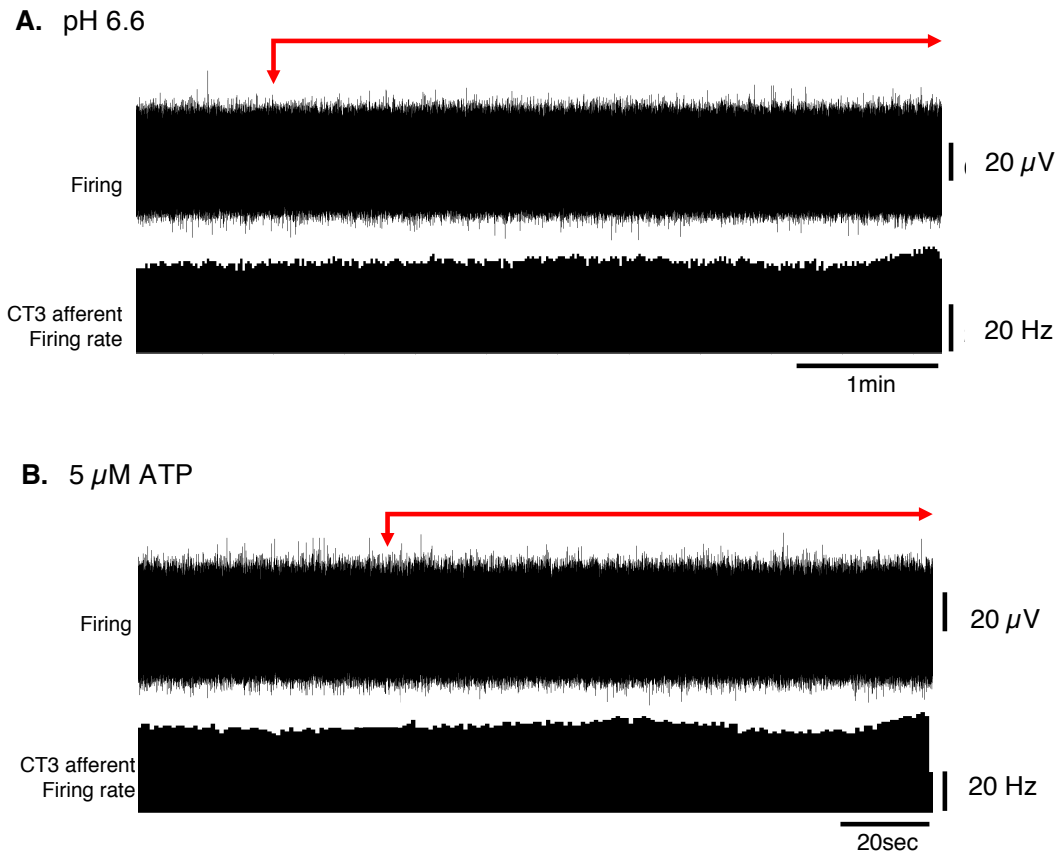

Figure 4.5 Responses of CT3 afferents to superfusion with single components of the low metabolite mix

A. Typical example of the effects of switching from a HEPES-based solution at pH 7.4 to a solution at pH 6.6 solution on an identified CT3 unit which was firing spontaneously at about 30Hz. There was no significant effect on the firing rate (lower trace) **B.** Typical example of the effects of application of 5μM ATP on the firing of the same identified CT3. No significant effects were seen although there is some small variation in spontaneous firing rate in both traces.

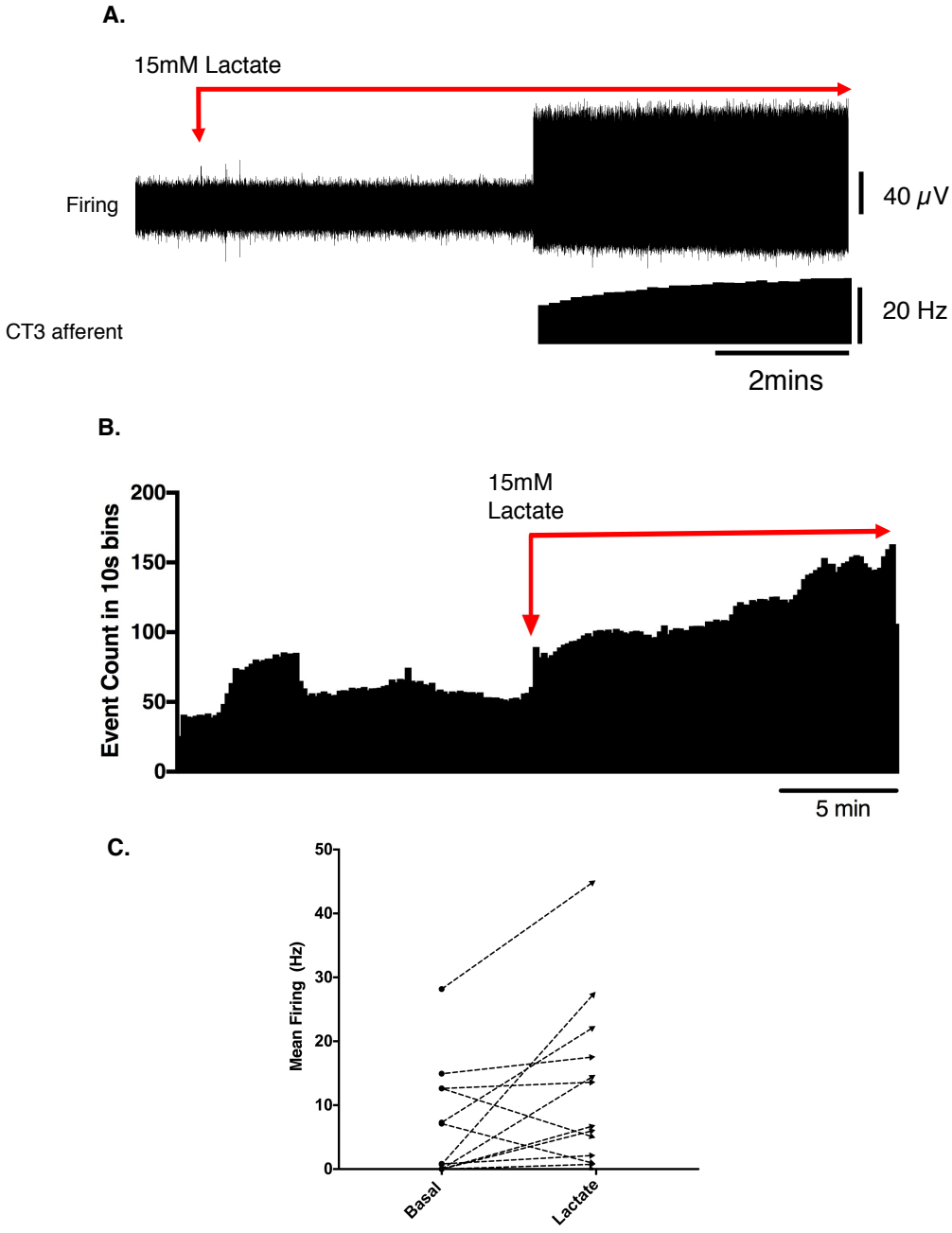

Figure 4.6. Activation of CT3 afferents by superfusion with 15 mM Lactate.
A. Typical example of the effects of application of the 15 mM lactate solution; CT3 unit firing rate (identified single unit) is shown on the lower trace. Note that the unit did not fire spontaneously but after several minutes of perfusion of lactate (15 mM) there was an abrupt start of firing at about 15 Hz which increased in frequency in the next few minutes. **B.** The mean response of 14 discriminated CT3 units is shown during the application of the 15 mM lactate solution averaged over 15 minutes in 10 second bins (14 units, $n = 13$). Note the large sustained increase in spontaneous firing in the presence of lactate. **C.** Comparison of basal firing (black dots) before and after the application of lactate for 14 identified CT3 units. Most units show an increase in firing in lactate, although 2 units showed a marked decrease in firing rate.

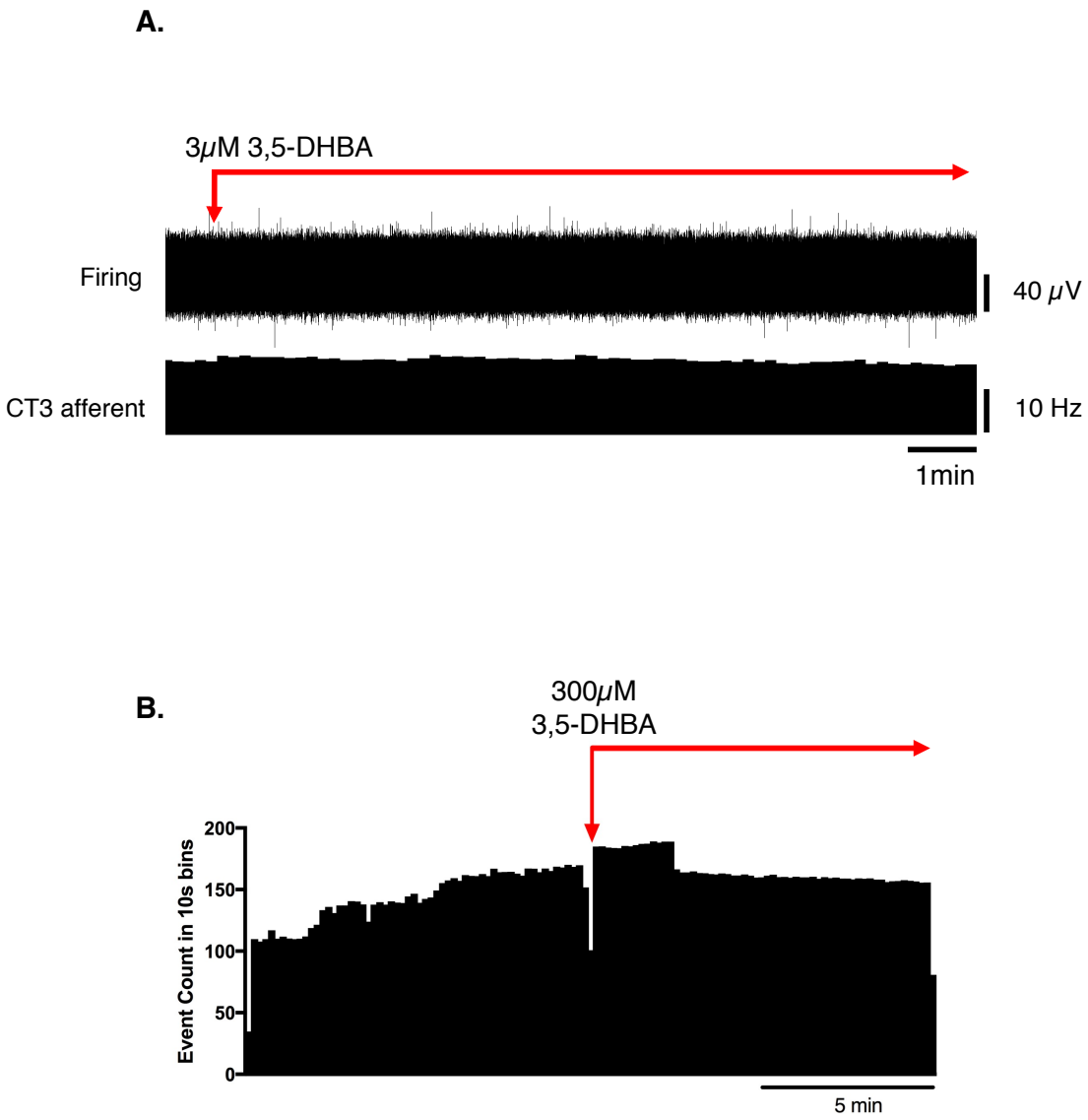

Figure 4.7. Application of HCAR1 agonist 3,5-dihydroxybenzenoic acid
A. Typical response of a single unit to application of a bath concentration of 3 µM 3,5-Dihydroxybenzenioc acid, a HCAR1 agonist. The agonist evoked no detectable change in spontaneous firing. **B.** Mean response of CT3 afferents to 3,5-Dihydroxybenzenioc acid applied in the bath. Again, inconsistent bursts of spontaneous activity led to variability in firing during the control period, but no significant effect was visible after the addition of the agonist. (units 7, $n = 6$).

Response of CT3 afferents to low calcium and magnesium ion 'mimic' solution

It has been reported that lactate can act by chelating calcium and magnesium ions in solution and thus reducing their effective concentration. This, in turn, strongly increases the permeability of the acid-sensing ion channel, ASIC3 to H+ ions. We tested whether a solution with [Ca^{2+}] and [Mg^{2+}] reduced to mimic their free concentration in 15 mM lactate (Immke and Mc Cleskey, 2001) would affect CT3 unit firing in a similar manner to lactate. Of 8 units recorded, 5 showed no response to the low calcium and low magnesium HEPES solution, 2 showed an increase in firing, and one unit showed a decrease in firing. Overall, there was no significant response of CT3 afferents to the low calcium and low magnesium HEPES solution (average basal firing 9.7 ± 8.7 Hz, average response 10.9 ± 10.3 Hz, $P < 0.05$, $p = 0.7431$, $t = 0.3411$, $df = 7$, paired t-test, (**Figure 4.8. and Figure 4.9.**)). This suggests that lactate does not solely act on CT3 afferents via this chelation of Ca^{2+} and Mg^{2+} ions.

After the mimic solution had been washed out, we then applied a 15 mM lactate solution in which [Ca^{2+}] and [Mg^{2+}] were raised ([Ca^{2+}] =2.35mM and [Mg^{2+}] = 1.12 mM) so that free [Ca^{2+}] and [Mg^{2+}] matched those in lactate-free HEPES solution. If reduced activity of the divalent cations was responsible for lactate effects; this compensated solution should be without effect. **Figure 4.8. B** shows that lactate still excited CT3 afferents under these conditions, supporting the idea that lactate was not working solely through chelation of calcium and magnesium ions. Of the 8 units recorded, 5 units showed an increased response to the 15 mM lactate (altered [Ca^{2+}] and [Mg^{2+}]) solution throughout the application, one unit showed an increased response, although this occurred 10 minutes after the application. Two units did not respond to the 15 mM lactate (altered [Ca^{2+}] and [Mg^{2+}]) solution.

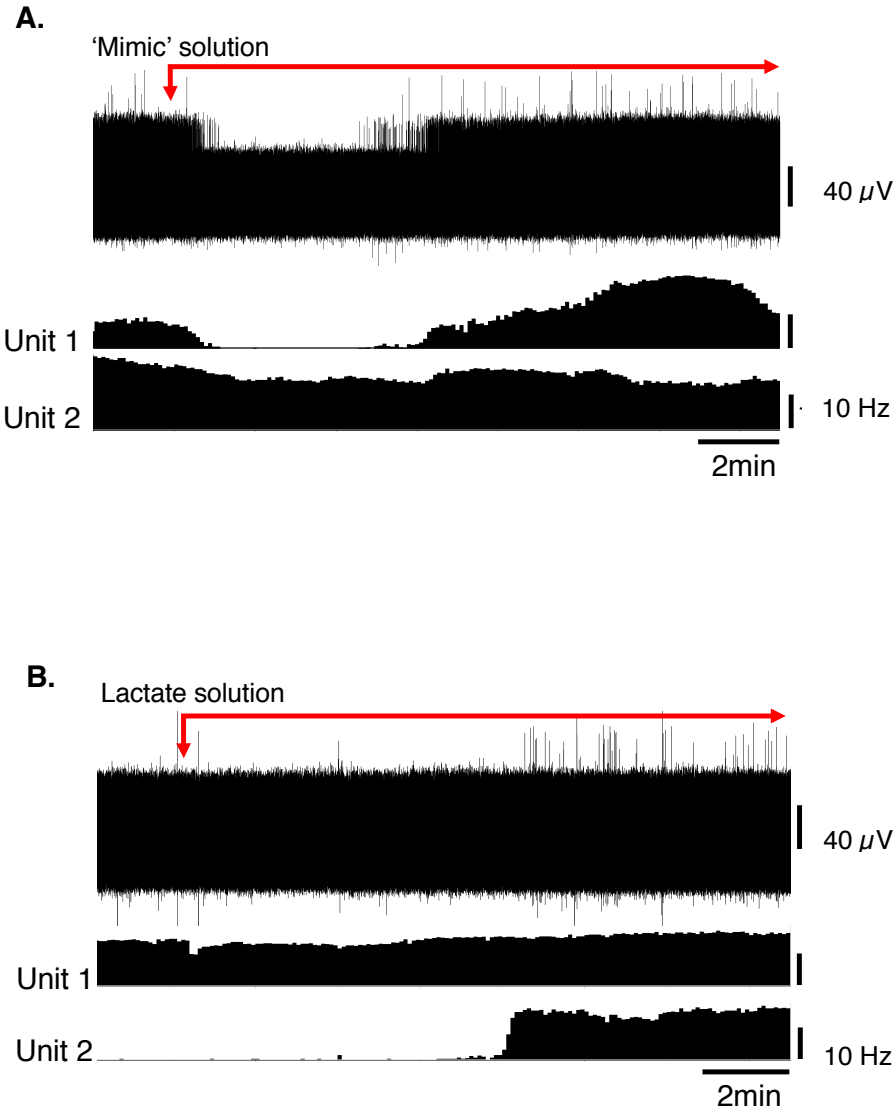

Figure 4.8. Response of CT3 afferents to low Ca^{2+} and Mg^{2+} 'mimic' solution and to 15 mM lactate.

Typical responses of two identified CT3 afferents recorded in a single nerve to the application 'mimic' solution' containing reduced concentrations of Ca^{2+} and Mg^{2+} ions, to mimic the chelating effects of lactate. One CT3 afferent (unit 1) increased in firing after switching to the mimic solution, while other decreased slightly. Overall there was no significant effect of the mimic solution ($p = 0.7431$, $t = 0.3411$, $df = 7$, paired t-test).

Note the other 6 units showed no response in the presence of the 'mimic' solution. **B.** The application of 15 mM lactate, with raised [Mg^{2+}] and [Ca^{2+}] (to counteract chelation effects of lactate) still activated some CT3 units (i.e. unit 2), indicating that its effect was not due to the reductions in the activity of the divalent cations.

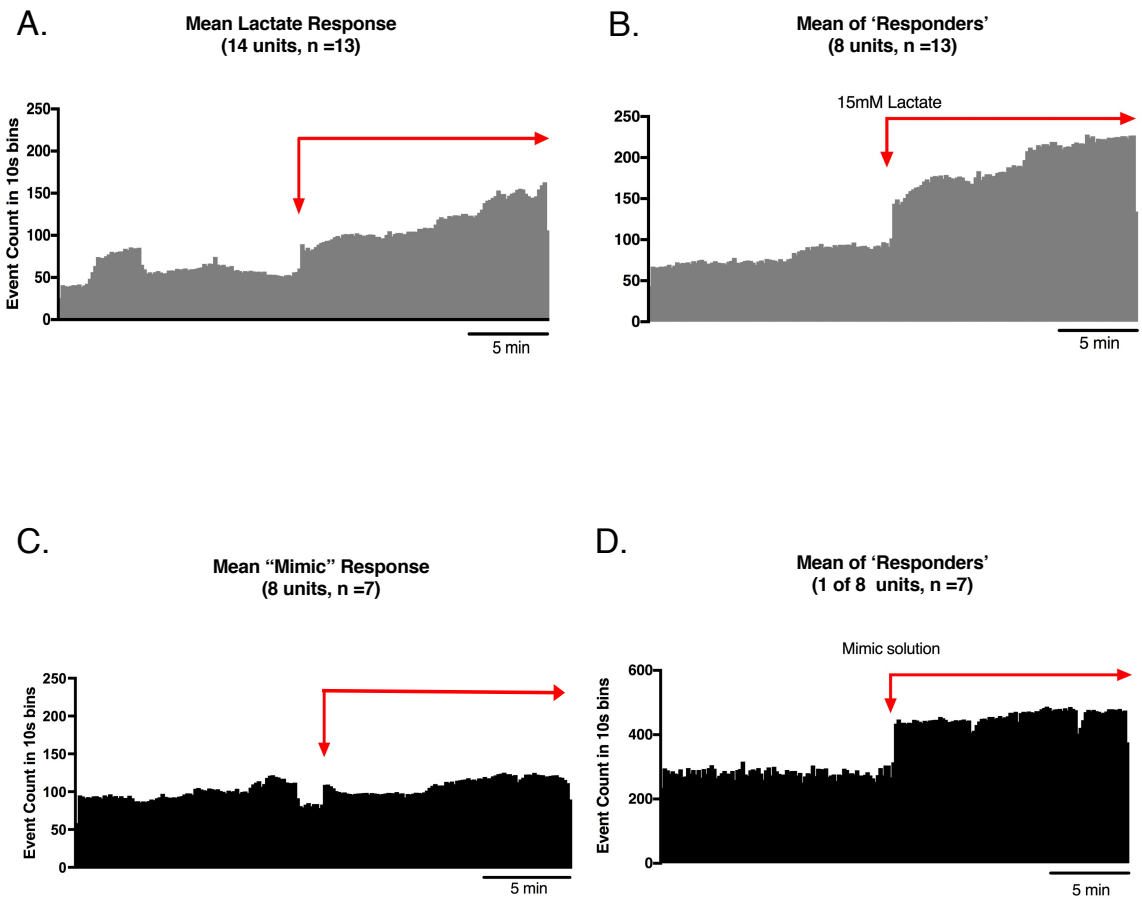

Figure 4.9. The overall mean response to 15 mM lactate and the 'mimic' solutions. **A.** The mean response of all 14 identified CT3 units, *n* = 13 to 15 mM lactate applied by superfusion. **B.** The mean response of the 8 "responder" units out of these 14 units (*n* = 13) which gave a visible response to 15 mM lactate. **C.** The mean response to low Ca^{2+} and Mg^{2+} 'mimic' solution for 8 identified CT3 units (*n* = 7); there was no significant change in firing. **D.** There was one "responder" unit to the mimic solution which showed an apparent increase in firing rate immediately after switching to the mimic solution. Note that the red arrows indicate when each solution was applied after a basal period.

HCAR1 Immunohistochemistry

Presence of HCAR1 immunoreactivity in dorsal root ganglia

HCAR1 immunoreactivity was detected in dorsal root ganglion cell bodies; the labelling was cytoplasmic, non-nuclear and is not detectably membrane bound. HCAR1 immunoreactivity labelled dorsal root ganglion nerve cell bodies with a range of intensities and, in many cases, the initial axon process was clearly labelled. It did not appear to label satellite cells in the ganglion. T11 - T13 DRG nerve cell bodies were assessed for HCAR1, CGRP and NF200 immunoreactive content in triple-labelled 12µm sections (n = 4). HCAR1 immunoreactivity was detected in 63.5 ± 8 % of all T11-T13 DRG cell bodies (n = 4). Cell bodies labelled with HCAR1 were very variable in size and had soma areas that ranged from 71 - 922µm^2. Of all neurons sampled, 28 ± 6 % were immunoreactive for HCAR1 alone (i.e.: HCAR1+/CGRP-/NF200-); 17.5 ± 7 % were HCAR1 co-localised with CGRP but lacking NF200 (HCAR1+/CGRP+/NF200-), 11 ± 10 % were HCAR1 co-localised with NF200 (HCAR1+/CGRP-/NF200+), and 7 ± 5 % were immunoreactive for all three neurochemical markers (HCAR1+/CGRP+/NF200+) **(Table 4.3 & Figure 4.10.)**. HCAR1 immunoreactivity coexisted with other markers in populations of neurons with a variety of soma sizes: HCAR1+/CGRP-/NF200- immunoreactive neurons had an average soma size of 186 ± 24 µm^2, HCAR1+/CGRP+/NF200- cell bodies were similar at 184 ± 32 µm^2 (n =4, NS P > 0.05, P = 0.9182, df =19, one-way ANOVA), HCAR1+/CGRP+/NF200+ were medium sized cells at 420 ± 49 µm^2 (n = 4, P < 0.05 * , P = 0.0132, df = 19, one-way ANOVA) and HCAR1+/CGRP-/NF200+ labelled cells were similarly medium in size with an average of 366 ± 126 µm^2 (n = 4, NS, P > 0.05 , P = 0.539, df = 19, one-way ANOVA) **(Table 4.3 & Figure 4.11.)**.

Table 4.3. Presence of HCAR1 immunoreactivity in dorsal root ganglia

Soma Size	186 ± 24. μm^2	184 ± 32 μm^2	366 ± 126 μm^2	420 ± 49 μm^2	297 ± 9 μm^2	364 ± 37 μm^2	513 ± 30 μm^2	313 ± 82 μm^2
% of cells	28 ± 8 %	17.5 ± 7 %	11 ± 10 %	7 ± 5 %	3.5 ± 3%	4.5 ± 7%	20.5 ± 7%	8 ± 6%
HCAR1	+	+	+	+	-	-	-	-
CGRP	-	+	-	+	+	+	-	-
NF200	-	-	+	+	-	+	+	-

Cell size and percentage of all neurons sampled are shown for the 8 possible combinations of HCAR1, CGRP and NF200 antisera. Cells that lacked all three markers were still detectable by autofluorescence. Counts are based on $n = 4$

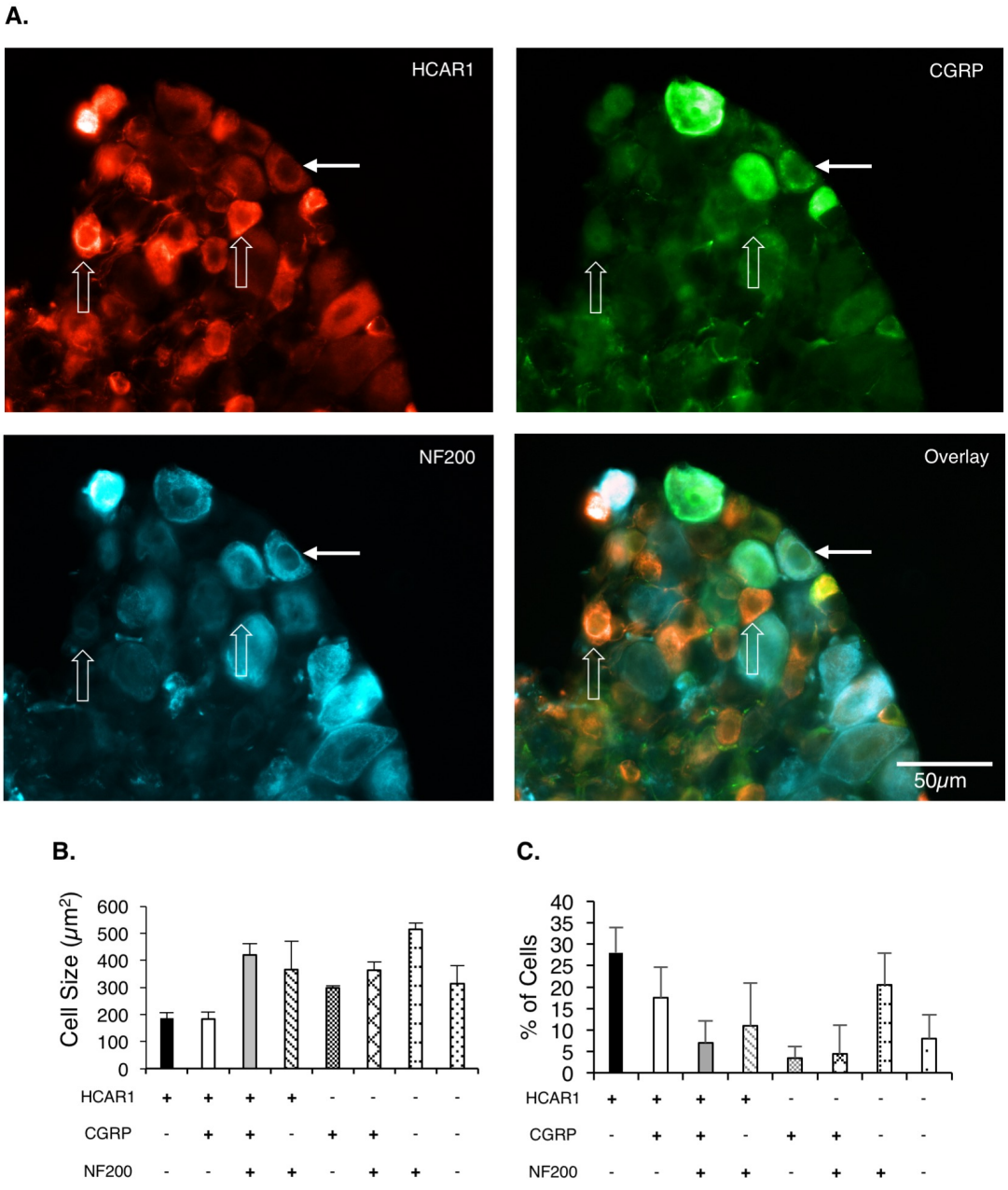

Figure 4.10. Localisation of HCAR1 in dorsal root ganglia and size of labelled cells of thoracic DRG neurons.

A. Thoracolumbar dorsal root ganglia contained HCAR1immunoreactive in small and medium cell bodies (open arrow). Some of these HCAR1 cell bodies were seen without CGRP and may correspond to CT3 afferents. Other HCAR1 cell bodies included large cells, with CGRP and NF200 labelling (solid arrows). **B.** A histogram depicting cell size profile of labelled cell bodies with combinations of markers (Error bars show 95% CI). **C.** The proportion of nerve cell bodies with various combinations of immunohistochemical profiles (n = 4).

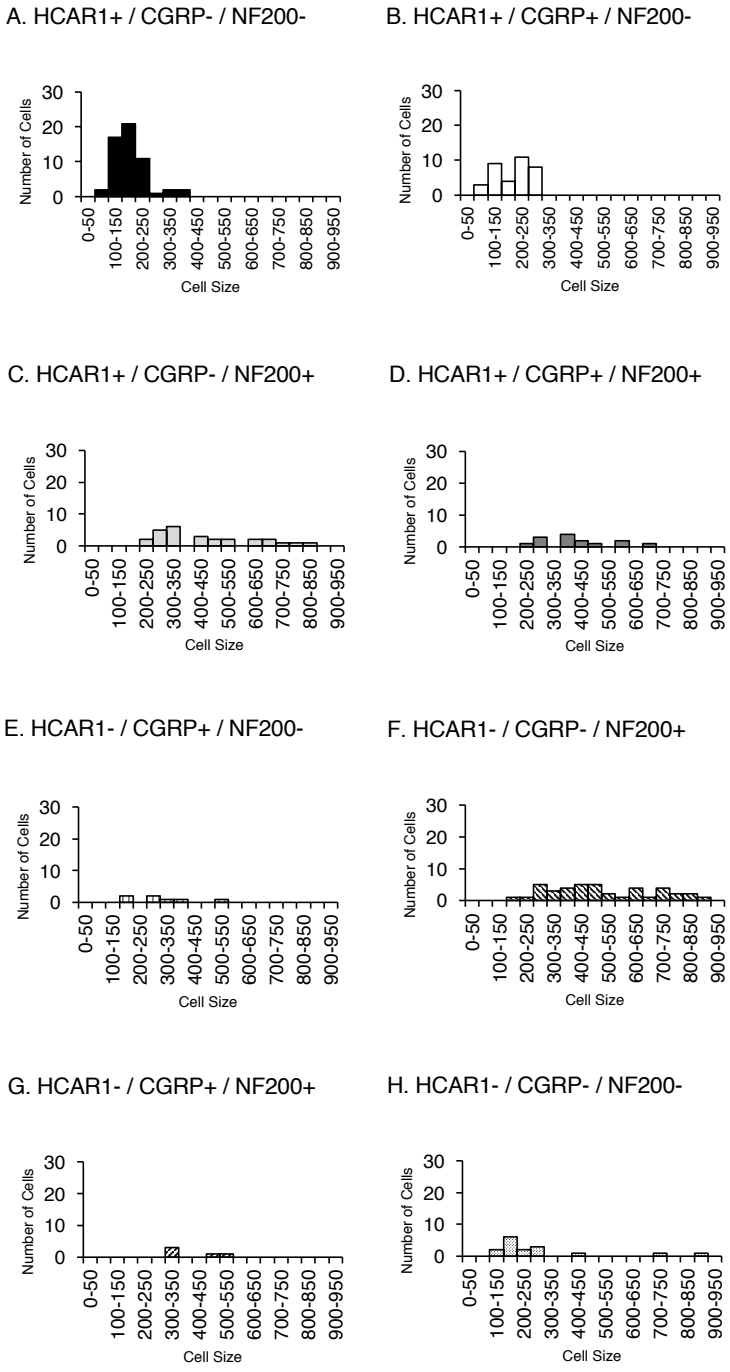

Figure 4.11. Size distribution of nerve cell bodies in DRG neurons (T10-T11) with combinations of HCAR1, CGRP, and NF200 immunoreactivity.

A. HCAR1+/CGRP-/NF200- identified neurons had small to medium soma sizes (0-250µm small, 250-500µm medium). **B.** Neurones co-labelled with HCAR1 +/CGRP+/NF200- had similar sizes to HCAR1+/CGRP-/NF200- neurons but were less numerous. **C.** HCAR1+/CGRP-/NF200+ neurons were identified as medium to large (>500µm) cells. **D.** Neurons labelled with all three neurochemical markers were the least frequent and had a tendency to be larger cells. **E.F.G.** show the relative sizes of cells that were not immunoreactive for HCAR1. **H.** shows cells that lacked immunoreactivity for any of the 3 markers; their size was measured from autofluorescence of their cell bodies.

Presence of HCAR1 in wholemounts of abdominal muscles

Individual nerve trunks innervating the abdominal muscles were labelled with biotinamide and HCAR1 to determine the distribution of HCAR1 immunoreactivity in relation to the nerve distribution in these muscle preparations (**Chapter 2**). Preparations were also labelled with antibodies to CGRP and NF200. HCAR1 immunoreactive nerve fibres mostly had smooth axons (**Figure 4.12.**) and did not appear beaded or varicose. Within large nerve trunks, HCAR1 labelled medium diameter axons (axons of passage as described in **Chapter 2, Figure 4.13.**) which often also co-labelled with NF200. These axons were also smooth rather than varicose (**Figure 4.12.**).

HCAR1 labelling was also present in nerve fibres in small nerve bundles throughout the muscles itself, as well as in the connective tissue layers. Within the connective tissue layers, HCAR1immunoreactive axons would also appear as small or fine continuous axons (**Figure 4.12.**). This pattern occurred in the muscle. These axons often ran alongside fine varicose, often CGRP labelled, nerve fibres. HCAR1 labelling was not only present in nerve fibres in the preparation. It also faintly labelled adipose tissue (white fat cells, **Figure 4.13.**). Other structures within these preparations, such as motor endplates and muscle spindles, were not immunoreactive for HCAR1.

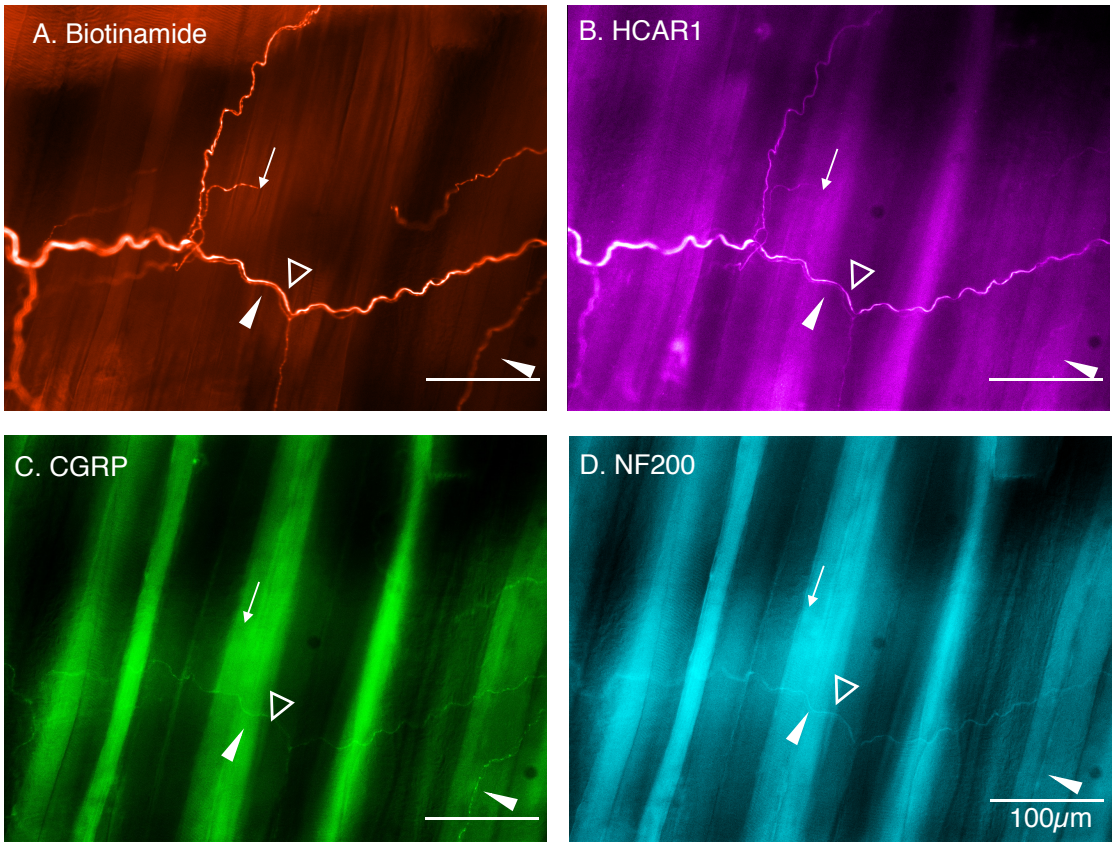

Figure 4.12. Anterograde labelling of extrinsic nerves to abdominal muscles with biotinamide combined with immunoreactivity for HCAR1, CGRP and NF200.
A. As shown previously, biotinamide labelled bundles of axons and single axons branching in connective tissue between muscle layers. **B**. HCAR1 was present in some of the axons in bundles (open arrow head), and also as single axons (white arrow). **C**. These HCAR1 labelled axons ran alongside CGRP immunoreactive axons (white closed arrow heads) but coexistence was not detected **D**. Some axons in the same bundles were also labelled with NF200 (open arrow head).

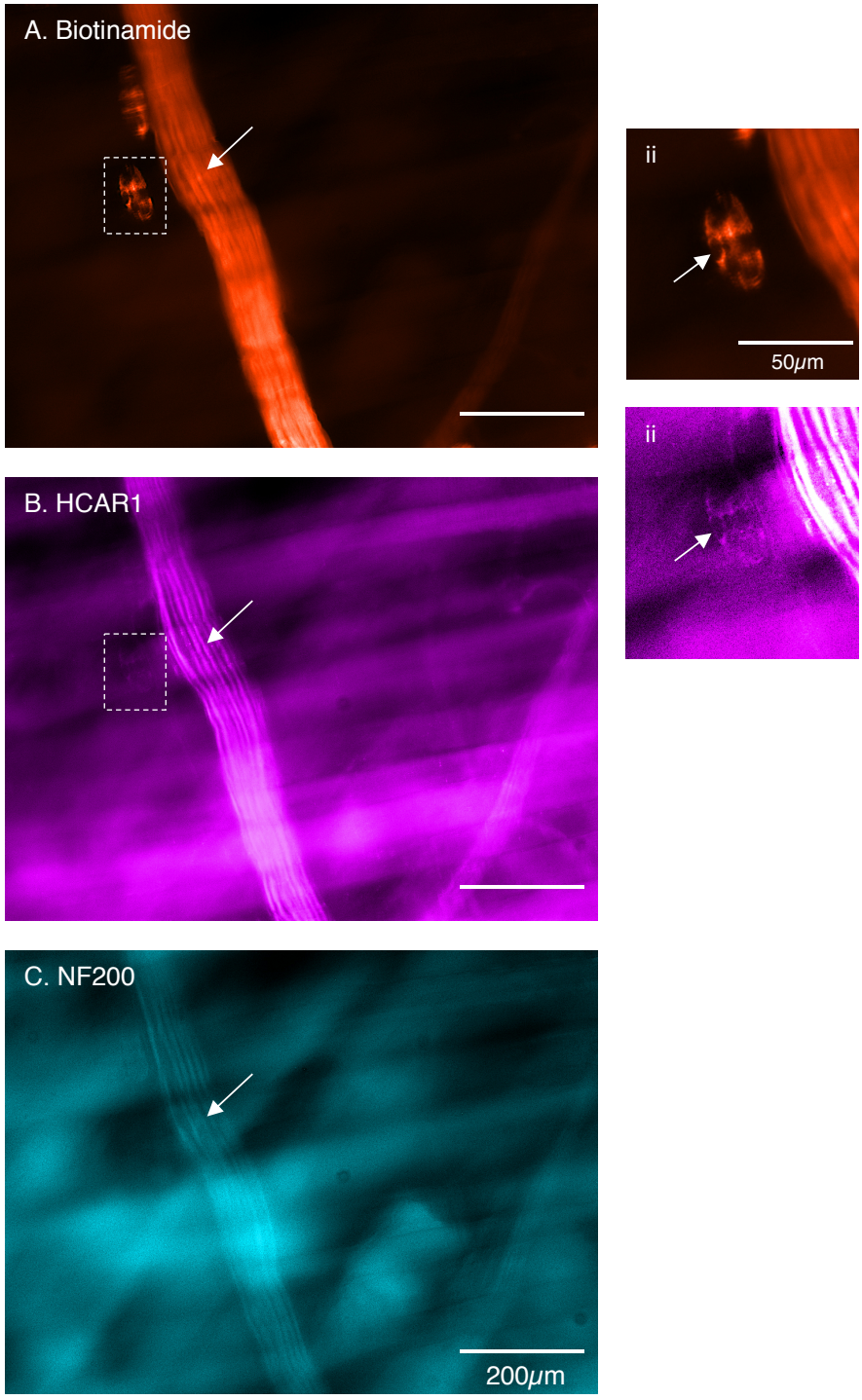

Figure 4.13. HCAR1 immunoreactivity was visible in axons of passage in major nerve trunks and in nearby fat cells.

A. Anterogradely labelled axons of passage labelled with biotinamide include some large diameter axons with characteristic constrictions that reflect myelination (arrow) **B.** some of these axons were HCAR1 immunoreactive (white arrow) and **C**. NF200+ immunoreactive. HCAR1 immunoreactivity was also visible in nearby fat cells (insert, small white arrows). Note that fat cells both contain endogenous biotin and were thus labelled by streptavidin CY3 together with HCAR1 immunoreactivity**.**

Retrograde tracing from the abdominal muscles

Cholera Toxin Subunit B conjugated to Alexa Fluor 488 (CTxB-AF488) was unilaterally injected into the abdominal muscles to retrogradely label DRG nerve cell bodies ($n = 4$). After at least 7 days of recovery, retrogradely labelled nerve cell bodies were detectable in ipsilateral but not contralateral thoracic and lumbar DRG (T9 – L1) (**Figure 4.14.)**. The number of CTxB-AF488 labelled cell bodies in DRG were counted in wholemount preparations of ganglia. On average, after application of CTxB-AF488 to 3 sites in the abdominal muscles, 63 ± 23 neurons were labelled per animal (n =4). These were located in a slightly skewed normal distribution extending from T9 to L1, with the majority of the cells located between T10 and T12 (See **Figure 4.14.**).

T11 thoracolumbar DRG ($n = 4$) contained the largest number of CTxB-488 labelled cells (**see Figure 4.14.**). These were sectioned and labelled with antisera against HCAR1, CGRP and NF200. The proportion of CTxB-488 labelled cells containing immunoreactivity for the different combinations of markers was quantified.

Abdominal-projecting cells in T11 CTxB-488 labelled cells bodies were randomly selected and analysed. Cell bodies that co-localised CTxB-488+/ HCAR1+/CGRP-/NF200- made-up 30% (6/20 cells) and had an average cell size of 198 ± 17 μm^2. HCAR1+/CGRP+/NF200- cells labelled by CTxB-488 (15% (3/20 cells)), averaged 176 ± 6 μm^2. One HCAR1+/CGRP-/ NF200+ immunoreactive cell was the largest filled cells, with the area of 828.8 μm^2 (**Figure 4.15.**). Of these, 50% (10/20) of labelled cells lacked HCAR1-/ CGRP-/NF200- and had an average cell size of 183 ± 37 μm^2.

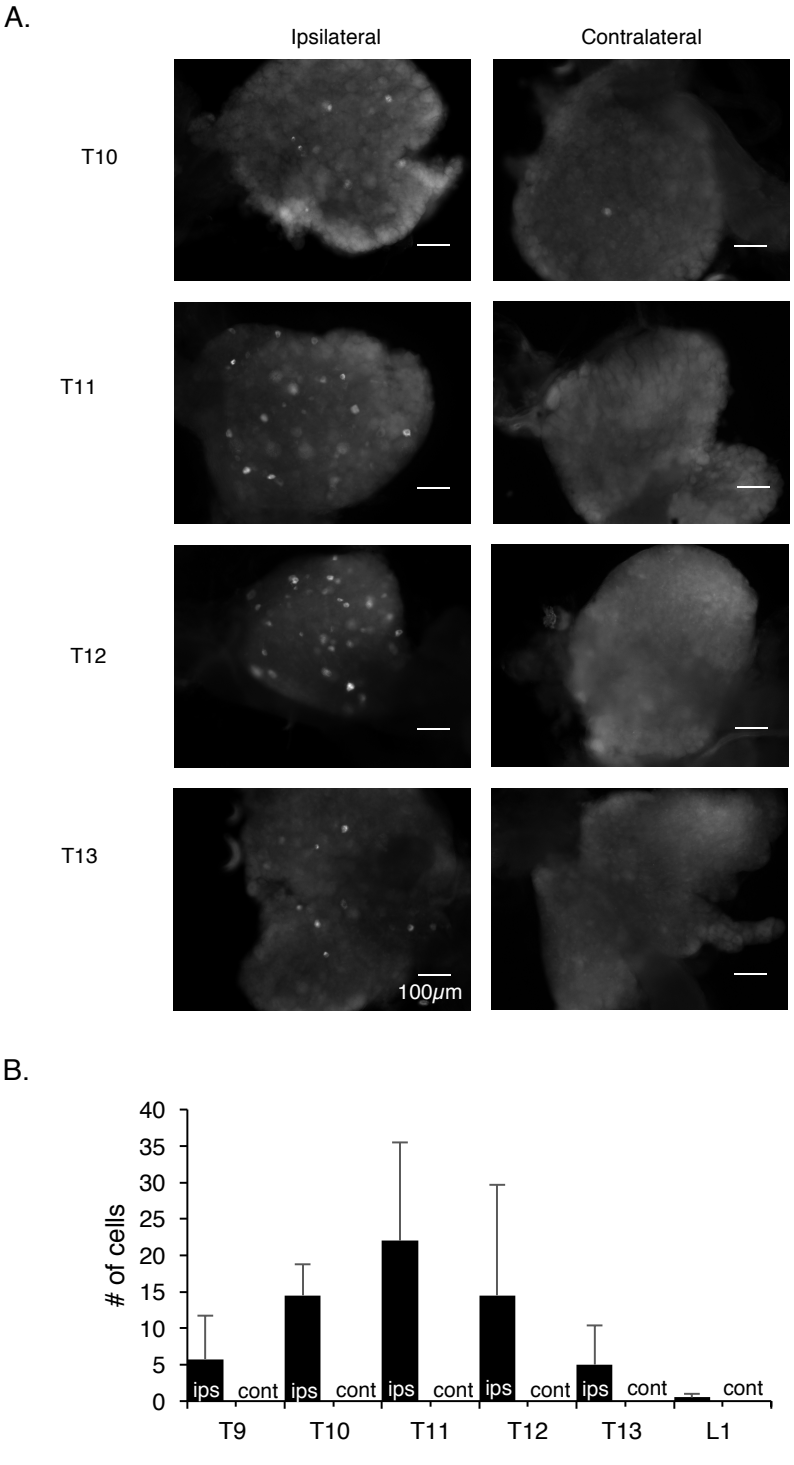

Figure 4.14. Distribution of retrogradely CTxB-AF488 labelled cells in the dorsal root ganglia after application to abdominal muscles

(**A**). CTxB-488 labelled cells were counted in glycerol-cleared wholemount ganglia. They were predominantly located in T10 to T12 ganglia, with a maximum at T11 (n = 4). The contralateral ganglia contained no labelled cells and served as a negative control. **B.** Average number of CTxB-488 cells at each segment for the 2 sides (error bars show 95% confidence intervals) show a distribution peaking at T11.

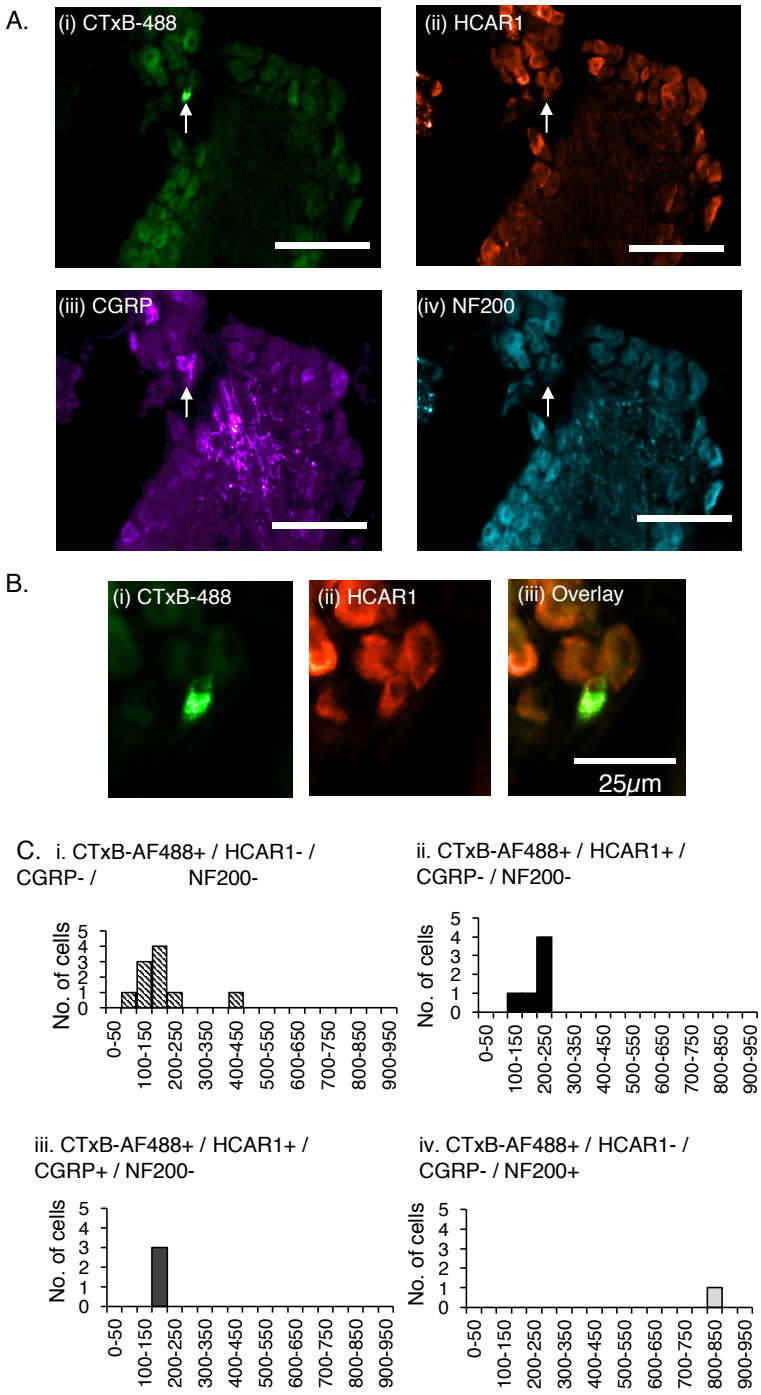

Figure 4.15. Nerve cell bodies in T11 mouse dorsal root ganglia retrogradely labelled from longitudinal muscle; immunohistochemical labelling for HCAR1, CGRP and NF2000.

Ai. Intense CTxB-AF488 labelling of nerve cell body (white arrow) is clearly more intense than autofluorescence unlabelled cells. The arrowed cell was immunoreactive for HCAR1 but not CGRP (**Aiii**) or NF200 (**Aiv**). **B.** shows higher magnification image of the same cell body with its immunoreactivity for HCAR1 clearly visible. **Ci-Civ.** Size distribution of 20 retrogradely labelled DRG neurones in T11 with combinations of HCAR1, CGRP and NF200. Neurons which lacked HCAR1, CGRP and NF200, had small to medium soma sizes. **ii.** Neurones with HCAR1 had similar small sizes but were less abundant. **iii.** HCAR1 neurons that contained CGRP immunoreactivity were small cells. **iv.** Neurons with NF200 were the least frequent and tended to be larger cells.

RNA isolation and Quantitative real-time PCR of HCAR1

We compared expression of mRNA for the GPCR receptor HCAR1, in the dorsal root ganglia, gastrocnemius muscle, hippocampus and abdominal fat of mice. A single PCR product was obtained for HCAR1 in each sample. GAPDH and β-actin were used as dual housekeeping genes as both had previously been compared to HCAR1 expression in these tissues (Lauritzen et al., 2014, Liu et al., 2009).

HCAR1mean normalised mRNA expression, relative to β-actin, was found to be most abundant in abdominal fat (4.29 ± 0.75 MNE), followed by the gastrocnemius muscle (3.59 ± 0.43 MNE), hippocampus (3.07 ± 0.73 MNE) and dorsal root ganglia (3.03 ± 0.23 MNE (**Figure 4.16.**)). However, there was no significant difference in abundance of HCAR1 relative to β-actin between these four tissues, based on a one-way ANOVA corrected for multiple comparisons (n = 4, P >0.05, NS, df = 11 one-way ANOVA).

Expression relative to GAPDH, HCAR1 was most abundant in the abdominal adipose tissue (3.59 ± 0.26 MNE), followed by the hippocampus (2.52 ± 0.70 Log10(MNE), then dorsal root ganglia (2.32 ± 0.12 MNE) and gastrocnemius muscle (1.50 ± 0.29 MNE) (**Figure 4.16.**). There was significantly more HCAR1 mRNA in adipose tissue compared to dorsal root ganglion (n = 4, P < 0.05 *, df =11, one-way ANOVA, **Figure 4.16.**) and the gastrocnemius muscle sample (n = 4, P < 0.05 ***, df = 11, one-way ANOVA, **Figure 4.16.**). However, it should be noted that GAPDH is enzymatic in nature and may itself have variable expression between types of tissues.

Resultant PCR products separated on a 2% SB agarose gel showed identified bands for each sample, which correspond to the predicted base pair mass for HCAR1 (82 bp), as well as housekeeping genes GAPDH (109 bp) and β-actin (143 bp) **(Figure 4.16.)**

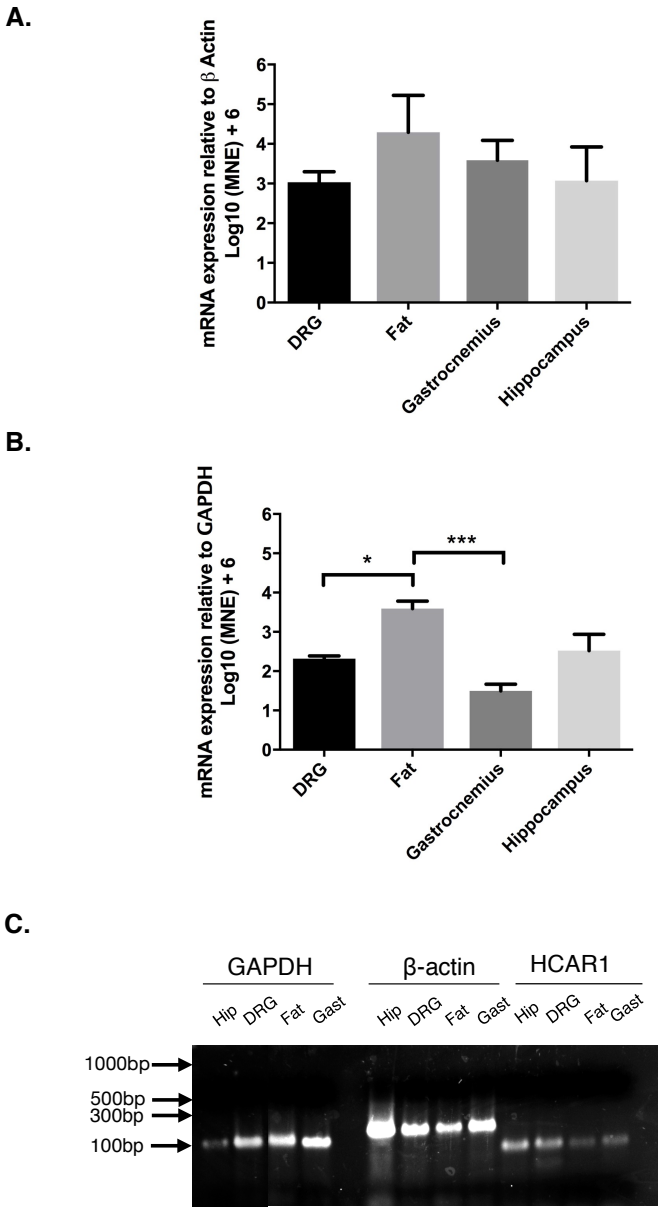

Figure 4.16. mRNA expression of HCAR1 across tissue samples (n=4).

A. Mean expression of GPR81 normalised relative to β-actin, in dorsal root ganglia (DRG), adipose tissue, gastrocnemius muscle and brain tissue (hippocampus). No differences in relative expression were significant. **B.** Mean expression of GPR81 normalised relative to GAPDH, indicated that content in adipose tissue was higher than in the DRG and hippocampus samples. **C.** Gel separation and molecular weight of PCR products of GRPR81 (~82 bp) for Hipp (Hippocampus), DRG (Dorsal root ganglia), Gast (Gastrocnemius) in lanes 9-12. Products for GAPDH (~ 109 bp) and b-actin (~149 bp) in lanes 1-4 and 5-8 respectively; these are both housekeeping genes commonly used to normalise expression levels.

DISCUSSION

Summary of Results

We show, for the first time, that the G-protein coupled lactate receptor, hydroxyl carboxylic acid receptor 1 (HCAR1), is expressed in a subset of primary afferents that innervate the abdominal muscles in mice. Our data is consistent with the proposal that lactate activates sensory afferent endings in striated muscle, at least in part, via HCAR1. Specifically, we have shown that lactate alone excites identified CT3 afferents, but not all sensory neurons. HCAR1 mRNA was localised in dorsal root ganglia that provide sensory innervation of the abdominal muscles. HCAR1 immunoreactivity was also visualised in the somata of dorsal root ganglion sensory neurons retrogradely labelled from abdominal muscles. A population of these cell bodies were HCAR1+/CGRP-; lack of CGRP immunoreactivity was a feature of CT3 afferents (see Chapter 3). Thus, some of these axons are likely to represent the lactate-sensitive CT3 afferents recorded in the present study. HCAR1 immunoreactivity was also present in nerve fibres and nerve endings in wholemounts of mouse abdominal muscle and in axons that had been anterogradely filled with biotinamide applied to the nerve trunks from which recordings of CT3 afferents were made.

Lactate in muscle

Lactate is produced from glucose through glycolysis and the conversion of pyruvate by lactate dehydrogenase to lactate (Meyerhof and Kiessling, 1935 see - (Ferguson et al., 2018)). Lactate is released in high concentrations from active muscle, particularly when oxygen supply is limited. Initially it accumulates in the sarcoplasm, before being transported out of the muscle into the extracellular fluid. Lactate is exchanged between glycolytic and oxidative muscle fibres or it can be released into the bloodstream (Fletcher and Hopkins, 1907, Margaria et al., 1933). The exchange of lactate from one cell/tissue to another occurs

via a family of four monocarboxylate transporters (MCTs) (Brooks, 2007, Brooks, 2009, Gladden, 2004). MCT's are expressed in many tissues and cellular organelles that rapidly exchange lactate. For example, MCT1 and MCT4 transport both lactate and protons out of skeletal muscle during exercise (Gladden, 2004, Domènech-Estévez et al., 2015, Brooks, 2018).

Lactate was long held to be an unwanted by-product of muscle metabolism, produced as a result of anaerobic glycolysis. It was thought that as lactate was transported out of the muscle, in parallel with protons, it caused the formation of lactic acid. The build-up of lactic acid was then believed to cause muscle fatigue and muscle soreness (Fletcher and Hopkins, 1907). Since then, it has been realised that this is not accurate (Hall et al., 2016). Lactate, and not lactic acid, is produced from pyruvate, and itself acts as a weak acid and thus tends to reduce the extracellular proton concentrations. The co-transport of H^+ ions explains the acidification that occurs during intense muscle activity. The characterisation of lactate as a fuel, and its production in fully aerobic conditions (Bendahan et al., 2017), changed the perception of this metabolite from a 'dead-end waste product of glycolysis' (Gladden, 2004, Nalbandian and Takeda, 2016)to a molecule that coordinates metabolism between cells and tissues in many parts of the body (Ferguson et al., 2018).

Lactate is produced in large quantities within active muscle. At rest, the concentration of lactate within the extracellular fluid may be as small as 1-2 mM. During exercise this can increase to 15 mM. When a muscle becomes ischemic, during maximal exertion, the concentration can reach 25-30 mM (Ferguson et al., 2018). Lactate had been proposed to play a role in many different pathophysiological conditions including ischemia (Immke and Mc Cleskey, 2001), muscle fatigue (Fletcher and Hopkins, 1907, Margaria et al., 1933), and acidosis (Robergs et al., 2004). A variety of different techniques have been used to

investigate the role of lactate in normal physiology. *In vivo* injections, of lactate, as part of a metabolite 'mix', containing ATP and protons, has been targeted intra-arterially(Rotto and Kaufman, 1988), intraperitoneally (Carrard et al., 2016), or intramuscularly in rats(Gregory et al., 2015) and human subjects (Pollak et al., 2014). It has repeatedly been shown to activate group III and group IV muscle afferents that signal sensations of fatigue and pain. Similarly, *ex vivo* application of the metabolite 'mix' was used to demonstrate that, at physiological levels, the metabolites produced by contracting muscles (ATP, lactate and protons) activate a population of spinal sensory neurons that innervate skeletal muscles. This 'mix' has also been applied to other *ex vivo* muscle preparations to demonstrate muscle afferents response ((Jankowski et al., 2013, Light et al., 2008) and see **Chapter 3**).

Human studies, have used pressure cuffs to occlude a working muscle's arterial supply, thus causing build-up of metabolites within the tissue. This can be carried out before, during or after exercises to determine, for example, whether the build-up of metabolites increases the afferent firing only while metabolites are present. By releasing the cuff, it can be determined whether firing rates recover once the metabolites have washed out(Kaufman and Hayes, 2002, Kaufman et al., 2002). These studies demonstrated that metaboreceptive endings increase their firing in the presence of the metabolites, but when the blood supply is re-established these afferents quickly reduce their excitability (Kaufman and Hayes, 2002, Kaufman et al., 2002). In other studies, in human subjects, the plasma concentrations of lactate have been obtained before, during and after exercise to determine the concentration changes during these states of activity (Amann et al., 2010, Amann et al., 2011b, Blain et al., 2016). Amann et al (2015) showed that metaboreceptive afferents activated by lactate have two different roles. This laboratory used a μ-opioid antagonist, fentanyl, applied intrathecally to block ascending spinal pathways that include those of metaboreceptor pathways. Using this manipulation, they showed that one role of these sensory neurons is

to activate adaptive cardiovascular and respiratory responses at the onset of exercise and throughout its duration. These reflexes ensure optimal availability of oxygenated blood to active muscle groups. The second role for metaboreceptors from muscle is to provide input which reduces central motor drive, thereby contributing to 'central fatigue' (Amann et al., 2008, Amann et al., 2009, Amann et al., 2010, Amann et al., 2011a, Amann, 2012, Rossman et al., 2012, Dempsey et al., 2014, Sidhu et al., 2014, Weavil et al., 2015, Broxterman et al., 2017). Central fatigue is also adaptive because it helps prevent damage to muscle by accumulating metabolites when they are driven excessively.

Lactate as a means to detect muscle activity

Ergoreceptors are the sensory neurons in muscle that are activated by contraction, stretch, and by metabolites released by working muscle fibres (Amann et al., 2015). CT3 afferents have the properties of ergoreceptors, as discussed in the previous chapter (**Chapter 3**). They respond to mechanical stimuli, as well as to a metabolite mix of lactate, ATP and protons. Muscle afferent responses to ATP have been well characterised and are largely mediated via P2X receptors; P2X3 receptors, in particular, are located on many afferent terminals (Burnstock et al., 2013, Fabbretti, 2019). pH changes have also been studied widely and are largely detected via ASICs channels, in particular in sensory neurons (Gautam and Benson, 2013, Gründer and Chen, 2010, Molliver et al., 2005). Our data has shown that lactate by itself can also activate some afferents. Our experiments have shown that this is not due to protons, osmolarity, temperature or mechanical artefacts during application. One limitation of our study was that only one concentration (15 mM) was used, however, this is within the range released by physiological muscle activity. A full concentration response curve would be highly informative. Previous studies have shown that individual components of the metabolite mix have little effect on afferent firing; they demonstrate considerable synergy when applied in combinations (Pollak et al., 2014). It also needs to be noted that in the

present study endogenous lactate released from the muscle cells during contraction, was not measured nor were effects of endogenous lactate on afferents determined. Further investigation is need to investigate the presence of endogenous lactate and determine its influence on these afferents.

How lactate affects sensory neurons

Our data suggests that lactate may have excitatory effects on some neurons, probably mediated via HCAR1. It has been suggested that lactate activate sensory afferents by enhancing the activity of ASICS channels, specifically ASICS3 (Naves and McCleskey, 2005). Lactate weakly chelates calcium and magnesium ions in solution, reducing the availability of these divalent ions in the extracellular fluid (Immke and Mc Cleskey, 2001). The proton binding sites that gate ASICs binds divalent cations. Thus, if high concentrations of lactate reduce the effective concentration of calcium and magnesium ions, this would decrease the concentration of protons required for ASICS3 activation (Babini et al., 2002, Birdsong et al., 2010). In one previous study lactate was proposed to act solely via ASIC3 (Immke and Mc Cleskey, 2001). It should be noted that this study was carried out in isolated cells in culture. In contrast, the preparation used in the present study was considerably more intact, and we applied the solutions to the nerve terminals within the muscle itself. We also studied a mimic solution, which did not replicate the response to lactate. Furthermore, a solution containing 15mM lactate with raised [Ca^{2+}] and [Mg^{2+}] to compensate for partial chelation was effective in exciting some afferents. Put together, these studies provide evidence that divalent ion chelation is not solely responsible for driving lactate-evoked firing in CT3 afferents.

A second mechanism has been suggested. Lactate has been shown to inhibit TRPV1 channel activation (de La Roche et al., 2016). Such a mechanism would be expected to reduce

activation of sensory neurons by lactate. However, in our hands lactate usually caused excitation in CT3 afferents. Furthermore, CT3 afferents do not express functional TRPV1 channels as no identified CT3 afferents (from 14 tested) responded to capsaicin (1 μM). This makes it unlikely that lactate affects CT3 afferents via TRPV1 channels, thus it is probable that lactate can activate afferents via another mechanism. HCAR1 immunoreactivity was shown to be present in sensory endings in abdominal muscles. It was also detected in sensory neurons cell bodies in the dorsal root ganglia retrogradely labelled from abdominal muscles. In fact, HCAR1 immunoreactivity was widespread in dorsal root ganglia, in several classes of neurons, co-localised with or without CGRP and/or NF200. Thus, HCAR1 is in the right places to play a role in the excitatory effects of lactate on some muscle afferents. There are no known HCAR1 antagonists commercially available at the present time (Offermanns, 2017). This is unfortunate as a selective receptor agonist could provide a useful test of whether exogenous lactate acts via HCAR1.

Lactate in the nervous system

Lactate is not only released by muscle cells; it is produced by many types of cells in the body. In the central nervous system, neurons and glia are exposed to lactate. Circulating lactate does not cross the blood brain barrier, but astrocytes and neurons can make and release it (Dienel, 2012). The astrocyte- neuron shuttle theory (Magistretti and Allaman, 2018, Pellerin and Magistretti, 1994) proposed that astrocyte-derived lactate could be an energy source for neurons. It has also been suggested that lactate signals the metabolic state of the brain, via changes in redox states (increasing pyruvate, to increase the NADH/NAD ratio) or that it may act as volume transmitter within the brain (Bergersen and Gjedde, 2012, Lauritzen et al., 2014).

Initial studies of HCAR1 in the brain indicated low-level expression compared to adipocytes (Cai et al., 2008). In follow-up studies, Lauritzen et al (2014) demonstrated that HCAR1 is actually expressed in multiple areas of the brain. Expression was high in Purkinje cells in the cerebellum and in pyramidal cells in the hippocampus. This supports the idea that lactate in the brain could act as a signalling molecule via HCAR1(Lauritzen et al., 2014). Calcium imaging in primary cortical cultures (Bozzo et al., 2013) showed that lactate reduced the frequency of calcium transients in 50% of principle and GABAergic interneurons, in a concentration-dependent manner. This supports the proposal that lactate could act as a signalling molecule. The authors suggested that it acts as a signal that adapts neuronal activity to the metabolic state of the brain.

Tang et al (2014) provided evidence for an unidentified excitatory G-Protein coupled receptor that could be activated by lactate, and which operates in a positive-feedback loop between glia and locus coeruleus noradrenergic neurons. Activated astrocytes release lactate, which excites noradrenergic neurons and stimulates the release of noradrenaline (Tang et al., 2014). This hypothesis has been questioned by others, as the authors did not identify the GPCR. One may speculate that HCAR1 via one or more mechanisms, may have contributed to this system perhaps via its downstream second messenger pathways (Morland et al., 2015).

Morland et al (2017) showed that lactate, released during exercise, increases brain vascular endothelial growth factor A (VEGF-A) and cerebral angiogenesis. This was mediated via the activation of HCAR1 receptors on pial fibroblast-like cells that line cerebral blood vessels and via pericytes in capillaries (Morland et al., 2017). This mechanism was proposed to explain the beneficial effects of exercise on brain function. Raised levels of lactate in the brain have been associated with migraine possibly driven by local hyoxia (Arngrim et al.,

2016). Lactate has been implicated in a range of other mechanisms in the brain, including neuronal excitability, plasticity and, memory (Magistretti and Allaman, 2018). Which of these play a significant role in normal physiology remains to be determined. The role of lactate in neurological dysfunction is similarly unclear. This may be a productive area of research in future.

HCAR1, a G-protein coupled receptor

HCAR1, also known as GPR81, HCA1, FKSG80 and TA-GPCR, is a hydroxyl-carboxylic acid receptor. It was first found and identified as an orphan G-protein coupled receptor GPR81 by BLAST analysis of a genomic sequence database, searching for known GPCR-encoding sequences (Lee et al., 2001). It is located on chromosome 12q.24.31 in humans and 5f in mouse. In 2008, lactate was first proposed as an endogenous agonist for this receptor (Cai et al., 2008). Liu et al 2009, went on to described lactate as a specific agonist of HCAR1. Confirmation that lactate was in fact a ligand for HCAR1 were tested by using GTPγS binding and direct inhibition of cAMP accumulation. The EC50 value for lactate-induced binding of GTPγS in CHO cells transfected with human HCAR1 was 4.87 mM. Similarly, the inhibition of cAMP formation in human neuroblastoma/cre-β-galactose cell line (SK-N-MC/CRE-β-gal) stably expressing human HCAR1 provided an EC50 value of 4.10 mM. While they are similar values, both are strikingly high concentrations, compared with values typically associated with GPCRs (nanomolar ranges). Thus, HCAR1 is a low affinity receptor. Functionally, this may allow it to detect the large dynamic range of lactate concentrations in the body under physiological conditions (Liu et al., 2009).

In studies of the downstream effects of HCAR1, a number of studies demonstrated that HCAR1 was sensitive to the pertussis toxin (Soga et al., 2003) pointing towards involvement of the G_i/G_o family of G-proteins. The activation of G_i/G_o G-proteins typically results in a decrease in adenylyl cyclase activity which reduces availability of cyclic AMP (cAMP)

(Yudin and Rohacs, 2018) and downregulates Protein Kinase A activity. This would be expected to lead to multiple and widespread effects in neurons and in other cell types.

Expression of HCAR1 receptor

The expression of HCAR1 was first described in the human pituitary gland (Lee et al., 2001) (although this has not been replicated to date). Since then several studies using quantitative RT-PCR have demonstrated the expression of HCAR1 mRNA in the brain (Ge et al., 2008, Liu et al., 2009)including the hippocampus, cerebellum (Lauritzen et al., 2014). It has also been detected in heart (Liu et al., 2009), kidney (Ge et al., 2008, Liu et al., 2009), intestine, liver, lung, skeletal muscle, spleen, stomach, thymus (Liu et al., 2009), gastric ghrelin cells (Engelstoft et al., 2013) and adipocytes (both brown and white adipose tissue) (Ahmed, 2011, Ahmed et al., 2009, Ahmed et al., 2010, Cai et al., 2008, Ge et al., 2008). Overall, HCAR1 is most abundant in adipose tissue (see above), with higher concentrations in brown fat than white fat (Liu et al., 2009). It is not surprising then that HCAR1 immunoreactivity was readily detected in fat cells within the preparations of abdominal muscles in the present study.

In some tissues, there has been uncertainly whether abundant HCAR1 in adipocytes occluded its expression in other cells (Offermanns, 2017). Using immunohistochemistry Lauritzen et al (2014) described the presence of HCAR1 in the hippocampus, cerebellum and neocortex (Lauritzen et al., 2014). Importantly, Lauritzen et al (2014) showed that the antibody used in their study (the same as used in the present study) labelled bands in Western blots corresponding to the known molecular mass of 39kDa. Thus, HCAR1 is expressed specifically by some neurons in the central nervous system. Our work extends this by showing that it is also expressed in many dorsal root ganglion sensory neurons. One limitation to of the present study regarding the visualisation of HCAR1in dorsal root ganglia,

was that the dorsal root ganglia were dissected from the animal before being immersion fixed compared to being perfusion fixed. This created an 'edge effect' around the edges of a few of the DRG's (**Figure 4.15**).

HCAR1 in adipocytes

In adipocytes, activation of HCAR1 receptors results in an anti-lipolytic effect via a decrease in adenylyl cyclase activity and reduction in cAMP. This occurs in both human and in mouse cells(Cai et al., 2008, Liu et al., 2009). Cyclic AMP is a major intracellular regulator of lipolysis, which acts by stimulating cAMP-dependant kinase (PKA), which in turn phosphorylates and activates hormone sensitive lipase. Thus, HCAR1 activation causes a reduction in cAMP production and an over-all anti-lipolytic effect (Offermanns, 2017). HCAR1-deficient mice gain less weight than wild type mice when given a high fat diet; suggesting that the antilipolytic effect is involved in weight gain (Ahmed et al., 2010, Offermanns, 2017). Whether this same mechanism operates in sensory neurons remains to be determined.

Physiology of lactate detection by CT3 afferents

CT3s are subset of group III muscle afferents and are likely to be non-nociceptive, as they respond to stimuli within the physiological ranges of muscle work and are not activated by capsaicin. Ergoreceptors, provide information to the CNS about the metabolic and contractile state of muscle groups. The CT3 afferents described in **Chapter3** are both mechanoreceptive and metaboreceptive and thus probably encode a mix of stimuli that generally reflect abdominal muscle activation. They respond vigorously to a 'metabolite mix' of low pH, ATP and lactate, and to lactate on its own. While sensory neuron responses to acidity and purines have been extensively described since the 1960s, this study suggests that lactate may contribute via its own specialised GPCR to ergoreceptor excitability. Clearly

synergistic interactions between pH, ATP and lactate occur and this needs further characterisation. CT3 afferents in mouse abdominal muscles would provide a preparation well suited to this type of study.

Lactate and ergoreceptor function

Ergoreceptors are involved in reflex adjustments of respiration and circulation during exercise (Amann and Calbet, 2008, Dempsey et al., 2008, Amann et al., 2015). Lactate concentrations found within skeletal muscle vary from 1 mM at rest to 30 mM in extreme exercise and ischemic muscle (Ferguson et al., 2018). CT3 afferents are activated by lactate alone at a physiological level (15 mM). Thus, these afferents act at least in part as lactate 'sensors' within skeletal muscle, however they also respond to other metabolites and mechanical stimuli. The presence of HCAR1 in these nerve fibres and endings may contribute to effects of lactate on CT3 neurons. The ability for CT3 afferents to be activated by lactate raises the possibility that these neurons play a role in the exercise pressor reflex, muscle fatigue, ischemia, and other exercise-related sensory activities. This is discussed in more detail in the following chapter.

CHAPTER FIVE

GENERAL DISCUSION

Structure-function correlation in group III & IV muscle afferents

One important requirement for understanding how primary afferent neurons function is to comprehensively describe the characteristics of individual neuronal populations. This allows the specific combinations of features of each class to be distinguished, rather than describing an "average" composite neuron which doesn't actually exist. Integrating structural and functional classification schemes represents a major challenge towards this goal. For the group I and II muscle afferents, this was achieved relatively early (Barker, 1948). The conspicuous and distinctive morphological and functional characteristics of large-diameter muscle afferents were amenable to structure-function correlation studies using simple techniques (Matthews, 1964). Thus, it was possible to histologically stain muscle afferent endings with silver (Banks et al., 1982) or gold (Andrew et al., 1973) impregnation and reconstruct the afferent ending from sectioned material. The same could not be readily achieved for the more diffuse and dispersed endings of group III and IV muscle afferents. Based on neuroanatomical studies, it was speculated that group III/IV muscle afferents terminate peripherally as free nerve endings (Stacey, 1969). However, concurrent electrophysiological recording (functional identification) and localization of their peripheral terminals (structural identification) has not been reported for either group III or IV muscle afferents to date (Jankowski et al., 2013, Mense and Gerwin, 2010). This means that despite many years of research, the exact adequate stimuli, combinations of receptors expressed, the types of ion channels contributing to group III and group IV muscle afferents function have not been established on a class-by-class basis (Amann and Light, 2015). Functional studies suggest that group III/IV afferents can be divided into several classes of mechanoreceptors, metaboreceptors, and nociceptors yet no neuroanatomical criteria have been described that differentiate between these classes (Mense and Gerwin, 2010). Thus, positive identification of functionally characterised group III or IV afferents combined with a means to identify the

morphological characteristics of their peripheral endings were both major aims of the present study.

Validation of preparation and technique

One particular difficulty in studying the morphological details of sensory neurons is the ability to study all parts of the entire neuron from its peripheral ending, where transduction and spike initiation occur, to the central processes where signals are transmitted into the central nervous system. As discussed in **Chapter 2,** many of the techniques currently available only allow a part of each sensory neuron to be investigated at any one time. Thus, spike trains from terminal endings can be recorded, or transmitter combinations can be ascertained immunohistochemically in the cell body, or central projections can be investigated by recording synaptic contacts onto follower neurons in the central nervous system. Combinations of features can be correlated. For example, it has been possible to activate peripheral nerve endings, while recording action potentials from the afferents' cell bodies in dorsal root ganglia or nodose ganglion (Jankowski et al., 2013, Williams et al., 2016). This makes it possible to combine information about stimulus/response characteristics with immunohistochemical expression of neuropeptides (Jankowski et al., 2013). However, this approach provides no data on the morphology of the neurons' peripheral endings. Applying tracers directly to sensory ganglia (nodose or dorsal root ganglia) can reveal morphological features of peripheral endings, but it is hard to combine this with functional characterisation on an ending-by-ending basis (Spencer et al., 2018a, Spencer et al., 2016). In **Chapter 2** we validated a method to establish the functional characteristics of muscle afferents and relate this to their morphology, using the well-described muscle spindles as a test-case. In **Chapter 3** we used these methods to correlate the morphology and function of a class of group III mechano- and metaboreceptive endings that are present within the connective tissue between the muscle layers.

Correlation of morphological and functional properties

We first demonstrated that muscle afferents can be recorded from a novel ex vivo preparation of mouse abdominal muscles. Spontaneously firing afferents were then recorded and dye filled and were shown to correspond to muscle spindle endings. This was an important validation of our ex vivo preparation and dye filling techniques (**Chapter 2**). We then concentrated on a single class of group III muscle afferents, which were readily distinguished by a combination of characteristics including spatially distributed responses to von Frey hair stimulation, large amplitude action potentials and saturating responses to stretch. We then correlated this class's activity with the presence of distinctive nerve endings in the connective tissue between layers of muscle fibres that were filled with the biotinamide tracer (**Chapter 3**).

In the present study, it was not possible to provide a detailed description of all different classes of group III/IV nerve endings which had been our original goal. Instead we established a method in which group III and group IV afferents can be individually characterised, class by class, combining the location of their endings within the muscle with their functional properties and neurochemical coding of their axons. In the course of the project, this validated approach was applied to a single recognisable class of afferents. However, there is no reason to believe that it would not be applicable to other classes of group III and IV muscle afferents that have not yet been fully characterised.

The number of specimens in which we identified positively a single ending corresponding to the recorded activity was small: 7 morphological endings were correlated with their functional characteristics (out of $n = 23$). This was due to the extensive and overlapping branching of nerves entering the muscle. In most cases it was not possible to identify a single axon corresponding to the discriminated unit because of the presence of multiple

biotinamide-labelled axons. In a few preparations, there were no filled endings within the marked receptive field due to a failure to fill. In two cases this was due to the carbon markers disappearing during tissue processing - a particular problem for CT3 afferents as their endings lay in the connective tissue layers to which the carbon particles did not always adhere tightly. Furthermore, probing with von Frey hairs occasionally damaged axons; this may have disrupted filling in a few preparations although we routinely used the lightest von Frey hairs that gave reliable responses. Improving the success rate of dye filling would need to be addressed for a comprehensive analysis of all classes of muscle afferents. One possible way to achieve this would be to reduce the total number of afferents/efferents dye filled from the recorded nerve trunk. Previous studies, have used a variety of techniques to ablate different populations of axons. For example, sympathetic neurons have been specifically destroyed using 6-hydroxydopamine (6-OHDA) (Rodrigues et al., 2018), while transient receptor potential vanilloid type 1 (TRPV1) neurons have been ablated via by pretreatment with capsaicin or resiniferatoxin (RTX) (Yu et al., 2018). Newer neurogenetic approaches have used the expression of diphtheria toxin under specific promoters to achieve this (Le Pichon and Chesler, 2014, Pogorzala et al., 2013). These methods could potentially be combined with the approaches used in the present study to reduce the number of types of axons filled by biotinamide and thus make identification of functionally characterised endings more productive.

In the current studies, we identified CT3 afferents by their spontaneous firing, responses to isotonic stretch, and responses to von Frey hair probing (**Chapter 2 and 3**). In doing so, we unavoidably biased recordings towards mechanosensitive afferents within these preparations. However, this did allow us to concentrate on one class of readily recognisable afferents (in **Chapter 3**), the so-called CT3 afferents. Correspondingly, we restricted our aim to functionally characterise these afferents further and then correlate this with their

morphology (Jankowski et al., 2013). From studying their chemoreceptive responses, we then obtained evidence that CT3 afferents were specifically responsive to the metabolic product, lactate. The detailed combination of criteria for positively identifying CT3 afferents then made it possible to study responses to lactate in this single class of sensory neurons, without the confounding effects that might arise if experiments were carried out on a mixed collection of unidentified muscle afferents. The location of the CT3 branching endings were primarily in the connective tissue between the muscle layers, rather than within specific muscle sheets or lying parallel to individual muscle fibres. This suggests that they are not immediately adjacent to the muscle fibres, which are the major source of lactate (among other substances). Thus, CT3 afferents are likely to be activated by the output of lactate from multiple muscle fibres within several different layers of the abdominal group. This is consistent with their putative roles as metaboreceptors that reflect generalised muscle activity. CT3 afferents were also mechanosensitive to stretch and compression. We were unable to test their responses to contraction because it proved impossible to stimulate all the muscle fibres in the preparation to contract simultaneously (data not shown). However, it is feasible that stretch and compression responses encode aspects of the animal's physical motor activity that can then activate the body's adaptive responses to the demands of exercise. Certainly, there is evidence that imposed movements on a limb can activate the exercise pressor response without requiring active voluntary activation of the muscle (Secher and Amann, 2012, Smith et al., 2006).

The question then arises whether responses of CT3 fibres in abdominal muscles are likely to be representative of metabo/mechanoreceptive group III afferents throughout the body. It should be noted that the abdominal muscles are often not considered to be primary locomotor muscles, which are primarily indicated as the drivers for the exercise pressor reflex. Thus, the actual contributions of abdominal CT3 afferents to the exercise pressor response are not

clear. It should be noted that group III and group IV muscle afferents have been detected in a wide variety of skeletal muscles (Michelini et al., 2015). It has also been reported that the abdominal muscles of dogs, including the transversus and oblique muscle, function as mixed locomotor, and ventilatory muscles (Deban and Carrier, 2002). It has also been suggested that trunk muscles and respiratory muscles do in fact contribute to pressor reflexes (Michelini et al., 2015). Further studies would be needed to determine the presence and impact of CT3 like afferents in locomotor muscles and their influence on the exercise pressor reflex as well as other exercise-related sensory activities. It would also be valuable to study whether there are sensory fibres with properties similar to CT3 afferents in, for example, locomotor limb muscles.

Sex as a biological variable

The sex of the animals needs to be noted as an important biological variable. Many studies have demonstrated the biological difference between males and females. A few examples of these differences include, but are not limited to, disease manifestation, prevalence, and responses to treatments (Clayton, 2018). Throughout the course of the studies at hand, 44 males and 47 female mice were utilised (Chapter 2, 9 males & 1 females; Chapter 3 15 males & 40 females; Chapter 4 20 males & 6 females). These small numbers of each sex, within each of the study groups, do not allow any comparisons to be made on the basis of the sex of the animal. The current study did not investigate the differences of CT3 afferents between males and females and to determine this effect, further investigation is required. This would be a valuable future study.

Group III&IV muscle afferents in the exercise pressor reflex

The exercise pressor reflex is a reflex that originates within skeletal muscles, and which plays an integral role in triggering and maintaining adaptive cardiovascular and

haemodynamic responses to exercise (Mitchell, 2012). Alam & Smirk (1937) were among the first to provide experimental evidence that a reflex was responsible for these physiological responses to exercise(Alam and Smirk, 1937). They demonstrated that muscle ischemia in response to handgrip exercise led to an increase in blood pressure. Later studies showed that blood pressure remains elevated for as long as the forearm is kept ischemic after exercise (Mitchell, 2012).

At the onset of exercise, the exercise pressor reflex is activated during muscle contraction by stimulation of receptors both on thinly myelinated (group III) and unmyelinated (group IV) muscle afferents, that respond to either mechanical distortion or metabolic by-products of exercising skeletal muscle (Secher and Amann, 2012). Once afferents have been excited, their activity is transmitted via the dorsal horn of the spinal cord to various sites within the central nervous system, only some of which have been positively identified. The areas that have been described include the nucleus tractus solitarius (NTS), rostral ventral medulla and the caudal ventral medulla (Murphy et al., 2011). From excitation of these areas, elevations in heart rate and blood pressure are generated predominantly by increasing sympathetic nerve activity.

Over the last 80 years, extensive studies of the pressor reflex and the muscle afferents involved have been vital to our understanding of how the circulatory and respiratory adjustments to exercise are mediated. More recently, this reflex has attracted significant attention due to its potential role in generating exaggerated cardiovascular response to exercise that occur in heart failure, hypertension, and peripheral artery disease. In these disease states, it has been suggested that exercise pressor reflexes are over-activated, thus reducing exercise tolerance and increasing the risk of adverse cardiac events and stroke during exercise. Group III and Group IV muscle afferents have also been implicated in other

conditions, including the development of peripheral and central fatigue, and chronic fatigue syndrome (Amann et al., 2015, Garry, 2011, Mense and Schiltenwolf, 2010, Mitchell, 2017, Sidhu et al., 2018, Staud et al., 2015, Stone et al., 2015, Stone and Kaufman, 2015).

Group III&IV muscle afferents (ergoreceptors) in muscle fatigue

Muscle fatigue is the reversible, progressive reduction in a muscle's ability to produce force and/or power during exercise (Allen et al., 2008, Gandevia, 2001, Taylor et al., 2016). A muscle's ability to produce force and/or power, ultimately depends on both the contractile mechanisms within the muscle fibres, and the mechanisms that precede muscle activation. Changes at any of these sites can result in the force and generation of the muscle becoming impaired ("fatigued") (Taylor et al., 2016).

It is well recognised that muscle fatigue has both central and peripheral components. Peripheral fatigue involves the biochemical changes that accumulate within the contracting muscle distal to the neuromuscular junction, which lead to attenuated force and/or power (Amann et al., 2015, Taylor et al., 2016). Central fatigue refers to the reduction in force and/power of the muscle caused by decreases in neural motor drive. Firing frequency and recruitment of motor units usually determine the level of activation of a muscle (Taylor et al., 2016) and thus determine the strength of voluntary muscle contraction. Mechanisms that reduce this central drive are responsible for central fatigue. Both central and peripheral fatigue have been previously associated with group III and group IV muscle afferent feedback (Sidhu et al., 2017).

Peripheral fatigue

Peripheral fatigue develops due to reduced contractility of muscle, caused by restricted delivery oxygen and nutrients via the blood, together with the accumulation of metabolic

products, during muscle activity. There is evidence that Group III and group IV muscle afferents delay the onset of peripheral fatigue via their contribution to the exercise pressor reflex, which helps optimise blood flow to active muscles, in parallel with increasing respiratory ventilation during exercise. Group III and IV ergoreceptors provide sensory information from the active muscles which leads to generalised arteriolar constriction, which, in turn, raises peripheral resistance. Together with increases in heart rate and stroke volume (sympathetic responses), this leads to increased blood pressure, providing additional driving force for blood through active muscles. Local vasodilation in active muscles then ensures that blood flow and oxygen delivery increase to meet the heightened demand; these are the key variables that predict the rate at which peripheral fatigue will occur. A decrease in either blood flow or oxygen delivery results in an increased rate of fatigue of exercising muscles. This is largely due to increased accumulation of protons, phosphate, lactate etc, which negatively affect excitation-contraction coupling within muscle fibres. The failure of excitation-contraction coupling is one of the main factors that evokes peripheral muscle fatigue, partly via disruption of calcium release and uptake by the sarcoplasmic reticulum (Amann and Calbet, 2008).

Early studies investigating the role of group III and group IV muscle afferents in both fatigue and pressor reflexes examined the effects of lumbar epidural application of the local anaesthetic lidocaine (0.5%) to block the ascending muscle afferent pathways in the spinal cord. Blockade of ascending sensory pathways with lidocaine, was carried out while the subjects were doing cycling exercise. These studies suggested that sensory feedback from working muscles affect central circuits during exercise, reducing central drive (Amann et al., 2008). However, it was found that the lumbar epidural application of lidocaine also affected efferent motor nerves directly, thus confounding the effects mediated via sensory pathways (Amann et al., 2008).

To avoid these confounding effects of lidocaine, a μ-opioid receptor agonist, fentanyl was later used to selectively block ascending sensory pathways of nociceptors and metabo-receptors, without affecting the motor nerve activity (Amann et al., 2009). Lumbar intrathecal fentanyl, attenuated 60% of group III and IV afferent signalling from the legs (Amann et al., 2009, Hureau et al., 2018) via the closing of n-type voltage gated calcium channels (Estrada and Kaufman, 2018). This modified technique has since been extensively used to investigate the role of group III and group IV in the development of pressor reflexes and fatigue.

Group III and IV afferents have been shown to play an important role in pressor reflexes, which optimise blood flow to active muscles, and thus delay peripheral fatigue. This was demonstrated by the use of intrathecal fentanyl to attenuate ascending central sensory pathways, including those from muscles during exercise. In the presence of fentanyl, ventilation failed to increase during exercise, while the exercise pressor reflex response was also attenuated. Thus, cardiac output (central) was elevated less and leg blood flow (peripheral) haemodynamic responses during exercise were also less marked when fentanyl was administered intrathecally (Amann and Calbet, 2008, Amann et al., 2009, Amann et al., 2010, Amann et al., 2011a, Amann et al., 2011b). Peripheral fatigue was quantified as a reduction in quadriceps twitch force evoked by a supramaximal femoral nerve stimulation. (Amann et al., 2011a). Peripheral fatigue accumulated 60% more rapidly during exercise in subjects with group III and group IV afferent blockade, compared to subjects with intact muscle afferent feedback (Amann et al., 2011a, Sidhu et al., 2014). This shows that group III and group IV afferent input is very effective in boosting muscles blood supply and oxygen delivery to active muscle during exercise and thereby prevents premature peripheral fatigue at the muscle level. Thus, the feedback from these afferents plays an important role in

controlling peripheral fatigue resistance during physical activity (Amann and Light, 2015, Amann et al., 2015).

Central fatigue

Group III and group IV muscle afferents also play a part in the development of central fatigue (Amann et al., 2015)via their ability to inhibit firing of spinal motor pathways (which activate the final neural drive to make muscles contract). This was also demonstrated using pharmacological blockade with either local anaesthetic lidocaine or intrathecal fentanyl (as described above). When ascending pathways from group III/IV muscle afferents were inhibited, spinal motor drive did not decline as quickly and was actually increased compared to when sensory pathways were intact (Amann, 2011, Amann et al., 2008, Amann et al., 2009, Gandevia, 2001, Sidhu et al., 2017, Sidhu et al., 2014). The mechanisms by which Group III/IV sensory pathways reduce corticospinal excitability to cause central fatigue was not clear.

To address this question, Sidhu et al (2017) used repeated fatiguing bouts of cycling performed with or without muscle afferent blockade. They examined the effects of this on cortico-spinal and lower motor neuron excitability. When muscle feedback was left intact, the corticospinal pathway was inhibited by fatiguing exercise, but lower motor neurons were not affected. Without feedback (i.e.: in the presence of fentanyl), corticospinal pathways were unaffected, as were lower motor neurons (Sidhu et al., 2017, Sidhu et al., 2018, Weavil and Amann, 2018). Sidhu et al (2018) used studied unconditioned or conditioned motor evoked potentials pre-and post-cycling exercise. To determine the spinal or cortical contributions to these motor evoked potentials, cervicomedullary stimulation was were used. Feedback from group III/IV muscle afferents innervating the locomotor (leg) muscles, at least in part, decreased the excitability of the motor cortex during fatiguing exercise, via

inhibitory intracortical $GABA_b$ interneurons (Sidhu et al., 2018). This appears to be one contributory mechanism to central fatigue.

In summary, Group III and group IV muscle afferents play a significant and complex role in exercise-induced fatigue. These sensory neurons contribute to the activation of autonomic responses to exercise, which ensure that blood flow and oxygen delivery to muscles increases to meet higher demand during physical activity. Thus, they help slow the onset of peripheral muscle fatigue by ensuring adequate oxygen and blood supplies. However, these same afferents also exert inhibitory effects on higher motor pathways in the CNS, which diminish the output of the spinal cord motor neurons i.e.: they play a key role in central fatigue. It is tempting to interpret this mixture of effects as an adaptation to ensure optimal muscle performance whilst minimising risk of damage by over-use. The characteristics of CT3 afferents, which signal both mechanical and metabolic activity, make them candidates for mediating some or all of these exercise-induced adaptations.

Group III muscle afferents in peripheral artery disease, hypertension and heart failure

Hypertension, peripheral artery disease, and heart failure are all conditions in which physical activity and exercise result in excessive increases in heart rate, blood pressure, and sympathetic activity. It is hypothesised that these pathological responses during exercise may involve an abnormality of the afferent arm of the exercise pressor reflex i.e.: group III and IV afferents (Garry, 2011, Mitchell, 2017, Stone and Kaufman, 2015).

Peripheral artery disease

Peripheral artery disease is the narrowing of arteries, predominantly in the lower extremities, caused by the build-up of atherosclerotic plaques which restrict arterial flow and hence oxygen delivery (Stone and Kaufman, 2015). The accumulation of plaques reduces blood

flow to the working muscles, resulting in augmented blood pressure response during dynamic exercise. It is hypothesised that this is due to, in part, an exaggerated exercise pressor reflex. This has been studied in a rat model. The femoral artery of a rat was ligated, to simulate impaired blood flow, as seen in patients with the disease. Ligation was set to allow adequate arterial flow to meet metabolic demand at rest, but during exercise it was inadequate to meet the increased demand (Harms et al., 2018, Kaufman and Rybicki, 1987, Kumazawa and Mizumura, 1977, Kaufman et al., 1984 Prior, 2004 #792). Tsuchimochi et al (2010) demonstrated that the exercise pressor reflex was augmented in decerebrate rats after 72 hours of femoral artery ligation(Tsuchimochi et al., 2010a). Again, the exercise pressor reflex evoked from the hind limb muscle with ligation, was significantly larger than from the non-ligated contralateral hind limb. This type of model has been further used to identify receptors/channels and modulators that may affect group III/IV muscle afferents involved in the exercise pressor reflex. These include ASICS3 channels, TRPV1, and μ-opioid receptors.

ASIC3

In the same ligation model, amiloride, a non-selective ASIC (Acid-Sensing Ion Channel) antagonist, or APETx2 (a selective inhibitor of the ASIC3), were injected into one femoral artery. The exaggerated exercise pressor reflex induced by femoral artery ligation was decreased by both ASIC inhibitors. When the femoral artery was left patent, inhibiting ASICs had no effect on the exercise pressor reflex from the freely perfused hind limb (Tsuchimochi et al., 2011). This suggests that ASIC channels, possibly ASIC3, are activated on metaboreceptive afferent neurons during ligation-induced partial ischemia, and that they may contribute to the exaggerated pressor response. It is possible that some of this effect of ASCI3 channels is actually mediated by chelation of calcium and magnesium ions by accumulating lactate (Immke and Mc Cleskey, 2001).

TRPV1

TRPV1 is an ion channel expressed on many small diameter spinal afferent neurons which is activated by heat, low pH and by capsaicin. Investigations into the role of the TRPV1 receptor and its effects on the exaggerated exercise pressor response have shown that: femoral artery ligation increased the expression of TRPV1 receptor expression in DRG cells, and increased their responses to capsaicin (Stone and Kaufman, 2015). However, TRPV1 receptors did not play a significant role in the exaggerated pressor response evoked by evoked muscle contraction in rats with ligated blood supply. The application of iodo-resiniferatoxin, a potent TRPV1 antagonist, had no effect on the exaggerated exercise pressor reflex, even though this same antagonist blocked the pressor reflex to capsaicin (Tsuchimochi et al., 2010a). From these studies, it is hypothesised that even though TRPV1 channels are upregulated in DRG neurons after arterial ligation, they do not play a significant role in the exaggerated exercise pressor response seen in these preparations (Stone and Kaufman, 2015).

Opioid receptors

The peptide agonist of μ-opioid receptors, DAMGO, applied intra-arterially, significantly attenuates the exercise pressor reflex in rats. DAMGO was injected into the femoral artery of rats which had been ligated for 72 hours before, and this significantly reduced the muscle activity-induced pressor response. This effect was not seen in the contralateral (non-ligated) hind limb, where DAMGO only had a minimal effect. The effect of DAMGO was blocked by the opioid receptor antagonist, naloxone (Tsuchimochi et al., 2010b). DAMGO was found to attenuate the responses of both group III and group IV afferents to contraction when femoral arteries had been ligated. While in the contralateral hind limbs (with patent vessels) DAMGO had no significant effect on group III/IV afferent responses to contraction (Harms

et al., 2018). This suggests that partial ligation induces increased expression of μ opioid receptors on group III/IV ergoreceptors.

Hypertension

Hypertension is a common and costly risk factor for many cardiovascular diseases (Pescatello et al., 2015). Individuals with hypertension present with abnormal cardiovascular haemodynamics in response to exercise, due to their already elevated blood pressure. Typically, they present with excessive increases in arterial blood pressure, heart rate, and sympathetic activity during both static and dynamic exercises (Mitchell, 2017, Smith et al., 2010, Smith et al., 2006).

A spontaneous hypertensive rat model has been used extensively to investigate the exercise pressor reflex and the contributions of mechano-reflexes and the metabo-reflexes (Mitchell, 2017). Smith et al (2006) demonstrated that the activation of the exercise pressor reflex caused a larger increase in blood pressure and heart rate in spontaneously hypertensive rats, compared to their wild-type controls (Smith et al., 2006). Mizuno et al (2011) described similar changes in blood pressure and heart rate and recorded renal sympathetic nerve activity. Spontaneously hypertensive rats showed greater integrated renal sympathetic nerve activity than controls (Mizuno et al., 2011). To determine the contribution of the mechano-reflex in this spontaneous hypertensive rat model, muscle stretch was used to selectively activate muscle mechanoreceptors. This stimulus had previously been shown by Leal et al (2008), in the triceps surae muscles of spontaneously hypertensive rats, to evoke an accentuated response (Leal et al., 2008). Mizuno et al (2011) used the same approach to activate the mechano-reflex, detecting exaggerated increases in arterial pressure, heart rate, and renal sympathetic nerve activity (Mizuno et al., 2011).

Group IV muscle afferents are described as being primarily metaboreceptors (Kaufman, 1984). The transient receptor potential vanilloid 1 (TRPV1) receptor is known to be present on some group IV muscle afferents (Hoheisel et al., 2004). Activating this receptor with its known agonist capsaicin has previously been suggested to increase blood pressure and heart rate, similar to that seen in responses to exercise (Kaufman et al., 1982). Due to the presence of TRPV1 receptors on group IV muscle afferents, and the role of group IV muscle afferents in relation to the exercise pressor reflex, TRVP1 receptors have been investigated to determine if they contribute or play a part of the metaboreflex, especially during hypertension (Smith et al., 2010). To determine the contribution of TPRV1 receptors on the metaboreflex in hypertension, selective activation of these chemically sensitive afferents was achieved by administering intra-arterial capsaicin to one hindlimb (Leal et al., 2008, Smith et al., 2010). Administration of capsaicin elicited a significant increase in blood pressure and heart rate in spontaneous hypertensive rats (Leal et al., 2008, Smith et al., 2010). The antagonist capsazepine, a blocker of TRPV1 channels, caused a decrease in arterial blood pressure and renal sympathetic nerve activity after metaboreceptor activation in these rats. This suggests that TRPV1 could have a partial effect on the metaboreflex (Mizuno et al., 2011).

Collectively, animal data supports the hypothesis that autonomic reflexes elicited by skeletal muscle activity are exaggerated in hypertension. The aetiology of the dysfunction is currently unclear but may result, in part, from a change in the sensitivity of metaboreceptors and mechanoreceptors (Murphy et al., 2011). This suggestion raises additional questions of how hypertension itself could affect metaboreceptors scattered throughout the body. Recent studies have also suggested a central component in blood pressure involving nitric oxide within the nucleus tractus solitarius. The data suggested a decrease in the expression/activity of NOS in the NTS which reduces the availability of nitric oxide which normally acts as a

brake on the pressor response to muscle activity. This could therefore result in an accentuated mechano-reflex in patients with hypertension (Smith et al., 2015). Further studies are needed to investigate these peripheral and central pathways involved in the exaggerated pressor responses seen in hypertension. The present study has shown that CT3-like afferents are likely to comprise part of the metabo-reflex and mechano-reflex pathways. Future experiments could test whether their sensitivity changes during experimental hypertension or in models of peripheral artery disease based on ligation of the blood supply.

Heart Failure

Patients with heart failure exhibit decreased cardiac output, chronically elevated sympathetic nerve activity and peripheral endothelial dysfunction. Additionally, exercise evokes excessive increase in blood pressure, heart rate, sympathetic activity, and ventilation. These alterations increase the risk of myocardial ischemia, infarction, cardiac arrest and/or stroke during or after exercise. (Ives et al., 2016, Olson et al., 2010). Thus, the exercise pressor reflex is exaggerated in heart failure patients. It has been hypothesised that this is due, in part, to muscle reflex abnormalities (Garry, 2011). Animal studies have investigated the pathways in the exercise pressor reflex, mechano-reflexes, and metabo-reflexes in heart failure. Studies have used passive muscle stretch, electrically induced static contractions, and intra-arterial injections of capsaicin into the arterial supply as stimuli. Gadolinium, a lanthanide which effectively blocks many mechano-gated ion channels, was used to differentiate group III and group IV afferents in a decerebrate rat model, and in a dilated cardiomyopathy rat model. These studies showed that the mechano-reflex was enhanced in heart failure, while the metabo-reflex was blunted. It was also demonstrated that the mechano-reflex mediated the exaggerated exercise pressor activity. Furthermore, decreased sensitivity of group IV afferent neurons was important for development of exercise pressor reflex hyperactivity (Smith Scott et al., 2003, Smith Scott et al., 2005a, Smith Scott et al.,

2005b). Using recordings from single afferent fibres, Wang et al (2010) demonstrated that responses of group III afferents to contraction and stretch were increased in rat models of hypertension, and that application of capsaicin reduced the exaggerated response to mechanical stimuli of some mechanosensitive group IV afferents(Wang et al., 2010). Thus, it has been shown that the exaggerated exercise pressor reflex is at least partly due to sensitised group III/IV afferent endings (Wang et al., 2012, Wang et al., 2010).

Human studies have also cast light on the roles of group III and IV muscle afferents in heart failure. Amann et al (2014) used lumbar intrathecal fentanyl to block ascending pathways activated by group III and group IV muscle afferent, in patients with heart failure(Amann et al., 2014). This laboratory had previously shown that leg extensor exercises evoked exaggerated sympathetic responses in patients. When i.t. fentanyl was present, sympathetic outflow was attenuated and leg blood flow/O_2 delivery were significantly increased compared to exercise without intrathecal fentanyl. Thus, in healthy controls, group III/IV muscle afferents decrease peripheral fatigue, by improving blood flow via the pressor reflex. In contrast, in heart failure patients, it appears that group III and IV muscle afferents are attenuated, as the blockade by fentanyl resulted in an increase in blood flow and oxygen delivery, instead of a decrease as would normally been seen if group III/IV afferents effects had been inhibited. Thereby, in heart failure patients it was suggested that group III/IV afferents have an abnormal inhibitory effect on the sympathetic outflow, blood flow, and oxygen delivery (Amann et al., 2014, Taylor et al., 2016).

A recent human study used the same basic pharmacological method to elucidate the role of mechanosensitive muscle afferents in the exercise pressor reflex in response to **passive** leg movements in patients with heart failure. This stimulus should minimise activation of muscle metaboreceptors. During the passive leg movements, ascending spinal pathways were again

attenuated with intrathecal fentanyl. Controls had no i.t. fentanyl. In patients under control conditions, passive leg movement caused an increase in femoral blood flow and conductance, but did not change ventilatory responses, heart rate, stroke volume, or cardiac output. In the presence of fentanyl, patients had much larger increases in femoral blood flow and conductance. Thus, in heart failure patients, muscle mechanoreceptors augment the sympathetic vasoconstriction during exercise, thus causing exercise intolerance (Ives et al., 2016). It is possible that CT3 afferents, with their combined mechanosensitivity and metabosensitivity may contribute to this phenomenon. Exactly how such afferents could be sensitised by heart failure is not currently clear.

Group III/IV muscle afferents: Lactate, HCAR1 and ergoreceptor function

Our ability to positively identify a single class of group III afferents, "CT3s", in extracellular recordings was exploited to investigate the effects of the metabolite, lactate (**Chapter 4**). CT3 endings had previously been shown to be activated by low and high metabolite mixes (see **Chapter 3)**. In Chapter 4 of the present study, we demonstrated that lactate at a high but physiological concentration (15 mM) activated CT3 afferents in the absence of either raised ATP or protons (the other components of the "metabolite mixes"). We detected the presence of a G-protein coupled receptor for lactate, the hydroxycarboxylic acid receptor 1 (HCAR1), in the peripheral nervous system and demonstrated the presence of HCAR1 mRNA in dorsal root ganglia. HCAR1 immunoreactivity was also detected in cell bodies of dorsal root ganglia neurons that were retrogradely labelled from skeletal muscle. Additionally, immunoreactivity was also visible in some, but not all nerve fibres in whole-mount preparations of abdominal muscles. The presence of HCAR1+/CGRP-immunoreactive cell bodies and muscle axons is consistent with expression of HCAR1 by CT3 afferents.

Lactate concentration within skeletal muscle can range from 1 mM at rest to 30 mM during extreme exercise or ischemia (Ferguson et al., 2018). In the current studies, we demonstrated that CT3 afferents are activated by physiological levels of lactate. The HCAR1 receptor is a low affinity receptor, which may allow it to detect across the wide range of lactate concentrations that occur naturally (Liu et al., 2009). Thus, CT3 afferents may act, in part, as lactate 'sensors', while still responding to other stimuli (including stretch and compression). While lactate responses by afferents have been described previously, these have been attributed to chelation of divalent cations by lactate, which then secondarily causes changes in ASIC channel properties. The present study is, to the best of our knowledge, the first to suggest that a G-protein coupled receptor may mediate some effects of lactate on primary afferent neurons. It has recently been suggested that sensitivity to lactate by spinal nociceptors may be involved in generating bone pain (Hasegawa et al., 2018). Additional experimental evidence for this role of HCAR1 in the body is needed. Studies using conditional HCAR1 knock-down in neurons or RNA interference might be valuable, as would the development of a selective antagonist for HCAR1 (see below).

The possibility that CT3 afferents are activated by lactate, via HCAR1, could have many physiological implications. The activation of the exercise pressor reflex is mediated, in part, via release of metabolites from active muscles (Alam and Smirk, 1937). This may involve CT3 detecting lactate via HCAR1. This would be a mechanism in which the switch to the glycolytic pathway that occurs during oxygen shortfall could be signalled to the central nervous system. At present, there are no available specific antagonists for HCAR1; if such agents become available it would be fascinating to assess the role of this mechanism in exercise responses.

Group III/IV muscle afferents involved in delaying the onset of peripheral fatigue by ensuring adequate blood supply, but they also protect the body by restricting the output of motor neurons within the spinal cord (Laurin et al., 2015, Sidhu et al., 2017, Sidhu et al., 2018, Weavil and Amann, 2018). This is probably a major mechanism of central fatigue which prevents the overuse of the muscles during exercise. Therefore, these afferents have a protective role, and this may involve HCAR1 in instances where the concentration of lactate is very high (30 mM).

Patients with Chronic Fatigue Syndrome described long-lasting fatigue that persists even after minor bouts of exercise. One current hypothesis suggests that build-up of muscle metabolites activate and/or sensitise fatigue pathways to an abnormal extent, thereby causing the symptoms of chronic fatigue (Staud et al., 2015). Patients with chronic fatigue report higher fatigue ratings than healthy controls after hand grip exercises to exhaustion. When the blood flow to the exercised arm was occluded, via a cuff, after the exercises were completed, chronic fatigue patients reported worse overall fatigue. This provides indirect evidence that metaboreceptive pathways, in these patients, are involved as the cuff slows the rate at which metabolites are washed away from the exhausted muscles. However, as an increase in overall fatigue was reported, both peripheral and central pathways may be affected in patients with chronic fatigue syndrome (Staud et al., 2015).

Lactate has also been suggested as a volume transmitter in the brain that may couple neuronal activity, cerebral blood flow, and cellular metabolism, via actions on HCAR1(Lauritzen et al., 2014, Morland et al., 2015, Mosienko et al., 2015).

Future directions on lactate

Further studies are needed to investigate the presence and role of HCAR1 in sensory transduction in skeletal muscles afferents. One important question is whether HCAR1 is only present on metaboreceptive endings, or whether it is expressed by multiple classes of afferents. If HCAR1 is selectively expressed, this would have major implications for understanding its role. Certainly, our retrograde tracing and immunohistochemical studies suggest that HCAR1 is expressed in subpopulations of both peptidergic (CGRP-containing) and non-peptidergic neurons. If HCAR1 is expressed in just a few classes, it might be possible to test its role using neurogenetic approaches to either up-regulate or down-regulate receptor expression in particular afferent classes (see below). In the absence of selective agonists or antagonists, this type of approach could be highly informative. In this way, it would be possible to determine the role of HCAR1 and CT3 afferents in physiological processes such as processes such as the exercise pressor reflex, ventilatory responses to exercise, and muscle fatigue.

In the present studies, we applied lactate to the preparations alone. Other studies, as well as the present one, lactate was applied to preparations as a part of a metabolite mix (Jankowski et al., 2013, Light et al., 2008, Pollak et al., 2014). Some of these studies have reported that when the metabolites are applied together it results in a bigger response, compared to the individual effects, thereby suggesting the possibility of these metabolite having a synergistic effect (Gregory et al., 2015, Light et al., 2008, Pollak et al., 2014) . In the present studies, we did not investigate the possible synergistic effects. This should be investigated in CT3 afferents, as all three together might activate these pathways more potently than lactate alone.

Group III/IV muscle afferents: Delayed onset muscle soreness

Delayed onset muscle soreness is a phenomenon in which unaccustomed exercise-induced eccentric contractions result in discomfort and/or pain 24-72 hours after the exercise has been completed (Armstrong, 1984). The tendency for this discomfort, soreness and pain to appear after 12-24 hours, is somewhat of a physiological mystery. Delayed onset muscle soreness results in a reduction in performance and/or the ability to optimally train. Some of the impacts delayed onset muscle soreness have on athletes include the perception of functional impairment, a reduction in strength and power, altered muscle recruitment patterns, and increased risk of further or more severe injuries (Cheung et al., 2003). The mechanisms that underlie delayed onset muscle soreness remain unclear (Cheung et al., 2003, Taguchi et al., 2005b). Due to the unknown causes of delayed onset muscle soreness, the treatment and management strategies of delayed onset muscle soreness are wide-ranging. Some of the more known treatments and management strategies for delayed onset muscle soreness include cryotherapy, stretching, anti-inflammatory drugs (NSAIDS), ultrasound, application of electrical currents, massage (Guo et al., 2017), and compression sportswear (Dupuy et al., 2018).

Hough in 1902 made the first report of the soreness that occurs 12 to 24 hours after 'quick', 'strong' contractions. Hough's hypothesis was that soreness arose from *"rupture of the muscle fibre (or connective tissue between muscle fibres"* (Hough, 1902). The relationship between eccentric contractions, but not concentric contractions, and the occurrence of delayed onset muscle soreness was proposed in the 1980's by Asmussen, and later confirmed by others. Because of this, researchers investigating delayed onset muscle soreness have widely used eccentric exercises in both human and animal studies. Methods include including downhill running, resisted cycling, lifting weights, and resistance training (Cheung et al., 2003).

Many causes for delayed onset muscle soreness have been proposed, which tried to explain the pain that occurs. Proposed mechanisms have included lactic acid build-up, muscle spasm, connective tissue damage, muscle fibre damage, and inflammation (Cheung et al., 2003, Mizumura and Taguchi, 2016). Studies using eccentric contraction to investigate delayed onset muscle soreness have found histological (Armstrong et al., 1983), ultrastructural (Newham et al., 1983), biochemical (Armstrong et al., 1983), and physical (see for review- (Proske and Morgan, 2001)), changes in within the muscle (Taguchi et al., 2005b). These studies described the presence of disrupted sarcomeres within myofibrils, including microscopic lesions, a broadening, smearing, or even total myofibrillar disruption of the z-line, in addition to more wide- spread disruption of sarcomere architecture (Proske and Morgan, 2001).

Overstretching during eccentric exercise can cause sarcomeres to lengthen non-uniformly beyond the point where thick and thin filaments overlap, leading to 'popped sarcomeres'. These alterations directly reduce the muscles ability to produce force, overloading the sarcolemma and T-tubule system. This overloading of the sarcolemma and T-tubule system leads to the dysfunction of the excitation-contraction coupling system. It is thought that an influx of calcium stimulates calpain, an enzyme that can degrade excitation-contraction coupling proteins, resulting in loss of muscle strength (Peake et al., 2016). From these studies, the current theory arose - that delayed onset muscle soreness is caused by micro-damage of the subcellular structures of muscle fibres which subsequently causes inflammation and sensitisation or activation of muscle nociceptors (Mizumura and Taguchi, 2016).

This theory has recently come into question. Delayed onset muscle soreness can be present without muscular damage (Taguchi et al., 2005a). The timescale of micro-injury occurrence

and the symptoms of delayed onset muscle soreness do not align well (Cheung et al., 2003). Furthermore, anti-inflammatory drugs (NSAIDs) are not effective in reducing DOMs (Cheung, 2003). Muscle contraction, stretch and palpation are mechanical stimuli which do not evoke pain in normal healthy subjects. In subjects with delayed onset muscle soreness the above stimuli have the ability to evoke pain. From this arose the idea that delayed onset muscle soreness is a form of hyperalgesia, that is distinct from other types of muscle pain (Proske, 2005).

Another theory that cannot be ruled out is the idea that inflammatory mediators or cytoplasmic components released by muscle cells due to the micro-injury sensitise muscle afferents to mechanical stimuli. These may include prostaglandins, adenosine 5'-triphosphate and bradykinin (Taguchi et al., 2005b). Taguchi et al (2005) studied the extensor digitorum longus muscle of anaesthetised rats, which was stimulated to contract eccentrically repeatedly, then the animals were allowed to recover. During early recovery rats demonstrated no behavioural evidence of muscle hyperalgesia. Two days after the exercise, one group was subjected to moderate compression of the exercised muscle. Muscle tenderness was detected by behavioral pain tests and by c-Fos protein expression in the spinal dorsal horn to mechanical stimulation. The authors also suggested that the diffuse and dull character of delayed onset muscle soreness may implicate thin-fibre muscle afferents (Taguchi et al., 2005a, Taguchi et al., 2005b).

The role of thin-fibre muscle afferents and their involvement in delayed onset muscle soreness was then investigated using single-fibre afferent recordings (Taguchi et al., 2005b). These recordings were made from sensory axons in the rat extensor digitorum longus muscle/peroneal nerve preparations *in vitro* two days after application of eccentric contractions (Taguchi et al., 2005b). These studies provided evidence that the mechanical

threshold of the muscle thin-fibre sensory receptors was reduced in rats subjected to eccentric contractions and the magnitude of their responses were increased. The responses to other stimuli chemical mediators (ATP, Bradykinin, Lactic acid, pH) and thermal stimuli (hot or cold Krebs) were not modified by prior exposure to eccentric contractions (Taguchi et al., 2005b).

The same *ex vivo* preparation was further used to investigate the roles of bradykinin and nerve growth factor in delayed onset muscle soreness, as both excite/ sensitise nociceptors (Ellrich and Makowska, 2007, Mense, 1981). It was demonstrated that bradykinin triggers the development of muscular mechanical hyperalgesia, as application of the B_2 receptor antagonist prevented the development of delayed onset muscle soreness. Nerve growth factor was shown to sensitise muscle C-fiber receptors to mechanical stimulation. This was demonstrated by mechanical hyperalgesia being partially reversed within 2 hours after an injection of an anti-NGF antibody(Murase et al., 2010).

Another study investigated the involvement of glial cell line-derived neurotrophic factor and prostaglandins (COX-2) in mechanical hyperalgesia induced by exercise. Using the same *in vivo* rat model (Taguchi et al., 2005a) along with bradykinin receptor antagonists and cyclooxygenase -1 and -2 inhibitors, it was shown that COX-2 was upregulated after exercise, triggered by an upregulation of glial cell line-derived neurotrophic factor. It was also shown that these effects could be reversed using an anti- glial cell line-derived neurotrophic factor antibody (Murase et al., 2014).

From these studies, a new theory for delayed onset muscle soreness was proposed. It suggested that nerve growth factor and glial cell line-derived neurotrophic factor produced by muscle fibres and/or satellite cells are responsible for the muscle hyperalgesia seen in

delayed onset muscle soreness (Mizumura and Taguchi, 2016). It was proposed that the mechanical hyperalgesia after eccentric contraction occurs through two pathways. The first, is via activation of the B_2-bradykinin receptor-nerve growth factor pathway. The second is the activation of the COX-2-glial cell line-derived neurotrophic factor pathway (Mizumura and Taguchi, 2016). It was suggested that the neurotrophic factors are produced within the muscle cells and/or surrounding satellite cells and directly excite muscle afferents(Mizumura and Taguchi, 2016).

The preparation described in the present study could be modified to characterise the morphological and functional properties of the muscle afferents stimulated by bradykinin, nerve growth factor and glial cell line-derived neurotrophic factor. This would be a method to identify which class(es) of muscle afferents mediate delayed onset muscle soreness and thus could be targeted for treatment of this unpleasant disorder.

Group III muscle afferents and Transversus Abdominal Plane Block

The anatomy of sensory and motor innervation of the muscles of the abdominal wall is not known with precision. There is a need for a detailed description of the course and distribution of sensory and motor nerves within the abdominal wall. Modern surgical and anaesthetic techniques can damage these nerves; and a detailed map of the innervation could help minimise surgical damage (Rozen et al., 2008).

The transversus abdominis plane lies between the internal oblique and the transversus abdominis muscle. It includes innervation from interscostal, subcostal, and lumber nerves that run alongside blood vessels (Rozen et al., 2008). Rafi (2001) identified the neurovascular plane as an optimal area to inject a local anaesthetic, to reduce pain after abdominal surgery (Rafi, 2001). The “TAP block” is now a widely used (Stoving et al.,

2015), and the technique has been improved by the use of ultrasound or laparoscopic cameras to guide the needle during administration of the local anaesthetic (Güner et al., 2015). How the TAP block works is largely unknown (Gadsden et al., 2015, Petersen et al., 2010, Stoving et al., 2015).

TAP block reduces pain scores in adults after abdominal surgery (Sforza et al., 2011), including pain from the incision after abdominoplasty. This pain delays mobilization and ambulation, increasing the risks of deep venous thrombosis and pulmonary embolism. TAP blocks reduce pain in these patients and facilitate rehabilitation (Sforza et al., 2011). The technique is also currently considered as a pain relief for paediatric surgery (Güner et al., 2015). However, the optimal indications for the use in children are lacking and the safety, pharmokinetic, and pharmodynamic effects are still to be investigated (Bergmans et al., 2015, Bryskin et al., 2015, Suresh and Chan, 2009). The present study provides an approach that allows individual classes of the nerve fibres that innervate muscle to be characterised. Using this approach, has the potential to not only establish the different classes of nerves fibres and their locations within the abdominal muscles (**Chapter 3**). It potentially can be used to investigate and identify the nerve fibres that are effected by the TAP block, along with investigating the safety, pharmacokinetic, and pharmacodynamics effects. Further investigations would need to be made in relation to the translational ability between that of a small animal model (the mouse) and the human abdominal muscles.

Reconstructive surgery

Parts of the adnominal wall are often used for reconstructive flaps in plastic surgery, in particular in breast reconstructions (Rozen et al., 2008, Young et al., 2012). A significant complication of with this type of surgery is damage to the rectus abdominis, which can result in the denervation, abdominal bulge, and frank herniation (Bottero et al., 2004, Duchateau

et al., 1988). An understanding of the anatomy and physiology of abdominal muscle innervation would be valuable for this surgery, to minimise damage to underlying layers and preserve sensation, in both the flap and the remaining rectus abdominis (Rozen et al., 2008). The present study has started to identify some details of the innervation of the abdominal muscles, albeit in a small animal model. It would be informative to test whether the arrangement of nerve trunks seen in the mouse holds true for human abdominal muscles.

Future prospects for studying group III muscle afferents

One of the major obstacles in identifying different types of spinal afferents is to positively distinguish them from motor axons and autonomic efferent axons, which travel along in the same mixed nerve trunks (Spencer et al., 2018b). The nerve cell bodies of spinal afferents reside in the dorsal root ganglia (DRG), but the morphology and location of peripheral nerve endings of spinal afferents that transduce various types of sensory stimuli is poorly understood in many parts of the body (Spencer et al., 2018a). This may be less of a problem in skeletal muscle than in viscera, where there is often a far more extensive autonomic innervation.

Over the last 30 years there has been significant advances in the techniques used to investigate and differentiate the different classes of sensory neurons and their functional roles. Genetic and tracing methods have been combined to investigate the molecular and functional diversity of sensory neurons. Examples below include anterograde and retrograde tracers, RNA interference, transgenic mice with reporters under the control of cell-specific promoters, viral tracing, calcium (Ca^{2+}) imaging, optogenetics, and single cell sequencing. These techniques can be used individually or in combination.

Transgenic models

Transgenic mice have been extensively used to investigate the molecular and functional diversity of sensory neurons. Transgenic mice have been engineered to either have a selective gene 'knocked in' or 'knocked out'. Reporter 'tags' can be expressed under the control of a cell-specific promoter, so that the distribution of one particular gene can be visualised, or one particular type of cell. For example, placental alkaline phosphates (PLAP), nuclear-localised-β-galactosidase gene (nLacZ), fluorescent reporter proteins (Green FP, Yellow FP) have all been used (Cavanaugh et al., 2011, Le Pichon and Chesler, 2014, Spencer et al., 2018b) . In regards to the present study, targeted HCAR1 knockout mice would be a useful tool. Likewise, GFP expression under the HCAR1 promoter would also be useful to identify with confidence which types of sensory neurons (and other cells) express the G-protein coupled receptor. Non-targeted HCAR1 knockout mice are viable, fertile and display few notable differences from wild-types (Liu et al., 2009) and have been used to investigate the role of HCAR1 in insulin dependent anti-lipolysis (Ahmed et al., 2010), agonist induced hypertensive effects (Wallenius et al., 2017) and exercise induced cerebral VEGF and angiogenesis (Morland et al., 2017).

Viral tracers

In recent years, viral tracers have been widely used to map neural circuits, establishing the input and output connectivity of specific neuronal populations (Zingg et al., 2017). Viral tracers allow the alteration of the genome in a flexible, and adaptable way, that can be rapidly exploited (Iyer et al., 2014). Adeno-associated viruses (AAV's) have been extensively used to deliver vectors via retrograde transport. Using viruses for gene delivery has exploited the tropisms of viruses. For example, canine adenovirus 2 (Junyent and Kremer, 2015) and herpes simplex virus (Han et al., 2018) can be transported anterogradely. Adenovirus 1 and 9 have also been described as being capable of anterograde and trans-synaptic transport

(Zingg et al., 2017). The ability to use a viral tracer would allow (if the HCAR1 receptor is specific to CT3 afferents (this remains to be determined)), a range of studies to be undertaken. It would be possible to determine the distribution and population of CT3 afferents in the abdominal muscles as well as the dorsal root ganglia. It would be possible to determine the ascending central pathways. A model that utilises viral vectors would be a useful tool to combine with other techniques such as calcium imaging and optogenetics to further understand the physiological properties of CT3 afferents.

Anterograde and Retrograde Tracers

Anterograde and retrograde tracers have been used extensively to visualise either the morphological endings of neurons in a tissue of interest or the visualisation of cell bodies supplying axons to a tissue of interest. Over the past decade, these techniques have been revitalised due to new methods. Selective anterograde tracing of vagal afferents was extensively studied since the 1990s (Berthoud et al., 1991, Berthoud and Powley, 1991). Similar techniques have been applied to dorsal root ganglia in mice more recently, using biotinylated dextran tracers. The extensive morphology of spinal sensory afferents has been described for the large intestine (Kyloh and Spencer, 2014), stomach and oesophagus (Spencer et al., 2016), and urinary bladder (Spencer et al., 2018a), and this has been combined with CGRP immunoreactivity to identify peptidergic classes. Tracing techniques have been further developed by the use of combinatorial viral approaches to achieve sensory neuron labelling. The ability to transfect regions of interest with adeno-associated virus carrying specific constructs (Cre-recombinase, fluorescent proteins – GFP, YFP) allows the endings of sensory neurons to be visualised, along with the ability to visualise sensory neuron activation using in vivo methods such as Ca^{2+} imaging, genetically-encoded calcium indicators (GECIs), or optogenetics to selectively activate neurons of interest (Han et al., 2018). These represent a rich trove of possibilities for targeted study of identified muscle

afferents, if promoters selective for specific classes can be identified and used to direct gene expression appropriately. We speculate that HCAR1 might be just such a marker for a subset of metabosensitive muscle afferents.

Single cell analysis

Single cell RNA sequencing is a powerful way to discriminate different populations of cells based on each cell's specific pattern of expression. Gene expression profiling of individual cells has revealed a rich variety of cell types and improved our understanding of the complexity of tissues, organs, and organisms (Lafzi et al., 2018). A strategy for cell classification based on expression analysis has been developed. It is based on the hypothesis that functionally different cell types will be reflected in the combination of genes that each express. Functional heterogeneity of sensory neurons investigated in this way has not always related closely to classifications based on functional properties or immunohistochemical markers (Usoskin et al., 2015). An un-biased analysis on single sensory nerve cell bodies, isolated from mouse lumbar (L4-L6) DRGs, described a high variance in gene expression between cells. Eleven groups were distinguished based on their combinations of genes expressed. The authors also noted some genes that had not previously been studied in sensory neurons that appeared to be markers for specific classes. For example, substance P (*tac1*) and family with sequence similarity 19, member A1 (FAM19A1) appeared to be selectively expressed by peptidergic nociceptors (Usoskin et al., 2015). Hockley et al (2018) used single cell RNA sequencing to identify seven subtypes of colonic sensory neurons based on their gene expression. Single cell PCR and immunohistochemistry for the identified genes were used to validate the derived subtypes. It is not clear how all of the 7 classes map onto 5-6 classes identified using morphological and functional techniques (Brookes et al., 2013), although some overlap was noted (Hockley et al., 2018).

Calcium (Ca2+) Imaging

Calcium imaging allows the visualisation of intracellular calcium signals in activated neurons (Grienberger and Konnerth, 2012) and has been used to investigate the activation of vagal afferents from the stomach, intestine, and lungs. Williams et al (2018) used the genetically encoded calcium indicator, GCaMP3, to record calcium transients - an optical proxy of activity. GCaMP3 expression was driven using a Cre driver line, *Glp1r-ires*-Cre, that targeted a particular type of vagal sensory neurons. Recordings from single neurons were made while stimuli were applied to the end organs including gastric distension, duodenal nutrient application, intestinal distension and lung inflation. The study demonstrated that not only are some afferents polymodal, responding to several different stimuli, but that some afferents activated by stretch in the stomach were also activated by nutrients; this was not the case for intestinal vagal afferent endings (Williams et al., 2016).

Wang et al (2018) demonstrated how cutaneous temperature is encoded by distinctively tuned thermoreceptive afferents. In vivo Ca^{2+} imaging from mouse dorsal root ganglia nerve cell bodies (L4 or L5) was achieved with the genetically encoded Ca^{2+} indicator GCaMP6s, that was transfected via an adeno-associated viral vector, into primary sensory neurons. Optical recording was performed using two-photon microscopy to ensure high spatial resolution and fast temporal scanning from large sets of neurons simultaneously. Controlled thermal stimuli were then applied to the skin of the hind limb and the Ca^{2+} transients recorded and visualised (Wang et al., 2018). Wang et al (2018) demonstrated that cutaneous temperature is represented by distinctive sets of thermo-receptive afferents and that heat-sensitive and cold-sensitive afferent use different coding strategies. It was shown that heating sensitive neurons responded in a graded fashion, while cold-sensitive neurons responded in an ungraded fashion. Even though many neurons were activated by multiple stimuli, this occurred via very distinctive patterns of activation (Wang et al., 2018). This type of approach could be usefully applied to muscle afferents in the future to investigate

transduction patterns of specific classes of neurons. It could potentially allow an *in vivo* investigation into the specific transduction patterns of CT3 afferents.

Optogenetics

Optogenetics is a powerful combination of techniques based on the expression of photo-activated proteins called opsins, in genetically-defined neural populations. Light mediated activation of opsins either excite or inhibit neurons or modulate subcellular functions (Iyer et al., 2014, Xie et al., 2018) depending on the opsin gene. Channelrhodopsin is a cation channel, activated by blue light, which causes cell depolarization and excitation. Halorhodopsin is an anion pump, activated by yellow light, which causes hyperpolarisation. The use of photonic stimuli, *ex vivo* or *in vivo*, enables tight control of the extent and patterning of activation with unprecedented temporal precision (Xie et al., 2018). For example, different functional classes of spinal afferents from the mouse large intestine could be distinguished by their responses to focal pulses of blue light to isolated segments of the distal colon (Feng et al., 2016).

One of the key challenges in using optogenetics is to delivery adequate light stimuli to the region of interest, during studies of complex behaviour without using acute invasive methods. Recent efforts have delivered light via wireless microLED systems (Montgomery et al., 2015) surgically implanted well before the experiment. Alternatively, external wireless illumination with LED arrays can be used to afferents in the periphery. The use of these arrays is often only sufficient for afferents close to the skin due to poor penetration of light and are often difficult to use in awake and moving animals. Indeed, the light stimuli may also impact on the animal's behaviour independent of opsin expression (Mickle and Gereau, 2018, Shin et al., 2017). Implanted Micro-LEDs adjacent to dorsal root ganglia do not have this problem and may be used to precisely activate or inhibit spinal afferents in

mice (Spencer et al., 2018b). Non-transgenic mouse models rely on viruses to express target genes in cell bodies of interest in the dorsal root ganglia. Typically, one virus is injected into the target organ and is transported back to the cell body in the dorsal root ganglia. The second virus is injected directly into one dorsal root ganglia of interest. Through the intersection of their effects, only the sensory neurons that project to the target organ express the opsins (Spencer et al., 2018b). Such an approach could be used to test whether HCAR1-expressing spinal afferents activate the exercise pressor response and ventilatory responses as hypothesised in the present study.

Recent studies have demonstrated how identity, peripheral axon anatomy, central anatomy, and physiological function of sensory neurons can be related *ex vivo* and *in vivo* (Williams et al., 2016). Han et al (2018) injected the duodenum and stomach of wild-type mice with a retrogradely transported adeno-associated virus, carrying a Cre-EBFP recombinase construct, which was transported to cell bodies in the nodose ganglion of the vagus nerve. The nodose ganglia were then transfected with channel channelrhodopsin2 in a Cre-inducible viral construct. The neurons that expressed the opsin were restricted to those that innervated the stomach and intestine. This study used cell specific targeted transneuronal tracing to identify the ascending pathways of vagal afferents within the gut. It was found that these vagal afferents with cell bodies within the nodose ganglia are a part of the nodose parabrachio-nigral pathway. Optical stimulation of this pathway replicated the rewarding effects of vagus excitation (Han et al., 2018). These techniques could be used to confirm whether CT3 afferent central projections terminate in brain structures that are known to be involved in the exercise pressor reflex.

Chemogenetics

DREADDS, are modified muscarinic receptors that respond specifically to a synthetic ligand; clozapine N-oxide (CNO). DREADDs allow subpopulations of neurons *in vivo* to be targeted by the administration of CNO (Manvich et al., 2018). CNO-activated DREADDs can be coupled to various GCPR signalling cascades (Urban and Roth, 2015). This could be a valuable way to investigate the downstream effects of HCAR1. The use of DREADDs, allow widespread modulation of neuronal activity throughout more of the body than optogenetic approaches, but at the cost of lower temporal resolution.

A detailed description of the structural, functional and molecular characteristics is needed for a comprehensive understanding of sensory neurons, including their peripheral and central pathways, and physiological roles. At the time that this project was started, the choice of tools to related structure to function in afferent endings was quite restricted. Today there is a myriad of techniques (some of these described above), which will revolutionise these types of studies. No single technique will answer all of the questions, but each can add hugely to future experimental design.

Mechanoreceptors, metaboreceptors, nociceptors, polymodal receptors

Despite a century of research, some of the basic anatomical and physiological properties of group III and group IV muscle afferents remain unknown (Jankowski et al., 2013). The repertoire of metabolites and receptors that modulate metabo-sensitive afferents has not been fully established (Amann and Light, 2015). Methods to correlate the morphology and function of identified group III and group IV afferents have not hitherto been available. If this approach is used to create a comprehensive account of afferent endings in muscles it will be possible to characterise and distinguish nociceptors, mechanoreceptors and

metaboreceptors. This would be invaluable for determining how their activity contributes to altered sensation in physiology and a range of disease states.

Group III and group IV muscle afferents have been described as being predominantly mechanoreceptive (Group III) or metaboreceptive (Group IV) (Hayes and Kaufman, 2001, Hayes et al., 2009, Kaufman et al., 2002). Many studies investigating the role of group III and IV afferents in physiology (exercise pressor reflex, muscle fatigue), and disease states (hypertension, heart failure, chronic fatigue syndrome) in animal and humans, have been based on this classification. This is problematic, not least because in the present study CT3 afferents, which are clearly group III afferents on the basis of their conduction velocities have been shown to combine mechano- and metabo-sensitive responses.

However, some group III and group IV muscle afferents have been described as polymodal; i.e. are activated by more than one type of stimulus (Mense, 1996, Kaufman et al., 2002, Jankowski et al., 2013#180, Queme et al., 2017, Ross et al., 2014).In addition, some mechanosensitive afferents are known to be sensitised by a range of metabolites (Murphy et al., 2011). Even though this is the case, group III and group IV afferents are still widely described in the literature as mechanoreceptors and metaboreceptors respectively. This is an important oversight when trying to understand these afferents and their roles in physiology and disease states. Our data suggest that this rigid characterisation of group III and group IV skeletal muscle afferents is not accurate. As roles of group III and group IV muscle afferents are identified, it will become increasingly important to discriminate the different classes and sub-classes. Then will it be possible to identify which specific neurons are affected in disorders and which actually contribute to each type of central pathway.

We have speculated that CT3 afferents may play roles in several of these physiological and diseases states. However, the likely existence of multiple classes of group III and group IV muscle afferents, makes it difficult to establish this definitively. Until each class has been systematically characterised, uncertainty will remain. Our findings confirm that at least some sensory neurons, including CT3 neurons that do not have the characteristics of nociceptors, have polymodal responses.

In the present study, we have developed a novel preparation and a method, that allows the morphological and functional characteristics of group III/IV muscle afferents to be related. This methodology will allow individual classes to be studied systematically and in detail, one at a time, without conflating their properties (**Chapter 2**). We have described a class of group III muscle afferents that are mechanosensitive metaboreceptors (CT3s) present within the connective tissue in skeletal muscles in mice (**Chapter 3**). We have also described a possible mechanism by which CT3 afferents are activated by lactate, via a specific G-protein coupled receptor HCAR1 (**Chapter 4**). This simple approach, in which essentially a single functional class is studied in detail, has the potential to contribute significantly to a better understanding of the basis of sensation from muscle groups.

REFERENCES

Abrahams, V. C. 1986. Group III and IV receptors of skeletal muscle. *Canadian Journal of Physiology and Pharmacology,* 64**,** 509-514.

Abrahams, V. C., Hilton, S. M. & Zbrozyna, A. 1960. Active muscle vasodilatation produced by stimulation of the brain stem: its significance in the defence reaction. *The Journal of Physiology,* 154**,** 491-513.

Ackermann, P. W., Li, J., Finn, A., Ahmed, M. & Kreicbergs, A. 2001. Autonomic innervation of tendons, ligaments and joint capsules. A morphologic and quantitative study in the rat. *Journal of Orthopaedic Research,* 19**,** 372-378.

Adal, M. 1984. The sensory and motor innervation of muscle spindles in cat tail dorsolateral muscles. *Journal of Anatomy,* 138**,** 237.

Adrian, E. D. & Zotterman, Y. 1926. The impulses produced by sensory nerve-endings: Part II. The response of a Single End-Organ. *The Journal of Physiology,* 61**,** 151-171.

Adrian, R. H. 1956. The effect of internal and external potassium concentration on the membrane potential of frog muscle. *The Journal of Physiology,* 133**,** 631-658.

Ahmed, K. 2011. Biological roles and therapeutic potential of hydroxy-carboxylic Acid receptors. *Frontiers in Endocrinology,* 2**,** 1-12.

Ahmed, K., Tunaru, S. & Offermanns, S. 2009. GPR109A, GPR109B and GPR81, a family of hydroxy-carboxylic acid receptors. *Trends in Pharmacological Sciences,* 30**,** 557-562.

Ahmed, K., Tunaru, S., Tang, C., Müller, M., Gille, A., Sassmann, A., Hanson, J. & Offermanns, S. 2010. An autocrine lactate loop mediates insulin-dependent inhibition of lipolysis through GPR81. *Cell metabolism,* 11**,** 311-319.

Alam, M. & Smirk, F. H. 1937. Observations in man upon a blood pressure raising reflex arising from the voluntary muscles. *The Journal of Physiology,* 89**,** 372-383.

Allen, D. G., Lamb, G. D. & Westerblad, H. 2008. Skeletal muscle fatigue: cellular mechanisms. *Physiological Reviews,* 88**,** 287-332.

Amann, M. 2011. Central and peripheral fatigue: interaction during cycling exercise in humans. *Medicine & Science in Sports & Exercise,* 43**,** 2039-2045.

Amann, M. 2012. Significance of Group III and IV muscle afferents for the endurance exercising human. *Proceedings of the Australian Physiological Society,* 43**,** 1-7.

Amann, M., Blain, G. M., Proctor, L. T., Sebranek, J. J., Pegelow, D. F. & Dempsey, J. A. 2011a. Implications of group III and IV muscle afferents for high- intensity endurance exercise performance in humans. *The Journal of Physiology,* 589**,** 5299-5309.

Amann, M. & Calbet, J. A. 2008. Convective oxygen transport and fatigue. *Journal of Applied Physiology,* 104**,** 861-870.

Amann, M., G, B., Proctor, L. T., Sebranek, J. J., Pegelow, D. F. & Dempsey, J. A. 2010. Group III and IV muscle afferents contribute to ventilatory and cardiovascular response to rhythmic exercise in humans. *Journal of Applied Physiology,* 109**,** 966–976.

Amann, M. & Light, A. R. 2015. From Petri dish to human: new insights into the mechanisms mediating muscle pain and fatigue, with implications for health and disease. *Experimental Physiology,* 100**,** 989-990.

Amann, M., Proctor, L. T., Sebranek, J. J., Eldridge, M. W., Pegelow, D. F. & Dempsey, J. A. 2008. Somatosensory feedback from the limbs exerts inhibitory influences on central neural drive during whole body endurance exercise. *Journal of Applied Physiology,* 105**,** 1714-1724.

Amann, M., Proctor, L. T., Sebranek, J. J., Pegelow, D. F. & Dempsey, J. A. 2009. Opioid-mediated muscle afferents inhibit central motor drive and limit peripheral muscle fatigue development in humans. *The Journal of Physiology,* 587**,** 271-283.

Amann, M., Runnels, S., Morgan, D. E., Trinity, J. D., Fjeldstad, A. S., Wray, D. W., Reese, V. R. & Richardson, R. S. 2011b. On the contribution of group III and IV muscle afferents to the circulatory response to rhythmic exercise in humans. *The Journal of Physiology,* 589**,** 3855-3866.

Amann, M., Sidhu, S. K., Weavil, J. C., Mangum, T. S. & Venturelli, M. 2015. Autonomic responses to exercise: group III/IV muscle afferents and fatigue. *Autonomic Neuroscience: Basic and Clinical,* 188**,** 19-23.

Amann, M., Venturelli, M., Ives, S. J., Morgan, D. E., Gmelch, B., Witman, M. A., Jonathan Groot, H., Walter Wray, D., Stehlik, J. & Richardson, R. S. 2014. Group III/IV muscle afferents impair limb blood in patients with chronic heart failure. *International Journal of Cardiology,* 174**,** 368–375.

Andres, K., Von Düring, M. & Schmidt, R. 1985. Sensory innervation of the Achilles tendon by group III and IV afferent fibers. *Anatomy and Embryology,* 172**,** 145-156.

Andres, K. H. & During, M. V. 1990. Comparative and functional aspects of the histological organisation of cutaneous receptors in vertebrates *In:* ZENKER, W. & NEUHUBER, W. L. (eds.) *The Primary Affernt Neuron* New York and London Plenum Press

Andrew, B., Leslie, G. & Thompson, J. 1973. Distribution and properties of muscle spindles in the caudal segmental muscles of the rat together with some comparisons with hind limb muscle spindles. *Quarterly Journal of Experimental Physiology and Cognate Medical Sciences,* 58**,** 19-37.

Arjmand, N., Shirazi-Adl, A. & Parnianpour, M. 2008. Trunk biomechanics during maximum isometric axial torque exertions in upright standing. *Clinical Biomechanics (Bristol, Avon),* 23**,** 969-78.

Armstrong, R. 1984. Mechanisms of exercise-induced delayed onset muscular soreness: a brief review. *Medicine & Science in Sports & Exercise,* 16**,** 529-538.

Armstrong, R., Ogilvie, R. & Schwane, J. 1983. Eccentric exercise-induced injury to rat skeletal muscle. *Journal of Applied Physiology,* 54**,** 80-93.

Arngrim, N., Schytz, H. W., Britze, J., Amin, F. M., Vestergaard, M. B., Hougaard, A., Wolfram, F., De Koning, P. J. H., Olsen, K. S., Secher, N. H., Larsson, H. B. W., Olesen, J. & Ashina, M. 2016. Migraine induced by hypoxia: an MRI spectroscopy and angiography study. *Brain,* 139**,** 723-737.

Asmussen, E. 1956. Observations on experimental muscular soreness. *Acta Rheumatologica Scandinavica,* 2**,** 109-116.

Babini, E., Paukert, M., Geisler, H.-S. & Gründer, S. 2002. Alternative splicing and interaction with di-and polyvalent cations control the dynamic range of acid-sensing ion channel 1 (ASIC1). *Journal of Biological Chemistry,* 277**,** 41597-41603.

Bandler, R. & Carrive, P. 1988. Integrated defence reaction elicited by excitatory amino acid microinjection in the midbrain periaqueductal grey region of the unrestrained cat. *Brain Research,* 439**,** 95-106.

Banks, R. W., Barker, D. & Stacey, M. 1982. Form and distribution of sensory terminals in cat hindlimb muscle spindles. *Philosophical Transactions of the Royal Society of London,* 299**,** 329-364.

Bárány, M. 1967. ATPase activity of myosin correlated with speed of muscle shortening. *The Journal of general physiology,* 50**,** 197-218.

Barker, D. 1948. The innervation of the muscle-spindle. *Journal of Cell Science,* 3**,** 143-185.

Barry, C. M., Kestell, G., Gillan, M., Haberberger, R. V. & Gibbins, I. L. 2015. Sensory nerve fibers containing calcitonin gene-related peptide in gastrocnemius, latissimus dorsi and erector spinae muscles and thoracolumbar fascia in mice. *Neuroscience,* 291**,** 106-117.

Basbaum, A. I., Bautista, D. M., Scherrer, G. & Julius, D. 2009. Cellular and Molecular Mechanisms of Pain. *Cell,* 139**,** 267-284.

Basbaum, A. I., Shepherd, G. M., Kaneko, A. & Westheimer, G. 2008. *The Senses: A Comprehensive Reference*, Academic Press, Elsevier.

Basnayake, S. D., Hyam, J. A., Pereira, E. A., Schweder, P. M., Brittain, J.-S., Aziz, T. Z., Green, A. L. & Paterson, D. J. 2010. Identifying cardiovascular neurocircuitry involved in the exercise pressor reflex in humans using functional neurosurgery. *Journal of Applied Physiology,* 110**,** 881-891.

Bendahan, D., Chatel, B. & Jue, T. 2017. Comparative NMR and NIRS analysis of oxygen-dependent metabolism in exercising finger flexor muscles. *American Journal of Physiology-Regulatory, Integrative and Comparative Physiology,* 313**,** R740-R753.

Benjamin, M. 2009. The fascia of the limbs and back-A review. *Journal of Anatomy,* 214**,** 1-18.

Benjamin, M., Kaiser, E. & Milz, S. 2008. Structure- function relationships in tendons: a review. *Journal of Anatomy,* 212**,** 211-228.

Benjamin, M., Redman, S., Milz, S., Büttner, A., Amin, A., Moriggl, B., Brenner, E., Emery, P., Mcgonagle, D. & Bydder, G. 2004. Adipose tissue at entheses: the rheumatological implications of its distribution. A potential site of pain and stress dissipation? *Annals of the Rheumatic Diseases,* 63**,** 1549-1555.

Bergersen, L. & Gjedde, A. 2012. Is lactate a volume transmitter of metabolic states of the brain? *Frontiers in Neuroenergetics,* 4**,** 1-6.

Bergersen, L. H. 2007. Is lactate food for neurons? Comparison of monocarboxylate transporter subtypes in brain and muscle. *Neuroscience,* 145**,** 11-19.

Bergmans, E., Jacobs, A., Desai, R., Masters, O. W. & Thies, K. C. 2015. Pain relief after transversus abdominis plane block for abdominal surgery in children: a service evaluation. *Local and Regional Anesthesia,* 8**,** 1-6.

Bernier, L. P., Ase, A. R. & Séguéla, P. 2018. P2X receptor channels in chronic pain pathways. *British Journal of Pharmacology,* 175**,** 2219-2230.

Berthoud, H., Carlson, N. & Powley, T. 1991. Topography of efferent vagal innervation of the rat gastrointestinal tract. *American Journal of Physiology-Regulatory, Integrative and Comparative Physiology,* 260**,** R200-R207.

Berthoud, H.-R. & Powley, T. L. 1991. Morphology and distribution of efferent vagal innervation of rat pancreas as revealed with anterograde transport of DiI. *Brain research,* 553**,** 336-341.

Bewick, G. S. & Banks, R. W. 2015. Mechanotransduction in the muscle spindle. *Pflügers Archiv-European Journal of Physiology,* 467**,** 175-190.

Birdsong, W. T., Fierro, L., Williams, F. G., Spelta, V., Naves, L. A., Knowles, M., Marsh-Haffner, J., Adelman, J. P., Almers, W. & Elde, R. P. 2010. Sensing muscle ischemia: coincident detection of acid and ATP via interplay of two ion channels. *Neuron,* 68**,** 739-749.

Blain, G. M., Mangum, T. S., Sidhu, S. K., Weavil, J. C., Hureau, T. J., Jessop, J. E., Bledsoe, A. D., Richardson, R. S. & Amann, M. 2016. Group III/IV muscle afferents limit the intramuscular metabolic perturbation during whole body exercise in humans. *The Journal of Physiology,* 594**,** 5303-5315.

Borg, G. A. 1973. Perceived exertion: a note on "history" and methods. *Medicine and Science in Sports,* 5**,** 90-93.

Bottero, L., Lefaucheur, J.-P., Fadhul, S., Raulo, Y., Collins, E. D. & Lantieri, L. 2004. Electromyographic assessment of rectus abdominis muscle function after deep inferior epigastric perforator flap surgery. *Plastic and Reconstructive Surgery,* 113**,** 156-161.

Bottinelli, R., Schiaffino, S. & Reggiani, C. 1991. Force-velocity relations and myosin heavy chain isoform compositions of skinned fibres from rat skeletal muscle. *The Journal of Physiology,* 437**,** 655-672.

Bowen, W. P. 1904. Changes in Heart-Rate, Blood-Pressure, and Duartion of Systole Resulting from Bicycling. *American Journal of Physiology - Legacy Content,* 11**,** 59-77.

Bozzo, L., Puyal, J. & Chatton, J.-Y. 2013. Lactate modulates the activity of primary cortical neurons through a receptor-mediated pathway. *PloS one,* 8**,** e71721-e71721.

Brain, S., Williams, T., Tippins, J., Morris, H. & Macintyre, I. 1985. Calcitonin gene-related peptide is a potent vasodilator. *Nature,* 313**,** 54.

Brooke, M. H. & K, K. K. 1970. Three" myosin adenosine triphosphatase" systems: the nature of their pH lability and sulfhydryl dependence. *Journal of Histochemistry & Cytochemistry,* 18**,** 670-672.

Brookes, S. J. H., Spencer, N. J., Costa, M. & Zagorodnyuk, V. P. 2013. Extrinsic primary afferent signalling in the gut. *Nature Reviews Gastroenterology and Hepatology,* 10**,** 286-296.

Brooks, G. A. Lactate:Glycolytic End Product and Oxidative Substrate During Sustained Exercise in Mammals — The “Lactate Shuttle”. *In:* GILLES, R., ed. Circulation, Respiration, and Metabolism, 1985// 1985 Berlin, Heidelberg. Springer Berlin Heidelberg, 208-218.

Brooks, G. A. 2007. Lactate: Link Between Glycolytic and Oxidative Metabolism. *Sports Medicine,* 37**,** 341-343.

Brooks, G. A. 2009. Cell–cell and intracellular lactate shuttles. *The Journal of Physiology,* 587**,** 5591-5600.

Brooks, G. A. 2018. The Science and Translation of Lactate Shuttle Theory. *Cell metabolism,* 27**,** 757-785.

Brown, A. G. 1975. *Handbook of Sensory Physiology. Vol. III/2: Muscle Receptors: Edited by C. C. Hunt. Springer-Verlag, Berlin-Heidelberg-New York, 1974. Pp. viii+312. DM 130*.

Brown, S. H., Banuelos, K., Ward, S. R. & Lieber, R. L. 2010. Architectural and morphological assessment of rat abdominal wall muscles: comparison for use as a human model. *Journal of Anatomy,* 217**,** 196-202.

Brown, S. H., Carr, J. A., Ward, S. R. & Lieber, R. L. 2012. Passive mechanical properties of rat abdominal wall muscles suggest an important role of the extracellular connective tissue matrix. *Journal of Orthopaedic Research,* 30**,** 1321-1326.

Brown, S. H., Ward, S. R., Cook, M. S. & Lieber, R. L. 2011. Architectural analysis of human abdominal wall muscles: implications for mechanical function. *Spine,* 36**,** 355.

Broxterman, R. M., Layec, G., Hureau, T. J., Morgan, D. E., Bledsoe, A. D., Jessop, J. E., Amann, M. & Richardson, R. S. 2017. Bioenergetics and ATP Synthesis during Exercise: role of Group III/IV Muscle Afferents. *Medicine & Science in Sports & Exercise,* 49**,** 2404-2413.

Bruce, A. N. 1913. Vasodilator axon-reflexes. *Quarterly Journal of Experimental Physiology,* 6**,** 339-354.

Bryskin, R. B., Londergan, B., Wheatley, R., Heng, R., Lewis, M., Barraza, M., Mercer, E. & Ye, G. 2015. Transversus Abdominis Plane Block Versus Caudal Epidural for Lower Abdominal Surgery in Children: A Double-Blinded Randomized Controlled Trial. *Anesthesia & Analgesia,* 121**,** 471-478.

Burnstock, G., Arnett, T. R. & Orriss, I. R. 2013. Purinergic signalling in the musculoskeletal system. *Purinergic Signalling,* 9**,** 541-572.

Burnstock, G. & Williams, M. 2000. P2 purinergic receptors: modulation of cell function and therapeutic potential. *Journal of Pharmacology and Experimental Therapeutics,* 295**,** 862-869.

Cai, T.-Q., Ren, N., Jin, L., Cheng, K., Kash, S., Chen, R., Wright, S. D., Taggart, A. K. & Waters, M. G. 2008. Role of GPR81 in lactate-mediated reduction of adipose lipolysis. *Biochemical and Biophysical Research Communications,* 377**,** 987-991.

Carrard, A., Elsayed, M., Margineanu, M., Boury-Jamot, B., Fragnière, L., Meylan, E., Petit, J., Fiumelli, H., Magistretti, P. J. & Martin, J. 2016. Peripheral administration of lactate produces antidepressant-like effects. *Molecular Psychiatry,* 23**,** 392–399.

Catterall, W. A., Wisedchaisri, G. & Zheng, N. 2017. The chemical basis for electrical signaling. *Nature Chemical Biology,* 13**,** 455.

Cavanaugh, D. J., Chesler, A. T., Bráz, J. M., Shah, N. M., Julius, D. & Basbaum, A. I. 2011. Restriction of transient receptor potential vanilloid-1 to the peptidergic subset of primary afferent neurons follows its developmental downregulation in nonpeptidergic neurons. *Journal of Neuroscience,* 31**,** 10119-10127.

Chen, B. N., Sharrad, D. F., Hibberd, T. J., Zagorodnyuk, V. P., Costa, M. & Brookes, S. J. H. 2015. Neurochemical characterization of extrinsic nerves in myenteric ganglia of the guinea pig distal colon. *The Journal of Comparative Neurology,* 523**,** 742-756.

Cheung, K., Hume, P. A. & Maxwell, L. 2003. Delayed onset muscle soreness. *Sports Medicine,* 33**,** 145-164.

Cholewicki, J., Juluru, K. & Mcgill, S. M. 1999. Intra-abdominal pressure mechanism for stabilizing the lumbar spine. *Journal of Biomechanics,* 32**,** 13-17.

Clayton, J. A. 2018. Applying the new SABV (sex as a biological variable) policy to research and clinical care. *Physiology & Behavior,* 187**,** 2-5.

Clifford, P. S. & Hellsten, Y. 2004. Vasodilatory mechanisms in contracting skeletal muscle. *Journal of Applied Physiology,* 97**,** 393-403.

Cooper, S. 1961. The responses of the primary and secondary endings of muscle spindles with intact motor innervation during applied stretch. *Quarterly journal of Experimental Physiology and Cognate Medical Sciences,* 46**,** 389-398.

Coote, J. H. & Dodds, W. N. 1976. The baroreceptor reflex and the cardiovascular changes associated with sustained muscular contraction in the cat. *Pflügers Archiv - European Journal of Physiology,* 363**,** 167-173.

Coote, J. H., Hilton, S. M. & Perez-Gonzalez, J. F. 1971. The reflex nature of the pressor response to muscular exercise. *The Journal of Physiology,* 215**,** 789-804.

Corey, D. P. & Holt, J. R. 2016. Are TMCs the Mechanotransduction Channels of Vertebrate Hair Cells? *The Journal of Neuroscience,* 36**,** 10921.

Cui, J., Blaha, C., Moradkhan, R., Gray, K. S. & Sinoway, L. I. 2006. Muscle sympathetic nerve activity responses to dynamic passive muscle stretch in humans. *The Journal of Physiology,* 576**,** 625-634.

Cui, J., Mascarenhas, V., Moradkhan, R., Blaha, C. & Sinoway, L. I. 2008. Effects of muscle metabolites on responses of muscle sympathetic nerve activity to mechanoreceptor (s) stimulation in healthy humans. *American Journal of Physiology-Regulatory, Integrative and Comparative Physiology,* 294**,** R458-R466.

Dahl, R., Larsen, S., Dohlmann, T. L., Qvortrup, K., Helge, J. W., Dela, F. & Prats, C. 2015. Three-dimensional reconstruction of the human skeletal muscle

mitochondrial network as a tool to assess mitochondrial content and structural organization. *Acta Physiologica,* 213**,** 145-155.

Dampney, R. A. 2016. Central neural control of the cardiovascular system: current perspectives. *Advances in Physiology Education,* 40**,** 283-296.

Day, I. N. & Thompson, R. J. 2010. UCHL1 (PGP 9.5): neuronal biomarker and ubiquitin system protein. *Progress in Neurobiology,* 90**,** 327-362.

De La Roche, J., Walther, I., Leonow, W., Hage, A., Eberhardt, M., Fischer, M., Reeh, P. W., Sauer, S. & Leffler, A. 2016. Lactate is a potent inhibitor of the capsaicin receptor TRPV1. *Scientific Reports,* 6**,** 36740.

De Nó, R. L. 1935. The synaptic delay of the motoneurones. *American Journal of Physiology-Legacy Content,* 111**,** 272-282.

Deban, S. M. & Carrier, D. R. 2002. Hypaxial muscle activity during running and breathing in dogs. *Journal of Experimental Biology,* 205**,** 1953-1967.

Dempsey, J. A., Amann, M., Romer, L. M. & Miller, J. D. 2008. Respiratory system determinants of peripheral fatigue and endurance performance. *Medicine & Science in Sports & Exercise,* 40**,** 457-461.

Dempsey, J. A., Blain, G. M. & Amann, M. 2014. Are type III–IV muscle afferents required for a normal steady- state exercise hyperpnoea in humans? *The Journal of physiology,* 592**,** 463-474.

Diehl, B., Hoheisel, U. & Mense, S. 1993. The influence of mechanical stimuli and of acetylsalicylic acid on the discharges of slowly conducting afferent units from normal and inflamed muscle in the rat. *Experimental Brain Research,* 92**,** 431-440.

Dienel, G. A. 2012. Brain lactate metabolism: the discoveries and the controversies. *Journal of Cerebral Blood Flow & Metabolism,* 32**,** 1107-1138.

Djouhri, L. & Lawson, S. N. 2004. Aβ-fiber nociceptive primary afferent neurons: a review of incidence and properties in relation to other afferent A-fiber neurons in mammals. *Brain Research Reviews,* 46**,** 131-145.

Do, M. T. H. & Yau, K.-W. 2010. Intrinsically photosensitive retinal ganglion cells. *Physiological reviews,* 90**,** 1547-1581.

Domènech-Estévez, E., Baloui, H., Repond, C., Rosafio, K., Médard, J.-J., Tricaud, N., Pellerin, L. & Chrast, R. 2015. Distribution of monocarboxylate transporters in the peripheral nervous system suggests putative roles in lactate shuttling and myelination. *Journal of Neuroscience,* 35**,** 4151-4156.

Drew, R. C. 2017. Baroreflex and neurovascular responses to skeletal muscle mechanoreflex activation in humans: an exercise in integrative physiology. *American Journal of Physiology-Regulatory, Integrative and Comparative Physiology,* 313**,** R654-R659.

Duchateau, J., Declety, A. & Lejour, M. 1988. Innervation of the rectus abdominis muscle: implications for rectus flaps. *Plastic and Reconstructive Surgery,* 82**,** 223-227.

Dupuy, O., Douzi, W., Theurot, D., Bosquet, L. & Dugué, B. 2018. An evidence-based approach for choosing post-exercise recovery techniques to reduce markers of muscle damage, soreness, fatigue and inflammation: a systematic review with meta-analysis. *Frontiers in Physiology,* 9**,** 403.

Edström, L. & Kugelberg, E. 1968. Histochemical composition, distribution of fibres and fatiguability of single motor units. Anterior tibial muscle of the rat. *Journal of Neurology, Neurosurgery, and Psychiatry,* 31**,** 424-433.

Eldridge, F. L., Millhorn, D. E., Killey, J. P. & Waldrop, T. G. 1985. Stimulation by central command of locomotion, respiration and circulation during exercise. *Respiration Physiology,* 59**,** 313-337.

Ellrich, J. & Makowska, A. 2007. Nerve growth factor and ATP excite different neck muscle nociceptors in anaesthetized mice. *Cephalalgia,* 27**,** 1226-1235.

Engelstoft, M. S., Park, W.-M., Sakata, I., Kristensen, L. V., Husted, A. S., Osborne-Lawrence, S., Piper, P. K., Walker, A. K., Pedersen, M. H., Nøhr, M. K., Pan, J., Sinz, C. J., Carrington, P. E., Akiyama, T. E., Jones, R. M., Tang, C., Ahmed, K., Offermanns, S., Egerod, K. L., Zigman, J. M. & Schwartz, T. W. 2013. Seven transmembrane G protein-coupled receptor repertoire of gastric ghrelin cells. *Molecular Metabolism,* 2**,** 376-392.

Erlanger, J. & Gasser, H. 1930. The action potential in fibers of slow conduction in spinal roots and somatic nerves. *American Journal of Physiology-Legacy Content,* 92**,** 43-82.

Estrada, J. A. & Kaufman, M. P. 2018. μ-Opioid receptors inhibit the exercise pressor reflex by closing N-type calcium channels but not by opening GIRK channels in rats. *American Journal of Physiology-Regulatory, Integrative and Comparative Physiology,* 314**,** R693-R699.

Fabbretti, E. 2019. P2X3 receptors are transducers of sensory signals. *Brain Research Bulletin,* In Press.

Fadel, P. 2015. Reflex control of the circulation during exercise. *Scandinavian journal of medicine & science in sports,* 25**,** 74-82.

Fadel, P., Ogoh, S., Watenpaugh, D., Wasmund, W., Olivencia-Yurvati, A., Smith, M. & Raven, P. 2001. Carotid baroreflex regulation of sympathetic nerve activity during dynamic exercise in humans. *American Journal of Physiology-Heart and Circulatory Physiology,* 280**,** H1383-H1390.

Falk, E. 2006. Pathogenesis of Atherosclerosis. *Journal of the American College of Cardiology,* 47**,** C7-C12.

Fallon, J., Blevins, F. T., Vogel, K. & Trotter, J. 2002. Functional morphology of the supraspinatus tendon. *Journal of Orthopaedic Research,* 20**,** 920-926.

Feng, B., Joyce, S. C. & Gebhart, G. F. 2016. Optogenetic activation of mechanically insensitive afferents in mouse colorectum reveals chemosensitivity. *American Journal of Physiology-Gastrointestinal and Liver Physiology,* 310**,** G790-G798.

Ferguson, B. S., Rogatzki, M. J., Goodwin, M. L., Kane, D. A., Rightmire, Z. & Gladden, L. B. 2018. Lactate metabolism: historical context, prior misinterpretations, and current understanding. *European Journal of Applied Physiology,* 118**,** 691-728.

Fisher, J. P. 2014. Autonomic control of the heart during exercise in humans: role of skeletal muscle afferents. *Experimental Physiology,* 99**,** 300-305.

Fisher, J. P., Young, C. N. & Fadel, P. J. 2015. Autonomic adjustments to exercise in humans. *Comprehensive Physiology,* 5**,** 475-512.

Fitts, R. H. 1994. Cellular mechanisms of muscle fatigue. *Physiological Reviews,* 74**,** 49-94.

Fletcher, W. M. & Hopkins, F. G. 1907. Lactic Acid in Amphibian Muscle *The Journal of physiology,* 35**,** 247-309.

Fock, S. & Mense, S. 1976. Excitatory effects of 5-hydroxytryptamine, histamine and potassium ions on muscular group IV afferent units: a comparison with bradykinin. *Brain research,* 105**,** 459-469.

Franco, J. A., Kloefkorn, H. E., Hochman, S. & Wilkinson, K. A. 2014. An In Vitro Adult Mouse Muscle-nerve Preparation for Studying the Firing Properties of Muscle Afferents. *Journal of Visualized Experiments: JoVE,* 91**,** e51948.

Franz, M. & Mense, S. 1975. Muscle receptors with group IV afferent fibres responding to application of bradykinin. *Brain research,* 92**,** 369-383.

Frontera, W. R. & Ochala, J. 2015. Skeletal muscle: a brief review of structure and function. *Calcified Tissue International,* 96**,** 183-95.

Fukami, Y. & Wilkinson, R. S. 1977. Responses of isolated Golgi tendon organs of the cat. *The Journal of Physiology,* 265**,** 673-689.

Furness, J., Morris, J., Gibbins, I. & Costa, M. 1989. Chemical coding of neurons and plurichemical transmission. *Annual Review of Pharmacology and Toxicology,* 29**,** 289-306.

Furness, J. B., Costa, M., Morris, J. L. & Gibbins, I. L. 1987. Novel Neurotransmitters and the Chemical Coding of Neurones. *In:* MCLENNAN, H., LEDSOME, J. R., MCINTOSH, C. H. S. & JONES, D. R. (eds.) *Advances in Physiological Research.* Boston, MA: Springer US.

Gadsden, J., Ayad, S., Gonzales, J. J., Mehta, J., Boublik, J. & Hutchins, J. 2015. Evolution of transversus abdominis plane infiltration techniques for postsurgical analgesia following abdominal surgeries. *Local and Regional Anesthesia,* 8**,** 113-117.

Gandevia, S. C. 2001. Spinal and supraspinal factors in human muscle fatigue. *Physiological Reviews,* 81**,** 1725-1789.

Garry, M. G. 2011. Abnormalities of the exercise pressor reflex in heart failure. *Exercise and Sport Sciences Reviews,* 39**,** 167-176.

Gasser, H. & Meek, W. J. 1914. A study of the mechanisms by which muscular exercise produces acceleration of the heart. *American Journal of Physiology-Legacy Content,* 34**,** 48-71.

Gautam, M. & Benson, C. J. 2013. Acid-sensing ion channels (ASICs) in mouse skeletal muscle afferents are heteromers composed of ASIC1a, ASIC2, and ASIC3 subunits. *The FASEB Journal,* 27**,** 793-802.

Ge, H., Weiszmann, J., Reagan, J. D., Gupte, J., Baribault, H., Gyuris, T., Chen, J.-L., Tian, H. & Li, Y. 2008. Elucidation of signaling and functional activities of an orphan GPCR, GPR81. *Journal of Lipid Research,* 49**,** 797-803.

Gibbins, I. L., Furness, J. B. & Costa, M. 1987. Pathway-specific patterns of the co-existence of substance P, calcitonin gene-related peptide, cholecystokinin and dynorphin in neurons of the dorsal root ganglia of the guinea-pig. *Cell and Tissue Research,* 248**,** 417-437.

Gilroy, A. M., Macpherson, B. R., Ross, L. M., SchüNke, M., Schulte, E. & Schumacher, U. 2012. *Atlas of anatomy,* New York, New York : Thieme.

Gladden, L. 2004. Lactate metabolism: a new paradigm for the third millennium. *The Journal of physiology,* 558**,** 5-30.

Goodwin, G., Mccloskey, D. & Mitchell, J. 1972. Cardiovascular and respiratory responses to changes in central command during isometric exercise at constant muscle tension. *The Journal of Physiology,* 226**,** 173-190.

Graven-Nielsen, T. & Arendt-Nielsen, L. 2003. Induction and assessment of muscle pain, referred pain, and muscular hyperalgesia. *Current Pain and Headache Reports,* 7**,** 443-451.

Green, A. L., Wang, S., Owen, S. L. F., Xie, K., Liu, X., Paterson, D. J., Stein, J. F., Bain, P. G. & Aziz, T. Z. 2005. Deep brain stimulation can regulate arterial blood pressure in awake humans. *NeuroReport,* 16**,** 1741-1745.

Gregory, J. E., Morgan, D. L. & Proske, U. 1985. Site of impulse initiation in tendon organs of cat soleus muscle. *Journal of Neurophysiology,* 54**,** 1383-1395.

Gregory, J. E. & Proske, U. 1979. The responses of Golgi tendon organs to stimulation of different combinations of motor units. *The Journal of Physiology,* 295**,** 251-262.

Gregory, N. S., Whitley, P. E. & Sluka, K. A. 2015. Effect of intramuscular protons, lactate, and ATP on muscle hyperalgesia in rats. *PloS one,* 10**,** e0138576.

Greising, S. M., Gransee, H. M., Mantilla, C. B. & Sieck, G. C. 2012. Systems biology of skeletal muscle: fiber type as an organizing principle. *Wiley Interdisciplinary Reviews: Systems Biology Medicine,* 4**,** 457-473.

Grienberger, C. & Konnerth, A. 2012. Imaging Calcium in Neurons. *Neuron,* 73**,** 862-885.

Gründer, S. & Chen, X. 2010. Structure, function, and pharmacology of acid-sensing ion channels (ASICs): focus on ASIC1a. *International Journal of Physiology, Pathophysiology and Pharmacology,* 2**,** 73-94.

Gulick, D. T. & Kimura, I. F. 1996. Delayed onset muscle soreness: what is it and how do we treat it? *Journal of Sport Rehabilitation,* 5**,** 234-243.

Güner, M. C., Göz, R., Berber, I., Kaspar, C. & Çakır, Ü. 2015. Ultrasound/Laparoscopic Camera-Guided Transversus Abdominis Plane Block for Renal Transplant Donors: A Randomized Controlled Trial. *Annals of Transplantation,* 20**,** 418-423.

Guo, J., Li, L., Gong, Y., Zhu, R., Xu, J., Zou, J. & Chen, X. 2017. Massage alleviates delayed onset muscle soreness after strenuous exercise: a systematic review and meta-analysis. *Frontiers in Physiology,* 8**,** 747.

Halestrap, A. P. 2013. The SLC16 gene family–structure, role and regulation in health and disease. *Molecular Aspects of Medicine,* 34**,** 337-349.

Hall, M. M., Rajasekaran, S., Thomsen, T. W. & Peterson, A. R. 2016. Lactate: friend or foe. *PM&R,* 8**,** S8-S15.

Hama, H., Hioki, H., Namiki, K., Hoshida, T., Kurokawa, H., Ishidate, F., Kaneko, T., Akagi, T., Saito, T., Saido, T. & Miyawaki, A. 2015. ScaleS: an optical clearing palette for biological imaging. *Nature Neuroscience,* 18**,** 1518.

Han, W., Tellez, L. A., Perkins, M. H., Perez, I. O., Qu, T., Ferreira, J., Ferreira, T. L., Quinn, D., Liu, Z.-W. & Gao, X.-B. 2018. A neural circuit for gut-induced reward. *Cell,* 175**,** 665-678. e23.

Haouzi, P., Chenuel, B. & Huszczuk, A. 2004. Sensing vascular distension in skeletal muscle by slow conducting afferent fibers: neurophysiological basis and implication for respiratory control. *Journal of Applied Physiology,* 96**,** 407-418.

Haouzi, P., Hill, J. M., Lewis, B. K. & Kaufman, M. P. 1999. Responses of group III and IV muscle afferents to distension of the peripheral vascular bed. *Journal of Applied Physiology,* 87**,** 545-553.

Harding, S. D., Sharman, J. L., Faccenda, E., Southan, C., Pawson, A. J., Ireland, S., Gray, A. J. G., Bruce, L., Alexander, S. P. H., Anderton, S., Bryant, C., Davenport, A. P., Doerig, C., Fabbro, D., Levi-Schaffer, F., Spedding, M., Davies, J. A. & Nc, I. 2017. The IUPHAR/BPS Guide to PHARMACOLOGY in 2018: updates and expansion to encompass the new guide to IMMUNOPHARMACOLOGY. *Nucleic Acids Research,* 46**,** D1091-D1106.

Harms, J. E., Stone, A. J. & Kaufman, M. P. 2018. Peripheral Mu-Opioid receptors Attenuate the Responses of Group III and IV Afferents to Contraction in Rats with Simulated Peripheral Artery Disease. *Journal of Neurophysiology,* 119**,** 2052-2058.

Hasegawa, K., Okui, T., Shimo, T., Ibaragi, S., Kawai, H., Ryumon, S., Kishimoto, K., Okusha, Y., Monsur Hassan, N. & Sasaki, A. 2018. Lactate Transporter Monocarboxylate Transporter 4 Induces Bone Pain in Head and Neck Squamous Cell Carcinoma. *International Journal of Molecular Sciences,* 19**,** 3317.

Hatt, H. 2004. Molecular and Cellular Basis of Human Olfaction. *Chemistry & Biodiversity,* 1**,** 1857-1869.

Hayashi, K., Katanosaka, K., Abe, M., Yamanaka, A., Nosaka, K., Mizumura, K. & Taguchi, T. 2017. Muscular mechanical hyperalgesia after lengthening contractions in rats depends on stretch velocity and range of motion. *European Journal of Pain,* 21**,** 125-139.

Hayes, S. G. & Kaufman, M. P. 2001. Gadolinium attenuates exercise pressor reflex in cats. *American Journal of Physiology-Heart and Circulatory Physiology,* 280**,** H2153-H2161.

Hayes, S. G., Kindig, A. E. & Kaufman, M. P. 2005. Comparison between the effect of static contraction and tendon stretch on the discharge of group III and IV muscle afferents. *Journal of Applied Physiology,* 99**,** 1891-1896.

Hayes, S. G., Mccord, J. L., Koba, S. & Kaufman, M. P. 2009. Gadolinium inhibits group III but not group IV muscle afferent responses to dynamic exercise. *The Journal of Physiology,* 587**,** 873-882.

Hearon Jr, C. M. & Dinenno, F. A. 2016. Regulation of skeletal muscle blood flow during exercise in ageing humans. *The Journal of physiology,* 594**,** 2261-2273.

Hertz, L. 2004. The Astrocyte-Neuron Lactate Shuttle: A Challenge of a Challenge. *Journal of Cerebral Blood Flow & Metabolism,* 24**,** 1241-1248.

Hikida, R. S., Staron, R. S., Hagerman, F. C., Sherman, W. M. & Costill, D. L. 1983. Muscle fiber necrosis associated with human marathon runners. *Journal of the Neurological Sciences,* 59**,** 185-203.

Hilger, D., Masureel, M. & Kobilka, B. K. 2018. Structure and dynamics of GPCR signaling complexes. *Nature Structural & Molecular Biology,* 25**,** 4-12.

Hille, B. 2001. *Ionic channels of excitable membranes (3rd ed.),* Sunderland, MA, Sinauer Associates.

Hinsey, J. C. 1927. Some observations on the innervation of skeletal muscle of the cat. *Journal of Comparative Neurology,* 44**,** 87-195.

Hockley, J. R. F., Taylor, T. S., Callejo, G., Wilbrey, A. L., Gutteridge, A., Bach, K., Winchester, W. J., Bulmer, D. C., Mcmurray, G. & Smith, E. S. J. 2018. Single-cell RNAseq reveals seven classes of colonic sensory neuron. *Gut***,** 1-12.

Hoffman, B. U., Baba, Y., Griffith, T. N., Mosharov, E. V., Woo, S.-H., Roybal, D. D., Karsenty, G., Patapoutian, A., Sulzer, D. & Lumpkin, E. A. 2018. Merkel Cells Activate Sensory Neural Pathways through Adrenergic Synapses. *Neuron,* 100**,** 1401-1413.e6.

Hoffmann, S., Ramm, J., Grittner, U., Kohler, S., Siedler, J. & Meisel, A. 2016. Fatigue in myasthenia gravis: risk factors and impact on quality of life. *Brain and Behavior,* 6**,** e00538-e00538.

Hogg, R. C., Buisson, B. & Bertrand, D. 2005. Allosteric modulation of ligand-gated ion channels. *Biochemical Pharmacology,* 70**,** 1267-1276.

Hoheisel, U., Reinöhl, J., Unger, T. & Mense, S. 2004. Acidic pH and capsaicin activate mechanosensitive group IV muscle receptors in the rat. *Pain,* 110**,** 149-157.

Hoheisel, U., Unger, T. & Mense, S. 2005. Excitatory and modulatory effects of inflammatory cytokines and neurotrophins on mechanosensitive group IV muscle afferents in the rat. *Pain,* 114**,** 168-176.

Holgate, S. T., Komaroff, A. L., Mangan, D. & Wessely, S. 2011. Chronic fatigue syndrome: understanding a complex illness. *Nature Reviews Neuroscience,* 12**,** 539.

Hough, T. 1902. Ergographic studies in muscular fatigue and soreness. *Journal of the Boston Society of Medical Sciences,* 5**,** 81.

Houk, J. & Henneman, E. 1967a. Feedback control of skeletal muscles. *Brain research,* 5**,** 433-451.

Houk, J. & Henneman, E. 1967b. Responses of Golgi tendon organs to active contractions of the soleus muscle of the cat. *Journal of Neurophysiology,* 30**,** 466-481

Hudspeth, A. J. 2014. Integrating the active process of hair cells with cochlear function. *Nature Reviews Neuroscience,* 15**,** 600.

Hunt, C. C. & Wilkinson, R. S. 1980. An analysis of receptor potential and tension of isolated cat muscle spindles in response to sinusoidal stretch. *The Journal of physiology,* 302**,** 241-262.

Hunt, C. C., Wilkinson, R. S. & Fukami, Y. 1978. Ionic basis of the receptor potential in primary endings of mammalian muscle spindles. *The Journal of General Physiology,* 71**,** 683.

Hureau, T. J., Weavil, J. C., Thurston, T. S., Broxterman, R. M., Nelson, A. D., Bledsoe, A. D., Jessop, J. E., Richardson, R. S., Wray, D. W. & Amann, M. 2018. Identifying the role of group III/IV muscle afferents in the carotid baroreflex control of mean arterial pressure and heart rate during exercise. *The Journal of physiology,* 596**,** 1373-1384.

Husmark, I. & Ottoson, D. 1971. Ionic effects on spindle adaptation. *The Journal of physiology,* 218**,** 257-269.

Huxley, A. F. & Niedergerke, R. 1954. Structural Changes in Muscle During Contraction: Interference Microscopy of Living Muscle Fibres. *Nature,* 173**,** 971.

Huxley, H. & Hanson, J. 1954. Changes in the Cross-Striations of Muscle during Contraction and Stretch and their Structural Interpretation. *Nature,* 173**,** 973-976.

Iggo, A. 1960. Cutaneous mechanoreceptors with afferent C fibres. *The Journal of Physiology,* 152**,** 337-353.

Iggo, A. & Andres, K. H. 1982. Morphology of cutaneous receptors. *Annual Review of Neuroscience,* 5**,** 1-31.

Iggo, A. & Muir, A. R. 1969. The structure and function of a slowly adapting touch corpuscle in hairy skin. *The Journal of physiology,* 200**,** 763-796.

Ikeda, R., Cha, M., Ling, J., Jia, Z., Coyle, D. & Gu, Jianguo g. 2014. Merkel Cells Transduce and Encode Tactile Stimuli to Drive Aβ-Afferent Impulses. *Cell,* 157**,** 664-675.

Immke, D. & Mc Cleskey, E. 2001. Lactate enhances the acid-sensing Na+ channel on ischemia-sensing neurons. *Nature neuroscience,* 4**,** 869-870.

Ives, S. J., Amann, M., Venturelli, M., Witman, M. A., Groot, H. J., Wray, D. W., Morgan, D. E., Stehlik, J. & Richardson, R. S. 2016. The mechanoreflex and hemodynamic response to passive leg movement in heart failure. *Medicine & Science in Sports & Exercise,* 48**,** 368-376.

Iwamoto, G., Waldrop, T., Kaufman, M., Botterman, B., Rybicki, K. & Mitchell, J. 1985. Pressor reflex evoked by muscular contraction: contributions by neuraxis levels. *Journal of Applied Physiology,* 59**,** 459-467.

Iwamoto, G. A., Mitchell, J. H., Mizuno, M. & Secher, N. H. 1987. Cardiovascular responses at the onset of exercise with partial neuromuscular blockade in cat and man. *The Journal of Physiology,* 384**,** 39-47.

Iyer, S. M., Montgomery, K. L., Towne, C., Lee, S. Y., Ramakrishnan, C., Deisseroth, K. & Delp, S. L. 2014. Virally mediated optogenetic excitation and inhibition of pain in freely moving nontransgenic mice. *Nature Biotechnology,* 32**,** 274.

Jami, L. 1992. Golgi tendon organs in mammalian skeletal muscle: functional properties and central actions. *Physiological Reviews,* 72**,** 623-666.

Jankowski, M. P., Rau, K. K., Ekmann, K. M., Anderson, C. E. & Koerber, H. R. 2013. Comprehensive phenotyping of group III and IV muscle afferents in mouse. *Journal of Neurophysiology,* 109**,** 2374-2381.

Jansen, J. & Matthews, P. 1962. The central control of the dynamic response of muscle spindle receptors. *The Journal of Physiology,* 161**,** 357-378.

Johnston, S. C., Staines, D. R. & Marshall-Gradisnik, S. M. 2016. Epidemiological characteristics of chronic fatigue syndrome/myalgic encephalomyelitis in Australian patients. *Clinical Epidemiology,* 17**,** 97-107.

Julius, D. & Nathans, J. 2012. Signaling by sensory receptors. *Cold Spring Habor Perspectives in Biology,* 4**,** a005991.

Junyent, F. & Kremer, E. J. 2015. CAV-2—why a canine virus is a neurobiologist's best friend. *Current Opinion in Pharmacology,* 24**,** 86-93.

Kaufman, M., Rybicki, K. J., Waldrop, T. G. & Ordway, G. A. 1984. Effect of ischemia on responses of group III and IV afferents to contraction. *Journal of Applied Physiology: Respiratory, Environmental, and Exercise Physiology,* 57**,** 644-650.

Kaufman, M. P. 2012. The exercise pressor reflex in animals. *Experimental physiology,* 97**,** 51-58.

Kaufman, M. P. & Hayes, S. G. 2002. The Exercise Pressor Reflex. *Clinical Autonomic Research,* 12**,** 429-439.

Kaufman, M. P., Hayes, S. G., Adreani, C. M. & Pickar, J. G. 2002. Discharge properties of group III and IV muscle afferents. *In:* GANDEVIA S.C., P. U., STUART D.G. (ed.) *Sensorimotor Control of Movement and Posture. Advances in Experimental Medicine and Biology.* Springer, Boston, MA.

Kaufman, M. P., Iwamoto, G. A., Longhurst, J. C. & Mitchell, J. H. 1982. Effects of capsaicin and bradykinin on afferent fibers with ending in skeletal muscle. *Circulation Research,* 50**,** 133-139.

Kaufman, M. P., Longhurst, J. C., Rybicki, K. J., Wallach, J. H. & Mitchell, J. H. 1983. Effects of static muscular contraction on impulse activity of groups III and IV afferents in cats. *Journal of Applied Physiology: Respiratory, Environmental, and Exercise Physiology,* 55**,** 105-112.

Kaufman, M. P., Rotto, D. M. & Rybicki, K. J. 1988. Pressor reflex response to static muscular contraction: its afferent arm and possible neurotransmitters. *The American Journal of Cardiology,* 62**,** 58E-62E.

Kaufman, M. P. & Rybicki, K. J. 1987. Discharge properties of group III and IV muscle afferents: their responses to mechanical and metabolic stimuli. *Circulation Research,* 61**,** I60-5.

Kestell, G. R., Anderson, R. L., Clarke, J. N., Haberberger, R. V. & Gibbins, I. L. 2015. Primary afferent neurons containing calcitonin gene- related peptide but not substance P in forepaw skin, dorsal root ganglia, and spinal cord of mice. *Journal of Comparative Neurology,* 523**,** 2555-2569.

Knellwolf, T. P., Burton, A. R., Hammam, E. & Macefield, V. G. 2019. Firing properties of muscle spindles supplying the intrinsic foot muscles of humans in unloaded and freestanding conditions. *Journal of Neurophysiology,* 121**,** 74-84.

Knežević, O. & Mirkov, D. 2013. Trunk muscle activation patterns in subjects with low back pain. *Vojnosanitetski pregled,* 70**,** 315-318.

Kniffki, K., Mense, S. & Schmidt, R. 1978. Responses of group IV afferent units from skeletal muscle to stretch, contraction and chemical stimulation. *Experimental Brain Research,* 31**,** 511-522.

Kniffki, K.-D., Schomburg, E. & Steffens, H. 1981. Synaptic effects from chemically activated fine muscle afferents upon α-motoneurones in decerebrate and spinal cats. *Brain research,* 206**,** 361-370.

Krogh, A. & Lindhard, J. 1913. The regulation of respiration and circulation during the initial stages of muscular work. *The Journal of physiology,* 47**,** 112-136.

Kumazawa, T. & Mizumura, K. 1977. Thin-fibre receptors responding to mechanical, chemical, and thermal stimulation in the skeletal muscle of the dog. *The Journal of Physiology,* 273**,** 179.

Kumka, M. & Bonar, J. 2012. Fascia: a morphological description and classification system based on a literature review. *The Journal of the Canadian Chiropractic Association,* 56**,** 179-191.

Kurima, K., Peters, L. M., Yang, Y., Riazuddin, S., Ahmed, Z. M., Naz, S., Arnaud, D., Drury, S., Mo, J., Makishima, T., Ghosh, M., Menon, P. S. N., Deshmukh, D., Oddoux, C., Ostrer, H., Khan, S., Riazuddin, S., Deininger, P. L., Hampton, L. L., Sullivan, S. L., Battey Jr, J. F., Keats, B. J. B., Wilcox, E. R., Friedman, T. B. & Griffith, A. J. 2002. Dominant and recessive deafness caused by mutations of a novel gene, TMC1, required for cochlear hair-cell function. *Nature Genetics,* 30**,** 277.

Kyloh, M. & Spencer, N. 2014. A novel anterograde neuronal tracing technique to selectively label spinal afferent nerve endings that encode noxious and innocuous stimuli in visceral organs. *Neurogastroenterology & Motility,* 26**,** 440-444.

Laframboise, W. A., Daood, M. J., Guthrie, R. D., Moretti, P., Schiaffino, S. & Ontell, M. 1990. Electrophoretic separation and immunological identification of type 2X myosin heavy chain in rat skeletal muscle. *Biochimica et Biophysica Acta (BBA) - General Subjects,* 1035**,** 109-112.

Lafzi, A., Moutinho, C., Picelli, S. & Heyn, H. 2018. Tutorial: guidelines for the experimental design of single-cell RNA sequencing studies. *Nature Protocols,* 13**,** 2742-2757.

Lamboley, C. R., Murphy, R. M., Mckenna, M. J. & Lamb, G. D. 2014. Sarcoplasmic reticulum Ca2+ uptake and leak properties, and SERCA isoform expression, in type I and type II fibres of human skeletal muscle. *The Journal of physiology,* 592**,** 1381-1395.

Larsson, L., Edstrom, L., Lindegren, B., Gorza, L. & Schiaffino, S. 1991. MHC composition and enzyme-histochemical and physiological properties of a novel fast-twitch motor unit type. *American Journal of Physiology-Cell Physiology,* 261**,** C93-C101.

Laurin, J., Pertici, V., Dousset, E., Marqueste, T. & Decherchi, P. 2015. Group III and IV muscle afferents: Role on central motor drive and clinical implications. *Neuroscience,* 290**,** 543-551.

Lauritzen, K. H., Morland, C., Puchades, M., Holm-Hansen, S., Hagelin, E. M., Lauritzen, F., Attramadal, H., Storm-Mathisen, J., Gjedde, A. & Bergersen, L. H. 2014. Lactate receptor sites link neurotransmission, neurovascular coupling, and brain energy metabolism. *Cerebral cortex,* 24**,** 2784-2795.

Lawson, S. 2002. Phenotype and Function of Somatic Primary Afferent Nociceptive Neurones with C- , Aδ- or Aα/β- Fibres. *Experimental physiology,* 87**,** 239-244.

Lawson, S. N. 1992. Morphological and biochemical cell types of sensory neurons. *Sensory neurons: diversity, development and plasticity*. *Oxford University Press, New York***,** 27-59.

Le Pichon, C. E. & Chesler, A. T. 2014. The functional and anatomical dissection of somatosensory subpopulations using mouse genetics. *Frontiers in Neuroanatomy,* 8**,** 21.1-18.

Leal, A. K., Williams, M. A., Garry, M. G., Mitchell, J. H. & Smith, S. A. 2008. Evidence for functional alterations in the skeletal muscle mechanoreflex and metaboreflex in hypertensive rats. *American Journal of Physiology-Heart and Circulatory Physiology,* 295**,** H1429-H1438.

Lee, D. K., Nguyen, T., Lynch, K. R., Cheng, R., Vanti, W. B., Arkhitko, O., Lewis, T., Evans, J. F., George, S. R. & O'dowd, B. F. 2001. Discovery and mapping of ten novel G protein-coupled receptor genes. *Gene,* 275**,** 83-91.

Lewis, T. 1926. The Blood Vessels of the Human Skin. *British Medical Journal,* 2**,** 61-62.

Li, C.-L., Li, K.-C., Wu, D., Chen, Y., Luo, H., Zhao, J.-R., Wang, S.-S., Sun, M.-M., Lu, Y.-J., Zhong, Y.-Q., Hu, X.-Y., Hou, R., Zhou, B.-B., Bao, L., Xiao, H.-S. & Zhang, X. 2015. Somatosensory neuron types identified by high-coverage single-cell RNA-sequencing and functional heterogeneity. *Cell Research,* 26**,** 83.

Liddell, E. G. T. & Sherrington, C. 1924. Reflexes in response to stretch (myotatic reflexes). *Proceedings of the Royal Society of London. Series B, Containing Papers of a Biological Character,* 96**,** 212-242.

Light, A. R., Hughen, R. W., Zhang, J., Rainier, J., Liu, Z. & Lee, J. 2008. Dorsal root ganglion neurons innervating skeletal muscle respond to physiological combinations of protons, ATP, and lactate mediated by ASIC, P2X, and TRPV1. *Journal of Neurophysiology,* 100**,** 1184-1201.

Light, A. R. & Perl, E. R. 2003. Unmyelinated afferent fibers are not only for pain anymore. *Journal of Comparative Neurology,* 461**,** 137-9.

Light, N. & Champion, A. E. 1984. Characterization of muscle epimysium, perimysium and endomysium collagens. *Biochemical Journal,* 219**,** 1017-1026.

Liu, C., Kuei, C., Zhu, J., Yu, J., Zhang, L., Shih, A., Mirzadegan, T., Shelton, J., Sutton, S. & Connelly, M. A. 2012. 3, 5-Dihydroxybenzoic acid, a specific agonist for hydroxycarboxylic acid 1, inhibits lipolysis in adipocytes. *Journal of Pharmacology and Experimental Therapeutics,* 341**,** 794-801.

Liu, C., Wu, J., Zhu, J., Kuei, C., Yu, J., Shelton, J., Sutton, S. W., Li, X., Yun, S. J. & Mirzadegan, T. 2009. Lactate inhibits lipolysis in fat cells through activation

of an orphan G-protein-coupled receptor, GPR81. *Journal of Biological Chemistry,* 284**,** 2811-2822.

Lloyd, D. P. 1943a. Conduction and synaptic transmission of the reflex response to stretch in spinal cats. *Journal of Neurophysiology,* 6**,** 317-326.

Lloyd, D. P. 1943b. Neuron patterns controlling transmission of ipsilateral hind limb reflexes in cat. *Journal of Neurophysiology,* 6**,** 293-315.

Loeb, G. E. & Mileusnic, M. 2016. Proprioceptors and Models of Transduction. *Scholarpedia of Touch.* Springer.

Longden, T. A., Dabertrand, F., Koide, M., Gonzales, A. L., Tykocki, N. R., Brayden, J. E., Hill-Eubanks, D. & Nelson, M. T. 2017. Capillary K+-sensing initiates retrograde hyperpolarization to increase local cerebral blood flow. *Nature Neuroscience,* 20**,** 717.

Lucia, A., Nogales-Gadea, G., Pérez, M., Martín, M. A., Andreu, A. L. & Arenas, J. 2008. McArdle disease: what do neurologists need to know? *Nature Clinical Practice Neurology,* 4**,** 568.

Lynn, P. A. & Brookes, S. J. 2011a. Function and morphology correlates of rectal nerve mechanoreceptors innervating the guinea pig internal anal sphincter. *Neurogastroenterology & Motility,* 23**,** 88-e9.

Lynn, P. A. & Brookes, S. J. 2011b. Pudendal afferent innervation of the guinea pig external anal sphincter. *Neurogastroenterology & Motility,* 23**,** 871-e343.

Lynn, P. A., Olsson, C., Zagorodnyuk, V., Costa, M. & Brookes, S. J. 2003. Rectal intraganglionic laminar endings are transduction sites of extrinsic mechanoreceptors in the guinea pig rectum. *Gastroenterology,* 125**,** 786-94.

Lynn, P. A., Zagorodnyuk, V., Hennig, G., Costa, M. & Brookes, S. 2005. Mechanical activation of rectal intraganglionic laminar endings in the guinea pig distal gut. *Journal of Physiology,* 564**,** 589-601.

Macefield, V. G. & Knellwolf, T. P. 2018. Functional properties of human muscle spindles. *Journal of Neurophysiology,* 120**,** 452-467.

Magistretti, P. J. & Allaman, I. 2018. Lactate in the brain: from metabolic end-product to signalling molecule. *Nature Reviews Neuroscience,* 19**,** 235-249.

Maksimovic, S., Nakatani, M., Baba, Y., Nelson, A. M., Marshall, K. L., Wellnitz, S. A., Firozi, P., Woo, S.-H., Ranade, S., Patapoutian, A. & Lumpkin, E. A. 2014. Epidermal Merkel cells are mechanosensory cells that tune mammalian touch receptors. *Nature,* 509**,** 617.

Manvich, D. F., Webster, K. A., Foster, S. L., Farrell, M. S., Ritchie, J. C., Porter, J. H. & Weinshenker, D. 2018. The DREADD agonist clozapine N-oxide (CNO) is reverse-metabolized to clozapine and produces clozapine-like interoceptive stimulus effects in rats and mice. *Scientific Reports,* 8**,** 3840. 1- 10.

Margaria, R., Edwards, H. & Dill, D. B. 1933. The possible mechanisms of contracting and paying the oxygen debt and the role of lactic acid in muscular contraction. *American Journal of Physiology-Legacy Content,* 106**,** 689-715.

Martell, A. 1977. *Other Organic Ligands*, Springer US.

Martin, V., Dousset, E., Laurin, J., Gondin, J., Gautier, M. & Decherchi, P. 2009. Group III and IV muscle afferent discharge patterns after repeated lengthening and shortening actions. *Muscle & Nerve,* 40**,** 827-837.

Masani, K., Sin, V. W., Vette, A. H., Thrasher, T. A., Kawashima, N., Morris, A., Preuss, R. & Popovic, M. R. 2009. Postural reactions of the trunk muscles to multi-directional perturbations in sitting. *Clinical Biomechanics (Bristol, Avon),* 24**,** 176-82.

Matthews, B. H. C. 1933. Nerve endings in mammalian muscle. *The Journal of Physiology,* 78**,** 1-53.

Matthews, P. 1964. Muscle spindles and their motor control. *Physiological Reviews,* 44**,** 219-288.

Matthews, P. B. 2015. Where Anatomy led, Physiology followed: a survey of our developing understanding of the muscle spindle, what it does and how it works. *Journal of Anatomy,* 227**,** 104-114.

Mccloskey, D. & Mitchell, J. 1972. Reflex cardiovascular and respiratory responses originating in exercising muscle. *The Journal of Physiology,* 224**,** 173.

Mcgill, S. & Norman, R. 1986. 1986 Volvo Award in Biomechanics: Partitioning of the L4-L5 Dynamic Moment into Disc, Ligamentous, and Muscular Components During Lifting. *Spine,* 11**,** 666-678.

Mcmahon, S. B. & Koltzenburg, M. 2006. *Wall & Melzack's Textbook of Pain*, Elsevier.

Mense, S. 1977. Nervous outflow from skeletal muscle following chemical noxious stimulation. *The Journal of Physiology,* 267**,** 75.

Mense, S. 1981. Sensitization of group IV muscle receptors to bradykinin by 5-hydroxytryptamine and prostaglandin E 2. *Brain research,* 225**,** 95-105.

Mense, S. 1993. Nociception from skeletal muscle in relation to clinical muscle pain. *Pain,* 54**,** 241-289.

Mense, S. 1996. Group III and IV receptors in skeletal muscle: are they specific or polymodal? *In:* T. KUMAZAWA, L. K., AND K. MIZUMURA (ed.) *The Polymodal Pathological Pain Receptor—A Gateway to Pathological Pain.* Progress in Brain Research.

Mense, S. 1997. Activity in nociceptive primary afferent fibers and clinical muscle pain. *Pain Forum,* 6**,** 213-216.

Mense, S. 2009. Algesic agents exciting muscle nociceptors. *Exp Brain Res,* 196**,** 89-100.

Mense, S. & Craig Jr, A. 1988. Spinal and supraspinal terminations of primary afferent fibers from the gastrocnemius-soleus muscle in the cat. *Neuroscience,* 26**,** 1023-1035.

Mense, S. & Gerwin, R. D. 2010. *Muscle pain: understanding the mechanisms*, Springer Science & Business Media.

Mense, S. & Meyer, H. 1985. Different types of slowly conducting afferent units in cat skeletal muscle and tendon. *The Journal of Physiology,* 363**,** 403-417.

Mense, S. & Schiltenwolf, M. 2010. Fatigue and pain; what is the connection? *Pain,* 148**,** 177-8.

Mense, S. & Schmidt, R. F. 1974. Activation of group IV afferent units from muscle by algesic agents. *Brain research,* 72**,** 305-310.

Mense, S. & Stahnke, M. 1983. Responses in muscle afferent fibres of slow conduction velocity to contractions and ischaemia in the cat. *Journal of Physiology,* 342**,** 383-397.

Merton, P. A. 1951. The silent period in a muscle of the human hand. *The Journal of physiology,* 114**,** 183-198.

Messlinger, K. 1996. Chapter 17. Functional morphology of nociceptive and other fine sensory endings (free nerve endings) in different tissues. *In:* KUMAZAWA, T., KRUGER, L. & MIZUMURA, K. (eds.) *Progress in Brain Research.* Elsevier.

Michelini, L. C., O'leary, D. S., Raven, P. B. & Nóbrega, A. C. 2015. Neural control of circulation and exercise: a translational approach disclosing interactions between central command, arterial baroreflex, and muscle metaboreflex. *American Journal of Physiology-Heart and Circulatory Physiology,* 309**,** H381-H392.

Mickle, A. D. & Gereau, R. W. I. 2018. A bright future? Optogenetics in the periphery for pain research and therapy. *PAIN,* 159**,** S65-S73.

Mileusnic, M. P. & Loeb, G. E. 2006. Mathematical Models of Proprioceptors. II. Structure and Function of the Golgi Tendon Organ. *Journal of Neurophysiology,* 96**,** 1789-1802.

Mitchell, J. H. 1990. J.B. Wolffe memorial lecture. Neural control of the circulation during exercise. *Medicine & Science in Sports & Exercise,* 22.

Mitchell, J. H. 2012. Neural control of the circulation during exercise: insights from the 1970–1971 Oxford studies. *Experimental Physiology,* 97**,** 14-19.

Mitchell, J. H. 2017. 2015 Ludwig Lecture. Abnormal Cardiovascular Responses to Exercise in Hypertension: Contribution of Neural factors. *American Journal of Physiology-Regulatory, Integrative and Comparative Physiology***,** ajpregu. 00042.2017.

Mizumura, K. & Taguchi, T. 2016. Delayed onset muscle soreness: Involvement of neurotrophic factors. *The Journal of Physiological Sciences,* 66**,** 43-52.

Mizuno, M., Murphy, M. N., Mitchell, J. H. & Smith, S. A. 2011. Antagonism of the TRPv1 receptor partially corrects muscle metaboreflex overactivity in spontaneously hypertensive rats. *The Journal of Physiology,* 589**,** 6191-6204.

Molliver, D. C., Immke, D. C., Fierro, L., Paré, M., Rice, F. L. & Mccleskey, E. W. 2005. ASIC3, an acid-sensing ion channel, is expressed in metaboreceptive sensory neurons. *Molecular pain,* 1**,** 35.

Montgomery, K. L., Yeh, A. J., Ho, J. S., Tsao, V., Mohan Iyer, S., Grosenick, L., Ferenczi, E. A., Tanabe, Y., Deisseroth, K., Delp, S. L. & Poon, A. S. Y. 2015. Wirelessly powered, fully internal optogenetics for brain, spinal and peripheral circuits in mice. *Nature Methods,* 12**,** 969.

Morland, C., Andersson, K. A., Haugen, Ø. P., Hadzic, A., Kleppa, L., Gille, A., Rinholm, J. E., Palibrk, V., Diget, E. H., Kennedy, L. H., Stølen, T., Hennestad, E., Moldestad, O., Cai, Y., Puchades, M., Offermanns, S., Vervaeke, K., Bjørås, M., Wisløff, U., Storm-Mathisen, J. & Bergersen, L. H. 2017. Exercise induces cerebral VEGF and angiogenesis via the lactate receptor HCAR1. *Nature Communications,* 8**,** 15557.

Morland, C., Lauritzen, K. H., Puchades, M., Holm- Hansen, S., Andersson, K., Gjedde, A., Attramadal, H., Storm- Mathisen, J. & Bergersen, L. H. 2015. The lactate receptor, G- protein- coupled receptor 81/hydroxycarboxylic acid receptor 1: Expression and action in brain. *Journal of Neuroscience Research,* 93**,** 1045-1055.

Mosienko, V., Teschemacher, A. G. & Kasparov, S. 2015. Is L-lactate a novel signaling molecule in the brain? *Journal of Cerebral Blood Flow & Metabolism,* 35**,** 1069-1075.

Mountcastle, V. B., Talbot, W. H., Darian-Smith, I. & Kornhuber, H. H. 1967. Neural basis of the sense of flutter-vibration. *Science,* 155**,** 597-600.

Murase, S., Kato, K., Taguchi, T. & Mizumura, K. 2014. Glial cell line- derived neurotrophic factor sensitized the mechanical response of muscular thin-fibre afferents in rats. *European Journal of Pain,* 18**,** 629-638.

Murase, S., Terazawa, E., Queme, F., Ota, H., Matsuda, T., Hirate, K., Kozaki, Y., Katanosaka, K., Taguchi, T. & Urai, H. 2010. Bradykinin and nerve growth factor play pivotal roles in muscular mechanical hyperalgesia after exercise (delayed-onset muscle soreness). *Journal of Neuroscience,* 30**,** 3752-3761.

Murphy, M. N., Mizuno, M., Mitchell, J. H. & Smith, S. A. 2011. Cardiovascular regulation by skeletal muscle reflexes in health and disease. *American Journal of Physiology-Heart and Circulatory Physiology,* 301**,** H1191-H1204.

Nalbandian, M. & Takeda, M. 2016. Lactate as a signaling molecule that regulates exercise-induced adaptations. *Biology,* 5**,** 38.

Naves, L. & Mccleskey, E. 2005. An acid-sensing ion channel that detects ischemic pain. *Brazilian Journal of Medical and Biological Research,* 38**,** 1561-1569.

Needham, D. M. 1926. RED AND WHITE MUSCLE. *Physiological Reviews,* 6**,** 1-27.

Newham, D. 1988. The consequences of eccentric contractions and their relationship to delayed onset muscle pain. *European journal of applied physiology and occupational physiology,* 57**,** 353-359.

Newham, D. J., Mcphail, G., Mills, K. R. & Edwards, R. H. T. 1983. Ultrastructural changes after concentric and eccentric contractions of human muscle. *Journal of the Neurological Sciences,* 61**,** 109-122.

Nitatori, T. 1988. The fine structure of human Golgi tendon organs as studied by three-dimensional reconstruction. *Journal of Neurocytology,* 17**,** 27-41.

Offermanns, S. 2017. Hydroxy-carboxylic acid receptor actions in metabolism. *Trends in Endocrinology & Metabolism,* 28**,** 227-236.

Offermanns, S., Colletti, S. L., Lovenberg, T. W., Semple, G., Wise, A. & Ijzerman, A. P. 2011. International Union of Basic and Clinical Pharmacology. LXXXII: nomenclature and classification of hydroxy-carboxylic acid receptors (GPR81, GPR109A, and GPR109B). *Pharmacological Reviews***,** pr. 110.003301.

Olson, T. P., Joyner, M. J. & Johnson, B. D. 2010. Influence of locomotor muscle metaboreceptor stimulation on the ventilatory response to exercise in heart failure. *Circulation Heart Failure,* 3**,** 212-219.

Ordway, G. A. & Garry, D. J. 2004. Myoglobin: an essential hemoprotein in striated muscle. *Journal of Experimental Biology,* 207**,** 3441.

Ottenheijm, C. a. C. & Granzier, H. 2010. Lifting the Nebula: Novel Insights into Skeletal Muscle Contractility. *Physiology,* 25**,** 304-310.

Paintal, A. 1960. Functional analysis of group III afferent fibres of mammalian muscles. *The Journal of Physiology,* 152**,** 250.

Pan, B., Akyuz, N., Liu, X.-P., Asai, Y., Nist-Lund, C., Kurima, K., Derfler, B. H., György, B., Limapichat, W., Walujkar, S., Wimalasena, L. N., Sotomayor, M., Corey, D. P. & Holt, J. R. 2018. TMC1 Forms the Pore of Mechanosensory Transduction Channels in Vertebrate Inner Ear Hair Cells. *Neuron,* 99**,** 736-753.e6.

Papelier, Y., Escourrou, P., Gauthier, J. & Rowell, L. 1994. Carotid baroreflex control of blood pressure and heart rate in men during dynamic exercise. *Journal of Applied Physiology,* 77**,** 502-506.

Peake, J. M., Neubauer, O., Della Gatta, P. A. & Nosaka, K. 2016. Muscle damage and inflammation during recovery from exercise. *American Journal of Physiology-Heart and Circulatory Physiology*.

Pellerin, L. & Magistretti, P. J. 1994. Glutamate uptake into astrocytes stimulates aerobic glycolysis: a mechanism coupling neuronal activity to glucose utilization. *Proceedings of the National Academy of Sciences of the United States of America,* 91**,** 10625-10629.

Perl, E. R. 1992. Function of Dorsal Root Ganglion Neurons: An Overview. *In:* SCOTT, S. A. (ed.) *Sensory Neurons: Diversity, Development, and Plasticity.* Oxford Press

Pescatello, L. S., Macdonald, H. V., Lamberti, L. & Johnson, B. T. 2015. Exercise for Hypertension: A Prescription Update Integrating Existing Recommendations with Emerging Research. *Current hypertension reports,* 17**,** 87-87.

Peter, J. B., Barnard, R. J., Edgerton, V. R., Gillespie, C. A. & Stempel, K. E. 1972. Metabolic profiles of three fiber types of skeletal muscle in guinea pigs and rabbits. *Biochemistry,* 11**,** 2627-2633.

Petersen, P. L., Mathiesen, O., Torup, H. & Dahl, J. B. 2010. The transversus abdominis plane block: a valuable option for postoperative analgesia? A topical review. *Acta Anaesthesiol Scand,* 54**,** 529-35.

Pogorzala, L. A., Mishra, S. K. & Hoon, M. A. 2013. The cellular code for mammalian thermosensation. *The Journal of neuroscience : the official journal of the Society for Neuroscience,* 33**,** 5533-5541.

Pollak, K. A., D., S. J., Vanhaitsma, T. A., Hughen, R. W., Jo, D., Light, K. C., Schweinhardt, P., Amann, M. & Light, A. R. 2014. Exogenously applied muscle metabolites synergistically evoke sensations of muscle fatigue and pain in human subjects. *Experimental Physiology,* 99**,** 368-380.

Poole, D. C., Hirai, D. M., Copp, S. W. & Musch, T. I. 2012. Muscle oxygen transport and utilization in heart failure: implications for exercise (in)tolerance. *American Journal of Physiology-Heart and Circulatory Physiology,* 302**,** H1050-H1063.

Proske, U. 2005. Muscle tenderness from exercise: mechanisms? *The Journal of physiology,* 564**,** 1-1.

Proske, U. & Morgan, D. L. 2001. Muscle damage from eccentric exercise: mechanism, mechanical signs, adaptation and clinical applications. *The Journal of Physiology,* 537**,** 333-345.

Pyne, D. B. 1994. Exercise-induced muscle damage and inflammation: a review. *Australian Journal of Science and Medicine in Sport,* 26**,** 49-49.

Queme, L. F., Ross, J. L. & Jankowski, M. P. 2017. Peripheral mechanisms of ischemic myalgia. *Frontiers in Cellular Neuroscience,* 11**,** 419.

Rafi, A. 2001. Abdominal field block: a new approach via the lumbar triangle. *Anaesthesia,* 56**,** 1024-1026.

Rebbeck, R. T., Karunasekara, Y., Board, P. G., Beard, N. A., Casarotto, M. G. & Dulhunty, A. F. 2014. Skeletal muscle excitation–contraction coupling: Who are the dancing partners? *The International Journal of Biochemistry & Cell Biology,* 48**,** 28-38.

Reeves, N. P., Narendra, K. S. & Cholewicki, J. 2007. Spine stability: the six blind men and the elephant. *Clinical Biomechanics,* 22**,** 266-274.

Reinöhl, J., Hoheisel, U., Unger, T. & Mense, S. 2003. Adenosine triphosphate as a stimulant for nociceptive and non-nociceptive muscle group IV receptors in the rat. *Neuroscience Letters,* 338**,** 25-28.

Ro, J. Y., Lee, J. S. & Zhang, Y. 2009. Activation of TRPV1 and TRPA1 leads to muscle nociception and mechanical hyperalgesia. *Pain,* 144**,** 270-7.

Robergs, R. A., Ghiasvand, F. & Parker, D. 2004. Biochemistry of exercise-induced metabolic acidosis. *American Journal of Physiology-Regulatory, Integrative and Comparative Physiology,* 287**,** R502-R516.

Roberts, D. 2018. Chronic fatigue syndrome and quality of life. *Patient Related Outcome Measures,* 9**,** 253-262.

Rodrigues, A. C. Z., Messi, M. L., Wang, Z. M., Abba, M. C., Pereyra, A., Birbrair, A., Zhang, T., O'meara, M., Kwan, P., Lopez, E. I. S., Willis, M. S., Mintz, A., Files, D. C., Furdui, C., Oppenheim, R. W. & Delbono, O. a.-O. H. O. O. 2018. The sympathetic nervous system regulates skeletal muscle motor innervation and acetylcholine receptor stability. *Acta Physiologica*

(Oxf), 30.

Ross, J. L., Queme, L. F., Shank, A. T., Hudgins, R. C. & Jankowski, M. P. 2014. Sensitization of group III and IV muscle afferents in the mouse after ischemia and reperfusion injury. *The Journal of Pain,* 15**,** 1257-70.

Rossman, M. J., Venturelli, M., Mcdaniel, J., Amann, M. & Richardson, R. S. 2012. Muscle mass and peripheral fatigue: a potential role for afferent feedback? *Acta physiologica,* 206**,** 242-250.

Rotto, D. M. & Kaufman, M. P. 1988. Effect of metabolic products of muscular contraction on discharge of group III and IV afferents. *Journal of Applied Physiology,* 64**,** 2306-2313.

Rozen, W. M., Tran, T. M., Ashton, M. W., Barrington, M. J., Ivanusic, J. J. & Taylor, G. I. 2008. Refining the course of the thoracolumbar nerves: a new understanding of the innervation of the anterior abdominal wall. *Clinical Anatomy,* 21**,** 325-33.

Ruffini, A. 1898. On the Minute Anatomy of the Neuromuscular Spindles of the Cat, and on their Physiological Significance. *The Journal of Physiology,* 23**,** 190-208.3.

Running, C. A., Craig, B. A. & Mattes, R. D. 2015. Oleogustus: The Unique Taste of Fat. *Chemical Senses,* 40**,** 507-516.

Saito, M., Tsukanaka, A., Yanagihara, D. & Mano, T. 1993. Muscle sympathetic nerve responses to graded leg cycling. *Journal of Applied Physiology,* 75**,** 663-667.

San-Millán, I. & Brooks, G. A. 2017. Reexamining cancer metabolism: lactate production for carcinogenesis could be the purpose and explanation of the Warburg Effect. *Carcinogenesis,* 38**,** 119-133.

Schiaffino, S. 2018. Muscle fiber type diversity revealed by anti-myosin heavy chain antibodies. *The FEBS Journal,* 285**,** 3688-3694.

Schiaffino, S., Ausoni, S., Gorza, L., Saggin, L., Gundersen, K. & Lomo, T. 1998. Myosin heavy chain isoforms and velocity of shortening of type 2 skeletal muscle fibres. *Acta Physiologica Scandinavica,* 134**,** 575-576.

Schiaffino, S., Gorza, L., Sartore, S., Saggin, L., Ausoni, S., Vianello, M., Gundersen, K. & Lømo, T. 1989. Three myosin heavy chain isoforms in type 2 skeletal muscle fibres. *Journal of Muscle Research & Cell Motility,* 10**,** 197-205.

Schiaffino, S. & Reggiani, C. 2011. Fiber Types in Mammalian Skeletal Muscles. *Physiological Reviews,* 91**,** 1447-1531.

Schleip, R., Jager, H. & Klingler, W. 2012. What is 'fascia'? A review of different nomenclatures. *Journal of Bodywork and Movement Therapies,* 16**,** 496-502.

Schleip, R., Naylor, I. L., Ursu, D., Melzer, W., Zorn, A., Wilke, H. J., Lehmann-Horn, F. & Klingler, W. 2006. Passive muscle stiffness may be influenced by active contractility of intramuscular connective tissue. *Medicial Hypotheses,* 66**,** 66-71.

Schoultz, T. W. & Swett, J. E. 1972. The fine structure of the Golgi tendon organ. *Journal of Neurocytology,* 1**,** 1-25.

Schoultz, T. W. & Swett, J. E. 1974. Ultrastructural organization of the sensory fibers innervating the Golgi tendon organ. *The Anatomical Record,* 179**,** 147-161.

Schwane, J. A., Watrous, B. G., Johnson, S. R. & Armstrong, R. B. 1983. Is lactic acid related to delayed-onset muscle soreness? *The Physician and Sportsmedicine,* 11**,** 124-131.

Scott Adam, C., Wensel, R., Davos Constantinos, H., Georgiadou, P., Kemp, M., Hooper, J., Coats Andrew, J. S. & Piepoli Massimo, F. 2003. Skeletal Muscle Reflex in Heart Failure Patients. *Circulation,* 107**,** 300-306.

Screen, H. R. C., Lee, D. A., Bader, D. L. & Shelton, J. C. 2004. An investigation into the effects of the hierarchical structure of tendon fascicles on micromechanical

properties. *Proceedings of the Institution of Mechanical Engineers, Part H: Journal of Engineering in Medicine,* 218**,** 109-119.

Secher, N. H. 1985. Heart rate at the onset of static exercise in man with partial neuromuscular blockade. *The Journal of physiology,* 368**,** 481-490.

Secher, N. H. & Amann, M. 2012. Human investigations into the exercise pressor reflex. *Experimental physiology,* 97**,** 59-69.

Sforza, M., Andjelkov, K., Zaccheddu, R., Nagi, H. & Colic, M. 2011. Transversus abdominis plane block anesthesia in abdominoplasties. *Plastic Reconstructive Surgery - Journal of the American Society of Plastic Surgeons,* 128**,** 529-35.

Sherrington, C. S. 1894. On the Anatomical Constitution of Nerves of Skeletal Muscles; with Remarks on Recurrent Fibres in the Ventral Spinal Nerve- root. *The Journal of physiology,* 17**,** 210-258.

Shin, G., Gomez, A. M., Al-Hasani, R., Jeong, Y. R., Kim, J., Xie, Z., Banks, A., Lee, S. M., Han, S. Y., Yoo, C. J., Lee, J.-L., Lee, S. H., Kurniawan, J., Tureb, J., Guo, Z., Yoon, J., Park, S.-I., Bang, S. Y., Nam, Y., Walicki, M. C., Samineni, V. K., Mickle, A. D., Lee, K., Heo, S. Y., Mccall, J. G., Pan, T., Wang, L., Feng, X., Kim, T.-I., Kim, J. K., Li, Y., Huang, Y., Gereau, R. W., Ha, J. S., Bruchas, M. R. & Rogers, J. A. 2017. Flexible Near-Field Wireless Optoelectronics as Subdermal Implants for Broad Applications in Optogenetics. *Neuron,* 93**,** 509-521.e3.

Sidhu, S. K., Weavil, J. C., Mangum, T. S., Jessop, J. E., Richardson, R. S., Morgan, D. E. & Amann, M. 2017. Group III/IV locomotor muscle afferents alter motor cortical and corticospinal excitability and promote central fatigue during cycling exercise. *Clinical Neurophysiology,* 128**,** 44-55.

Sidhu, S. K., Weavil, J. C., Thurston, T. S., Rosenberger, D., Jessop, J. E., Wang, E., Richardson, R. S., Mcneil, C. J. & Amann, M. 2018. Fatigue- related group III/IV muscle afferent feedback facilitates intracortical inhibition during locomotor exercise. *The Journal of physiology,* 596.

Sidhu, S. K., Weavil, J. C., Venturelli, M., Garten, R. S., Rossman, M. J., Richardson, R. S., Gmelch, B. S., Morgan, D. E. & Amann, M. 2014. Spinal mu-opioid receptor-sensitive lower limb muscle afferents determine corticospinal responsiveness and promote central fatigue in upper limb muscle. *The Journal of Physiology,* 592**,** 5011-24.

Simon, P. 2003. Q-Gene: processing quantitative real-time RT–PCR data. *Bioinformatics,* 19**,** 1439-1440.

Sluka, K. A., Danielson, J., Rasmussen, L. & Dasilva, L. F. 2012. Exercise-induced pain requires NMDA receptor activation in the medullary raphe nuclei. *Medicine & Science in Sports & Exercise,* 44**,** 420.

Smith, S. A., Leal, A. K., Murphy, M. N., Downey, R. M. & Mizuno, M. 2015. Muscle mechanoreflex overactivity in hypertension: a role for centrally-derived nitric oxide. *Autonomic Neuroscience,* 188**,** 58-63.

Smith, S. A., Leal, A. K., Williams, M. A., Murphy, M. N., Mitchell, J. H. & Garry, M. G. 2010. The TRPv1 receptor is a mediator of the exercise pressor reflex in rats. *The Journal of physiology,* 588**,** 1179-1189.

Smith, S. A., Williams, M. A., Leal, A. K., Mitchell, J. H. & Garry, M. G. 2006. Exercise pressor reflex function is altered in spontaneously hypertensive rats. *The Journal of physiology,* 577**,** 1009-1020.

Smith Scott, A., Mammen Pradeep, P. A., Mitchell Jere, H. & Garry Mary, G. 2003. Role of the Exercise Pressor Reflex in Rats With Dilated Cardiomyopathy. *Circulation,* 108**,** 1126-1132.

Smith Scott, A., Mitchell Jere, H., Naseem, R. H. & Garry Mary, G. 2005a. Mechanoreflex Mediates the Exaggerated Exercise Pressor Reflex in Heart Failure. *Circulation,* 112**,** 2293-2300.

Smith Scott, A., Williams Maurice, A., Mitchell Jere, H., Mammen Pradeep, P. A. & Garry Mary, G. 2005b. The Capsaicin-Sensitive Afferent Neuron in Skeletal Muscle Is Abnormal in Heart Failure. *Circulation,* 111**,** 2056-2065.

Soga, T., Kamohara, M., Takasaki, J., Matsumoto, S.-I., Saito, T., Ohishi, T., Hiyama, H., Matsuo, A., Matsushime, H. & Furuichi, K. 2003. Molecular identification of nicotinic acid receptor. *Biochemical and Biophysical Research Communications,* 303**,** 364-369.

Song. X., C. B. N., Zagorodnyuk. V. P., Lynn. P. A., Blachshaw L. A., Grundy. D., Brunsden. A. M., Costa. M., and Brookes. S.J.H. 2009. Identification of Medium/ High- Threshold Extrinsic Mechanosensitive Afferent Nerves to the Gastrointestinal Tract.(Report). *Gastroenterology,* 137**,** 274-284.e1.

Spencer, N. J., Greenheigh, S., Kyloh, M., Hibberd, T. J., Sharma, H., Grundy, L., Brierley, S. M., Harrington, A. M., Beckett, E. A. & Brookes, S. J. 2018a. Identifying unique subtypes of spinal afferent nerve endings within the urinary bladder of mice. *Journal of Comparative Neurology,* 526**,** 707-720.

Spencer, N. J., Hibberd, T. J., Lagerström, M., Otsuka, Y. & Kelley, N. 2018b. Visceral pain–Novel approaches for optogenetic control of spinal afferents. *Brain research,* 1693**,** 159-164.

Spencer, N. J., Kyloh, M., Beckett, E. A., Brookes, S. & Hibberd, T. 2016. Different types of spinal afferent nerve endings in stomach and esophagus identified by anterograde tracing from dorsal root ganglia. *Journal of Comparative Neurology,* 524**,** 3064-3083.

Stacey, M. 1969. Free nerve endings in skeletal muscle of the cat. *Journal of Anatomy,* 105**,** 231.

Statistics, A. B. O. 2018. National Health Survey - First Results Australia 2017-2018. Canberra: Australian Bureau of Statistics.

Staud, R., Mokthech, M., Price, D. D. & Robinson, M. E. 2015. Evidence for sensitized fatigue pathways in patients with chronic fatigue syndrome. *Pain,* 156**,** 750.

Stecco, C., Gagey, O., Belloni, A., Pozzuoli, A., Porzionato, A., Macchi, V., Aldegheri, R., De Caro, R. & Delmas, V. 2007. Anatomy of the deep fascia of the upper limb. Second part: study of innervation. *Morphologie,* 91**,** 38-43.

Stecco, C., Macchi, V., Barbieri, A., Tiengo, C., Porzionato, A. & De Caro, R. 2018. Hand fasciae innervation: The palmar aponeurosis. *Clinical Anatomy,* 31**,** 677-683.

Steffens, H., Dibaj, P. & Schomburg, E. 2012. In vivo measurement of conduction velocities in afferent and efferent nerve fibre groups in mice. *Physiological research,* 61**,** 203-214.

Stilwell, D. L. 1957. The innervation of tendons and aponeuroses. *American Journal of Anatomy,* 100**,** 289-317.

Stone, A. J., Copp, S. W. & Kaufman, M. P. 2015. Role played by NaV 1.7 channels on thin-fiber muscle afferents in transmitting the exercise pressor reflex. *American Journal of Physiology-Regulatory, Integrative and Comparative Physiology,* 309**,** R1301-R1308.

Stone, A. J. & Kaufman, M. P. 2015. The exercise pressor reflex and peripheral artery disease. *Autonomic Neuroscience,* 188**,** 69-73.

Stoving, K., Rothe, C., Rosenstock, C. V., Aasvang, E. K., Lundstrom, L. H. & Lange, K. H. 2015. Cutaneous Sensory Block Area, Muscle-Relaxing Effect, and Block Duration of the Transversus Abdominis Plane Block: A Randomized,

Blinded, and Placebo-Controlled Study in Healthy Volunteers. *Regional Anesthesia and Pain Medicine,* 40**,** 355-62.

Suresh, S. & Chan, V. W. 2009. Ultrasound guided transversus abdominis plane block in infants, children and adolescents: a simple procedural guidance for their performance. *Paediatric Anaesthesia,* 19**,** 296-9.

Szolcsányi, J. 1987. Selective responsiveness of polymodal nociceptors of the rabbit ear to capsaicin, bradykinin and ultra-violet irradiation. *The Journal of physiology,* 388**,** 9-23.

Taguchi, T., Matsuda, T., Tamura, R., Sato, J. & Mizumura, K. 2005a. Muscular mechanical hyperalgesia revealed by behavioural pain test and c- Fos expression in the spinal dorsal horn after eccentric contraction in rats. *The Journal of Physiology,* 564**,** 259-268.

Taguchi, T., Sato, J. & Mizumura, K. 2005b. Augmented mechanical response of muscle thin-fiber sensory receptors recorded from rat muscle-nerve preparations in vitro after eccentric contraction. *Journal of Neurophysiology,* 94**,** 2822-31.

Tamura, R., Mizumura, K. & Kumazawa, T. 1996. Coexistence of calcitonin gene-related peptide-and substance P-like immunoreactivity in retrogradely labeled superior spermatic neurons in the dog. *Neuroscience research,* 25**,** 293-299.

Tang, F., Lane, S., Korsak, A., Paton, J., Gourine, A., Kasparov, S. & Teschemacher, A. 2014. Lactate-mediated glia-neuronal signalling in the mammalian brain. *Nature communications,* 5**,** 3284.

Tassicker, B. C., Hennig, G. W., Costa, M. & Brookes, S. J. H. 1999. Rapid anterograde and retrograde tracing from mesenteric nerve trunks to the guinea- pig small intestine in vitro. *Cell Tissue Research,* 295**,** 437-452.

Taylor, J. L., Amann, M., Duchateau, J., Meeusen, R. & Rice, C. L. 2016. Neural contributions to muscle fatigue: from the brain to the muscle and back again. *Medicine & Science in Sports & Exercise,* 48**,** 2294.

Tesarz, J., Hoheisel, U. & Mense, S. 2013. Tetrodotoxin-resistant fibres and spinal Fos expression: differences between input from muscle and skin. *Experimental brain Research,* 224**,** 571-80.

Tibes, U. 1977. Reflex inputs to the cardiovascular and respiratory centers from dynamically working canine muscles. Some evidence for involvement of group III or IV nerve fibers. *Circulation Research,* 41**,** 332-341.

Tiegs, O. W. 1953. Innervation of Voluntary Muscle. *Physiological Reviews,* 33**,** 90-144.

Tsuchimochi, H., Mccord, J. L., Hayes, S. G., Koba, S. & Kaufman, M. P. 2010a. Chronic femoral artery occlusion augments exercise pressor reflex in decerebrated rats. *American journal of physiology. Heart and circulatory physiology,* 299**,** H106-H113.

Tsuchimochi, H., Mccord, J. L. & Kaufman, M. P. 2010b. Peripheral mu-opioid receptors attenuate the augmented exercise pressor reflex in rats with chronic femoral artery occlusion. *American Journal of Physiology-Heart and Circulatory Physiology,* 299**,** H557-H565.

Tsuchimochi, H., Yamauchi, K., Mccord, J. L. & Kaufman, M. P. 2011. Blockade of acid sensing ion channels attenuates the augmented exercise pressor reflex in rats with chronic femoral artery occlusion. *The Journal of physiology,* 589**,** 6173-6189.

Tsukagoshi, M., Funakoshi, K., Goris, R. C. & Kishida, R. 2002. Differential distribution of nerve fibers immunoreactive for substance P and calcitonin gene-related peptide in the superficial and deep muscle layers of the dorsum of the rat. *Brain research bulletin,* 58**,** 439-446.

Tsukagoshi, M., Goris, R. C. & Funakoshi, K. 2006. Differential distribution of vanilloid receptors in the primary sensory neurons projecting to the dorsal skin and muscles. *Histochemistry and Cell Biology,* 126**,** 343-52.

Urban, D. J. & Roth, B. L. 2015. DREADDs (Designer Receptors Exclusively Activated by Designer Drugs): Chemogenetic Tools with Therapeutic Utility. *Annual Review of Pharmacology and Toxicology,* 55**,** 399-417.

Urquhart, D. M., Barker, P. J., Hodges, P. W., Story, I. H. & Briggs, C. A. 2005. Regional morphology of the transversus abdominis and obliquus internus and externus abdominis muscles. *Clinical Biomechanics,* 20**,** 233-241.

Usoskin, D., Furlan, A., Islam, S., Abdo, H., Lonnerberg, P., Lou, D., Hjerling-Leffler, J. a.-O., Haeggstrom, J., Kharchenko, O., Kharchenko, P. V., Linnarsson, S. & Ernfors, P. 2015. Unbiased classification of sensory neuron types by large-scale single-cell RNA sequencing. *Nature Neuroscience,* 18.

Viana, F. 2016. TRPA1 channels: molecular sentinels of cellular stress and tissue damage. *The Journal of Physiology,* 594**,** 4151-4169.

Von Düring, M. & Andres, K. H. 1990. Topography and Ultrastructure of Group III and IV Nerve Terminals of the Cat's Gastrocnemius-Soleus Muscle. *In:* ZENKER, W. & NEUHUBER, W. L. (eds.) *The Primary Afferent Neuron: A Survey of Recent Morpho-Functional Aspects.* Boston, MA: Springer US.

Waldrop, T. G., Mullins, D. C. & Millhorn, D. E. 1986. Control of respiration by the hypothalamus and by feedback from contracting muscles in cats. *Respiration Physiology,* 64**,** 317-328.

Walgenbach, S. C. & Donald, D. E. 1983. Cardiopulmonary reflexes and arterial pressure during rest and exercise in dogs. *American Journal of Physiology-Heart and Circulatory Physiology,* 244**,** H362-H369.

Wallenius, K., Thalén, P., Björkman, J.-A., Johannesson, P., Wiseman, J., Böttcher, G., Fjellström, O. & Oakes, N. D. 2017. Involvement of the metabolic sensor GPR81 in cardiovascular control. *JCI insight,* 2.

Wang, F., Bélanger, E., Côté, S. L., Desrosiers, P., Prescott, S. A., Côté, D. C. & De Koninck, Y. 2018. Sensory Afferents Use Different Coding Strategies for Heat and Cold. *Cell reports,* 23**,** 2001-2013.

Wang, H., Zucker, I. H. & Wang, W. 2012. Muscle reflex in heart failure: the role of exercise training. *Frontiers in physiology,* 3**,** 398.

Wang, H.-J., Li, Y.-L., Gao, L., Zucker, I. H. & Wang, W. 2010. Alteration in skeletal muscle afferents in rats with chronic heart failure. *The Journal of Physiology,* 588**,** 5033-5047.

Weavil, J. C. & Amann, M. 2018. Chapter 13 - Corticospinal excitability during fatiguing whole body exercise. *In:* MARCORA, S. & SARKAR, M. (eds.) *Progress in Brain Research.* Elsevier.

Weavil, J. C., Sidhu, S. K., Mangum, T. S., Richardson, R. S. & Amann, M. 2015. Intensity-dependent alterations in the excitability of cortical and spinal projections to the knee extensors during isometric and locomotor exercise. *American Journal of Physiology-Regulatory, Integrative and Comparative Physiology,* 308**,** R998-R1007.

Weddell, G. & Harpman, J. 1940. The neurohistological basis for the sensation of pain provoked from deep fascia, tendon, and periosteum. *Journal of Neurology and Psychiatry,* 3**,** 319.

Wenk, H. N. & Mccleskey, E. W. 2007. A novel mouse skeletal muscle-nerve preparation and in vitro model of ischemia. *Journal of Neuroscience Methods,* 159**,** 244-251.

Westerberg, E., Molin, C. J., Nees, S. S., Widenfalk, J. & Punga, A. R. 2018. The impact of physical exercise on neuromuscular function in myasthenia gravis patients: a single-subject design study. *Medicine,* 97.

White, M. J. 2014. Muscle afferents and cardiorespiratory control: the Birmingham connection. *Experimental physiology,* 99**,** 306-11.

Wilkinson, K. A., Kloefkorn, H. E. & Hochman, S. 2012. Characterization of muscle spindle afferents in the adult mouse using an in vitro muscle-nerve preparation. *PloS one,* 7**,** e39140.

Willard, F. H., Vleeming, A., Schuenke, M. D., Danneels, L. & Schleip, R. 2012. The thoracolumbar fascia: anatomy, function and clinical considerations. *Journal of Anatomy,* 221**,** 507-36.

Williams, E. K., Chang, R. B., Strochlic, D. E., Umans, B. D., Lowell, B. B. & Liberles, S. D. 2016. Sensory Neurons that Detect Stretch and Nutrients in the Digestive System. *Cell,* 166**,** 209-221.

Williamson, J. 2010. The relevance of central command for the neural cardiovascular control of exercise. *Experimental Physiology,* 95**,** 1043-1048.

Williamson, J., Fadel, P. & Mitchell, J. 2006. New insights into central cardiovascular control during exercise in humans: a central command update. *Experimental Physiology,* 91**,** 51-58.

Williamson, J. W., Nobrega, A. C., Winchester, P. K., Zim, S. & Mitchell, J. H. 1995. Instantaneous heart rate increase with dynamic exercise: central command and muscle-heart reflex contributions. *Journal of Applied Physiology,* 78**,** 1273-1279.

Wong, R., Lopaschuk, G., Zhu, G., Walker, D., Catellier, D., Burton, D., Teo, K., Collins-Nakai, R. & Montague, T. 1992. Skeletal Muscle Metabolism in the Chronic

Fatigue Syndrome: In Vivo Assessment by 31P Nuclear Magnetic Resonance Spectroscopy. *Chest,* 102**,** 1716-1722.

Woo, S.-H., Lukacs, V., De Nooij, J. C., Zaytseva, D., Criddle, C. R., Francisco, A., Jessell, T. M., Wilkinson, K. A. & Patapoutian, A. 2015. Piezo2 is the principal mechanotransduction channel for proprioception. *Nature Neuroscience,* 18**,** 1756.

Woo, S.-H., Ranade, S., Weyer, A. D., Dubin, A. E., Baba, Y., Qiu, Z., Petrus, M., Miyamoto, T., Reddy, K., Lumpkin, E. A., Stucky, C. L. & Patapoutian, A. 2014. Piezo2 is required for Merkel-cell mechanotransduction. *Nature,* 509**,** 622.

Xie, Y.-F., Wang, J. & Bonin, R. P. 2018. Optogenetic exploration and modulation of pain processing. *Experimantal Neurology,* 306**,** 117-121.

Xu, J., Gu, H. & Brennan, T. J. 2010. Increased sensitivity of group III and group IV afferents from incised muscle in vitro. *Pain,* 151**,** 744-55.

Young, M. J., Gorlin, A. W., Modest, V. E. & Quraishi, S. A. 2012. Clinical implications of the transversus abdominis plane block in adults. *Anesthesiology Research and Practice,* 2012**,** 731645.

Yu, L., Yang, F., Luo, H., Liu, F.-Y., Han, J.-S., Xing, G.-G. & Wan, Y. 2008. The role of TRPV1 in different subtypes of dorsal root ganglion neurons in rat chronic inflammatory nociception induced by complete Freund's adjuvant. *Molecular pain,* 4**,** 61-61.

Yu, S.-Q., Ma, S. & Wang, D. H. 2018. Selective ablation of TRPV1 by intrathecal injection of resiniferatoxin in rats increases renal sympathoexcitatory responses and salt sensitivity. *Hypertension Research,* 41**,** 679-690.

Yudin, Y. & Rohacs, T. 2018. Inhibitory Gi/O-coupled receptors in somatosensory neurons: Potential therapeutic targets for novel analgesics. *Molecular pain,* 14**,** 1-16.

Zaffagnini, S., Golano, P., Farinas, O., Depasquale, V., Strocchi, R., Cortecchia, S., Marcacci, M. & Visani, A. 2003. Vascularity and neuroreceptors of the pes anserinus: anatomic study.

Zagorodnyuk, V. P. & Brookes, S. J. 2000. Transduction sites of vagal mechanoreceptors in the guinea pig esophagus. *Journal of Neuroscience,* 20**,** 6249-55.

Zagorodnyuk, V. P., Chen, B. N. & Brookes, S. J. H. 2001. Intraganglionic laminar endings are mechano-transduction sites of vagal tension receptors in the guinea-pig stomach. *The Journal of Physiology,* 534**,** 255-268.

Zagorodnyuk, V. P., Chen, B. N., Costa, M. & Brookes, S. J. H. 2003. Mechanotransduction by intraganglionic laminar endings of vagal tension receptors in the guinea-pig oesophagus. *The Journal of Physiology,* 553**,** 575-587.

Zeng, H. & Sanes, J. R. 2017. Neuronal cell-type classification: challenges, opportunities and the path forward. *Nature Reviews Neuroscience,* 18**,** 530.

Zingg, B., Chou, X.-L., Zhang, Z.-G., Mesik, L., Liang, F., Tao, H. W. & Zhang, L. I. 2017. AAV-Mediated Anterograde Transsynaptic Tagging: Mapping Corticocollicular Input-Defined Neural Pathways for Defense Behaviors. *Neuron,* 93**,** 33-47.